



Copyright Statement

The digital copy of this thesis is protected by the Copyright Act 1994 (New Zealand). This thesis may be consulted by you, provided you comply with the provisions of the Act and the following conditions of use:

- Any use you make of these documents or images must be for research or private study purposes only, and you may not make them available to any other person.
- Authors control the copyright of their thesis. You will recognise the author's right to be identified as the author of this thesis, and due acknowledgement will be made to the author where appropriate.
- You will obtain the author's permission before publishing any material from their thesis.

To request permissions please use the Feedback form on our webpage.
<http://researchspace.auckland.ac.nz/feedback>

General copyright and disclaimer

In addition to the above conditions, authors give their consent for the digital copy of their work to be used subject to the conditions specified on the Library [Thesis Consent Form](#)

Thalidomide Metabolism and Metabolites

**A thesis submitted to the University of Auckland
in fulfilment of the requirements for the degree of
Doctor of Philosophy**

By

Jun Lu

**Auckland Cancer Society Research Centre
Department of Molecular Medicine and Pathology
Faculty of Medical and Health Sciences
University of Auckland
Auckland, New Zealand**

April 2004

ABSTRACT

Thalidomide, renowned for causing birth defects in the late 1950s when used for the relief of morning sickness, has attracted new interest for the treatment of inflammatory conditions such as erythema nodosum leprosum and human malignancies such as multiple myeloma. Different species have different sensitivities to thalidomide that could be related to differences in its metabolism. In this study, methodologies using liquid chromatography-mass spectrometry were developed to identify thalidomide metabolites formed *in vivo* and *in vitro* in liver microsomes from mice, rabbits and humans, firstly to seek explanations for inter-species differences in sensitivity, and secondly to determine whether thalidomide or its metabolite(s) is the active agent.

Four hydrolysis products were detected in plasma and urine samples from multiple myeloma patients (MMPs) on thalidomide therapy, and mice and rabbits after oral administration of thalidomide. Six hydroxylated metabolites were detected in mice and rabbits, but not in plasma and urine from MMPs. *In vitro* studies confirmed that murine and rabbit liver microsomes catalysed the hydroxylation of thalidomide efficiently, but significant production of hydroxylation of thalidomide was not observed using human liver microsomes. The degree of hydroxylation both *in vivo* and *in vitro* was highest in mice and lowest in humans with rabbits in between. It is unlikely that hydroxylated metabolites are responsible for the effects of thalidomide in the treatment of multiple myeloma, since they were not present in quantifiable amounts in patients who were responding to the treatment. The three major hydrolysis products that were detected in patients were compared with thalidomide for their ability to inhibit tube formation in an *in vitro* angiogenesis assay, to inhibit TNF production induced with LPS in human peripheral blood leucocytes, and to modulate DMXAA-induced TNF production and antitumour activity in mice. One of the three, *N*-(*o*-carboxybenzoyl)glutamic acid imide (CG) was found to be as active as thalidomide in all the assays at concentrations (1-2 µg/ml) that are achievable in MMPs. Since CG has been shown by other laboratories to be non-teratogenic, the studies in this

thesis indicate that CG would be a more favourable, non-teratogenic approach to cancer therapy compared with thalidomide.

ACKNOWLEDGMENTS

Constructing a PhD thesis is like building a house. I was very lucky to have a group of great “architects”, my supervisors, to guide me and supply me with a “blue print” and “building materials”.

I am indebted to my main supervisor, Associate Professor Lai-Ming Ching, for providing me with the opportunity to work on this project, and for her patient teaching, constant encouragement, valuable advice and technical and financial support. I’d like to thank my co-supervisor, Professor and centre Co-Director Professor Bruce Baguley, for his guidance, intelligent advice, unconditional support and ever-opening door to students. I am also indebted to my co-supervisor, Dr. Philip Kestell, for his expertise in pharmacology, technical guidance, frequent discussion, and casual chat. I also need to thank Drs. Malcolm Tingle and Nuala Helsby for their help and advice on metabolism studies of thalidomide *in vitro* and in rabbits. I thank Professor Peter Browett, head of Molecular Medicine and Pathology department, for providing clinical samples and outcomes of multiple myeloma patients. I need to thank Associate Professor Brian Palmer for synthesising all the authentic standards of thalidomide metabolites and support in chemistry. I thank all the patients with multiple myeloma who volunteered themselves to provide blood and urine samples; the seven volunteers in the Auckland Cancer Society Research Centre who donated blood for my TNF studies; and all the nursing staff who helped me collect blood samples. I thank Professor William A Denny for his support to students as the director of the Auckland Cancer Society Research Centre; Ms Elaine Marshall for her support and care as the manager of the centre; Rachel Sutherland for her assistance in animal surgery and other laboratory techniques; Dianne Ferry for her support in LC-MS analysis; Angela Ding for her assistant in pharmacological works; Sandy Hung and Derek Wu for assistance in cell culture experiments; Jack Zhao and Steve Wang for discussion and chats in our office; Ellen Semb and Mary Spellman for secretarial and IT support. I need to give special thanks to Francisco Chung, who has been working together with me on this project for three

years. We helped and cooperated with each other to carry out tough experiments, and produced a paper together, which has been submitted to *Clinical Cancer Research*.

As a “trainee builder”, a PhD student, I am very grateful that I was paid. I’d like to express my sincere gratitude to the Marsden Fund of the Royal Society of New Zealand, which supplied me with a fellowship to enable me to finish my PhD without sacrificing my financial integrity. The generous support of the Marsden Fund was instrumental to the achievement of this work. I also would like to express my acknowledgment to the University of Auckland Research Committee and Auckland Cancer Society for their travel grants, which enabled me to attend the 94th Annual Meeting of American Association for Cancer Research in Washington D.C., USA in 2003. A poster of my work has been presented at the conference.

Finally, I’d like to thank my parents, Jinlin Lu and Qindi Zhang, for their moral support and encouragement. I need to thank my wife, Liang-Ni Liu, for her contribution to my life and her understanding of my work. My son, Si-Cong Lu, although you are too young to know this, this is for you.

TABLE OF CONTENTS

ABSTRACT	I
ACKNOWLEDGMENTS	IV
TABLE OF CONTENTS.....	VI
LIST OF FIGURES	X
LIST OF TABLES	XVI
LIST OF TABLES	XVI
LIST OF ABBREVIATIONS.....	XVII
CHAPTER 1. GENERAL INTRODUCTION.....	1
1.1. THE HISTORY OF THALIDOMIDE AND ITS ROLE IN CANCER THERAPY	1
1.2. THALIDOMIDE AS AN ANTI-CANCER AGENT	4
1.2.1. <i>Pre-clinical Studies</i>	4
1.2.2. <i>Clinical Studies</i>	5
1.2.2.1. Thalidomide in Solid Tumours	5
1.2.2.2. Thalidomide in Haematological Malignancies.....	6
1.3. MECHANISM OF ACTION IN CANCER TREATMENT	10
1.3.1. <i>Anti-angiogenesis</i>	10
1.3.2. <i>Cytokine Modulation</i>	11
1.3.3. <i>Inhibition of Adhesion Molecule Expression</i>	14
1.3.4. <i>Stimulation of Lymphocytes and Natural Killer Cells</i>	15
1.3.5. <i>Induction of Apoptosis</i>	16
1.4. PHARMACOKINETICS, METABOLISM AND METABOLITES.....	18
1.4.1. <i>Pharmacokinetics and Pharmacokinetic Interaction with Other Drugs</i>	18
1.4.1.1. Pharmacokinetics	18
1.4.1.2. Pharmacokinetic Interactions with Other Drugs	20
1.4.2. <i>Metabolism and Metabolites</i>	20
1.5. SUMMARY OF THE REVIEW	23

1.6. OBJECTIVES OF THIS STUDY	24
CHAPTER 2. DETECTION AND IDENTIFICATION OF THALIDOMIDE METABOLITES IN MICE	26
2.1. INTRODUCTION	26
2.2. METHODS	27
2.2.1. <i>Mice and Tumour</i>	27
2.2.2. <i>Drug Administration</i>	27
2.2.3. <i>Metabolite Detection Using LC-MS and HPLC</i>	28
2.2.3.1. Preparation of Murine Plasma and Urine Samples	28
2.2.3.2. LC-MS Analysis.....	28
2.2.3.3. Resolution of Phthaloylglutamine (PG) and Phthaloylisoglutamine (PiG) by HPLC.....	30
2.2.5.8. Thalidomide Glucuronide Identification.....	31
2.3. RESULTS.....	31
2.3.1. <i>Detection of Metabolites</i>	31
2.3.2. <i>Identification of Metabolites</i>	32
2.4. DISCUSSION.....	44
CHAPTER 3. IDENTIFICATION OF THALIDOMIDE METABOLITES IN MULTIPLE MYELOMA PATIENTS.....	47
3.1. INTRODUCTION	47
3.2. METHODS	48
3.2.1. <i>Preparation of Urine and Plasma Samples</i>	48
3.2.2. <i>Metabolite Detection and Identification</i>	48
3.3. RESULTS	48
3.3.1. <i>Detection and Identification of Metabolites in MMPs</i>	48
3.3.2. <i>Intra-patient Metabolite Detection Study</i>	49
3.4. DISCUSSION.....	55
CHAPTER 4. COMPARISON OF THALIDOMIDE METABOLITE FORMATION IN MICE, RABBITS AND MULTIPLE MYELOMA PATIENTS	58

4.1. INTRODUCTION	58
4.2. METHODS	59
4.2.1. <i>Murine Studies</i>	59
4.2.2. <i>Rabbit Studies</i>	59
4.2.3. <i>Clinical Studies</i>	60
4.2.4. <i>Metabolite Detection and Identification</i>	60
4.3. RESULTS	61
4.3.1. <i>Thalidomide Metabolite Profile in Mice</i>	61
4.3.2. <i>Thalidomide metabolites in rabbits</i>	66
4.3.3. <i>Thalidomide Metabolites in Patients</i>	66
4.4. DISCUSSION	73
CHAPTER 5. IN VITRO METABOLISM OF THALIDOMIDE IN MURINE, RABBIT AND HUMAN LIVER MICROSOMES	75
5.1. INTRODUCTION	75
5.2. METHODS	76
5.2.1. <i>Liver Microsome Preparation</i>	76
5.2.2. <i>Bicinchoninic Acid (BCA) Protein Assay</i>	76
5.2.3. <i>In Vitro Metabolism</i>	77
5.2.4. <i>Detection of Metabolites Formed in vitro</i>	77
5.2.5. <i>Assay of 5-OH Th</i>	78
5.3. RESULTS	79
5.3.1. <i>Detection of Metabolites</i>	79
5.3.2. <i>Relative Abundance of Metabolites</i>	84
5.3.3. <i>Rate of Metabolism of Thalidomide to 5-OH Th</i>	84
5.4. DISCUSSION	96
CHAPTER 6. BIOLOGICAL ACTIVITY OF THALIDOMIDE'S HYDROLYSIS METABOLITES	99
6.1. INTRODUCTION	99
6.2. METHODS	100
6.2.1. <i>Tumour Growth Delay Determinations</i>	100

6.2.2. <i>Modulation of TNF Production in Mice</i>	101
6.2.3. <i>Modulation of TNF Production In vitro</i>	101
6.2.4. <i>TNF Assay</i>	102
6.2.5. <i>Inhibition of Tube Formation In vitro</i>	102
6.2.6. <i>Cytotoxicity Assay</i>	103
6.2.7. <i>Stability and Plasma Concentrations of CG</i>	103
6.2.7.1. <i>Calibration Curves and Quality Controls</i>	103
6.2.7.2. <i>Determination of CG Stability in vitro</i>	104
6.2.7.3. <i>Calculation of Plasma C_{max}, T_{max}, AUC and t_{1/2} of CG in MMPs</i>	104
6.3. RESULTS	105
6.3.1. <i>Potentiation of Anti-tumour Activity of DMXAA in Mice by Thalidomide, PG, PiG and CG</i>	105
6.3.2. <i>Effects of Thalidomide, PG, PiG and CG on DMXAA-Induced TNF Production in Mice</i>	108
6.3.3. <i>Effects of Thalidomide, PG, PiG and CG on LPS-induced TNF Production by HPBL in Culture</i>	108
6.3.4. <i>Inhibition of Tube Formation in Matrigel</i>	112
6.3.5. <i>Stability of CG at Different pHs</i>	112
6.3.6. <i>Plasma concentrations of CG in MMPs</i>	117
6.4. DISCUSSION	119
CHAPTER 7. GENERAL DISCUSSION	121
7.1. INTER-SPECIES DIFFERENCES IN THALIDOMIDE METABOLISM	121
7.2. THE ACTIVE AGENT IN THALIDOMIDE THERAPY	122
7.3. DEVELOPMENT OF CG AS A CLINICAL AGENT	123
APPENDICES	126
APPENDIX 1. CHEMICALS AND REAGENTS	126
APPENDIX 2. PUBLICATIONS DERIVED FROM THIS THESIS	127
REFERENCES	128

LIST OF FIGURES

Figure 1.1	Chemical structures of racemic thalidomide and its stereoisomers.	1
Figure 1.2	A model for the role of TNF in pathophysiology of multiple myeloma (MM). TNF secreted from MM cells induces modest proliferation, as well as MEK/MAPK and NF- κ B activation, in MM cells. It also augments IL-6 secretion, as well as activates MEK/MAPK and NF- κ B, in BMSCs. Importantly, TNF upregulates expression of CD49d (VLA-4), CD11a (LFA-1), and Muc-1 on MM-1S cells, as well as CD54 (ICAM-1) and CD106 (VCAM-1) on BMSCs, which is mediated via NF- κ B activation. Adapted from Hideshima et al., 2001b.	12
Figure 1.3	Possible role of thalidomide on multiple myeloma (MM) cells' and BMSCs' microenvironment <i>in vivo</i> . (A) Thalidomide directly inhibits myeloma cell growth. (B) Thalidomide inhibits MM cell adhesion to BMSCs. (C) thalidomide blocks IL-6, TNF and IL1 β secretion from BMSCs. (D) Thalidomide blocks the ability of VEGF and bFGF to stimulate neovascularisation of bone marrow. (E) Thalidomide induces IL-2 and IFN- γ secretion from T-cells. Adapted from Richardson et al., 2002.	17
Figure 1.4	Hydrolysis pathway of thalidomide (Adapted from Schumacher et al., 1965b).	22
Figure 2.1	UV-detected chromatograms of urine samples from mice without treatment (dotted lines) and up to 4 h following oral administration of thalidomide (Thal) (50 mg/kg, solid lines).	35
Figure 2.2	(A) Total ion MS-detected (Signal 1) chromatogram of urine from mice without treatment (dotted line) and up to 4 h following oral administration of Thal (50 mg/kg, solid line). (B) Mass spectrum of Peak 6 using negative ion-scan mode showing an [M-H] ⁻ mass of 273 amu. (C) Mass spectrum at the retention time corresponding to Peak 6 in untreated mouse urine.	36
Figure 2.3	(A) Negative SIM mode (Signal 3) MS-detected chromatogram of urine from mice without treatment (dotted line) and up to 4 h following p.o. of Thal (50	

mg/kg, solid line). (B) Mass spectrum using negative single-ion monitoring mode of Peak 6 showing a $[M-H]^-$ response of 273 amu. Note: Peaks 5 & 7 also corresponded to $[M-H]^-$ of 273 amu, while Peaks 1 & 4 corresponded to $[M-H]^-$ of 275 amu, Peak 2 corresponded to $[M-H]^-$ of 291 amu and Peak 3 corresponded to $[M-H]^-$ of 449 amu (spectrum not shown).	37
Figure 2.4 LC-MS chromatograms of urine samples from Colon 38 tumour-bearing mice up to 4 h following oral administration of Thal (50 mg/kg). (A) UV-detected chromatogram, and (B) SIM mode (Signal 3) MS-detected chromatogram.	38
Figure 2.5 UV spectra of metabolite peaks (dotted lines) compared with UV spectra of corresponding authentic standards (solid lines). (A) Peak 1 and CG. (B) Peak 5 and <i>cis</i> -5'-OH Th. (C) Peak 6 and <i>trans</i> -5'-OH Th. (D) Peak 7 and 5-OH Th.	39
Figure 2.6 (A) UV-detected chromatogram of Peak 3 following treatment with β -glucuronidase (solid line) and without treatment (dotted line). (B) Mass spectrum of the Peak II formed following β -glucuronidase treatment showing an $[M-H]^-$ mass of 273 amu corresponding to 5-OH Th. (C) Mass spectrum at the retention time corresponding to Peak II in the untreated control.	40
Figure 2.7 HPLC chromatograms using mobile phase containing cetyltrimethylammonium bromide and 1-octanesulfonic acid showing complete separation of: (A) PG and PiG authentic standards; and (B) separation of the Peak 4 fraction from mouse urine into two peaks showing the presence of both PG and PiG.	41
Figure 2.8 Comparison of UV-detected chromatograms of urine from mice administered Thal p.o. (solid line) or i.p. (dotted line).	42
Figure 2.9 Comparison of UV-detected chromatograms of urine (solid line) or plasma (dotted line) from mice given Thal (50 mg/kg) p.o.	43
Figure 2.10 Proposed pathways of biotransformation of thalidomide in mice. Unconfirmed steps or metabolites are shown in dashed lines.	46
Figure 3.1 LC-MS chromatograms of urine from MMP1 on Thal therapy (100 mg/day, solid lines) and from a healthy volunteer (dotted lines) recorded by: (A) UV at 230 nm, (B) MS at negative TIC mode (Signal 1), (C) MS at positive SIM mode (Signal 2), (D) MS at negative SIM mode (Signal 3).	50

Figure 3.2	UV chromatograms of urine samples of MMPs on thalidomide therapy (solid lines) and before treatment (dotted line). A-F correspond to Patients 2-7 respectively.....	51
Figure 3.3	HPLC chromatograms using mobile phase containing cetyltrimethylammonium bromide and 1-octanesulfonic acid showing complete separation of: (A) PG and PiG authentic standards; and (B) separation of the Peak 4 fraction from MMPs' urine into two peaks showing the presence of both PG and PiG.	52
Figure 3.4	UV chromatograms of urine samples of Patient 1 collected on three occasions after Thal therapy. (A) one month, (B) two months, (C) three months.	53
Figure 3.5	Comparison of UV-detected chromatograms of urine (solid lines) or plasma (dotted lines) from (A) mice given Thal (50 mg/kg, p.o.); and (B) patient 1 approximately 15 h after a prior dose of Thal (100 mg/day p.o.).	54
Figure 4.1	Chromatograms of urine from mice without treatment (dotted lines) and up to 4 h following oral administration of Thal (2 mg/kg, solid lines) recorded by: (A) UV at 230 nm, (B) MS at negative TIC mode (Signal 1), (C) MS at positive SIM mode (Signal 2), (D) MS at negative SIM mode (Signal 3).....	62
Figure 4.2	Negative SIM mode (Signal 3) MS-detected chromatograms of mouse plasma samples collected before (dotted lines) and after (solid lines) p.o. treatment of Thal (2 mg/kg). (A) 5 min, (B) 30 min, (C) 4 h.	64
Figure 4.3	Negative SIM mode (Signal 3) MS-detected chromatograms of mouse plasma samples collected before (dotted lines) and after (solid lines) i.v. treatment of Thal (2 mg/kg). (A) 1 h, (B) 2 h, (C) 4 h.....	65
Figure 4.4	Negative SIM mode (Signal 3) MS-detected chromatograms of rabbit plasma samples collected before (dotted lines) and after p.o. treatment (solid lines). (A) 30 min, (B) 2h, (C) 6 h.....	67
Figure 4.5	Negative SIM mode (Signal 3) MS-detected chromatograms of rabbit urine samples collected before (dotted lines) and after treatment (solid lines). (A) 3 h after p.o. administration, (B) 3 h after i.v. injection.	68
Figure 4.6	Negative SIM mode (Signal 3) MS-detected chromatograms of rabbit plasma samples collected before (dotted lines) and after i.v. treatment (solid lines). (A) 30 min, (B) 2h, (C) 4 h.....	69

Figure 4.7	Negative SIM mode (Signal 3) MS-detected chromatograms of MMP plasma samples collected before (dotted lines) and after treatment (solid lines). (A) 1 h, from MMP 8, (B) 4 h, from MMP 10, (C) 24 h, from MMP 11.	70
Figure 4.8	Negative SIM mode (Signal 3) MS-detected chromatograms of MMP 12 urine samples collected before (dotted lines) and after treatment (solid lines). (A) 4 h, (B) 8 h, (C) 24 h.	71
Figure 4.9	Thalidomide metabolism by hydrolysis (arrows with dashed lines) and CYP hydroxylation and UDPG transferase-mediated glucuronidation (arrows with solid lines) in mice, rabbits and MMPs. Unconfirmed metabolites are shown in dotted lines. Structures in bold are products formed via hydrolysis only. Numbers in brackets represent metabolite peak number in chromatograms.	72
Figure 5.1	LC-MS chromatograms of Thal metabolites following incubation (60 min; 37°C) of Thal (400 µM) with liver microsomes (solid lines) of (A) human HL18, (B) rabbits and (C) mice, or with boiled liver microsomes (dotted lines). Metabolites were detected by SIM mode (Signal 3) of MS as described in methods.	81
Figure 5.2	HPLC chromatograms with UV detection of Thal metabolites following incubation (60 min; 37°C) of Thal (400 µM) with (A) human HL18, (B) rabbits and (C) mice liver microsomes (solid lines), or with boiled liver microsomes (dotted lines).	82
Figure 5.3	LC-MS chromatograms with UV (A) or MS negative SIM (B) detection of Thal metabolites following incubation (60 min; 37°C) of Thal (400 µM) with 2 mg/ml human HL5 liver microsomes.	83
Figure 5.4	Enzymatic hydrolysis of PiG by rabbit liver microsomal protein in the presence of NADPH (4mM).	88
Figure 5.5	Concentration of 5-OH Th with different microsomal protein concentrations after incubating 400 µM of thalidomide with mouse, rabbit and human liver microsomes for 60 min.	90
Figure 5.6	Concentration of 5-OH Th at different times after incubating 400 µM of thalidomide with 2 mg/ml of mouse, rabbit and human liver microsomes.	91

Figure 5.7	HPLC chromatograms showing complete separation of cis-5'-OH Th, trans-5'-OH Th, 5-OH Th, Phencacetin and Thal using UV detection at (A) 220 nm or (B) 248 nm.	92
Figure 5.8	Formation of 5-OH Th in rabbit and mouse liver microsomes following incubation with Thal.....	93
Figure 5.9	Lineweaver-Burk plots of thalidomide 5-hydroxylation by rabbit and mouse liver microsomes	94
Figure 5.10	Eadie-Hofstee plots of thalidomide 5-hydroxylation by rabbit and mouse liver microsomes	95
Figure 6.1	Tumour growth delay in mice untreated, or treated with DMXAA or DMXAA combined with Thal or hydrolysis products/metabolites of Thal.....	106
Figure 6.2	Colon 38 tumour volumes 21 days after treatment in mice. “*” represents significant difference ($p < 0.05$, student's <i>t</i> -test) compared with DMXAA alone treatment.....	107
Figure 6.3	TNF levels in (A) serum and (B) tumour tissue of mice untreated, or treated with DMXAA alone or DMXAA combined with Thal or hydrolysis products/metabolites of Thal. “*” represents significant difference ($p < 0.05$, student's <i>t</i> -test) compared with DMXAA alone treatment.....	109
Figure 6.4	TNF production by HPBL from seven healthy volunteers at different concentrations of LPS.	110
Figure 6.5	The effect of Thal, CG, PG or PiG on LPS-induced TNF production by HPBL from healthy human volunteers. (A) average TNF activity, (B) average percentage of inhibition.....	111
Figure 6.6	Effects of Thal, CG, PG and PiG on tube formation of ECV 304 cells in Matrigel. Cells were treated with medium only, medium with vehicle only and indicated concentrations of drugs.....	113
Figure 6.7	Inhibition of the tube formation of ECV 304 cells in Matrigel by Thal and CG at different concentrations.	114
Figure 6.8	HPLC chromatograms showing complete separation of CG, phenacetin and Thal at wavelength of (A) 220 nm or (B) 248 nm.....	115

Figure 6.9 CG and Thal concentrations in PBS solutions at different pH during 24 h of incubation at 37 °C.	116
Figure 6.10 Plasma concentration-time profiles of CG (from samples of three MMPs) compared with that of thalidomide (redrawn from Chung et al., 2004a) after the treatment of 200 mg oral dose fo thalidomide	118
Figure 7.1 Proposed analogues of CG.	125

LIST OF TABLES

Table 1.1	List of diseases in which thalidomide has been trialed.	3
Table 1.2	Pharmacokinetic parameters of orally administered (<i>R</i> -, <i>S</i> -)-racemic-thalidomide (unless stated otherwise).	19
Table 2.1	Metabolite peaks in UV profiles from murine urine following thalidomide treatment.	34
Table 3.1	Comparison of metabolites in mouse and MMP urine samples.	57
Table 4.1	Metabolite peaks in mouse urine LC-MS profiles after thalidomide oral treatment.	63
Table 5.1	Metabolite formed after incubating thalidomide with mouse and rabbit liver microsomes.	80
Table 5.2	Comparison of relative levels of hydroxylated metabolites formed following a 60 min incubation of Thal with liver microsomal protein (2 mg/ml). Metabolites were determined by mass spectral detection using single ion monitoring. The response of each metabolite peak produced by mouse liver microsomes was normalized to 1.	86
Table 5.3	Comparison of relative levels of hydrolysis products formed following a 60 min incubation of Thal with liver microsomal protein (2 mg/ml). Hydrolysis products were determined by mass spectral detection using single-ion monitoring. The response of each peak produced by mouse liver microsomes was normalized to 1. ..	87
Table 5.4	Comparison of the total products of hydrolysis and hydroxylation formed following a 60 min incubation of Thal with liver microsomal protein (2 mg/ml).	89
Table 6.1	Comparison of PK parameters of CG and Thal in MMPs.	117

LIST OF ABBREVIATIONS

5-OH Th	5-hydroxythalidomide
5'-OH CG	5'-hydroxy- <i>N</i> -(<i>o</i> -carboxybenzoyl)glutamic acid imide
5'-OH Th	5'-hydroxythalidomide
α -MEM	α -minimal essential medium
μ g	microgram
μ l	microlitre
μ M	micromolar
ACN	acetonitrile
amu	atomic molecular unit
APCI	atmospheric pressure chemical ionisation
AU	arbitrary unit(s)
AUC	area under the concentration-time curve
bFGF	basic fibroblast growth factor
BMSC	bone marrow stromal cell
C _{max}	maximal drug concentration following administration
CG	<i>N</i> -(<i>o</i> -carboxybenzoyl)glutamic acid imide
CL _{int}	intrinsic clearance
Cox	cyclooxygenase
Cl/F	apparent clearance rate
CV	coefficient of variation
CYP	cytochrome P450 enzymes
DMSO	dimethylsulphoxide
DMXAA	5,6-dimethylxanthenone-4-acetic acid
ELISA	enzyme linked immunosorbent assay
FBS	fetal bovine serum
g	gram
<i>g</i>	gravity
h	hour

HCl	hydrochloric acid
HIV	human immunodeficiency virus
HPBL	human peripheral blood leucocytes
HPCD	2-hydroxypropyl- β -cyclodextrin
HPLC	high performance liquid chromatography
HUVEC	human umbilical vein endothelial cell
ICAM	intercellular cell adhesion molecule
IFN	interferon
IGF	insulin-like growth factor
IL	interleukin
i.p.	intraperitoneal
i.v.	intravenous
KCl	potassium chloride
K_M	Michaelis-Menten constant
kg	kilogram
LC-MS	liquid chromatography-mass spectrometry
LPS	lipopolysaccharide
mAU	milli arbitrary unit(s)
mg	milligram
min	minute
ml	milliliter
mM	millimolar
MMP	multiple myeloma patient
MRI	magnetic resonance imaging
MS	mass spectrometry
MSD	mass spectral detection
MTT	3-(4,5-dimethylthiazol-2-yl)-2,5-diphenyl tetrazolium bromide
NADPH	β -nicotinamide adenine dinucleotide phosphate reduced form
NF- κ B	nuclear factor- κ B
NMR	nuclear magnetic resonance
PBS	phosphate buffered saline

PG	phthaloylglutamine
PiG	phthaloylisoglutamine
p.o.	oral
SEM	standard error of mean
SIM	single ion monitoring
$t_{1/2}$	drug half-life
T_{\max}	time when C_{\max} is achieved
TCA	trichloroacetic acid
Thal	thalidomide
TIC	total ion current
TNF	tumour necrosis factor- α
UDPG	uridine diphosphate glucuronide
UDPG-transferase	uridine diphosphate glucuronosyl transferase
UV	ultraviolet
V	velocity of the reaction
V_{\max}	maximum velocity of the reaction
V/F	volume of distribution
v/v	volume/volume
VCAM	vascular cell adhesion molecule
VEGF	vascular endothelial growth factor

CHAPTER 1. GENERAL INTRODUCTION

1.1. The History of Thalidomide and Its Role in Cancer Therapy

Thalidomide (*N*- α -phthalimidoglutarimide, Thal, Figure 1.1), contains a phthalimide ring and a glutarimide ring. It has a chiral centre from a single asymmetric carbon in the glutarimide ring. Thalidomide is usually used as a racemic mixture of dextrorotatory (*R*) and levorotatory (*S*) forms in a ratio of 1:1 (Figure 1.1).

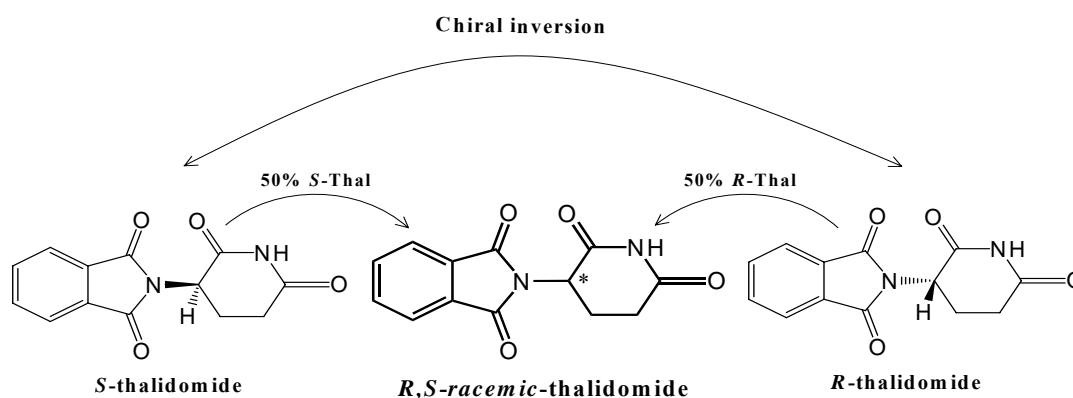


Figure 1.1 Chemical structures of racemic thalidomide and its stereoisomers.

The chemical formula of thalidomide is $C_{13}H_{10}N_2O_4$, and it has a molecular weight of 258.23. It is an off-white to white crystalline powder with a melting point of $275-7^\circ\text{C}$ (Schumacher et al., 1965b). It is poorly soluble in water and ethanol with a maximum aqueous solubility of around $50\text{ }\mu\text{g/ml}$ (Krenn et al., 1992), and undergoes rapid non-enzymatic hydrolysis with increasing pH (Schumacher et al., 1965b; Boughton et al., 1995; Huupponen and Pyykko, 1995; Lyon et al., 1995). Thalidomide was first

synthesized in 1953 by the Swiss pharmaceutical company Ciba, who did not continue with its development because of apparent lack of pharmacologic effects (Randall, 1990). However, the German company Chemie Grunenthal, re-synthesized the drug in 1954, and developed it as an anticonvulsant for the treatment of epilepsy (Zwingenberger and Wnendt, 1996). Thalidomide proved ineffective for this purpose, but it was found to cause deep sleep promptly and without any hangover effects. Nor did it show any acute toxicity even at large doses (Somers, 1960). Thalidomide was subsequently remarketed as a sedative and tranquilizer in 1956 and soon became the most widely used sleeping pill in Germany (Zwingenberger and Wnendt, 1996). By the end of the 1950s, 14 pharmaceutical companies were marketing thalidomide in 46 countries. Approval in the United States was delayed however by the Food and Drug Administration (FDA) because of concerns over neuropathy (Fullerton and Kremer, 1961; Kelsey, 1988; Randall, 1990).

In 1961, both Lenz and McBride simultaneously warned of a probable association between the use of thalidomide and the escalation of the number of cases of phocomilia and other congenital abnormalities (McBride, 1961; Lenz, 1962), and thalidomide was quickly withdrawn from the German and other world markets (Zwingenberger and Wnendt, 1996). In 1965, Sheskin (1965) reported that thalidomide was effective in treating erythema nodosum leprosum (ENL), an acute complication associated with leprosy. That serendipitous discovery by Sheskin renewed interest in thalidomide, and since then, it has been trialed for the treatment of numerous diseases (summarized in Table 1.1).

In 1965, thalidomide was demonstrated to reduce the growth of 7,12-dimethylbenzanthracene-induced tumours in rats (Muckter, 1965; Muckter and More, 1966), but the clinical results reported in the same year using thalidomide in cancer patients were inconclusive (Grabstald and Golbey, 1965; Olson et al., 1965). It was not until 1994 that interest in thalidomide for cancer treatment was renewed following a report that thalidomide was an inhibitor of angiogenesis (D'Amato et al., 1994). Subsequently, thalidomide has been trialed for the treatment of a number of human cancers. The most outstanding results have come from trials for the treatment of refractory and relapsed multiple myeloma, where response rates of over 30% have been reported (Larkin, 1999; Singhal et al., 1999). To date, thalidomide has been trialed

against many types of cancers and has been developed as second-line or salvage treatment of multiple myeloma (Streicher et al., 2003). Despite its clinical success, its anti-cancer mechanism is not completely understood. Nor is it clear as to whether the parent drug or one of its metabolites is the active agent.

Table 1.1 List of diseases in which thalidomide has been trialed.

Literature	Disease
Sheskin, 1965	ENL
Londono, 1973	Actinic prurigo
Grosshans and Illy, 1984	Behcet's syndrome
Gutierrez-Rodriguez, 1984	Rheumatoid arthritis
Vogelsang et al., 1988	Graft-versus-host disease
Johnke and Zachariae, 1993	Prurigo nodularis
Carlesimo et al., 1995	Sarcoidosis
Minor and Piscitelli, 1996; Reyes-Teran et al., 1996	Cachexia
Jacobson et al., 1997	Aphthous ulcers
Wettstein and Meagher, 1997	Crohn's disease
Stevens et al., 1997	Lupus erythematosus
Fife et al., 1998	AIDS-related Kaposi's sarcoma
Breban et al., 1999	Ankylosing spondylitis
Figg et al., 1999; Eisen, 2000; Fine et al., 2000	Solid tumours
Larkin, 1999; Singhal et al., 1999; Rajkumar et al., 2000a	Multiple myeloma
Parentin et al., 2001	Uveitis
Barosi et al., 2001; Dimopoulos et al., 2001b; Raza et al., 2001; Steins et al., 2002	Other hematologic malignancies
Agoston et al., 2002; Gullestad et al., 2002	Heart failure
Gupta et al., 2003	plexiform neurofibroma

1.2. Thalidomide as an Anti-cancer Agent

1.2.1. Pre-clinical Studies

The early interest in thalidomide as an anti-cancer agent began following reports that it was a teratogen (McBride, 1961; Lenz, 1962). Because of its teratogenicity, it was considered to be cytostatic and was tested against a wide variety of animal tumour models, but the results were not encouraging (reviewed by De and Pal, 1975). After the demonstration by D'Amato and co-workers that thalidomide is an inhibitor of angiogenesis in 1994, the interest of thalidomide in pre-clinical studies was renewed. However, thalidomide does not show any anti-tumour activity as a single agent in the majority of murine and rat tumour models. Ching and co-workers showed that daily intraperitoneal (i.p.) injection of thalidomide at 100 mg/kg did not inhibit the growth of the implanted Colon 38 tumour in C57Bl/6 mice (Ching et al., 1995). Gutman and co-workers demonstrated that daily oral (p.o.) administration of 0.3-1.0 mg thalidomide did not inhibit the growth of implanted B16-F10 melanoma and CT-26 colon carcinoma cells in mice (Gutman et al., 1996). Similarly, negative results have been reported using murine SCCVII and Lewis Lung tumours models (Minchinton et al., 1996). One report even showed that thalidomide promoted metastasis of prostate adenocarcinoma in the L-W rat model (Pollard, 1996). Myoung and co-workers studied a melanoma model in nude mice, and although there was no tumour growth inhibition, vascular endothelial growth factor (VEGF) expression was significantly decreased (Myoung et al., 2001). Activity has been reported against implanted human esophageal cancers in nude mice, however. Daily thalidomide i.p. treatment at 200mg/kg/day lowered microvessel density and inhibited tumour growth (Kotoh et al., 1999). Tumour growth delay has also been shown in severe combined immuno-deficient mice implanted with human multiple myeloma (Lentzsch et al., 2002), and in a syngeneic C6 glioma rat model (Arrieta et al., 2002). In general, thalidomide does not show potent anti-tumour effects in rodents. In rabbits, there is a single report of p.o. treatment with thalidomide at 200 mg/kg/day causing a reduction in tumour volume, and tumour microvessel density in V2 carcinomas (Verheul et al., 1999). Belo and co-workers studied the anti-angiogenic effect of thalidomide in sponge-induced granulomatous tissue and implanted solid Ehrlich tumour in Swiss mice. They demonstrated that

thalidomide inhibited sponge-induced angiogenesis but not tumour angiogenesis. They concluded that the anti-angiogenic effect of thalidomide is tissue-specific rather than species-specific (Belo et al., 2001).

In view of the poor activity as a single agent, combination studies involving thalidomide and other clinical or novel anti-cancer agents were explored and found to be more effective. For example, mice treated with thalidomide combined with cyclophosphamide or adriamycin had significantly smaller tumours than those given the two chemotherapeutic agents alone in a mouse model of breast cancer (Nguyen et al., 1997). Thalidomide combined with the anti-cancer drug 5,6-dimethylxanthenone-4-acetic acid (DMXAA) also exhibited higher cure rates and longer growth delays than DMXAA alone against implanted Colon 38 tumour in mice (Ching et al., 1999). In another study, co-administration of thalidomide (100 mg/kg) with cyclophosphamide (220 mg/kg) cured mice of their transplanted Colon 38 tumours, compared with cyclophosphamide alone which induced growth delays of only 11-13 days with no cures (Ding et al., 2002).

1.2.2. Clinical Studies

1.2.2.1. Thalidomide in Solid Tumours

The demonstration that thalidomide inhibits angiogenesis (D'Amato et al., 1994) and reduces microvessel density of tumour in animal models (Kotoh et al., 1999), led to its clinical trials in solid tumours. In the treatment of renal cell carcinoma, Stebbing and co-workers reported that 2 out of 22 patients (9%) taking thalidomide at 200 mg/day had stable disease for over 12 months, and 5 patients (23%) had stable disease for 6-12 months (Stebbing et al., 2001). Another report showed 16 out of 26 patients (62%) with renal carcinoma had stable disease for 6 months (Motzer et al., 2002). Fine and co-workers evaluated thalidomide efficacy in 37 patients with malignant gliomas. They found 2 patients (6%) had over 50% tumour size reduction using magnetic resonance imaging (MRI) and 12 (32%) had stable disease (Fine et al., 2000). Figg and co-workers conducted a Phase II study in patients with androgen-independent prostate cancer who had failed to respond to previous therapy. They reported that 18% of patients who took thalidomide 200 mg daily had a decrease of over 50% in prostate-

specific antigen level, with the overall median survival being 15.8 months (Figg et al., 2001). Thalidomide has also been trialed in Kaposi's sarcoma, an oncologic condition associated with human immunodeficiency virus (HIV) infection. Fife and co-workers reported that 6 of 17 patients (35%) who took a daily dose of thalidomide at 100 mg achieved a partial response, and 4 (24%) had stable disease (Fife et al., 1998). Another report involving 20 patients with Kaposi's sarcoma showed 8 patients achieved partial response and 2 had stable disease (Little et al., 2000). In the clinical trial of colorectal carcinoma, Govindarajan presented reports that irinotecan combined with thalidomide (400 mg/day) achieved a complete response in 2 out of 20 patients (10%), partial responses in 4 patients (20%), while 5 (25%) had stable disease (Govindarajan, 2000, 2002). Hsu and co-workers conducted a clinical trial on 68 patients with unresectable hepatocellular carcinoma using thalidomide at doses of 200-300 mg/day. One patient had a complete response and 3 had partial responses. Another 6 patients had a more than 50% decrease in their alpha-FP levels. The median overall survival for all of the 68 patients was 18.7 weeks with a 1-year survival rate of 27.6%. The median overall survival of the 10 patients with an objective response to thalidomide was 62.4 weeks (Hsu et al., 2003). Thalidomide also achieved long-term survival in a patient suffering from small-cell lung cancer (Mall et al., 2002). On the other hand, thalidomide as a single agent in advanced melanoma, ovarian carcinoma, breast cancer, and squamous cell carcinoma of the head and neck clinical trials has failed to provide any beneficial effects (Baidas et al., 2000; Eisen, 2000; Tseng et al., 2001). Since thalidomide alone only produced marginal benefit in many types of solid tumours, more clinical studies tried to combine thalidomide with other anti-cancer agents and the combination therapy showed more effectiveness in treating solid tumours (Singhal and Mehta, 2002).

1.2.2.2. Thalidomide in Haematological Malignancies

Based on the demonstration that multiple myeloma has an increased bone marrow microvasculature which is associated with disease progression (Vacca et al., 1994; Vacca et al., 1995; Vacca et al., 1999), thalidomide entered clinical trial as an anti-angiogenic agent for multiple myeloma. Singhal and co-workers were among the first to investigate thalidomide in multiple myeloma, and they conducted a study using thalidomide as a single agent in 84 patients with advanced and refractory multiple

myeloma. Thalidomide was initiated at a daily dose of 200 mg, and the dose was increased by 200 mg every 2 weeks to a maximum of 800 mg/day if tolerated. Eighty-three percent of the patients achieved a dose of 400 mg/day, 62% achieved 600 mg/day and 47% reached 800 mg/day. Response was defined in terms of decreases in serum and urine paraprotein levels of at least 25%, 50%, 75% and 90% on 2 occasions at least 6 weeks apart. A complete response was defined as the finding of less than 5% plasma cells in the biopsy specimen or aspirate. After 12 months of follow-up, the study reported that 2 patients had a complete remission, 6 had at least 90% reduction in paraprotein levels, another 6 had at least 75% reduction, 7 had at least 50% reduction and 6 had at least 25% reduction. The rates of total response, event-free survival and overall survival were 32%, $22 \pm 5\%$ and $58 \pm 5\%$, respectively. There was no statistical difference in bone marrow microvessel density between responders and non-responders, however, although responding patients had a reduction in bone marrow plasmacytosis and serum β_2 -microglobulin concentrations and an increase in hemoglobin levels (Singhal et al., 1999).

Following this landmark report, thalidomide has entered a number of clinical trials in which most of the patients have refractory or relapsed multiple myeloma. Barlogie and co-workers continued the preceding study and increased patient numbers to 169. Over a median follow-up of 22 months, they reported an overall response rate of 37% and a complete and near-complete remission rate of 14%. They also found that patients receiving more than 42 g of thalidomide in 3 months had higher response rate and longer survival time (Barlogie et al., 2001a). A French group also reported a dose-response relationship of thalidomide in a trial with 83 patients. They reported an overall response rate of 66%, and patients who received 34.4 g or over of thalidomide in the first 90 days of treatment had a better outcome than those who received less than 34.4 g (Yakoub-Agha et al., 2000; Yakoub-Agha et al., 2002). However, Larkin reported that low-doses (50-400 mg/day) of thalidomide were effective and recorded a 24% response rate in 33 patients (Larkin, 1999). Leleu and co-workers have reported similar observation, where thalidomide showed efficacy at the same dose range (Leleu et al., 2002). Wechalekar and co-workers further demonstrated that thalidomide at a dose of 200 mg/day was as effective as higher doses and less toxic in a clinical trial where 43% of 30 patients responded (Wechalekar et al., 2003). Juliusson and co-workers trialed 23 patients with doses of 200 – 800 mg/day in Sweden, and reported a 43% response rate

(Juliussen et al., 2000). Rajkumar and co-workers from the Mayo Clinic studied 16 patients treated with a dose range of 200 – 800 mg/day, and found all the responses occurred between doses ranging from 200 – 400 mg/day and could be sustained with doses as low as 100 mg/day. The overall response rate was 31% in that study (Rajkumar et al., 2000a). Another later report from Mayo Clinic assessed 32 patients with a dose range of 200 – 800 mg/day. The overall response rate of that study was 53% and the median overall survival for the entire group was 22 months after a median follow-up of 18.7 months (Kumar et al., 2003). Tosi and co-workers studied 65 patients in Italy with a dose range of 100 – 800 mg/day and reported that the total response rate was 46.6%. Among those responding patients, 15 are alive and progression-free after a median follow-up of 9 months. They also studied cytokine secretion in 24 patients and found that VEGF secretion by bone marrow plasma cells was significantly lower in responders compared with non-responders (Tosi et al., 2002). Dmoszynska and co-workers studied 30 patients with a dose of 400 mg/day in Poland and reported an overall response rate of 60%. They also found that the concentrations of cytokines such as VEGF, basic fibroblast growth factor (bFGF), interleukin-6 (IL-6) and tumour necrosis factor- α (TNF), were significantly lower in both bone marrow and peripheral blood in responders than non-responders after 4-8 weeks of thalidomide treatment (Dmoszynska et al., 2002). In another trial in Germany, Neben and co-workers studied 83 patient over 2 years and found no difference in plasma levels of cytokines, including VEGF, bFGF, IL-6 and TNF, between responders and non-responders or before and after treatment in 51 patients studied (Neben et al., 2001). The dose of thalidomide in that study was 100 to 400 mg/day and the 12-month progression-free survival and overall survival rates were 45% and 86%, respectively. They analysed all factors that may be related to overall survival rate and found that the high cumulative initial 3-month thalidomide dosage is one of the major prognostic factors in predicting better responses (Neben et al., 2002a). Li and co-workers treated 28 patients and analysed their plasma VEGF and bFGF levels as well as the expressions of intercellular cell adhesion molecule-1 (ICAM-1) and vascular cell adhesion molecule-1 (VCAM-1) of bone marrow stromal cells (BMSCs). They found VEGF and bFGF levels were higher after treatment than before treatment, while ICAM-1 and VCAM-1 were significantly lower after treatment in responders, but were not changed in non-responders (Li et al., 2003). Thompson and co-workers studied bone marrow microvessel density and plasma

levels of VEGF, bFGF, IL-6, IL-8 and TNF in 38 patients with previously untreated multiple myeloma. They found there was no difference in microvessel density and plasma cytokines levels before and after treatment. However, higher pre-treatment TNF level and increased IL-6 level after treatment predicted worse progression-free survival (Thompson et al., 2003).

Thalidomide also has been combined with other agents to treat multiple myeloma. The combination of thalidomide/dexamethasone is the most commonly used. This combination enhances the overall response rate of thalidomide generally from over 30% to over 50% (Rajkumar et al., 2000b; Barlogie et al., 2001b; Dimopoulos et al., 2001a; Palumbo et al., 2001; Tosi et al., 2001; Rajkumar et al., 2002). Weber and co-workers compared the efficacies of thalidomide alone and thalidomide combined with dexamethasone in 69 patients with previously untreated multiple myeloma. Twenty-nine patients were treated by thalidomide alone with a doses ranging from 150 to 600 mg/day and the remaining forty patients were treated with thalidomide (150 – 400 mg/day) plus dexamethasone (20 mg/m² for 4 days and repeated twice in 3 months). Disease remission was noted in 36% of patients with thalidomide alone but reached 72% with combination therapy (Weber et al., 2003). Thalidomide has also been combined with cisplatin, cyclophosphamide, etoposide, doxorubicin, vincristine, melphalan and clarithromycin (Biaxin), and some of those combinations showed better response rate than thalidomide alone (Barlogie et al., 2001b; Moehler et al., 2001; Coleman et al., 2002; Garcia-Sanz et al., 2002; Srkalovic et al., 2002; Hussein, 2003; Lee et al., 2003; Offidani et al., 2003).

Thalidomide has also been used as a single agent at a dose of 200 mg/day in 16 patients with previously untreated smoldering or indolent multiple myeloma, and 38% patients had clear responses with at least 50% reduction in serum and urine monoclonal protein. The total response rate was 69% (Rajkumar et al., 2001).

Following the clinical success in multiple myeloma, thalidomide has been used in many trials to treat other haematologic malignancies. It has been shown to have therapeutic effects in Waldenstrom's macroglobulinemia either used alone or combined with clarithromycin (Dimopoulos et al., 2001b; Coleman et al., 2002). Thalidomide also showed beneficial effects in clinical trials of myelodysplastic syndromes (Raza et al.,

2001; Strupp et al., 2002), acute myeloid leukemia (Steins et al., 2002), myelofibrosis with myeloid metaplasia (Barosi et al., 2001; Elliott et al., 2002) and acute leukemia (Wang et al., 2003).

The common adverse effects of thalidomide are teratogenicity, peripheral neuropathy (Fullerton and Kremer, 1961), sedation, deep vein thrombosis (Osman et al., 2001), severe toxic epidermal necrolysis (Horowitz and Stirling, 1999) and hypertension (Stirling, 1998). As little as one single dose of thalidomide at 27-40 days of gestation may cause teratogenicity in humans (Mellin and Katzenstein, 1962; Neubert and Neubert, 1997). However, the risk is manageable through education and strict use of contraceptives. Other adverse effects are manageable, not life-threatening or rare.

The exact mechanism of action of thalidomide in the treatment of cancer is still under investigation, and a number of hypotheses as summarised in the next section have been proposed.

1.3. Mechanism of Action in Cancer Treatment

1.3.1. Anti-angiogenesis

D'Amato et al. (1994) demonstrated that thalidomide could inhibit angiogenesis in the cornea of rabbits implanted with bFGF. Bauer and co-workers co-cultured rat aortic rings with thalidomide in the presence of microsomes from rabbits or humans and found improved anti-angiogenesis, while rat microsomes showed negative results. They therefore suggested that the anti-angiogenic activity of thalidomide required species-dependent metabolic activation (Bauer et al., 1998). However, the corneal anti-angiogenesis assay has been performed both in rabbits (Kruse et al., 1998; Jousen et al., 1999), and in mice, a species thought to be incapable of producing active thalidomide metabolites (Bauer et al., 1998), using bFGF and VEGF as inducers (Kenyon et al., 1997). The mechanism of thalidomide's anti-angiogenesis is not fully understood. It is thought thalidomide inhibits the production of angiogenic cytokines, such as bFGF and VEGF, to inhibit endothelial cell proliferation (Kruse et al., 1998). However, a recent report showed thalidomide inhibited tube formation of human

umbilical vein endothelial cells (HUVECs) in Matrigel but did not affect their proliferation (Ng et al., 2003).

Although thalidomide entered clinical trials for multiple myeloma as an anti-angiogenic agent (Singhal et al., 1999), a decrease in microvessel density was not observed in patients who were responding to thalidomide therapy (Singhal et al., 1999; Thompson et al., 2003), suggesting thalidomide may act through other mechanism apart from anti-angiogenesis.

1.3.2. Cytokine Modulation

Thalidomide has the ability to modulate the biosynthesis of a number of cytokines, which is thought to provide the basis for its biological effects, including anti-tumour and anti-inflammation activities. However, the exact target or receptor of thalidomide is not yet identified. Thalidomide reduces elevated levels of TNF in patients with ENL (Sampaio et al., 1991) and HIV-infected patients with tuberculosis (Klausner et al., 1996). A decrease in plasma and bone marrow concentrations of bFGF, VEGF, TNF and IL-6 in multiple myeloma patients (MMPs) responding to thalidomide treatment compared with non-responders has been reported (Dmoszynska et al., 2002). Another clinical trial showed a decrease of IL-6 in plasma and bone marrow in MMPs after thalidomide treatment compared with pre-treatment (Li et al., 2002). It is also reported that polymorphism of the promoter for the TNF gene was associated with response of thalidomide therapy, indicating that genetically-defined high TNF producers have better clinical responses (Neben et al., 2002b). Another recent clinical report demonstrated that altered expression of cytokine genes was necessary in order for thalidomide to achieve its therapeutic effect in MMPs (Zhang et al., 2003).

The most notable effect of thalidomide on cytokine production is that it decreases lipopolysaccharide (LPS)-induced TNF production in human monocytes and macrophages *in vitro* (Sampaio et al., 1991; Rowland et al., 1998). It has been shown that thalidomide has the ability to enhance the degradation of TNF messenger RNA (mRNA), thus inhibiting TNF production (Moreira et al., 1993). Turk and co-workers showed that photo-affinity labelled thalidomide bound to α_1 -acid glycoprotein, which

is a regulator of the immune system and in inflammation, *in vitro* in bovine thymus tissues. Thalidomide-bound α_1 -acid glycoprotein inhibited TNF production of human monocytes. They suggested that the binding of thalidomide to α_1 -acid glycoprotein caused down-regulation of TNF production (Turk et al., 1996). TNF is regarded as a survival and proliferation factor for human myeloma cells (Jourdan et al., 1999; Hideshima et al., 2001a), and inhibition of TNF may restrict tumour growth and cause tumour cell death. Furthermore, thalidomide's ability to modulate TNF production may have indirect effects on the myeloma/BMSC microenvironment (Figure 1.2) (Hideshima et al., 2001b) to inhibit the localization and growth of multiple myeloma cells.

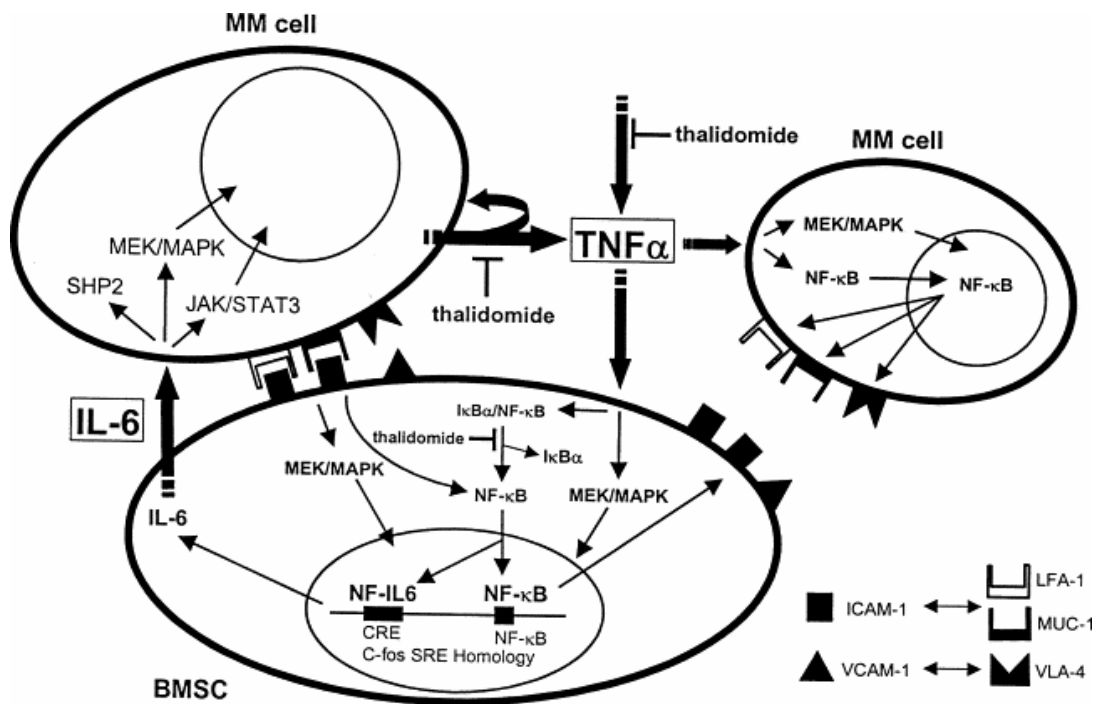


Figure 1.2 A model for the role of TNF in pathophysiology of multiple myeloma (MM). TNF secreted from MM cells induces modest proliferation, as well as MEK/MAPK and NF- κ B activation, in MM cells. It also augments IL-6 secretion, as well as activates MEK/MAPK and NF- κ B, in BMSCs. Importantly, TNF upregulates expression of CD49d (VLA-4), CD11a (LFA-1), and Muc-1 on MM-1S cells, as well as CD54 (ICAM-1) and CD106 (VCAM-1) on BMSCs, which is mediated via NF- κ B activation. Adapted from Hideshima et al., 2001b.

Thalidomide also has the ability to modulate the production of other cytokines, such as IL-1 β , IL-2, IL-4, IL-5, IL-6, IL-8, IL-10, IL-12, interferon-gamma (IFN- γ), bFGF and VEGF (Zwingerberger and Wnendt, 1996; Haslett et al., 1997; Kenyon et al., 1997; Moller et al., 1997; Hallek et al., 1998; Rowland et al., 1998; Corral et al., 1999; Dunzendorfer et al., 1999; Haslett et al., 1999; Bekker et al., 2000; Shannon et al., 2000; Verbon et al., 2000). Moraes and co-workers showed that the inhibition of cytokines, such as IFN- γ , IL-6, IL-10 and IL-12 p40, by thalidomide is also linked with mRNA degradation (Moraes et al., 2000). IL-6 is considered a potent growth factor for malignant plasma cells (Anderson et al., 1989; Bataille et al., 1989; Nilsson et al., 1990), and its inhibition is likely to affect tumour cell growth and survival. VEGF and bFGF are regarded as cytokines related to tumour angiogenesis (Kruse et al., 1998; Bellamy et al., 1999), and the inhibition of those cytokines is considered to be the cause of anti-angiogenesis in tumours and suppress tumour growth (Podar et al., 2001). The enhanced secretion of IFN- γ and IL-2 can induce T-cell response to act against tumours (Haslett et al., 1998). More recently, a report demonstrated that thalidomide was able to decrease the stability of cyclooxygenase-2 (Cox-2) mRNA and thus inhibit LPS-mediated Cox-2 induction in murine macrophage culture; providing basis for its anti-inflammatory and anti-neoplastic properties (Fujita et al., 2001).

In addition to mRNA degradation and Cox-2 inhibition, thalidomide may modulate cytokine production via damaging DNA. Based on the observation that thalidomide binds to DNA in animals (Schumacher et al., 1968a), Jonsson proposed that thalidomide exert its biological effects by intercalation of DNA (Jonsson, 1972). Later, Koch and Czejka showed that thalidomide could intercalate into DNA (Koch and Czejka, 1986), and Huang and McBride demonstrated that thalidomide was able to alter DNA secondary structure in rat embryos (Huang and McBride, 1990). Two reports further pointed out that free radical-mediated DNA damage might be the cause of thalidomide's biological effects (Liu and Wells, 1995; Parman et al., 1999). Huang and co-workers linked the effects of DNA damage to its immunosuppression (Huang et al., 1999). Recently, Stephens and co-investigators proposed a model explaining thalidomide's mechanism of action that combined a number of hypotheses (Stephens et al., 2000). The model was derived from previous observations that thalidomide was able to inhibit insulin-like growth factor-I (IGF-I) and fibroblast growth factor-2 pathways (Stephens et al., 1998). Both pathways encompass genes with promoters

lacking nucleotide sequence TATA, but instead containing GC-rich boxes, such as GGGCGG. Based on computational modeling, Stephens and co-workers suggested that S-thalidomide intercalated into the major groove of DNA in GC rich domains, thus down-regulate the expression of genes with promoters that have GC-rich boxes. The down-regulation of those genes might be the cause of thalidomide's anti-angiogenesis and immunomodulation. Recently, Drucker and co-workers reported that thalidomide down-regulated transcript levels of GC-rich promoter genes in multiple myeloma cell lines, supporting the hypothesis that thalidomide acts through intercalating itself into DNA and changing the expression of certain genes to exert its anti-myeloma effects (Drucker et al., 2003).

1.3.3. Inhibition of Adhesion Molecule Expression

Thalidomide may change tumour microenvironment through its effects on cytokine production (Hideshima et al., 2001a; Hideshima et al., 2001b). In addition, thalidomide has been shown to be able to change tumour microenvironment more effectively through inhibition of surface adhesion molecule expression. Thalidomide was shown initially to inhibit tumour cell attachment to concanavalin-A coated surfaces (Braun and Dailey, 1981), and was later found to reduce platelet/endothelial cell adhesion molecule *in vitro* (Zwingenberger and Wnendt, 1996). Further studies showed thalidomide was able to modulate the expression of cell surface adhesion molecules, such as ICAM-1 and VCAM-1, as well as their receptors. Geitz and co-workers investigated the modulation of the adhesion cascade of thalidomide using cultured HUVECs and human leukocytes *in vitro*. Density shifts of these molecules were measured by flow cytometry. They found thalidomide altered the expressions of ICAM-1 and VCAM-1, as well as E- and L-selectin (Geitz et al., 1996). Settles and co-worker studied cell adhesion molecule expression and cell-cell contact in a HUVEC-human T-leukemic cell mixed cell culture system using thalidomide at concentrations of 0, 10 and 50 µg/ml. They found that thalidomide down-regulated ICAM expression and inhibited HUVECs-human T-leukemic cell adhesion in a dose-dependent manner (Settles et al., 2001).

It is well recognized that the tumour microenvironment is important to tumour survival and growth (Paget, 1889), and there is increasing evidence that the bone marrow microenvironment plays an important role in haematologic malignancies (Caligaris-Cappio et al., 1992; Vidriales and Anderson, 1996; Hallek et al., 1998; Cheng et al., 1999; Tricot, 2000; Roodman, 2002; Mohla et al., 2003). The high expression of cell surface adhesion molecules is associated with multiple myeloma progression (Kim et al., 1994; Vacca et al., 1995; Faid et al., 1996). These molecules are much needed for the interaction between tumour cells and BMSCs to enable myeloma cells to bind strongly to the bone marrow cell layers as well as fibronectin (Uchiyama et al., 1992; Kim et al., 1994; Faid et al., 1996; Urashima et al., 1997). Observations of high expression of those molecules in other human malignancies have also been reported (Banks et al., 1993). Therefore, thalidomide's inhibitory effects on surface adhesion molecules are likely to cause changes in the tumour microenvironment and influence tumour localization, progression and survival. Furthermore, thalidomide also has direct effects on BMSCs to inhibit their growth and survival (Anderson, 2001; Richardson et al., 2002).

1.3.4. Stimulation of Lymphocytes and Natural Killer Cells

Thalidomide is able to exert its immunomodulatory effects not only through cytokine modulation but also through stimulation of immune cells themselves. Thalidomide increased the number of lymphocytes in systemic lupus erythematosus patients (Walchner et al., 2000). Haslett and co-workers showed that when purified T-cells were stimulated by antibodies to CD3, thalidomide provided an essential co-stimulatory signal for T-cell proliferation and lymphokine production, such as IFN- γ and IL-2. Thalidomide also increased the primary CD8⁺ cytotoxic T-cell response induced by allogeneic dendritic cells. The co-stimulatory effects of thalidomide could be achieved at concentrations as low as the 1 – 2 $\mu\text{g/ml}$ attained in the plasma of human subjects after thalidomide treatment (Haslett et al., 1998; Haslett et al., 2003). They also reported that thalidomide stimulated T-lymphocyte proliferation and cytokine production, such as IL-12, in patients infected with HIV (Haslett et al., 1997; Haslett et al., 1999). Not only can thalidomide co-stimulate the proliferation and function of T-cells directly (Corral et al., 1999), but it can also improve T-cell function through

inducing cytokine production by type 2 T-helper cells and concomitantly inhibiting cytokine production by type 1 T-helper cells in mitogen- and antigen-stimulated human peripheral blood mononuclear cell cultures (McHugh et al., 1995). Davies and co-workers demonstrated that co-culture of thalidomide with peripheral mononuclear cells and multiple myeloma cell lines significantly increased natural killer cell numbers and the lysis of multiple myeloma cells. Coupled with clinical observations that thalidomide increased natural killer cell numbers and function in MMPs responding to thalidomide therapy, they suggested that thalidomide could enhance the immune response against tumours by increasing natural killer cell numbers and function in humans (Davies et al., 2001).

1.3.5. Induction of Apoptosis

Thalidomide has been shown to directly induce apoptosis or G₁ growth arrest in multiple myeloma cells, as well as causing apoptosis through changing the microenvironment of multiple myeloma, both *in vitro* and *in vivo* (Hideshima et al., 2000; Chauhan and Anderson, 2003; Ezell et al., 2003; Zhai and Lu, 2003). Thalidomide induced apoptosis in cultured multiple myeloma cell lines directly that was associated with the activation of related adhesion focal tyrosine kinase (Hideshima et al., 2000; Anderson, 2001). Thalidomide also down-regulated constitutive nuclear factor- κ B (NF- κ B) activity of multiple myeloma cell lines to induce apoptosis (Hideshima et al., 2002; Mitsiades et al., 2002a). Keifer and co-workers further identified that thalidomide inhibited NF- κ B activity through suppression of I κ B kinase activity in human Jurkat T-cells *in vitro* (Keifer et al., 2001), while another group of investigators demonstrated that the inhibition of NF- κ B was due to thalidomide-induced redox changes in rat and rabbit limb buds (Hansen et al., 2002). NF- κ B is crucial in protecting tumour cells from apoptosis by attenuating death-receptor-induced apoptosis (Mitsiades et al., 2002b). Blocking that pathway removes the apoptotic protection of tumour cells, thus causing tumour cell death.

Thalidomide may exert its effects through one or a combination of the above 5 aspects. A summary of the above mechanism in multiple myeloma is shown in Figure 1.3 (Anderson, 2001; Richardson et al., 2002). Since it has been suggested that it is an

active metabolite which mediates its anti-tumour effects (Fabro et al., 1965; Braun and Dailey, 1981; Price et al., 2002), a closer examination of thalidomide pharmacokinetics and metabolism will further our understanding of its mode of action.

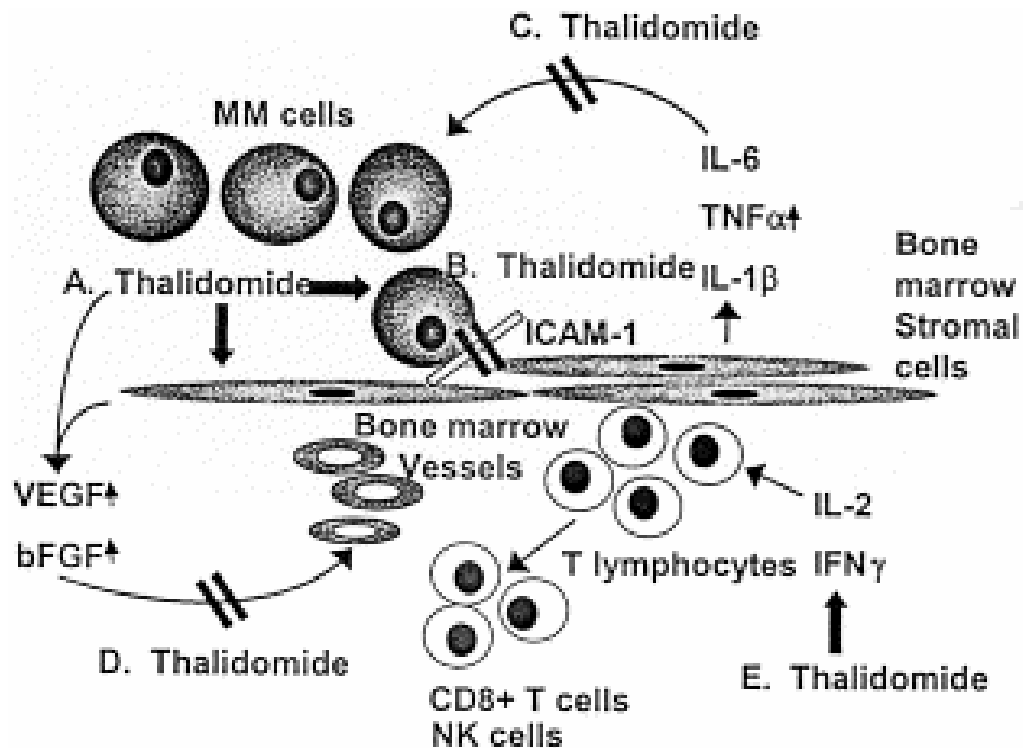


Figure 1.3 Possible role of thalidomide on multiple myeloma (MM) cells' and BMSCs' microenvironment *in vivo*. (A) Thalidomide directly inhibits myeloma cell growth. (B) Thalidomide inhibits MM cell adhesion to BMSCs. (C) thalidomide blocks IL-6, TNF and IL1 β secretion from BMSCs. (D) Thalidomide blocks the ability of VEGF and bFGF to stimulate neovascularisation of bone marrow. (E) Thalidomide induces IL-2 and IFN- γ secretion from T-cells. Adapted from Richardson et al., 2002.

1.4. Pharmacokinetics, Metabolism and Metabolites

1.4.1. Pharmacokinetics and Pharmacokinetic Interaction with Other Drugs

1.4.1.1. Pharmacokinetics

Studies of the pharmacokinetics of thalidomide in animals have not yet been reported. The majority of the studies on thalidomide pharmacokinetics were carried out in humans using racemic thalidomide since that is the form which is used in the clinic. The results from previous pharmacokinetic studies are summarized in Table 1.2.

Orally-administered thalidomide is absorbed slowly in humans and usually takes more than 2.5 h to reach maximum concentration (C_{\max}) in plasma. While the time to reach C_{\max} (T_{\max}) increases with increasing dose, the increase is not strictly dose proportional (Teo et al., 2001). However, the area under the concentration-time ($AUC_{0-\infty}$) increased proportionally with dose between 50 to 400 mg/day. This study also showed that the overall amount of thalidomide absorbed is independent of dose over this range (Teo et al., 2001). In humans, the apparent volume of distribution (V/F) of thalidomide at the dose of 200 mg/day is around 100 L (see Table 1.2), indicating a wide tissue distribution. The terminal elimination rate constant was associated more with the absorption rather than the elimination (Teo et al., 1999), and as a result, the V/F increased with dose between 200 to 400 mg/day (Teo et al., 2001). The variability in V/F observed in elderly prostate cancer patients was suggested to be due to altered absorption and plasma protein binding rates (Figg et al., 1999). Little unchanged parent compound is found in the urine (Williams et al., 1965; Chen et al., 1989), and thalidomide is excreted in urine mainly as metabolites (Smith et al., 1965). Unabsorbed drug however is excreted unchanged in faeces (Faigle, 1962; Schumacher et al., 1965a). The renal clearance rate of thalidomide has been shown to be 0.08 L/h, suggesting that the major route of elimination is non-renal (Chen et al., 1989). The apparent clearance rate (Cl/F) is normally around 10 L/h and terminal half-life ($t_{1/2}$) is between 4 – 8 h (see Table 1.2).

Table 1.2 Pharmacokinetic parameters of orally administered (*R*-, *S*-)-racemic-thalidomide (unless stated otherwise).

Reference	No. of Subjects	Dose mg/day	C _{max} µM	T _{max} h	AUC _{0-∞} µM·h	CI/F L/h	V/F L	t _{1/2} h
Chen et al., 1989	8 Hv*	200	4.7	4.4	-	10	121	8.7
Eriksson et al., 1995	6 Hv	1 ^a (<i>R</i>)	2.7	4	-	-	48	4.7
		1 ^a (<i>S</i>)	1.9	4			72	
Piscitelli et al., 1997	5 HIV	100	4.7	3.4	43	9	88	6.5
	4 HIV	300	13.6	3.4	155	8	78	5.7
Trapnell, 1998	9 Hv	200	12.4	5.8	159	5.4	-	6.7
Figg et al., 1999	13 PC	200	7.8	3.3	-	7.4	67	6.5
	11 PC	800	17.1	4.4	-	7.2	166	18.3
Noormohamed et al., 1999	14 HIV	100	4.5	2.5	38	10.4	70	4.6
		200	7.4	3.3	75	10.8	83	5.3
Scheffler et al., 1999	10 Hv	200	8.9	5.8	89	9.2	40	3.0
Teo et al., 1999	17 Hv	200	8.1	3.5	70	10	77	5.4
Eriksson et al., 2000	6 Hv (i.v.)	50 (<i>R</i>)	-	-	17	10	-	4.7
		50 (<i>S</i>)	-	-	11	21	-	3.9
Fine et al., 2000	34 G	800	15.9	4.7	-	14	146	8.3
Teo et al., 2000b	13 Hv	200 ^b	7.7	4.0	96	-	-	5.8
		200 ^c	8.4	6.1	91	-	-	5.1
Aweeka et al., 2001	7 HIV	200	8.1	6.3	21	9.6	79	5.7
Teo et al., 2001	15 Hv	50	2.4	2.9	19	10.4	81	5.5
		200	6.8	3.5	73	10.9	88	5.5
		400	10.9	4.3	141	11.7	122	7.3
Wohl et al., 2002	8 HIV	50	3.1	2.3	22	0.12 ^d	0.72 ^e	4.2
		100	4.7	2.9	48	0.12 ^d	1.14 ^e	7.4
		150	10.9	2.9	92	0.14 ^d	1.13 ^e	5.9
Dal Lago et al., 2003	4 CC	200	6.5	4.4	78	10.5	133	7.8
Chung et al., 2004a	5 MMP	200	5.4	4.8	81	10.8	111	7.3

* Hv = Healthy Volunteers; HIV = Human Immunodeficiency Virus-Infected Patients; PC = Prostate Cancer Patients; G = Patients with Gliomas; CC = Colorectal Cancer Patients; (*R*) = *R*-thalidomide isomer; (*S*) = *S*-thalidomide isomer.

^a 1mg/kg; ^b fast conditions, ^c high fat meal conditions, ^d L/h/kg, ^e L/kg.

1.4.1.2. Pharmacokinetic Interactions with Other Drugs

Thalidomide is often combined with other drugs for therapy, but little information is available on thalidomide interactions with co-administered drugs. It has been shown that chronic thalidomide administration does not affect the pharmacokinetics of ethinyl estradiol and norethindrone in healthy women volunteers (Trapnell et al., 1998; Scheffler et al., 1999). This study was important to establish if hormonal contraception will be effective during thalidomide therapy. The pharmacokinetic interactions of thalidomide with other cancer chemotherapies have been investigated in a preclinical murine model in this laboratory. Thalidomide was shown to alter the pharmacokinetics of DMXAA in Colon 38 tumour bearing mice (Kestell et al., 2000), leading to increased anti-tumour activity and TNF production (Cao et al., 1999). Thalidomide also altered the pharmacokinetics of co-administered cyclophosphamide in the same model, resulting in longer $t_{1/2}$ and greater AUC of both the parent drug and its active metabolite, 4-hydroxycyclophosphamide. The prolonged exposure of 4-hydroxycyclophosphamide enhanced the anti-tumour activity of cyclophosphamide (Ding et al., 2002). Thalidomide pharmacokinetics was conversely altered by DMXAA and cyclophosphamide (Chung et al., 2004b).

1.4.2. Metabolism and Metabolites

Biotransformation of thalidomide occurs by enzymatic or non-enzymatic hydrolysis (Faigle, 1962; Schumacher et al., 1965a, b; Williams et al., 1965), or by hepatic cytochrome P450-mediated hydroxylation in various species (Eriksson et al., 1998a; Ando et al., 2002a; Ando et al., 2002b). Both enzyme-catalysed and non-enzyme-catalysed products are generally referred to as metabolites. Most studies in the literature indicate that at physiologic conditions, thalidomide undergoes rapid non-enzymatic hydrolysis only (Faigle, 1962; Schumacher et al., 1965a, b; Williams et al., 1965) (Figure 1.4). The rate of hydrolysis of thalidomide in biological fluids increases with increasing pH and temperature (Kerberle et al., 1965; Williams et al., 1965; Huupponen and Pyykko, 1995; Lyon et al., 1995; Eriksson and Bjorkman, 1997; Eriksson et al., 1998b). Teo and co-workers reported that although 5-hydroxythalidomide (5-OH Th)

was detected in the urine below limits of quantitation, hydroxylation metabolites were not detectable in plasma of patients with Hansen's disease receiving thalidomide at a dose of 400 mg/day, nor could they be detected by incubating thalidomide with human liver microsomes or cloned human cytochrome P-450 (CYP) isozymes (Teo et al., 2000a). Eriksson and co-workers studied hydroxylated metabolite formation in 8 healthy male human volunteers. Three volunteers received 1 mg/kg of *R*- or *S*-thalidomide on separate occasions and their plasma was collected to test for 5-OH Th. Six volunteers took 1 mg/kg and two volunteers took 2.5 mg/kg of racemic thalidomide and their plasma was collected for the detection of 5'-hydroxythalidomide (5'-OH Th). 5-OH Th was not detectable in plasma samples, but trace amount of 5'-OH Th was detected in all volunteers. The same study also reported that both 5-OH Th and 5'-OH Th were formed after 4 h of incubation with human S9 liver fraction preparations. However, dihydroxy metabolites, such as 4,5-dihydroxythalidomide and 5,6-dihydroxythalidomide, were not detected *in vivo* or *in vitro* (Eriksson et al., 1998a). Ando and co-workers investigated hydroxylated metabolite formation in the plasma of prostate cancer patients on thalidomide therapy with a dose of 200 mg/day or 1200 mg/day. They found very low concentrations of 5-OH Th and 5'-OH Th in plasma in less than half of the patients (Ando et al., 2002b). In another report, Ando and co-workers showed that hydroxylated metabolites, such as 5-OH Th, 5'-OH Th and 5,6-dihydroxythalidomide were formed after incubating thalidomide with microsomes of mice, rats, rabbits, dogs and humans. They demonstrated that the enzymes responsible for the hydroxylation of thalidomide in humans are CYP2C9, CYP2C19 and CYP1A1, while in rats CYP2C6, CYP2C11, CYP2C12 and CYP1A1 are responsible (Ando et al., 2002a). The rate of thalidomide metabolism *in vivo* is not known. *In vitro* studies show that the rate of 5-OH Th formation is fastest in mice, followed by rabbits, then humans (Ando et al., 2002a). It has also been shown that the hydrolysis and hydroxylated metabolites are more soluble and have longer $t_{1/2}$ than thalidomide (Keberle et al., 1965; Schumacher et al., 1965b; Ando et al., 2002a).

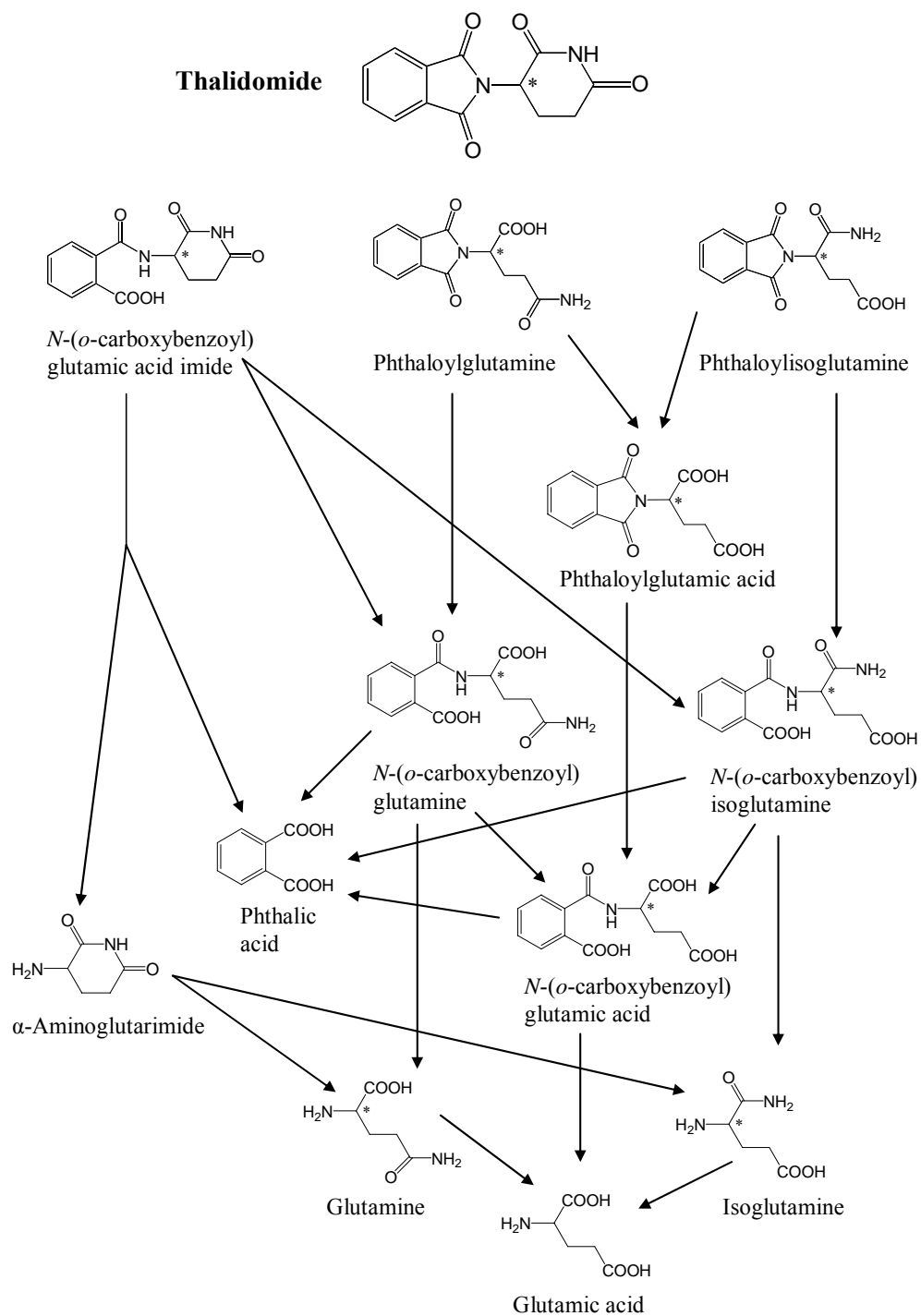


Figure 1.4 Hydrolysis pathway of thalidomide (Adapted from Schumacher et al., 1965b).

While the number of metabolites that can theoretically be generated from thalidomide has been estimated to be higher than 100 (Schumacher et al., 1965a; Zhu et al., 1999), to date only twelve major metabolites have been observed in animals and humans, seven of which are hydrolysis products and three are hydroxylated metabolites (Schumacher et al., 1965b; Eriksson et al., 1998a).

Hydrolysis metabolites were tested for teratogenicity in the 1960s and most studies showed negative results (Fabro et al., 1965; Smith et al., 1965; Fabro et al., 1967b). Later, some of them were tested for immunomodulation and were found to be inactive (Gunzler et al., 1986). Apart from these results, little can be found in the literature about the biological activities of the hydrolysis metabolites of thalidomide. On the other hand, hydroxylated metabolites have been tested for anti-angiogenic activities in a number of studies. Marks and co-workers demonstrated that both thalidomide and 5-OH Th inhibited the blood vessel formation on chorioallantoic membrane of a growing chicken embryo, suggesting that 5-OH Th is an active anti-angiogenic agent (Marks et al., 2002). Price and co-workers synthesized *cis*-5'-OH Th and tested its anti-angiogenic effects. They showed that *cis*-5'-OH Th inhibited the microvessel outgrowth of rat aortic ring cultured in Matrigel and microtubule formation of HUVECs in Marigel (Price et al., 2002). Hydroxylated metabolites were shown not to inhibit gene transcription in cultured multiple myeloma cell lines, however (Drucker et al., 2003).

1.5. Summary of the Review

Although thalidomide has a tragic history, its established therapeutic effects in autoimmune diseases and cancers warrants further investigation. The mechanism of action of thalidomide in cancer treatment still remains to be clarified. A number of hypotheses have been proposed, some of which are supported by some clinical observations. However, none of the hypotheses can provide an overall comprehensive explanation of the effects of thalidomide. Whether thalidomide itself, or its hydroxylated metabolite(s) or its hydrolysis metabolite(s) is the active compound is currently still controversial.

It is known that thalidomide has different biological effects in different species. However, the pharmacological disposition of thalidomide in different species remains unstudied. Complexities arise from chirality, enzymatic and non-enzymatic hydrolysis, enzymatic biotransformation, metabolic pathways and metabolite characterization. With the aid of modern technology, such as high performance liquid chromatography (HPLC) and liquid chromatography-mass spectrometry (LC-MS), and progress in the synthesis of potential thalidomide metabolites, it is now feasible to investigate the pharmacological properties of thalidomide in various species. Further studies of metabolism, metabolites and pharmacokinetics across species, both *in vitro* and *in vivo*, will likely provide answers as to the active metabolite, the basis for inter-species difference in biological response, and why thalidomide's anti-cancer activity appears to be species-dependent and tumour type-dependent.

As thalidomide's teratogenicity is still remembered, searching for a non-teratogenic analogue of thalidomide with the desired pharmacological and toxicological properties is likely to be the future direction of its development. The hydroxylated metabolites of thalidomide have been tested for their anti-tumour activities and shown to be moderately effective, but the ring-open/hydrolysis products have not yet been tested for anti-tumour activities. Since most of thalidomide's hydrolysis products are not teratogenic, should we find an active ring-opened product, it will provide more possibilities in the design and synthesis for new analogues that are non-teratogenic.

1.6. Objectives of This Study

This study addresses some fundamental questions concerning thalidomide's mode of action and inter-species differences in biological activity. It is hypothesized that the activities of thalidomide are closely related to its pharmacokinetics, metabolism and metabolite formation in different species. By detecting metabolites formed in different species and identifying the biological activity of the metabolites that are found in MMPs responding to thalidomide therapy, it should be possible to identify the active agent.

The objectives of this study are:

- 1) To develop methodologies that will allow the detection of all the thalidomide metabolites formed in mice, rabbits and MMPs.
- 2) To determine the metabolic rate and metabolite formation *in vitro* using liver microsomes of the same species tested *in vivo*.
- 3) To compare metabolite formation, metabolism rate and pharmacokinetics with biological effects of thalidomide in those species studied.
- 4) To test all the metabolites found in MMPs for anti-tumour and TNF modulatory activities.
- 5) To study the chemical and biochemical properties, both *in vitro* and *in vivo*, of the active metabolite(s).

CHAPTER 2. DETECTION AND IDENTIFICATION OF THALIDOMIDE METABOLITES IN MICE

2.1. Introduction

Thalidomide undergoes non-enzymatic hydrolysis and enzymatic biotransformation in various species to form numerous metabolites, and the possible number of metabolites can reach more than 100 (Schumacher et al., 1965b; Zhu et al., 1999). Schumacher and co-workers studied thalidomide hydrolysis in solution and identified 12 major breakdown products using paper chromatography (Schumacher et al., 1965b). Hydrolysis metabolites have also been detected in plasma and urine of mice, rats, guinea-pigs, rabbits and dogs in early studies using ultraviolet (UV) spectroscopy, paper chromatography, electrophoresis and radio-labelling technologies (Faigle, 1962; Schumacher et al., 1965a; Tanaka et al., 1965; Fabro et al., 1967a). However, the formation of hydroxylated metabolites has been more difficult to detect. Recent studies have used advanced HPLC and LC-MS technology to detect hydroxylated metabolites formed *in vitro* from the incubation of thalidomide with liver microsomes of mice, rats, rabbits, dogs and humans (Eriksson et al., 1998a; Meyring et al., 2000; Teo et al., 2000a; Ando et al., 2002a), and *in vivo* in human plasma (Eriksson et al., 1998a; Teo et al., 2000a; Ando et al., 2002a; Ando et al., 2002b). However, these studies focussed only on hydroxylated metabolites and the formation of hydrolysis products and other possible metabolites were not pursued, even though unidentified metabolite peaks were reported (Eriksson et al., 1998a; Meyring et al., 2000; Ando et al., 2002a).

Since thalidomide metabolites have been implicated in its mechanism of action and linked with inter-species biological sensitivity (Fabro et al., 1965; Gordon et al., 1981; Neubert and Neubert, 1997), this study has developed methodologies where all the major metabolites formed can be identified. The aims of this study are:

- a) To develop an analytical method to detect all the major metabolites of thalidomide formed in mice using LC-MS technology.
- b) To identify all the major metabolites formed in mice.

2.2. Methods

2.2.1. Mice and Tumour

Male or female C57Bl/6 mice bred at the Animal Resources Unit, Faculty of Medical and Health Sciences, University of Auckland, were housed under conditions of constant temperature and humidity and used between 8-12 weeks old. All animal experiments were carried out according to institutional ethical guidelines. The murine Colon 38 adenocarcinoma was originally obtained from the Mason Research Institute (Worcester, MA, USA). Tumour-bearing mice were killed by cervical dislocation. Tumour was removed and cut into 1 mm³ fragments in a Petri dish (Falcon Labware, Franklin Lakes, NJ, USA) containing 10 ml phosphate buffered saline (PBS). Recipient C57Bl/6 mice, either male or female, were anaesthetised using i.p. administration of sodium pentobarbitone (81 mg/kg in a volume of 10 µl/g body weight) and Colon 38 tumour fragments were placed subcutaneously in an opening made in the left flank. The incision was closed using a small Michel wound clip (Aesculap, Tuttlingen, Germany). Tumours were used when they had reached about 5-7 mm in diameter, generally 9-12 days after implantation.

2.2.2. Drug Administration

For i.p. administration at a dosage of 100 mg/kg, thalidomide was dissolved in dimethylsulphoxide (DMSO) at 40 mg/ml and injected i.p. into mice in a volume of 2.5 µl/g body weight using 0.5 ml syringe. For p.o. administration, thalidomide was suspended in 0.3% hydroxypropylcellulose (10 mg/ml) and administered using a gavage needle (5 µl/g body weight), and given at a dosage of 50 mg/kg, the maximum dosage possible due to difficulties in solubility.

2.2.3. Metabolite Detection Using LC-MS and HPLC

2.2.3.1. Preparation of Murine Plasma and Urine Samples

Following drug administration, mice were placed in metabolic cages with water and food, and urine over a 4 h period was collected. After 4 h, murine blood samples were collected in heparinised tubes through ocular bleeding during terminal halothane (NZ Pharmacology Ltd., Christchurch, New Zealand) anaesthesia, centrifuged (3,000 x g), and the plasma removed. Mouse plasma samples (300 µl each) and urine samples (100 µl each) were then acidified by adding 1N HCl up to 1 ml, because thalidomide is stable at low pH and does not undergo hydrolysis (Schumacher et al., 1965b). Acidified samples were loaded onto 1 ml/100 mg preconditioned C18 Bond Elut columns (Varian, Harbor City, CA) using an automated extraction column system (ASPEC, Gilson Medical, Meddleton, Wis.). The columns were washed with 1 ml Milli-Q water and the compounds of interest were then eluted using 1 ml 100% acetonitrile (ACN). The eluates were evaporated to dryness using a centrifugal evaporator (Jouan, St. Nazaire, France) and residues reconstituted in 100 µl mobile phase for LC-MS analysis.

2.2.3.2. LC-MS Analysis

LC-MS analysis was performed using an Agilent 1100 LC/MSD single quadrupole system in which an Agilent 1100 UV diode array detector was coupled in series. All synthesized standards and samples were analysed initially using the mass spectral detector (MSD) set on simultaneous negative-ion and positive-ion scan modes between 70 and 1000 atomic molecular units (amu). This was carried out using either an atmospheric pressure chemical interface (APCI) or an electrospray interface in order to determine the best conditions under which thalidomide and related compounds would ionize. This in turn would determine the responsiveness of the MSD. It was found that mass spectrometric signals produced from thalidomide were very poor under all the conditions described above. However, all of the metabolites and hydrolysis products of this compound (i.e. hydroxylated products) gave good responses in the MSD when the APCI interface was used in the negative mode. These compounds were detected as

their [M-1] ions with no evidence of adduction formation. In addition, it was found that the APCI interface was equally as good in detecting the hydrolysis products of thalidomide but not the hydroxylated metabolites when used in the positive-ion mode. In complete contrast, none of these compounds could be detected by the MSD when the electrospray interface was used. Therefore, it was decided to utilize the APCI interface in all of the LC-MS analyses set to produce negative ions. However, it was also necessary to use it in the positive mode to provide supplementary data which would substantiate metabolite identification. Thus, for the majority of the LC-MS analyses, operation of the MSD was performed using the APCI interface set on simultaneous negative-ion and positive-ion scan modes.

During the analyses of biological samples, it was found that background noise or peaks associated with endogenous substances interfered with the quality of chromatograms by co-eluting with the peaks related to the metabolites of thalidomide. In order to minimize this it was considered that the MSD was best set in the single ion monitoring (SIM) mode as well as monitoring the total ion current (TIC). Therefore, the MSD was programmed for both TIC and SIM in which one group of SIM signals were associated with the negative single ion detection of the metabolites and hydrolysis products of thalidomide and another set of SIM signals associated with positive single ions which would detect the hydrolysis products of thalidomide. It was thought that this was the best strategy to detect and quantitate the known metabolites and hydrolysis products of thalidomide in biological matrixes as well identifying any which might be unknown.

Thus, aliquots of reconstituted samples (50 µl each) were injected into an Agilent 1100 Series LC/MSD system (Agilent Technologies, Avondale, PA, USA) and analysis was performed using an APCI interface and three MSD signals simultaneously: **Signal 1**, which takes 50% of the MS analysing cycle, was set on negative-ion scan (TIC) mode with a molecular weight range of 70 to 1000; **Signal 2**, which also takes 25% of the MS analysing cycle, was set on positive SIM mode at the molecular weights 259, 275, 277, 278, 291, 293, 295, 296 and 451; **Signal 3**, which takes 25% of the MS analysing cycle, was set on negative SIM mode at the molecular weights 257, 273, 275, 276, 289, 291, 293, 294 and 449 (corresponding to each of the peaks and possible metabolites). Negative SIM detection provided higher sensitivity, reduced background noise and better chromatograms (Figure 2.3 for example). The other MS conditions were:

fragmentor and capillary voltage of the interface, 100 and 3500 volt, respectively, drying gas flow rate, 5 L/min, corona current, 10 μ A, gas temperature, 350 °C, vaporizing temperature, 500 °C, and nebulising pressure, 35 psi. Samples were also concurrently analysed using diode array UV detection at 230 nm with UV at 590 nm as reference. The UV spectra of individual metabolite peaks were compared with those generated by the authentic standards and the percentage match between the spectra determined using ChemStation Rev. A.08.04 (Agilent Technologies, Avondale, PA, USA). Chromatographic separation was achieved with a LUNA 5 μ Phenylhexyl 100 x 4.6 mm stainless steel column (Phenomenex, Torrence, CA, USA) using a combination of the following solutions: Solution A, which contained 80% ACN and 1% acetic acid in water and Solution B, which contained 10% ACN and 1% acetic acid in water. The elution program was 100% solution B at 0.5 ml/min over 0-20 min, addition of 0-20 % solution A in a linear gradient at 0.7 ml/min over 20-45 min, and 100% solution B at 0.5 ml/min over 45-55 min.

2.2.3.3. Resolution of Phthaloylglutamine (PG) and Phthaloylisoglutamine (PiG) by HPLC

The chromatographic conditions used in the LC-MS analyses did not allow the separation of PG and PiG. The mobile phase was modified by the addition of the ion pair reagents cetyltrimethylammonium bromide and 1-octanesulfonic acid. Analysis of these two compounds was performed using a Waters HPLC system (Waters Associates, Milford, MA, USA) consisting of a 717PLUS auto sampler, 1525 binary HPLC pump, 100 x 10.0 mm stainless steel LUNA 5 μ phenylhexyl column (Phenomenex, Torrence, CA, USA) and a model 2487 dual λ absorbance detector set at 230 nm, and the peak containing a mixture of PiG and PG was collected with a Gilson model-202 fraction collector (Gilson Medical Electronics, Middleton, MI, USA). The mobile phase consisted of 10% ACN and 1% acetic acid in Milli-Q water and the flow rate was 0.5 ml/min isocratic. The collected eluant was dried using a Virtis Freeze-Mobile 6 model freeze drier (Virtis Co. Inc., Gardiner, NY, USA). The reconstituted dried samples were analysed by the same Waters HPLC system but using a LUNA 5 μ Phenylhexyl 100 x 4.6 mm stainless steel column instead of 100 x 10.0 mm stainless steel LUNA 5 μ Phenylhexyl column, and a mobile phase of 10% ACN and 1% acetic acid in Milli-Q

water, 48 mg/l 1-octanesulfonic acid, and 32 mg/l cetyltrimethylammonium bromide. Peaks were monitored by UV at 230 nm using an isocratic flow rate of 0.5 ml/min.

2.2.5.8. Thalidomide Glucuronide Identification

The fraction containing the glucuronide metabolite of thalidomide was separated using 100 x 10.0 mm column, collected, and dried using the same procedure as that described above for the PiG/PG fraction. The method of identification was adapted from that of Webster et al. (Webster et al., 1995) used to identify glucuronidation of 5,6-dimethylxanthenone-4-acetic acid. In brief, the dried residue was reconstituted in 0.1 M sodium phosphate buffer (pH 5.5) and two aliquots of 500 µl reconstituted metabolite solution were incubated at 37 °C for 45 minutes and 90 minutes with 2,000 units/ml β-glucuronidase plus 20 mM D-saccharic acid 1,4-lactone respectively. Another two aliquots of 500 µl reconstituted metabolite solution were incubated together without β-glucuronidase as control. The reaction was initiated by addition of β-glucuronidase and D-saccharic acid 1,4-lactone, and stopped by addition of 50 µl of 10% trichloroacetic acid. The mixture was centrifuged at 3,000 x g for 15 minutes to remove precipitated protein. The supernatant was removed, then injected into LC-MS and analysed using the same procedure described above.

2.3. Results

2.3.1. Detection of Metabolites

Colon 38 tumour-bearing and normal mice were treated with thalidomide either i.p. (100 mg/kg) or p.o. (50 mg/kg), and urine and plasma samples collected at 4 h and analysed using LC-MS. Both tumour-bearing mice and normal mice were used in this study in order to establish whether the tumour-bearing status had any effect on thalidomide metabolism in mice. It was reported that cancer patients had reduced CYP metabolic activity compared with healthy people (Williams et al., 2000).

The UV profiles of urine and plasma from both untreated and treated mice showed a number of peaks (Figure 2.1) and differences in the UV profiles were used to detect metabolites. Peaks were considered to be metabolite peaks if they gave signals on MS negative ion scan mode and negative single-ion monitoring mode (Figures. 2.2A & 2.3A), and if the mass spectrum of the peak contained additional ions to those in untreated control samples. An example for Peak 6, is shown for scan mode in Figures 2.2B & 2.2C and for single ion monitoring in Figures 2.3A & 2.3B. By these criteria, 7 metabolite peaks, in addition to the thalidomide peak, were identified in the urine from mice treated with thalidomide (Figure 2.1). There was no difference between chromatographic profiles of samples from male and female mice, neither were there any differences between Colon 38 tumour-bearing and non-tumour-bearing mice (Figure 2.4).

2.3.2. Identification of Metabolites

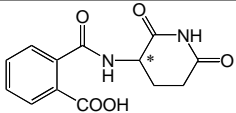
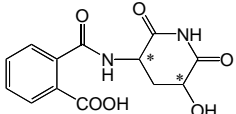
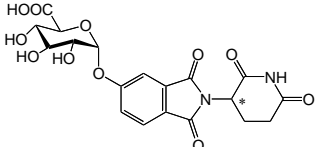
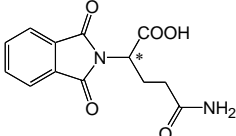
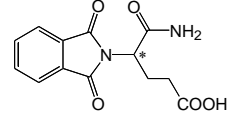
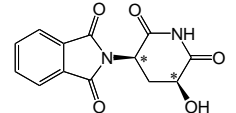
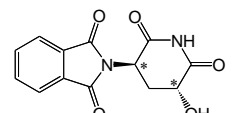
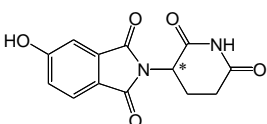
Possible metabolites with molecular weights corresponding to the MS signals of each of the peaks were deduced and authentic samples of the majority of these were either synthesised courtesy of Associate Professor Brian Palmer or bought (Appendix 1). The retention times, UV spectra, mass spectra and single ion monitoring chromatographic profiles of metabolite peaks and authentic standards were compared. Results are summarized in Table 2.1. Peak 1, with a molecular mass of 276, was identified as *N*-(*o*-carboxybenzoyl)glutamic acid imide (CG) on the basis that they had the same retention time and their UV spectra shared 93.5% identity to each other (Figure 2.5A). Peak 2, with a mass of 292, could correspond to a variety of possible hydroxylated hydrolysis products. Authentic 5- and 4-hydroxyphthaloylisoglutamine, 5- and 4-hydroxy-*N*-(*o*-carboxybenzoyl)glutamic acid imide, and 5- and 4-hydroxyphthaloylglutamine were synthesized courtesy of Associate Professor Brian Palmer, and it was found they all had different retention times to Peak 2. *N*'-hydroxy-*N*-(*o*-carboxybenzoyl)glutamic acid imide also has a mass of 292, but metabolites resulting from *N*-hydroxylation of the imide ring of thalidomide have never been detected, and it is unlikely that this is the compound in Peak 2. A likely candidate for Peak 2 is 5'-hydroxy-*N*-(*o*-carboxybenzoyl)glutamic acid imide (5'-OH CG), although the authentic compound is not yet available for confirmation.

Peak 3, a major component of the urine extracts, showed two molecular ions, corresponding to components with molecular weights of 450 and 274. It eluted just before an unidentified host component (present in urine of untreated mice) that had a molecular weight of 179. The molecular weight of the larger component suggested that it was an *O*-glucuronide derivative of thalidomide, while that of the smaller component suggested that it was a fragment ion resulting from loss of glucuronic acid. Peak 3 was therefore collected, a portion was treated with β -glucuronidase, and both portions were re-chromatographed (Figure 2.6A). Exposure to β -glucuronidase caused the appearance of a new component, Peak II, with a mass spectrum corresponding to a molecular weight of 274 (Figure 2.6B). This was identified as 5-OH Th on the basis that it has the same retention time and its UV spectrum shares more than 99% identity with that of authentic material. Peak I has a molecular weight of 450 (its reduced retention time was due to the lower loading of the column), and the decrease in its proportion following exposure to β -glucuronidase indicated that it was thalidomide-5-*O*-glucuronide. The peak eluting at 12.8 minutes (molecular weight 179) corresponded to an unidentified host component. No evidence of glucuronidation at the 5'- position was found.

Peak 4 had a molecular mass of 276 and identical UV spectra and mass spectra to authentic PiG. However, authentic PG also has the same mass and has a very similar retention time and it was necessary to determine whether both might be present in Peak 4. This fraction was therefore collected and re-analysed by HPLC using the mobile phase containing cetyltrimethylammonium bromide and 1-octanesulfonic acid that allows separation of PiG and PG with respective retention times of 15.1 min and 12.7 min (Figure 2.7A). The sample collected from Peak 4 resolved into two fractions (Figure 2.7B), indicating that both PG and PiG were present.

Peaks 5, 6 and 7 were identified as *cis*-5'-OH Th, *trans*-5'-OH Th and 5-OH Th, respectively on the basis of similarity of UV spectra (Figures 2.5B, 2.5C, and 2.5D) and identity of retention time (Table 2.1). The same number of metabolite peaks in UV profiles was obtained in urine following p.o. or i.p. administration (Figure 2.8). The profile obtained in plasma contained smaller sized peaks but the number of peaks was the same compared with the urine profile from mice administered thalidomide i.p. at the same dose (Figure 2.9).

Table 2.1 Metabolite peaks in UV profiles from murine urine following thalidomide treatment.

Peak #	Retention Time (min)	Molecular Weight	Match of UV spectra ^c	Metabolite	Structure
1	7.4	276	93.5%	CG	
2	9.1	292		5'-OH CG ^b	
3	12.8	450		thalidomide-5-O-glucuronide	
4a ^a	16.5	276		PG	
4b ^a	16.5	276		PiG	
5	25.4	274	98%	<i>cis</i> -5'-OH Th	
6	31.3	274	98%	<i>trans</i> -5'-OH Th	
7	33.3	274	>99%	5-OH Th	

^aPeak 4 separates into 4a and 4b with retention times of 12.7 and 15.1 min respectively on HPLC with mobile phase containing cetyltrimethylammonium bromide and 1-octanesulfonic acid.

^bproposed metabolite.

^cSee Figure 2.5.

*Chiral center

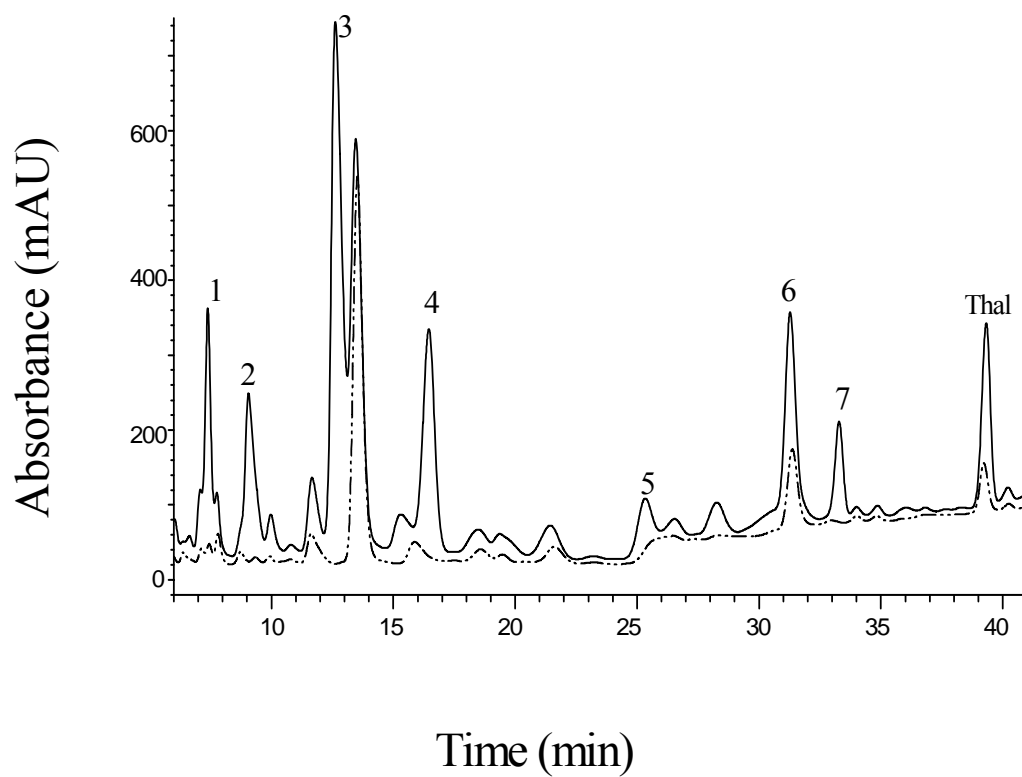


Figure 2.1 UV-detected chromatograms of urine samples from mice without treatment (dotted lines) and up to 4 h following oral administration of thalidomide (Thal) (50 mg/kg, solid lines).

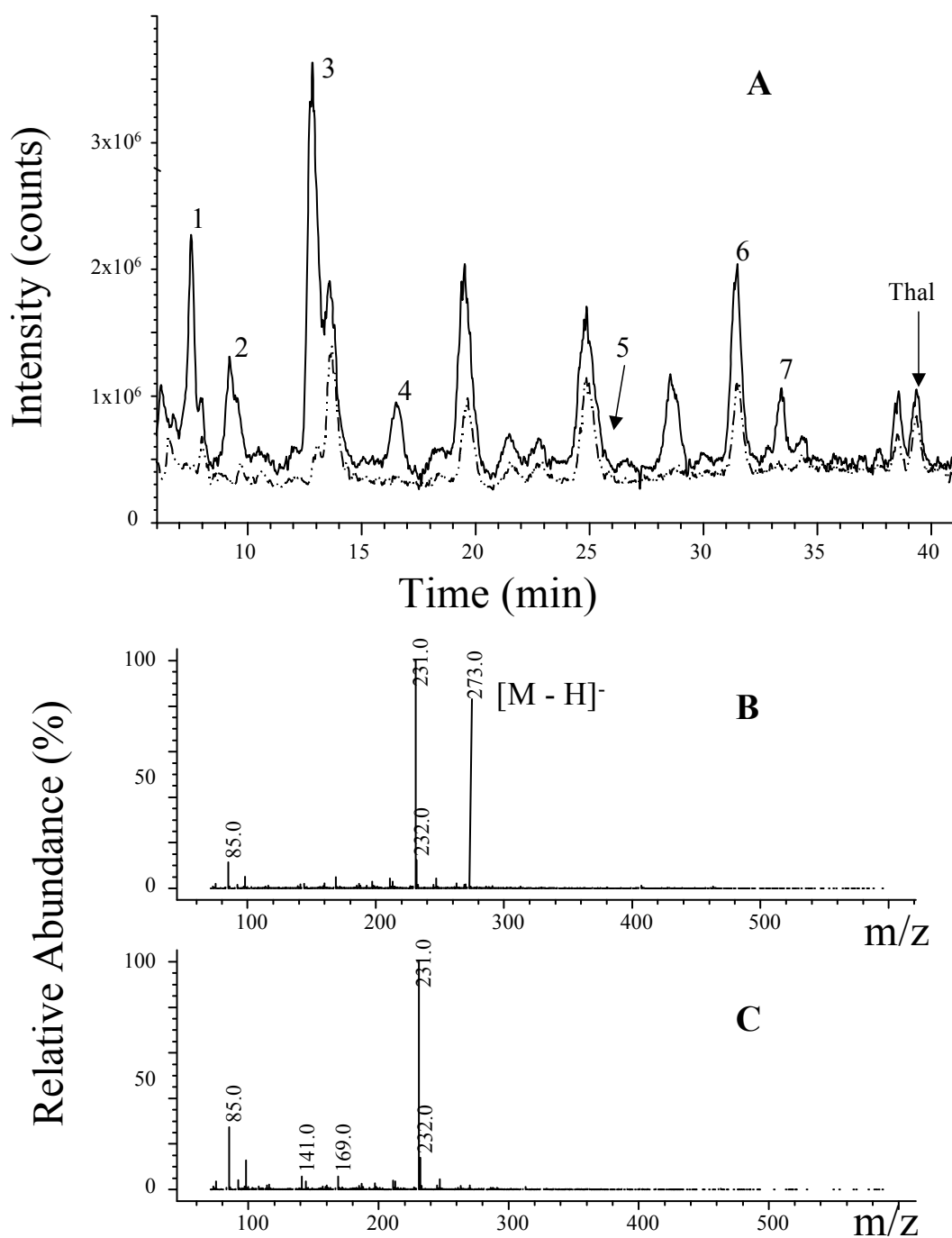


Figure 2.2 (A) Total ion MS-detected (Signal 1) chromatogram of urine from mice without treatment (dotted line) and up to 4 h following oral administration of Thal (50 mg/kg, solid line). (B) Mass spectrum of Peak 6 using negative ion-scan mode showing an $[M - H]^-$ mass of 273 amu. (C) Mass spectrum at the retention time corresponding to Peak 6 in untreated mouse urine.

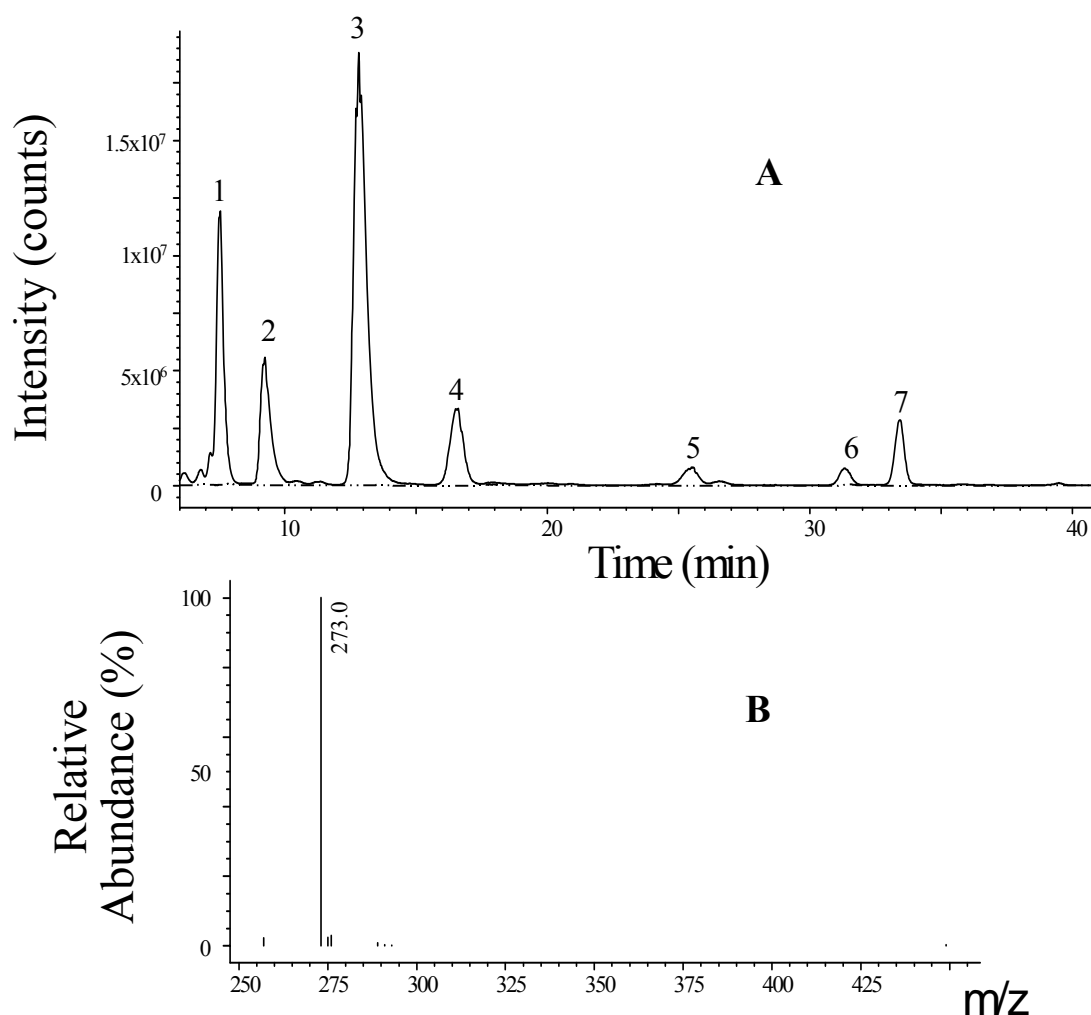


Figure 2.3 (A) Negative SIM mode (Signal 3) MS-detected chromatogram of urine from mice without treatment (dotted line) and up to 4 h following p.o. of Thal (50 mg/kg, solid line). (B) Mass spectrum using negative single-ion monitoring mode of Peak 6 showing a $[M-H]^-$ response of 273 amu. Note: Peaks 5 & 7 also corresponded to $[M-H]^-$ of 273 amu, while Peaks 1 & 4 corresponded to $[M-H]^-$ of 275 amu, Peak 2 corresponded to $[M-H]^-$ of 291 amu and Peak 3 corresponded to $[M-H]^-$ of 449 amu (spectrum not shown).

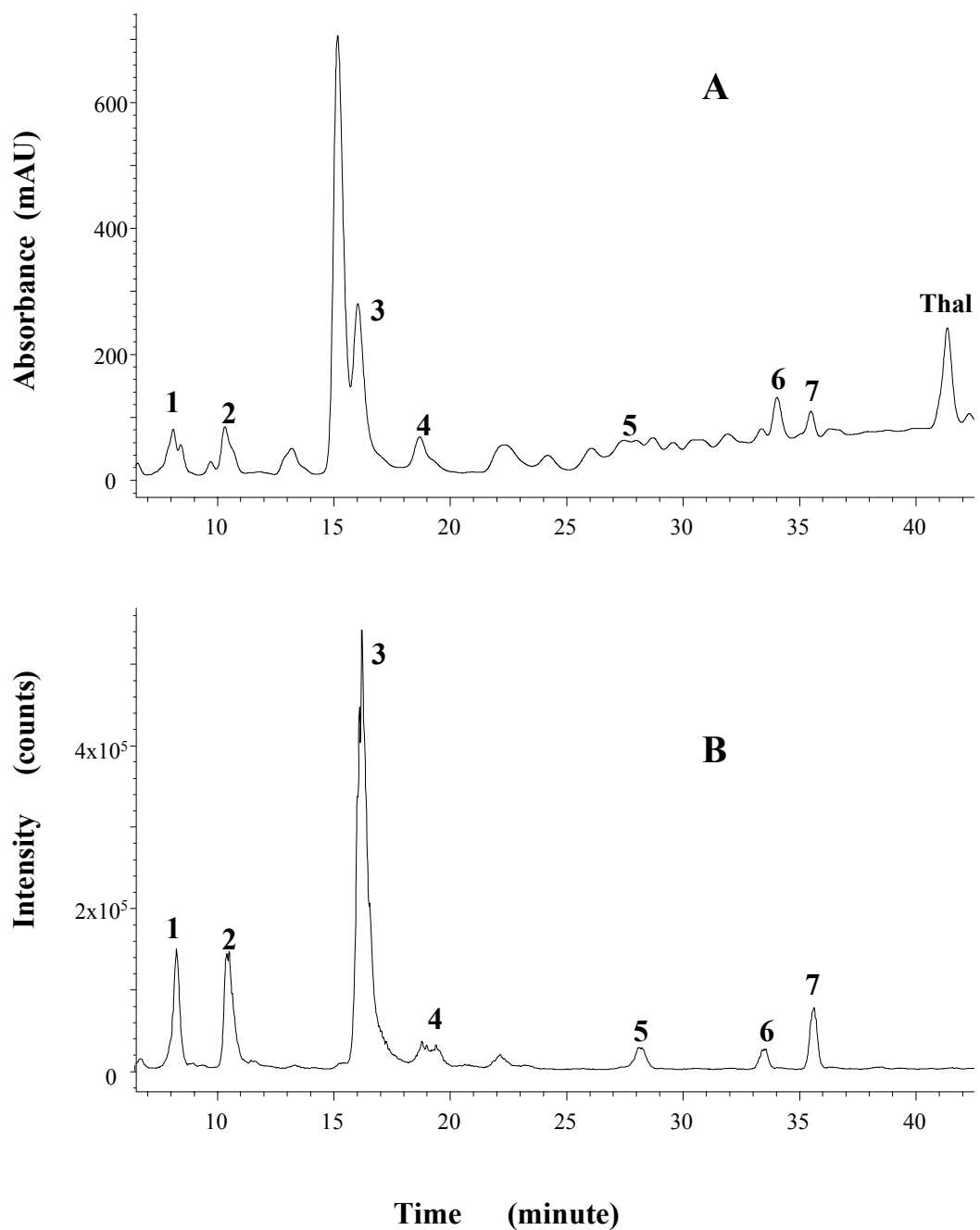


Figure 2.4 LC-MS chromatograms of urine samples from Colon 38 tumour-bearing mice up to 4 h following oral administration of Thal (50 mg/kg). (A) UV-detected chromatogram, and (B) SIM mode (Signal 3) MS-detected chromatogram.

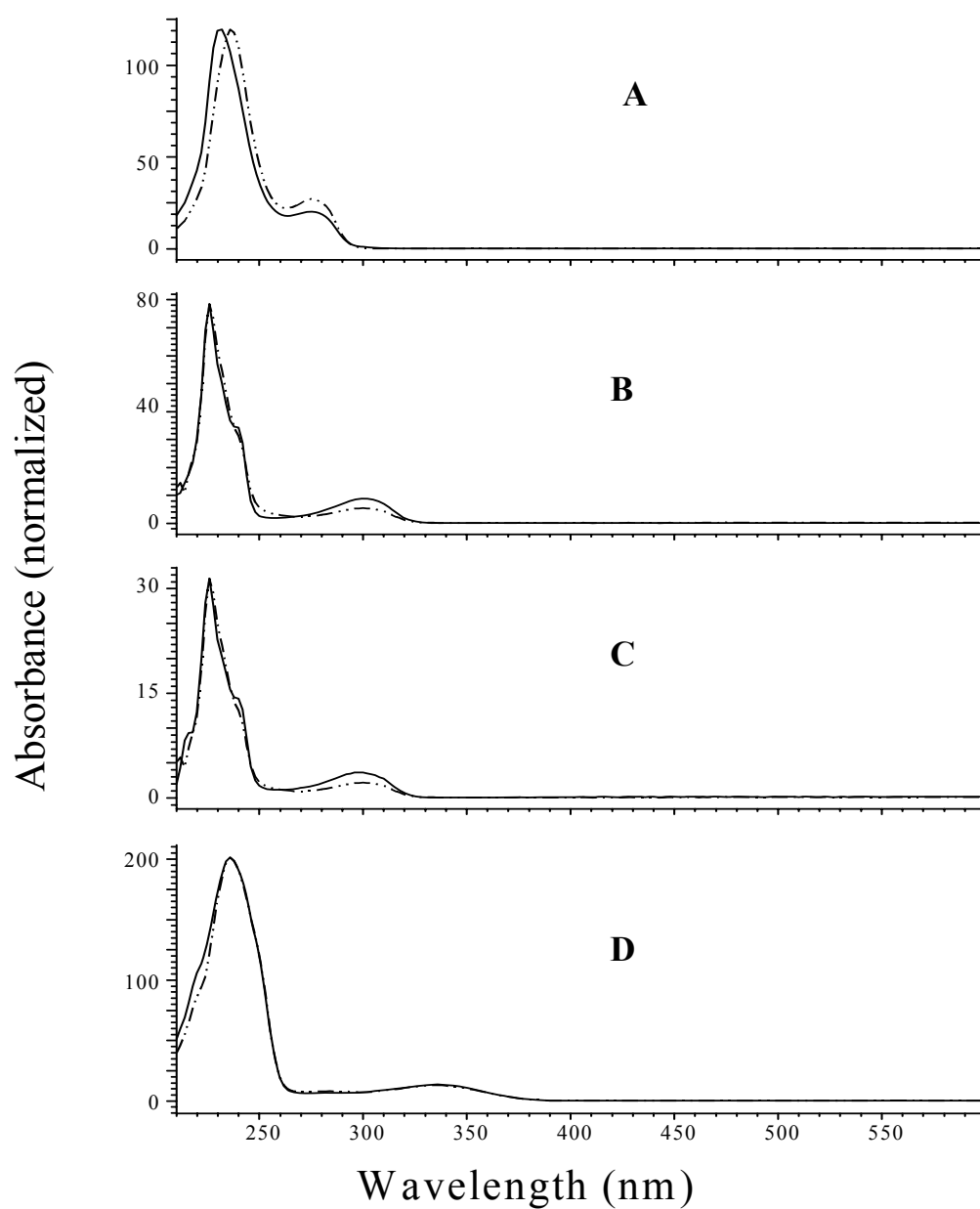


Figure 2.5 UV spectra of metabolite peaks (dotted lines) compared with UV spectra of corresponding authentic standards (solid lines). (A) Peak 1 and CG. (B) Peak 5 and *cis*-5'-OH Th. (C) Peak 6 and *trans*-5'-OH Th. (D) Peak 7 and 5-OH Th.

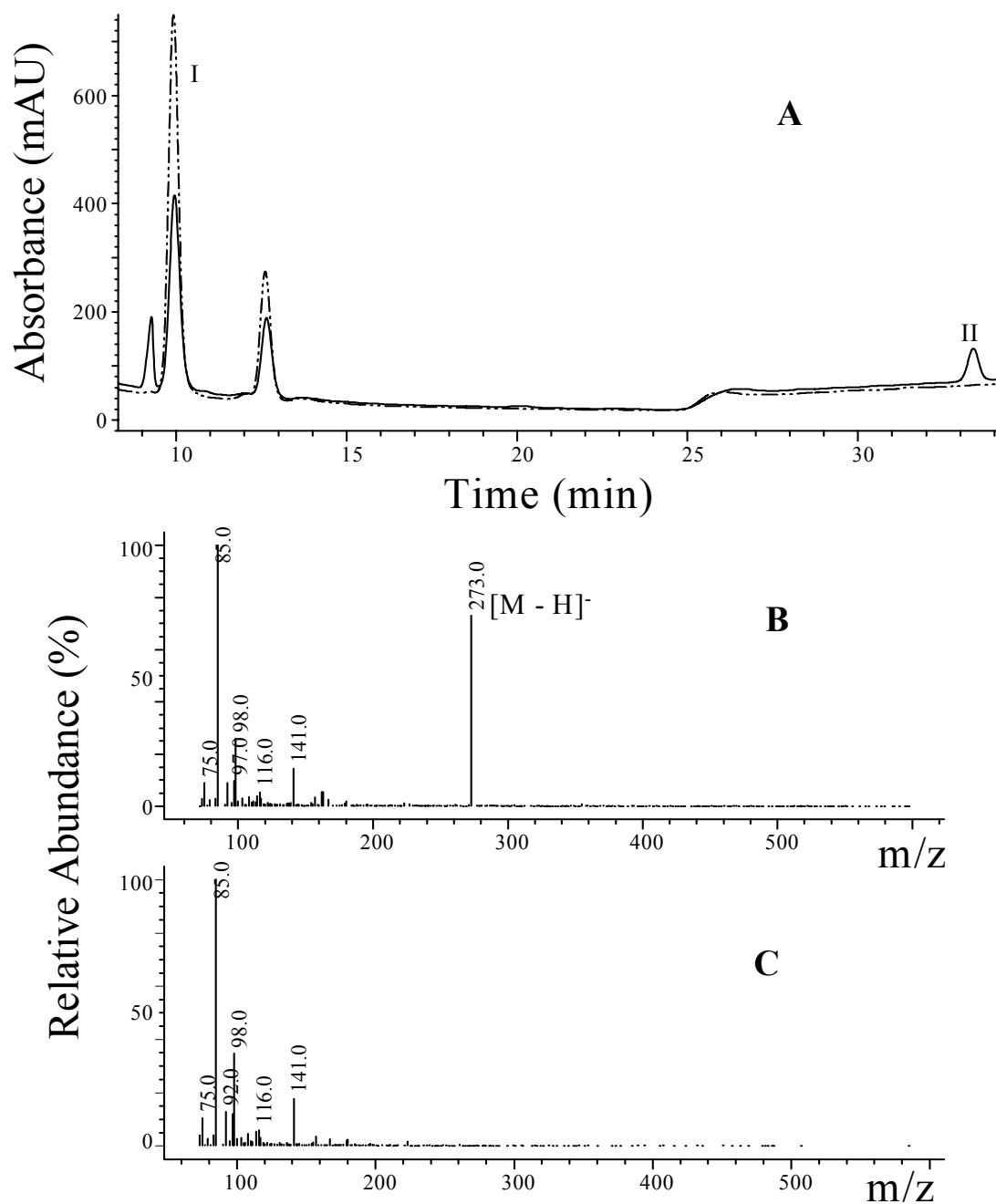


Figure 2.6 (A) UV-detected chromatogram of Peak 3 following treatment with β -glucuronidase (solid line) and without treatment (dotted line). (B) Mass spectrum of the Peak II formed following β -glucuronidase treatment showing an $[M-H]^-$ mass of 273 amu corresponding to 5-OH Th. (C) Mass spectrum at the retention time corresponding to Peak II in the untreated control.

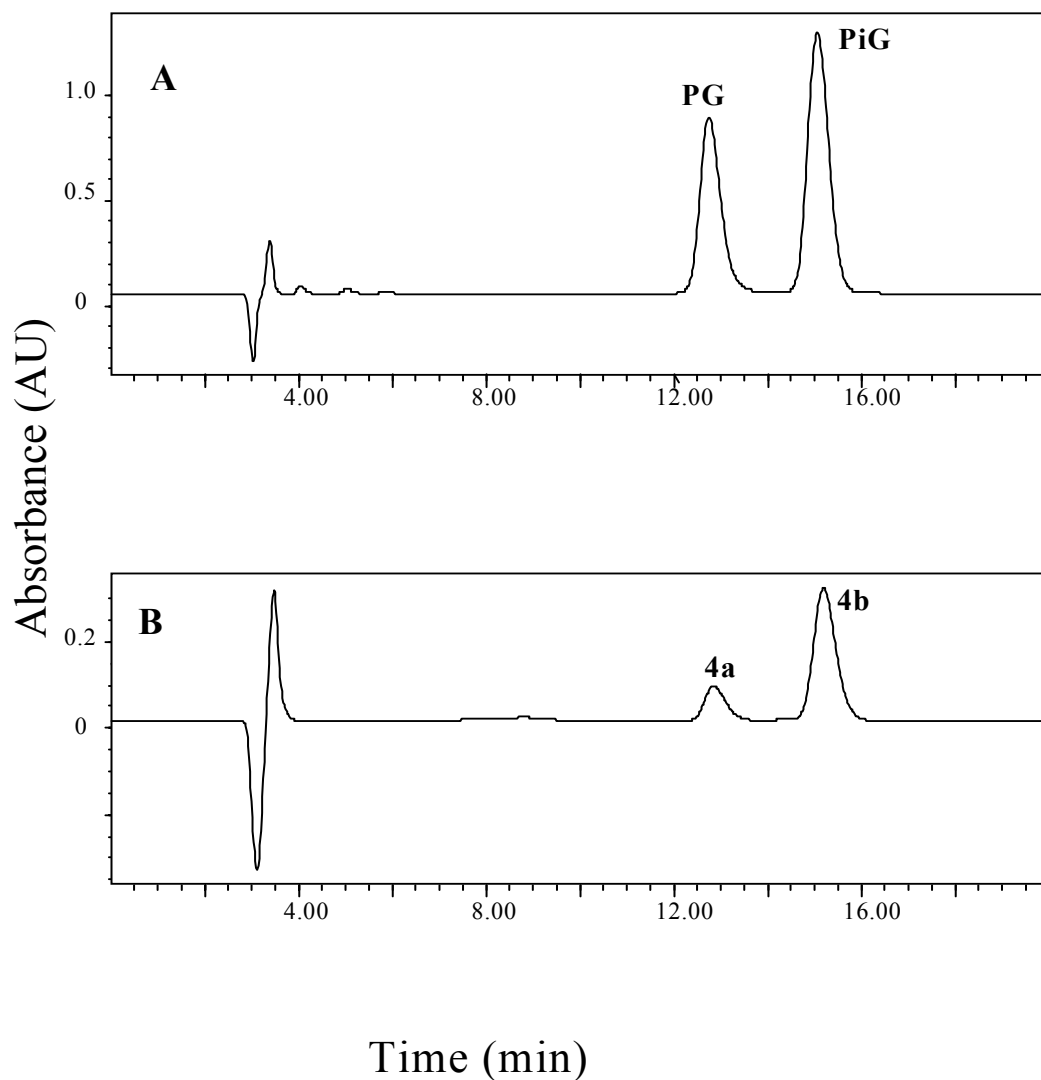


Figure 2.7 HPLC chromatograms using mobile phase containing cetyltrimethyl-ammonium bromide and 1-octanesulfonic acid showing complete separation of: (A) PG and PiG authentic standards; and (B) separation of the Peak 4 fraction from mouse urine into two peaks showing the presence of both PG and PiG.

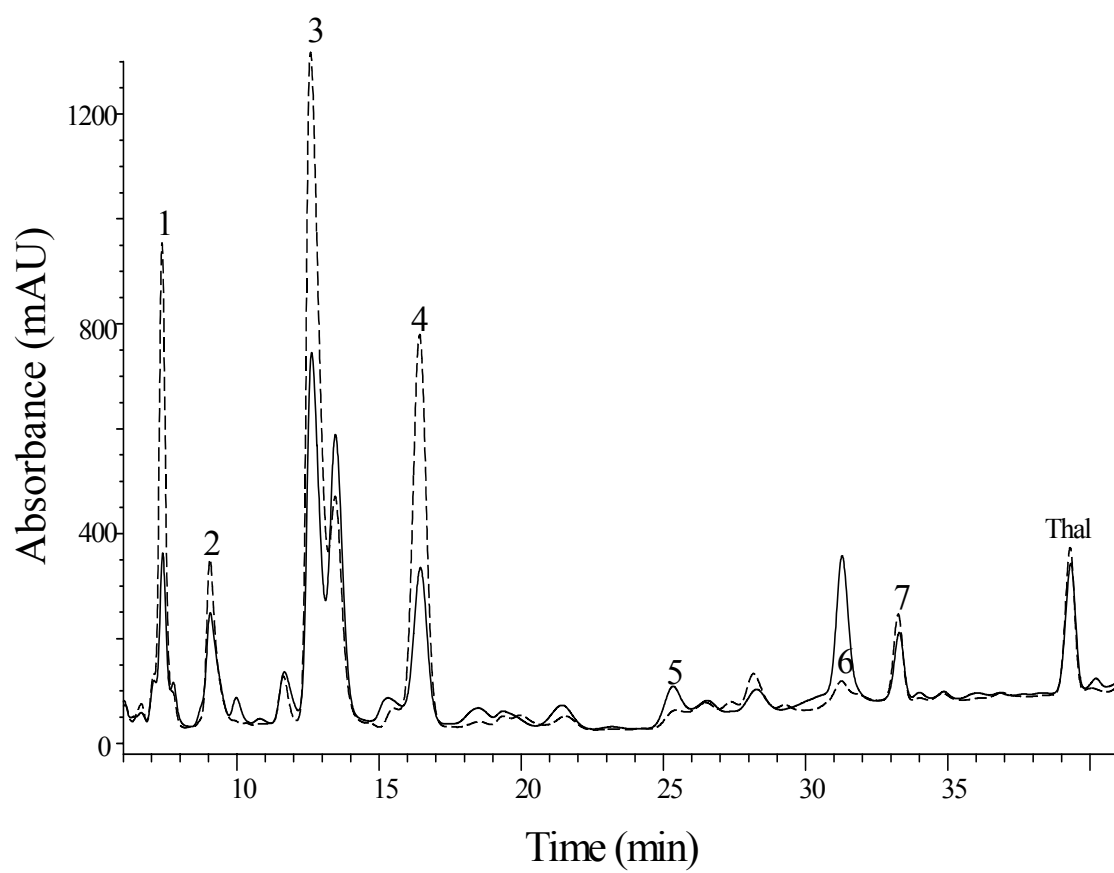


Figure 2.8 Comparison of UV-detected chromatograms of urine from mice administered Thal p.o. (solid line) or i.p. (dotted line).

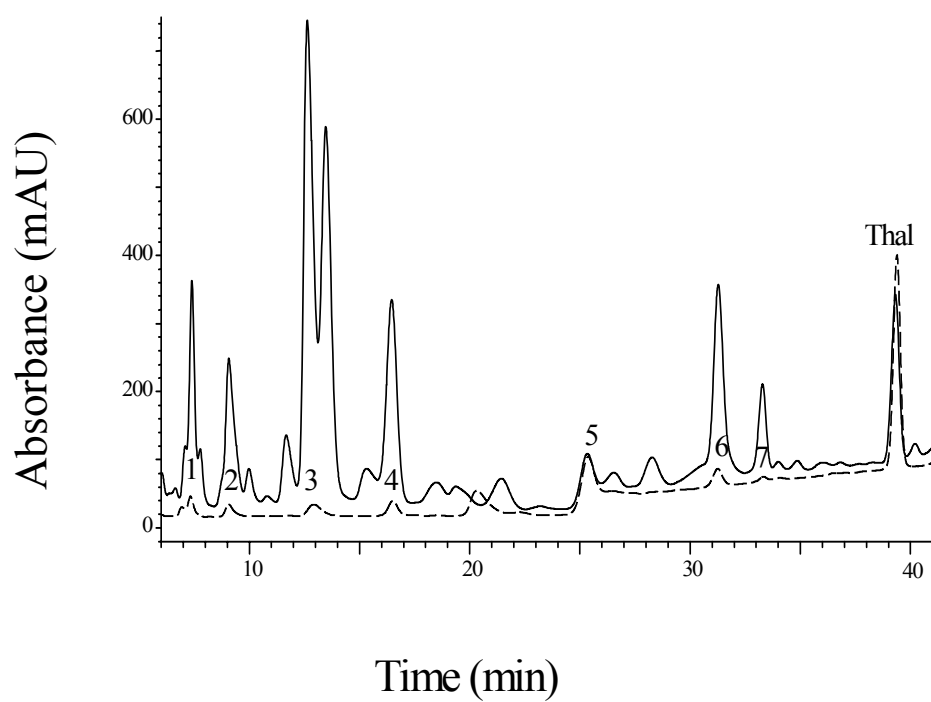


Figure 2.9 Comparison of UV-detected chromatograms of urine (solid line) or plasma (dotted line) from mice given Thal (50 mg/kg) p.o.

2.4. Discussion

The results confirm the formation in mice of three first step hydrolysis products, CG, PiG and PG, as well as three first step hydroxylation products, 5-OH Th and *cis*- and *trans*-5'-OH Th. In addition, evidence of a second step transformation of 5-OH Th to produce thalidomide-5-*O*-glucuronide was provided. A scheme for these transformation steps is shown in Figure 2.10. Although several studies report the presence of unidentified metabolite peaks (Eriksson et al., 1998; Meyring et al., 2000; Ando et al., 2002), glucuronidated thalidomide metabolites have not been previously documented. Glucuronidation is a uridine diphosphate glucuronide (UDPG) transferase-mediated phase II metabolism and confers greater solubility to a compound. The formation of glucuronidated metabolites may facilitate faster metabolism and excretion via this route. Indeed, the thalidomide-5-*O*-glucuronide was the largest metabolite peak in mouse urine (Figure 2.1). Glucuronidation occurred only at the 5-position and no evidence for the formation of thalidomide-5'-*O*-glucuronide was found.

The concentration of glucuronidase used in the experiment was high, and yet not all the thalidomide-5-*O*-glucuronide had been transformed into 5-OH Th. It was realised after the experiment had been carried out that D-saccharic acid 1,4-lactone was actually an inhibitor of β -glucuronidase and was used to eliminate microsomal glucuronidase activity in the original protocol (Webster et al., 1995). The use of D-saccharic acid 1,4-lactone was not really necessary in these experiments and explained the high concentration of glucuronidase that was used in the experiment here.

Although it has not been possible to validate the structure by comparison with authentic material, the metabolite in Peak 2 (Figures 2.1-3) is suggested to be 5'-OH CG, which can be formed either by second step hydrolysis of 5'-OH Th or second step hydroxylation of CG. Other authentic standards with the same mass have been ruled out as they have different HPLC retention times.

Thalidomide is extensively metabolised in mice resulting in seven metabolite peaks comprising hydrolysis, hydroxylation and glucuronidation of the parent compound. The

same number of peaks was obtained regardless of the route of administration. A previous *in vitro* study identified that CYP2C subfamily in liver was the major isoenzymes responsible for thalidomide's hydroxylation in rodents (Ando et al., 2002a). The same study also reported that the amount of 5-OH Th formed by mice liver microsomes was the highest among 5 species studied, namely Sprague Dawley rats, humans, New Zealand White rabbits, Beagle dogs and CD1 mice. 5-OH Th formation in murine liver microsomes after a 50-min incubation with 0.4 mM thalidomide was more than 20-fold higher than that formed by human liver microsomes. The presence of hydroxylated metabolites in mice (Figure 2.1) strongly suggests that metabolism by CYP2C subfamily isoenzymes is involved. The fast elimination of thalidomide via CYP2C-mediated hydroxylation route would result in relative short $t_{1/2}$ and low bioavailability in mice.

In summary, eight major metabolites have been identified to be formed in mice resulting from hydrolysis, CYP-mediated hydroxylation and UDPG-transferase-mediated glucuronidation.

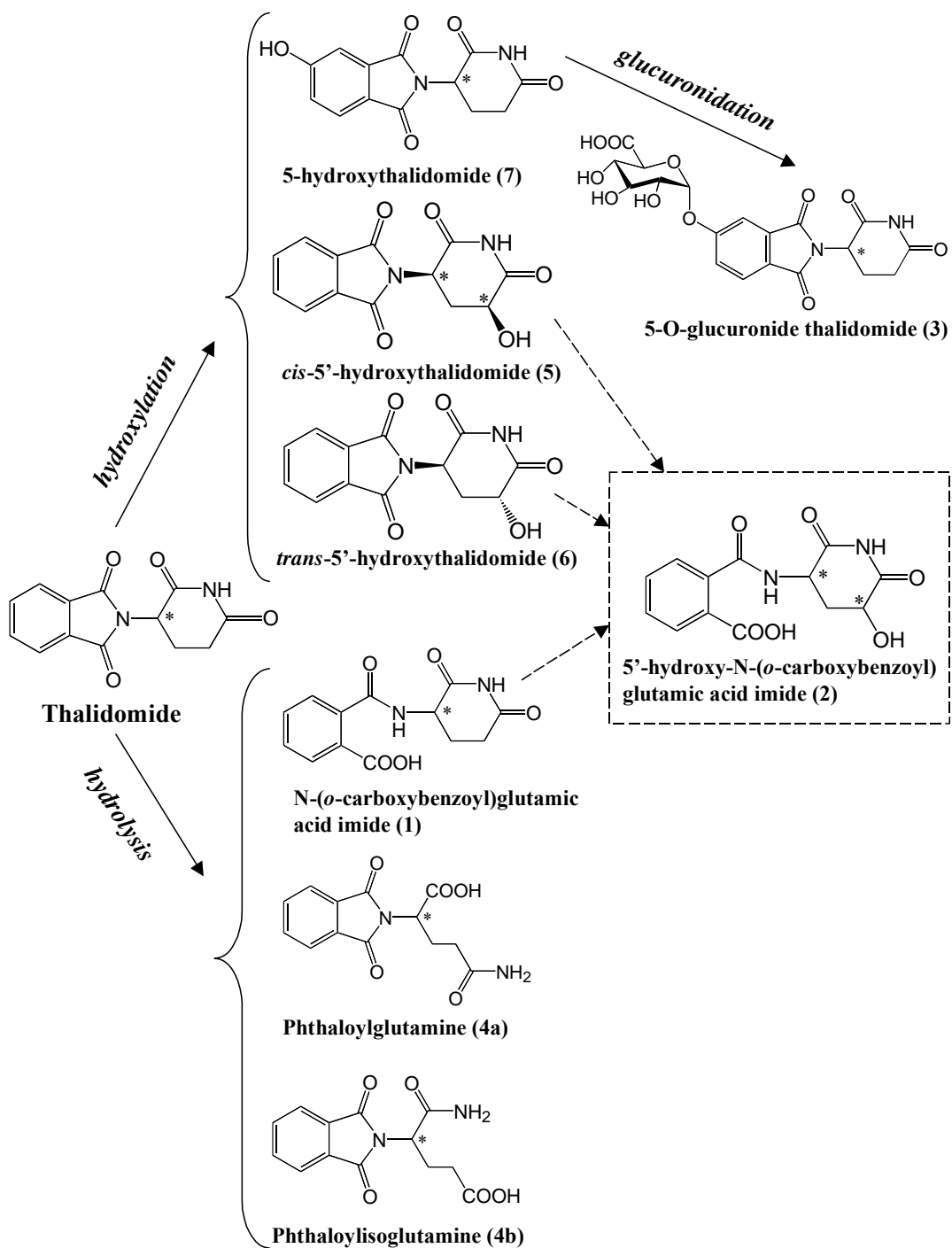


Figure 2.10 Proposed pathways of biotransformation of thalidomide in mice.
Unconfirmed steps or metabolites are shown in dashed lines.

CHAPTER 3. IDENTIFICATION OF THALIDOMIDE METABOLITES IN MULTIPLE MYELOMA PATIENTS

3.1. Introduction

Hydroxylated thalidomide metabolites have been proposed as the active compound(s) in thalidomide cancer treatment, since they have anti-angiogenic activities (Marks et al., 2002; Price et al., 2002). The synthesis of hydroxylated thalidomide analogues has also provided a number of compounds with potent anti-angiogenic/anti-metastatic activities (Luzzio et al., 2000; Luzzio et al., 2003), strengthening the hypothesis that hydroxylated thalidomide metabolites are responsible for thalidomide's anti-angiogenic effects. The formation of thalidomide metabolites appears to be highly species-dependent, and while microsomal preparations from human, primates or rabbits support the production of active metabolites, microsomes from rodents generally produce negative results (Gordon et al., 1981; Bauer et al., 1998). These *in vitro* studies are consistent with the greater *in vivo* sensitivity to the effects of thalidomide observed in humans and rabbits as compared to that in rodents, where thalidomide showed greater teratogenicity and anti-tumour activities in humans and rabbits but is generally ineffective in rodents (Neubert and Neubert, 1997) (also see reviewed in Section 1.2). However, inhibition of angiogenesis by thalidomide can be demonstrated in both rabbit and murine corneal assays (D'Amato et al., 1994; Kenyon et al., 1997; Kruse et al., 1998).

Since hydroxylated thalidomide metabolites have been proposed to be responsible for its anti-angiogenic effects, this study uses methodologies developed in Chapter 2 to search for these metabolites in the urine of MMPs undergoing thalidomide therapy. The objectives are:

- a) To identify thalidomide metabolites present in urine of MMPs on thalidomide therapy.
- b) To compare metabolite profiles in urine of mice and that of MMPs.

3.2. Methods

3.2.1. Preparation of Urine and Plasma Samples

With ethical approval, four male and three female Caucasian patients undergoing treatment with thalidomide for refractory multiple myeloma at Auckland Hospital were recruited for urine metabolite detection studies. The oral dosages of thalidomide for those patients ranged between 100 – 400 mg/day. Control samples of urine were obtained from healthy volunteers as well as a pre-treatment sample from one of the patients. Urine samples on three consecutive months of treatment as well as a plasma sample on one occasion was obtained from one patient with a >75% reduction in his IgG paraprotein on 100 mg thalidomide per day. Urine samples (3.33 ml) were acidified by adding 1N hydrochloride acid (HCl) to 10 ml and one plasma sample (100 µl) was acidified by adding 10% trichloroacetic acid (TCA) to 1 ml. Both urine and plasma samples were processed as described for murine samples (Section 2.2.3.1). Dried residues of the plasma sample and urine samples were reconstituted in 100 µl and 500 µl mobile phase respectively for LC-MS study.

3.2.2. Metabolite Detection and Identification

Thalidomide metabolites in samples from MMPs were detected and identified using the same methods and procedures described in Sections 2.2.3.2 & 2.2.3.3.

3.3. Results

3.3.1. Detection and Identification of Metabolites in MMPs

Urine samples from patients on thalidomide therapy were analysed for metabolites using the same procedure as that for murine samples. A pre-treatment sample from one patient (Patient 2, Figure 3.2A) showed no significant difference to those from healthy individuals, and peaks observed in untreated controls were not included in the analysis. Applying the same criteria as those used for defining murine metabolite peaks (Section

2.3.2), only two metabolite peaks were detected in the UV profile of all 7 of the patients' urine (Figures 3.1 & 3.2). The first of these peaks was the same as Peak 1 in the murine profile, corresponding to CG, while the second was identical to Peak 4 (Peak number here corresponds to the peak numbers in Section 2.3.1 and Figures 2.1-3). This second peak was re-analysed by HPLC using the ion-paired mobile phase, and like the corresponding peak in mice it could be resolved into two components corresponding to PG and PiG (Figure 3.3).

3.3.2. Intra-patient Metabolite Detection Study

Patient 1 who showed a greater than 75 % reduction in paraprotein levels on thalidomide was studied while on a dose of 100 mg per day. Urine samples collected on three consecutive months of treatment were analysed but no variation in the metabolite profiles were seen over this period (Figure 3.4). This patient also provided a blood sample 15 h after one of his daily thalidomide doses. Unlike in mice, thalidomide metabolites were not detected in this plasma even though they were detectable in a urine sample collected at the same time (Figure 3.5B).

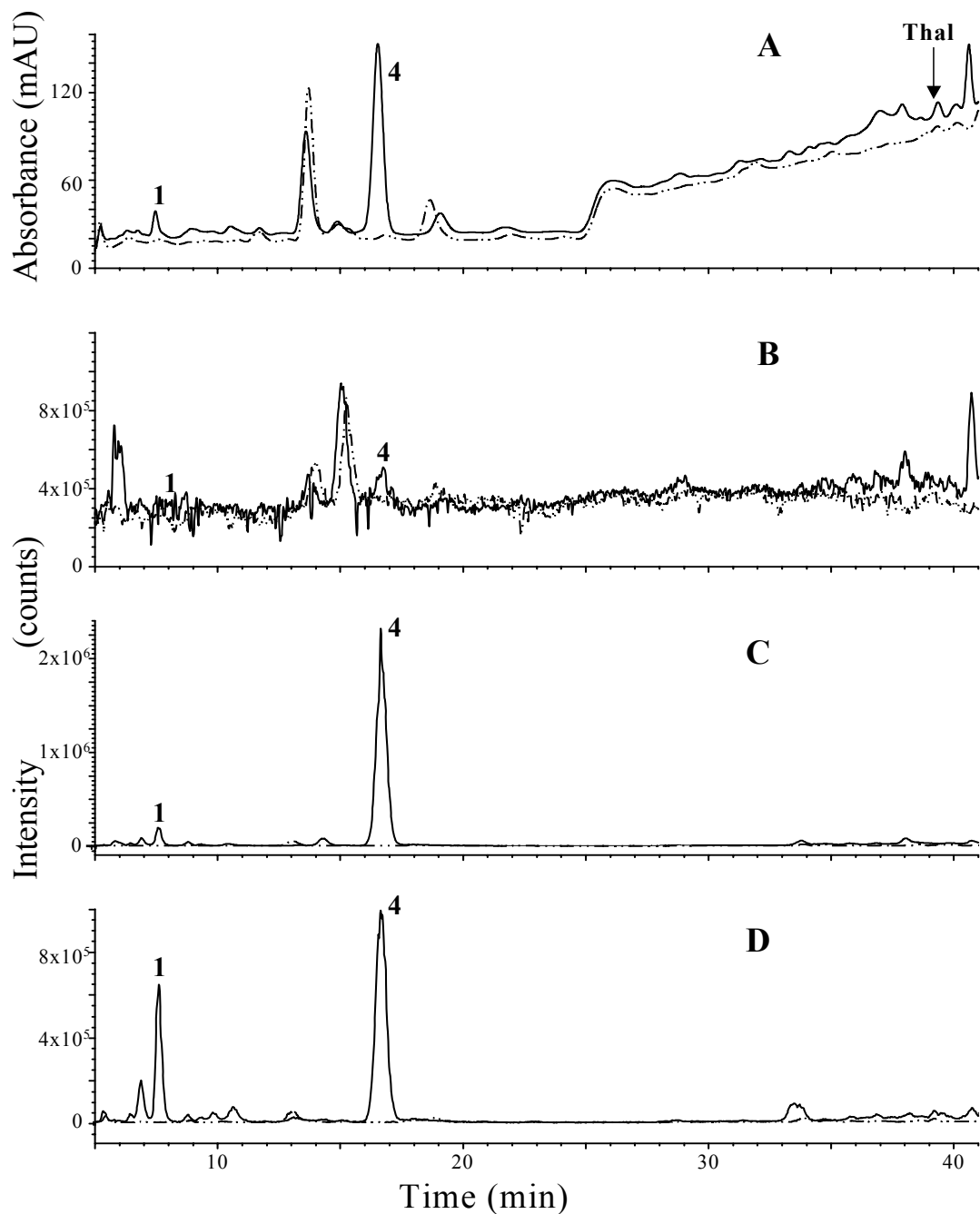


Figure 3.1 LC-MS chromatograms of urine from MMP1 on Thal therapy (100 mg/day, solid lines) and from a healthy volunteer (dotted lines) recorded by: (A) UV at 230 nm, (B) MS at negative TIC mode (Signal 1), (C) MS at positive SIM mode (Signal 2), (D) MS at negative SIM mode (Signal 3).

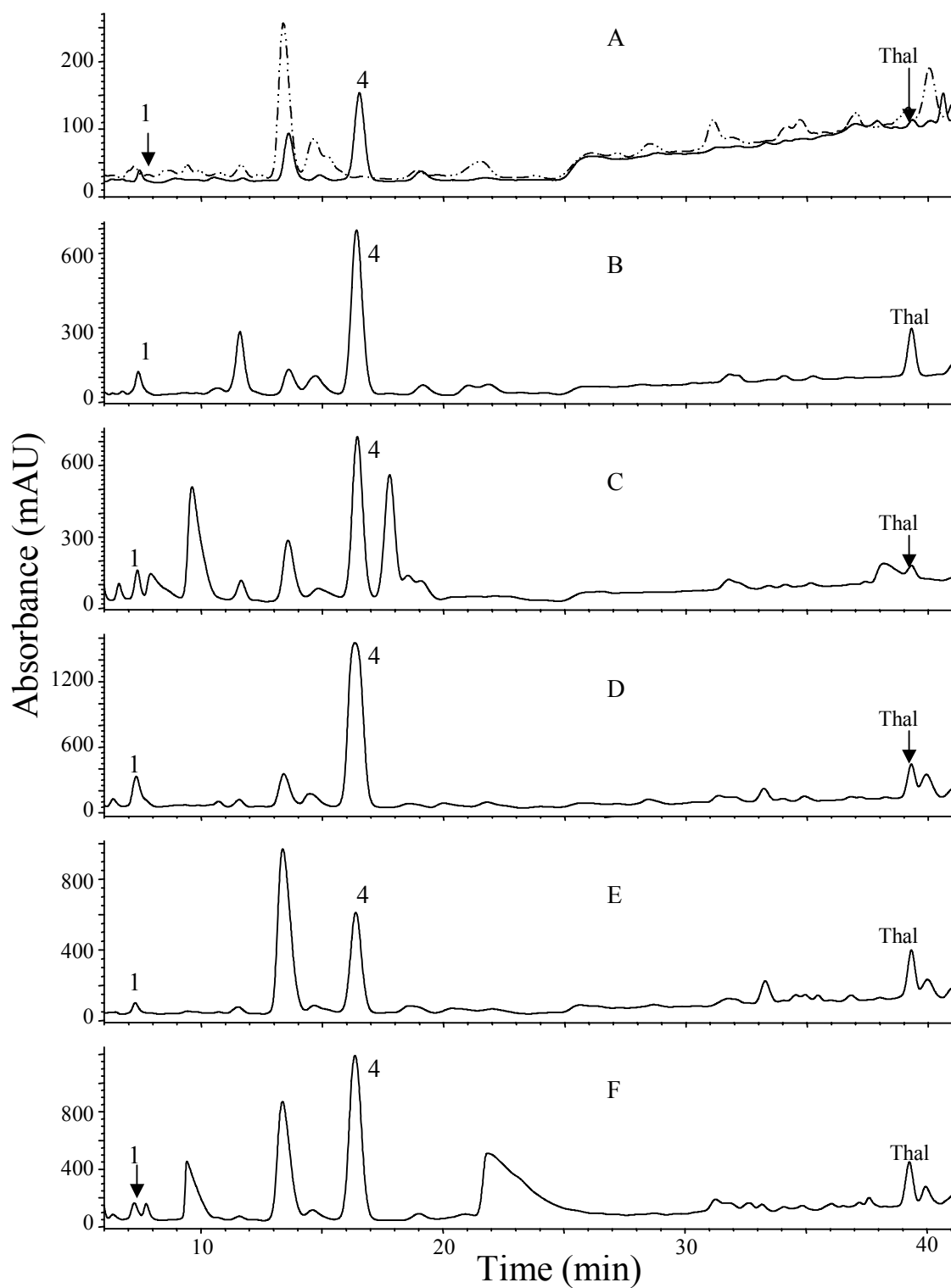


Figure 3.2 UV chromatograms of urine samples of MMPs on thalidomide therapy (solid lines) and before treatment (dotted line). A-F correspond to Patients 2-7 respectively.

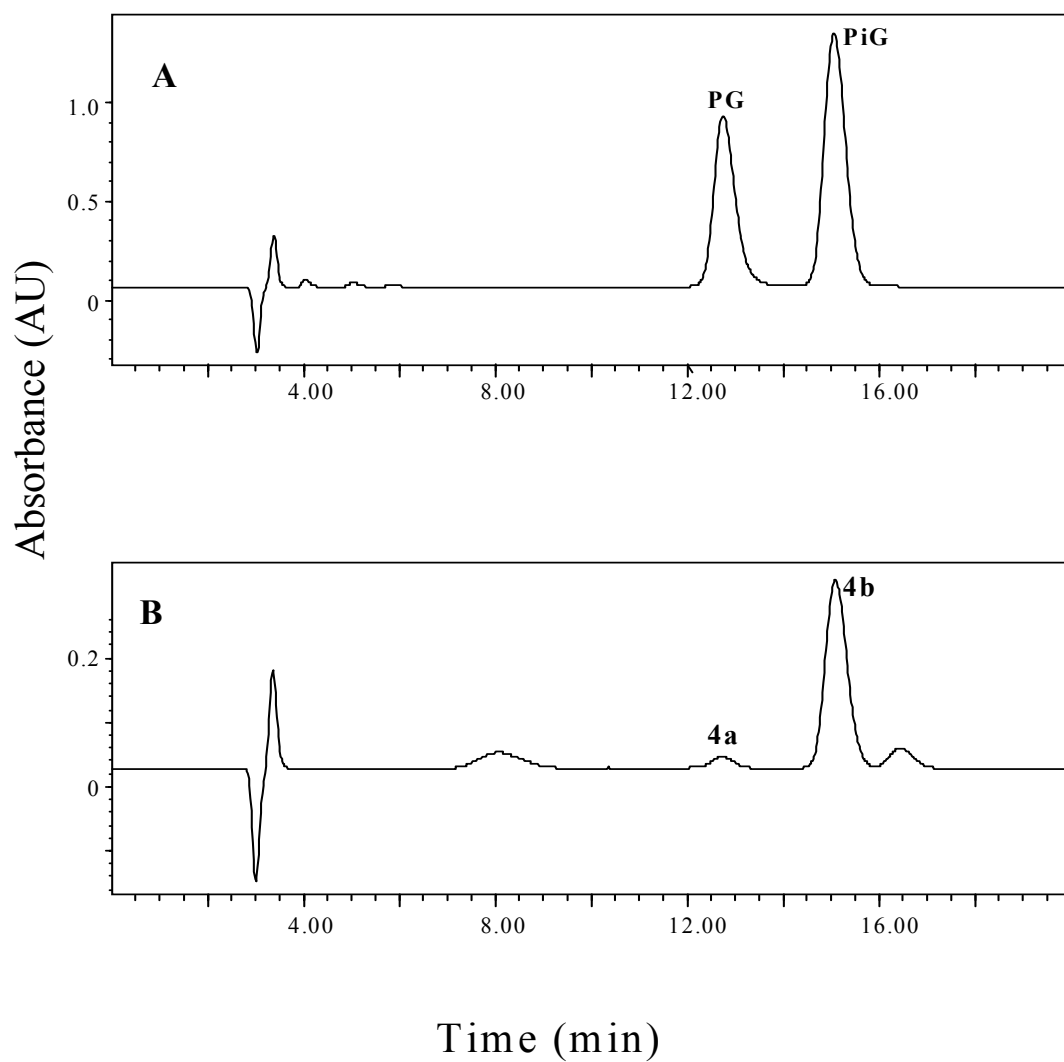


Figure 3.3 HPLC chromatograms using mobile phase containing cetyltrimethyl-ammonium bromide and 1-octanesulfonic acid showing complete separation of: (A) PG and PiG authentic standards; and (B) separation of the Peak 4 fraction from MMPs' urine into two peaks showing the presence of both PG and PiG.

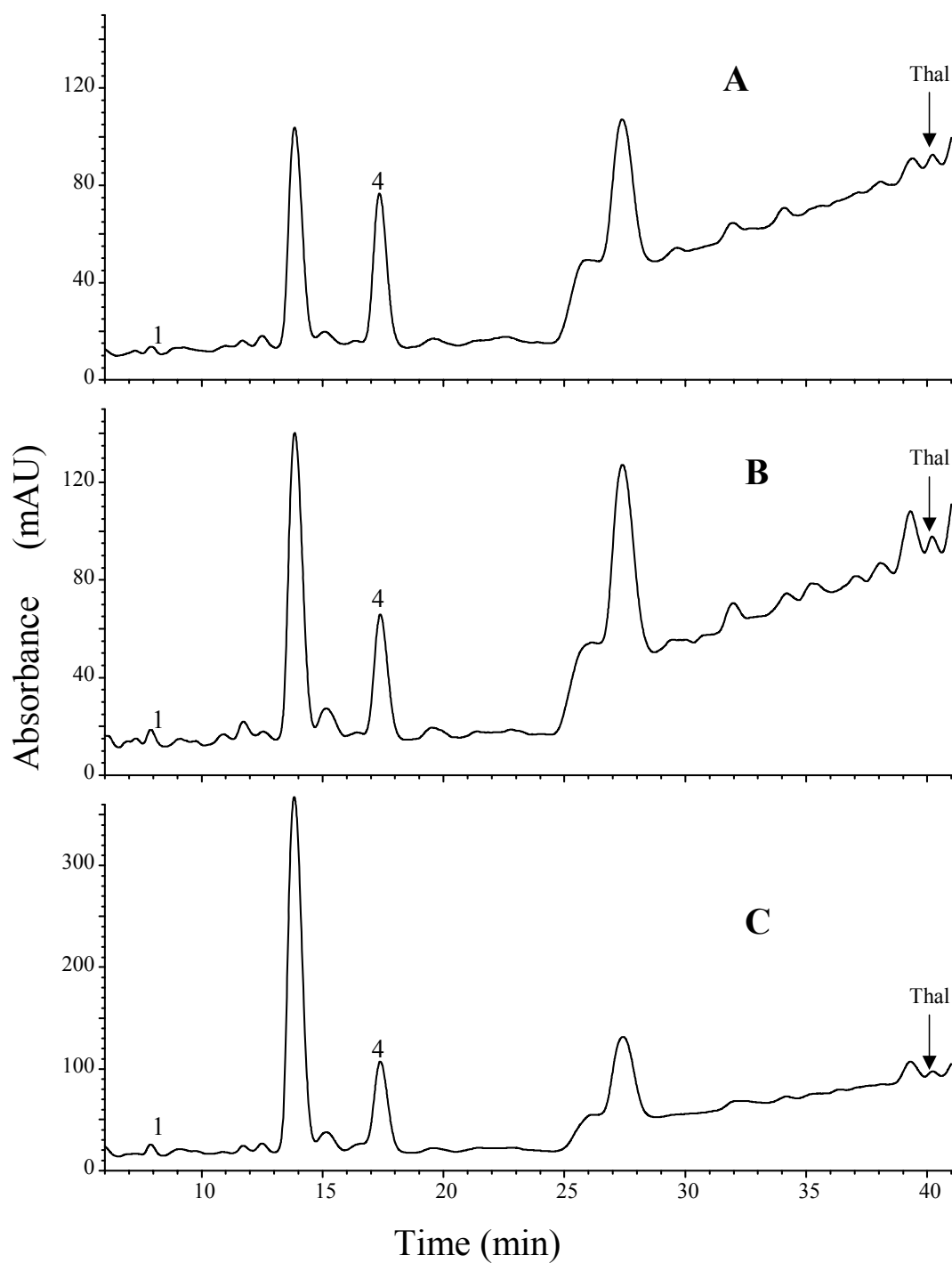


Figure 3.4 UV chromatograms of urine samples of Patient 1 collected on three occasions after Thal therapy. (A) one month, (B) two months, (C) three months.

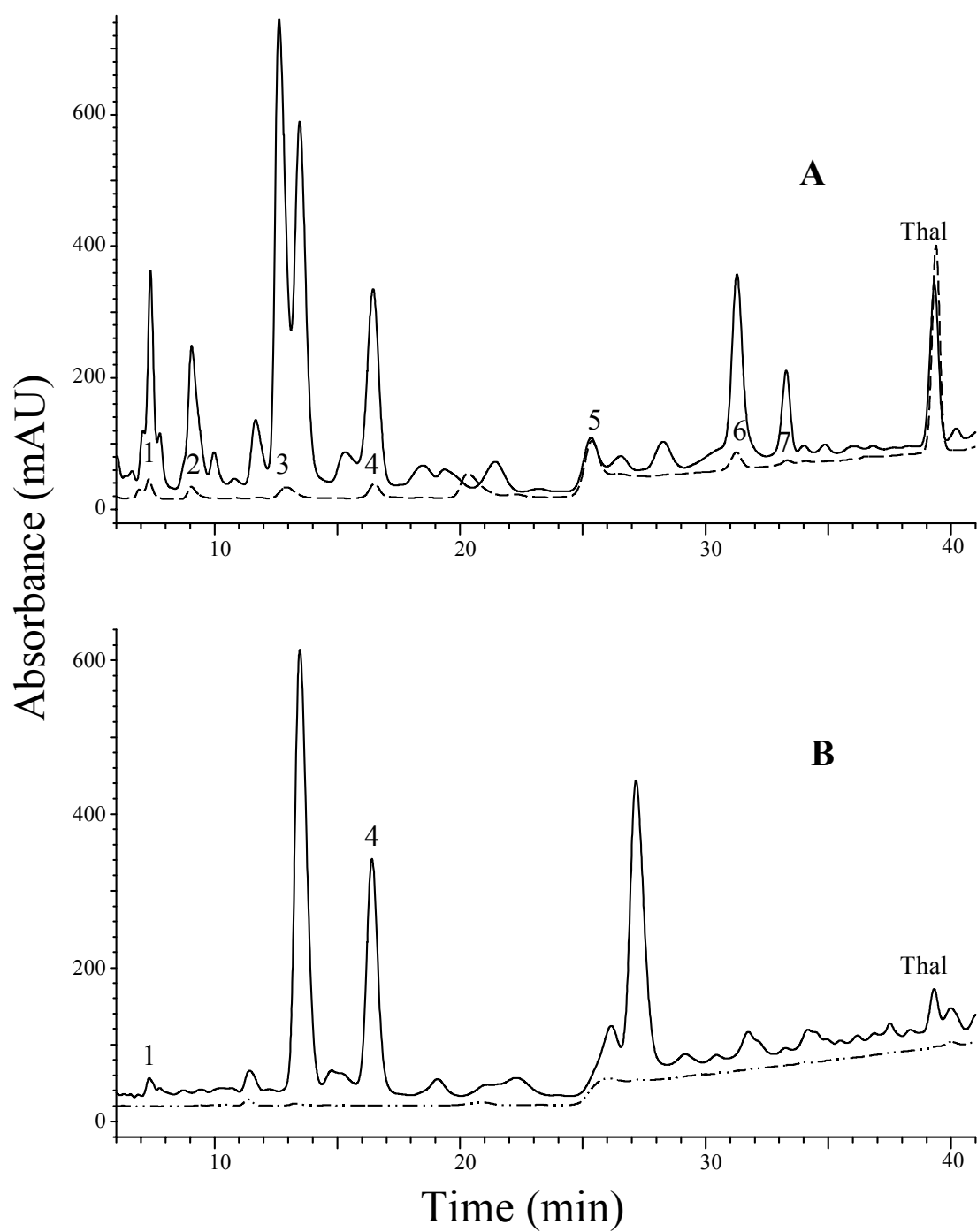


Figure 3.5 Comparison of UV-detected chromatograms of urine (solid lines) or plasma (dotted lines) from (A) mice given Thal (50 mg/kg, p.o.); and (B) patient 1 approximately 15 h after a prior dose of Thal (100 mg/day p.o.).

3.4. Discussion

Striking differences were found in the urinary thalidomide metabolite profiles between mice and patients with multiple myeloma. In the murine profiles, 7 peaks containing 8 metabolites formed by hydrolysis or hydroxylation were observed (Figure 2.1), while in the profiles of patients with multiple myeloma, only 3 products were detectable, all produced by hydrolysis (Figure 3.5, Table 3.1). Since p.o. and i.p. administration of thalidomide to mice produced essentially identical metabolite profiles (Figure 2.7), the differences are unlikely to be due to an altered route of administration. The differences therefore reflect differences in metabolism of thalidomide between mice and MMPs. Quantities of 5- and 5'-hydroxy thalidomide metabolites, thought to be produced by CYP2C19 activity in human liver microsomes, are approximately 20-fold and 10-fold lower than those obtained with liver microsomes from rodents respectively, where CYP2C6 is the primary enzyme responsible (Ando et al., 2002a). Thus, thalidomide appears a much poorer substrate for the human CYP enzymes involved compared with the equivalent rodent enzymes, explaining the lower level of hydroxylation of thalidomide in humans.

Since plasma samples were analysed in one patient only after 15 h of drug administration (Figure 3.5), the possibility that hydroxylated thalidomide metabolites are produced in plasma of humans but do not appear in urine cannot be excluded. However, in patients with Hansen's disease given a single oral dose of 400 mg thalidomide, no hydroxylated metabolites were detected in plasma and the 5-hydroxy metabolite, although detected in urine, was below the limits of quantitation (Teo et al., 2000a). Furthermore, in a study using healthy male volunteers, the plasma concentration of 5'-OH Th was of the order of 0.1% of that of thalidomide, even though both 5'- and 5-hydroxy metabolites were formed *in vitro* in the presence of human S9 liver fractions (Eriksson et al., 1998a). In addition to the intrinsically lower amounts of hydroxylation in humans, it is possible that this pathway is suppressed in MMPs as a result of their disease. A study involving 16 patients with advanced cancer showed a reduction in metabolic activity, correlating with decreased CYP2C19 activity, as

compared to healthy volunteers (Williams et al., 2000). However, Colon 38 tumour did not appear to influence the metabolite formation in mice (Section 2.3.1).

The lack of detectable hydroxylated metabolites in MMPs who were responding to thalidomide therapy, including 2 patients who had > 75% reduction in paraprotein levels, suggests that such metabolites are not responsible for the therapeutic effect in multiple myeloma. Furthermore, thalidomide alone does not exhibit anti-tumour activity in mice (Ching et al., 1995; Cao et al., 1999) although hydroxylation metabolites are present in plasma (Figure 2.9). Since hydroxylated metabolites have been implicated in the inhibition of angiogenesis, the results also imply that the primary mechanism of action of thalidomide in responding MMPs does not involve anti-angiogenesis. The results of this study are consistent with the proposed mechanism reviewed in Section 1.3.2 where thalidomide itself is the active agent and exerts its activity through immunomodulation. The progression of multiple myeloma is strongly dependent on TNF, IL-6, VEGF and bFGF production triggered by adhesion of the tumour cells to BMSCs (Suzuki et al., 1992; Gupta et al., 2001) (also see Section 1.3.2). Thalidomide's ability to inhibit the biosynthesis of a range of cytokines, including IL-1 β , IL-2, IL-4, IL-5, IL-6, IL-8, IL-10, IL-12, IFN- γ , bFGF, VEGF, TNF and Cox-2, is well documented (reviewed in Section 1.3.2), and the inhibition of growth factors necessary for tumour cell survival by thalidomide provides an alternative mechanism of action other than anti-angiogenesis in the therapy of multiple myeloma. Inhibition of cytokine biosynthesis by thalidomide is not dependent on prior hepatic activation, and occurs efficiently *in vitro* in the absence of metabolic enzymes (Sampaio et al., 1991). Rather, this activity is dependent on the intact parent compound and is lost upon hydrolysis (Shannon et al., 1997).

In summary, three major urinary metabolites in MMPs have been identified, all of which have resulted from hydrolysis. The lack of hydroxylation products in MMPs suggests that hydroxylated metabolites are not responsible for thalidomide's therapeutic effects against multiple myeloma.

Table 3.1 Comparison of metabolites in mouse and MMP urine samples.

Metabolites	Mice oral 50 mg/kg	Patient 1 Female 81y 100 mg	Patient 2 Female 47y 400 mg	Patient 3 Male 50y 200 mg	Patient 4 Male 55y 100 mg	Patient 5 Male 63y 400 mg	Patient 6 Male 68y 200 mg	Patient 7 Female 75y 300 mg
<u>Hydrolysis</u>								
CG (1)*	+	+	+	+	+	+	+	+
PG (4a)	+	+	+	+	+	+	+	+
PiG (4b)	+	+	+	+	+	+	+	+
<u>Hydroxylation</u>								
5'-OH CG (2)	+	-	-	-	-	-	-	-
Thal-5- <i>O</i> -G** (3)	+	-	-	-	-	-	-	-
<i>cis</i> -5'-OH Th (5)	+	-	-	-	-	-	-	-
<i>trans</i> -5'-OH Th (6)	+	-	-	-	-	-	-	-
5-OH Th (7)	+	-	-	-	-	-	-	-

*Numbers in brackets represent peak numbers observed in chromatograms (see Figures 2.1 & 3.1).

** Thalidomide-5-*O*-glucuronide.

CHAPTER 4. COMPARISON OF THALIDOMIDE METABOLITE FORMATION IN MICE, RABBITS AND MULTIPLE MYELOMA PATIENTS

4.1. Introduction

The biological effects of thalidomide vary in different species. Thalidomide is teratogenic in humans as well as in rabbits, but is non-teratogenic in rodents (Fabro et al., 1965; Schumacher et al., 1968b; Scott et al., 1977; Neubert and Neubert, 1997). The anti-tumour activity of thalidomide is generally in line with its teratogenicity in those species. Thalidomide does not exhibit significant anti-tumour activity in mice (Ching et al., 1995; Gutman et al., 1996; Myoung et al., 2001) (reviewed in Section 1.2.1), but has shown some activity in a rabbit tumour model (Verheul et al., 1999). It is effective in treating human malignancies particularly against multiple myeloma (Fife et al., 1998; Singhal et al., 1999; Barlogie et al., 2001a; Figg et al., 2001) (reviewed in Section 1.2). The basis for the inter-species differences in its biological effects is not clear.

The studies of Chapters 2 and 3 showed that thalidomide metabolite profiles in mice and MMPs were different. Hydroxylated metabolites were found in plasma and urine of mice but not in urine of MMPs. However, the dose of thalidomide administered was higher in mice than in humans, raising the question of whether the difference was due to different plasma concentrations of thalidomide. Furthermore, MMPs may have suppressed metabolic enzyme activity due to their disease. In this Chapter, healthy New Zealand White rabbit, a species that is similar to human in its sensitivity to thalidomide, is included in this study, and metabolite formation in mice, rabbit and MMPs, all receiving thalidomide at similar doses, is compared using a modified analytical method that allows PG and PiG to be resolved in one HPLC run. The objectives of this study are:

- a) To detect and identify all the major metabolites formed *in vivo* in three species, mice, rabbits and MMPs, administered with similar doses of thalidomide.
- b) To compare metabolite formation of those three species to determine if there is a relationship to their responsiveness to thalidomide.

4.2. Methods

4.2.1. Murine Studies

Thalidomide was dissolved in 2-hydroxypropyl- β -cyclodextrin (HPCD) (1 mg/ml) and administered p.o. using gavage needle or intravenous (i.v.) via tail-vein (2 mg/kg, 2 μ l/g body weight). In another set of experiments, thalidomide was administered p.o. or i.v. at a dose of 20 mg/kg dissolved in 30% DMSO in polypropylene glycol solution (8 mg/ml). Mice were bled at 5 min, 15 min, 30 min, 1 h, 2 h, 4 h, and 6 h after treatment. Three mice were used for each time point plus an untreated control group. The mice used for the 6 h time point were placed in metabolic cages with water and food, and urine collected over the first 4 h after treatment. Blood samples were collected into heparinized tubes during terminal halothane (NZ Pharmacology Ltd., Christchurch, New Zealand) anaesthesia, centrifuged, and the plasma removed. Plasma (300 μ l), and urine (100 μ l) were acidified by adding 10% TCA up to 1 ml. Samples were centrifuged at 3000 $\times g$ for 10 min to remove precipitated protein, and then processed using solid phase extraction as previously described (Section 2.2.3.1). Dried plasma and urine residues were reconstituted in 100 μ l and 1000 μ l mobile phase respectively for analysis.

4.2.2. Rabbit Studies

Three female New Zealand White rabbits supplied by Animal Resource Unit of the University of Auckland were used between 6-12 months old for all the experiments according to institutional ethical guidelines. Thalidomide was dissolved in HPCD (1 mg/ml) and administered p.o. using a polyethylene plastic tube, or i.v. via ear-vein injection (2 mg/kg in a volume of 2 ml/kg). Following drug administration, rabbits

were placed in metabolic cages with water and food for urine collection over a 6 h period. Blood samples were collected into heparinized tubes from the ear-vein at 15 min, 30 min, 1 h, 2 h, 3 h, 4 h, 6 h and 8 h for the p.o. studies, and at 15 min, 30 min, 1 h, 1.5 h, 2 h, 3 h, 4 h and 8 h for i.v. studies. Control urine and plasma samples for each rabbit were obtained prior to thalidomide administration. Plasma (300 µl) and urine (100 µl) were processed as described for the murine samples (see Section 4.2.1). Dried residues were reconstituted in 200 µl or 100 µl mobile phase respectively for urine and plasma samples.

4.2.3. Clinical Studies

Three male and two female Caucasian patients who were beginning their thalidomide therapy for refractory multiple myeloma at Auckland Hospital were recruited for these studies with ethical approval and consent. Their ages ranged from 42-81 years, and weights from 52-105 kg. All patients had been instructed not to take non-prescription medications or to drink alcohol. Patients received their first dose of thalidomide (2 x 100 mg tablets p.o.) after a meal. Blood was collected into heparinized tubes at various times up to 24 h after thalidomide, and urine samples were collected whenever possible. A control sample of blood and urine were obtained from the patients before treatment. Blood samples were centrifuged and plasma collected and quickly stored at –80°C until analysis. Plasma (300 µl) were acidified by adding 10% TCA up to 1 ml and centrifuged to remove precipitated protein. Urine samples (3.33 ml each) were acidified by adding 10% TCA up to 10 ml. All samples were processed as described for murine samples (see Section 4.2.1). Dried residues from plasma and urine samples were reconstituted in 100 µl and in 1000 µl mobile phase, respectively.

4.2.4. Metabolite Detection and Identification

Metabolite detection and identification performed using LC-MS and HPLC procedures described in Sections 2.2.3.2 & 2.2.3.3 does not allow the separation of PG and PiG in one HPLC run. The studies in this section have used a modified procedure that resolves PG from PiG in the same HPLC run. This was achieved by altering the proportions of

mobile phase: solution A (80% ACN, 1% glacial acetic acid and 19% Milli Q water) and solution B (9.5% ACN, 1% glacial acetic acid and 89.5% Milli Q water) to improve the resolution. In addition, the mass spectral detection was also simultaneously set on 3 signals: **Signal 1**, negative TIC mode, with a molecular weight range of 70 to 1000 amu; **Signal 2**, positive SIM mode at the molecular weights 259, 275, 277, 278, 291, 293, 295, 296 and 451; and **Signal 3**, negative single-ion monitoring mode, with the sensitivity of 1 pg, at the molecular weights 257, 273, 275, 276, 289, 291, 293, 294 and 449 (corresponding to each of the metabolite peak or possible metabolite). This provided greater sensitivity in metabolite detection with reduced background noise using SIM detection, and still maintaining background information from UV and MS TIC detections.

4.3. Results

4.3.1. Thalidomide Metabolite Profile in Mice

The metabolite profiles in mouse plasma and urine after administering thalidomide 2 mg/kg was similar to those after high dose (50 mg/kg or 100 mg/kg), with the exception that using the modified method, PiG (Peak 5) is separated from PG (Peak 7) and *cis*- and *trans*- 5'-OH CG were separated into two peaks (Peaks 2 & 4) (Figure 4.1). Based on their relative polarities, peak 2 and peak 4 would be expected to be the *cis*- and the *trans*-isomer respectively, but this has yet to be validated with authentic standards. With this method, Peaks 1, 5 and 7 corresponded to hydrolysis products, while Peaks 2, 4, 6, 8, 9 and 10 corresponded to hydroxylated and glucuronidated metabolites (Table 4.1; Figure 4.1). Urine samples contained the same peaks with the addition of Peak 3, *N*-(*o*-carboxybenzoyl)isoglutamine, which was masked in plasma samples by a background component present in untreated controls (Figures 4.1 & 4.2). Although i.v. or p.o. administration produced the same number of metabolite peaks, the plasma metabolite peaks at 2 h or earlier were higher after i.v. administration (Figure 4.3) compared with p.o. administration (Figure 4.1).

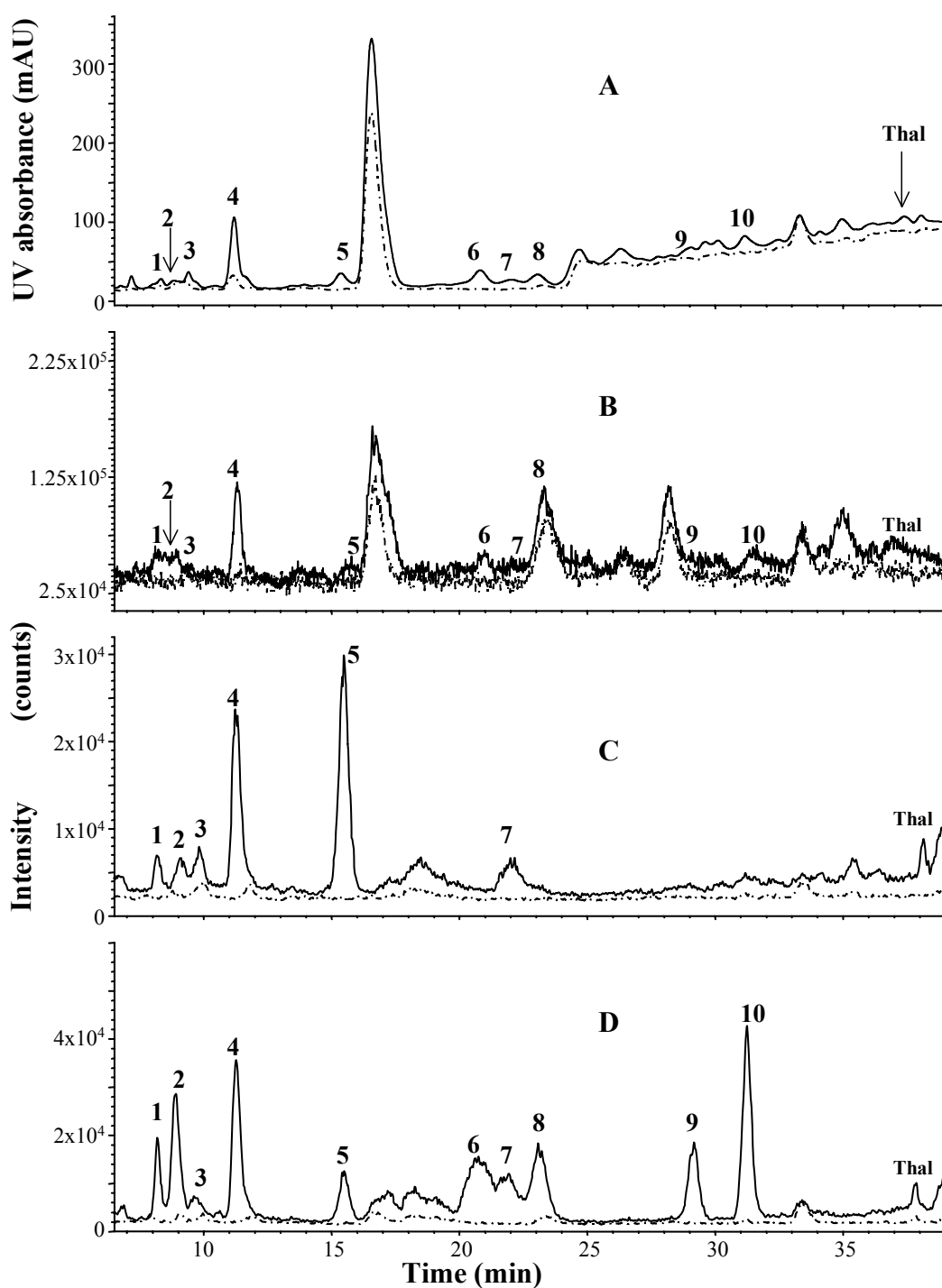
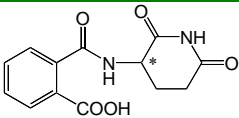
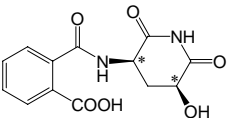
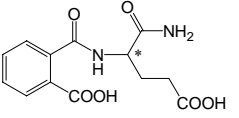
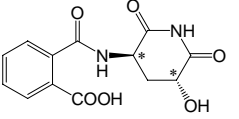
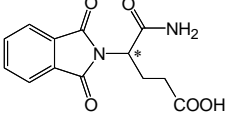
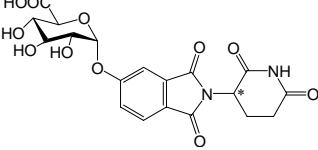
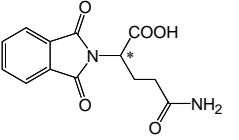
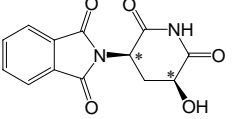
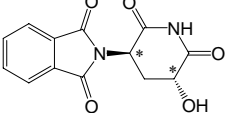
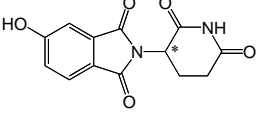


Figure 4.1 Chromatograms of urine from mice without treatment (dotted lines) and up to 4 h following oral administration of Thal (2 mg/kg, solid lines) recorded by: (A) UV at 230 nm, (B) MS at negative TIC mode (Signal 1), (C) MS at positive SIM mode (Signal 2), (D) MS at negative SIM mode (Signal 3).

Table 4.1 Metabolite peaks in mouse urine LC-MS profiles after thalidomide oral treatment.

Peak No.	Molecular Weight	Metabolite	Structure
1*	276	CG	
2 ^{# a}	292	<i>cis</i> -5'-OH CG	
3*	294	<i>N</i> -(<i>o</i> -carboxybenzoyl)isoglutamine	
4 ^{# a}	292	<i>trans</i> -5'-OH CG	
5*	276	PiG	
6 [#]	450	thalidomide-5- <i>O</i> -glucuronide	
7*	276	PG	
8 [#]	274	<i>cis</i> -5'-OH Th	
9 [#]	274	<i>trans</i> -5'-OH Th	
10 [#]	274	5-OH Th	

* hydrolysis metabolite, [#] metabolite formed via hydroxylation, ^a Proposed metabolite.

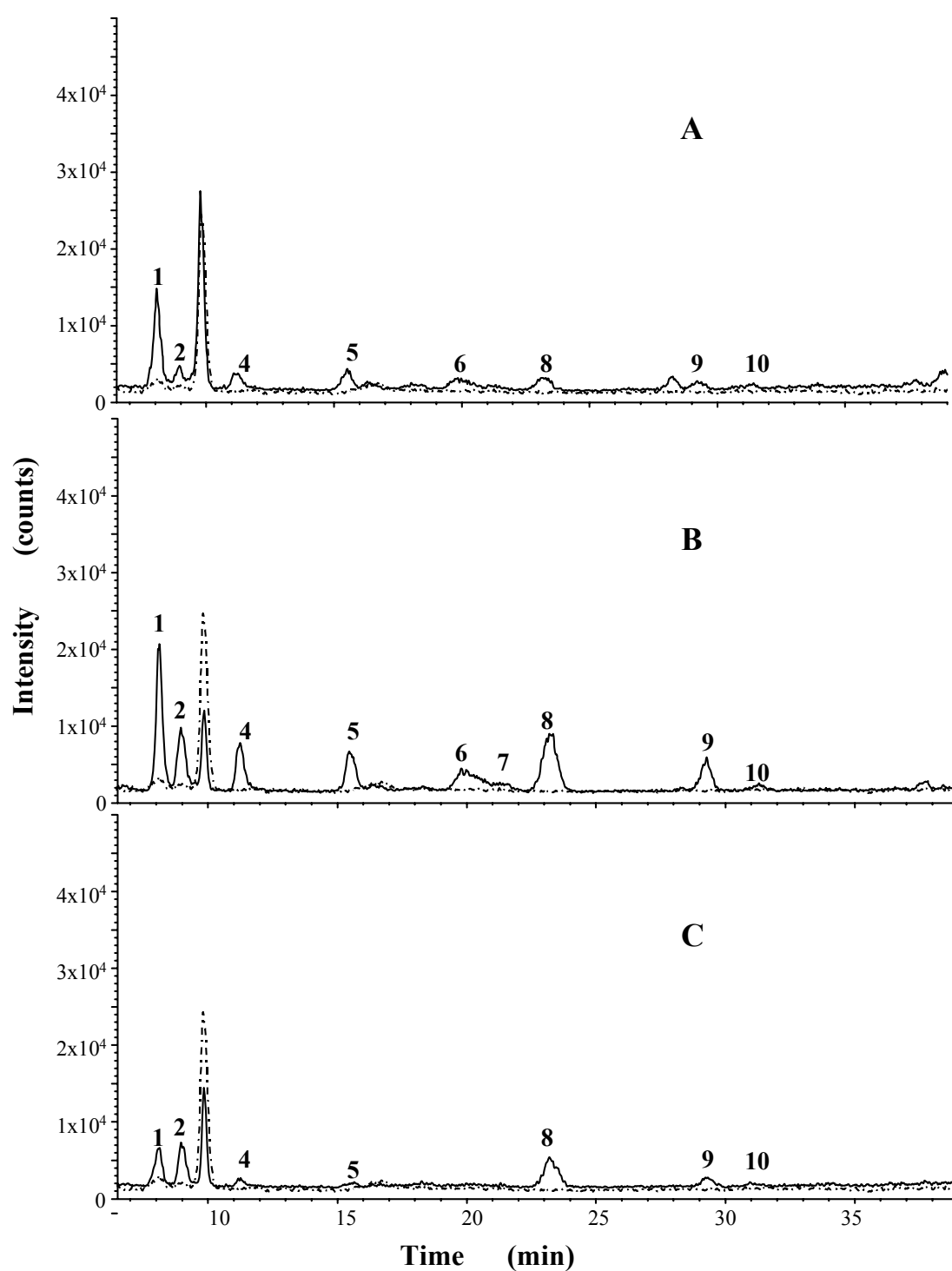


Figure 4.2 Negative SIM mode (Signal 3) MS-detected chromatograms of mouse plasma samples collected before (dotted lines) and after (solid lines) p.o. treatment of Thal (2 mg/kg). (A) 5 min, (B) 30 min, (C) 4 h.

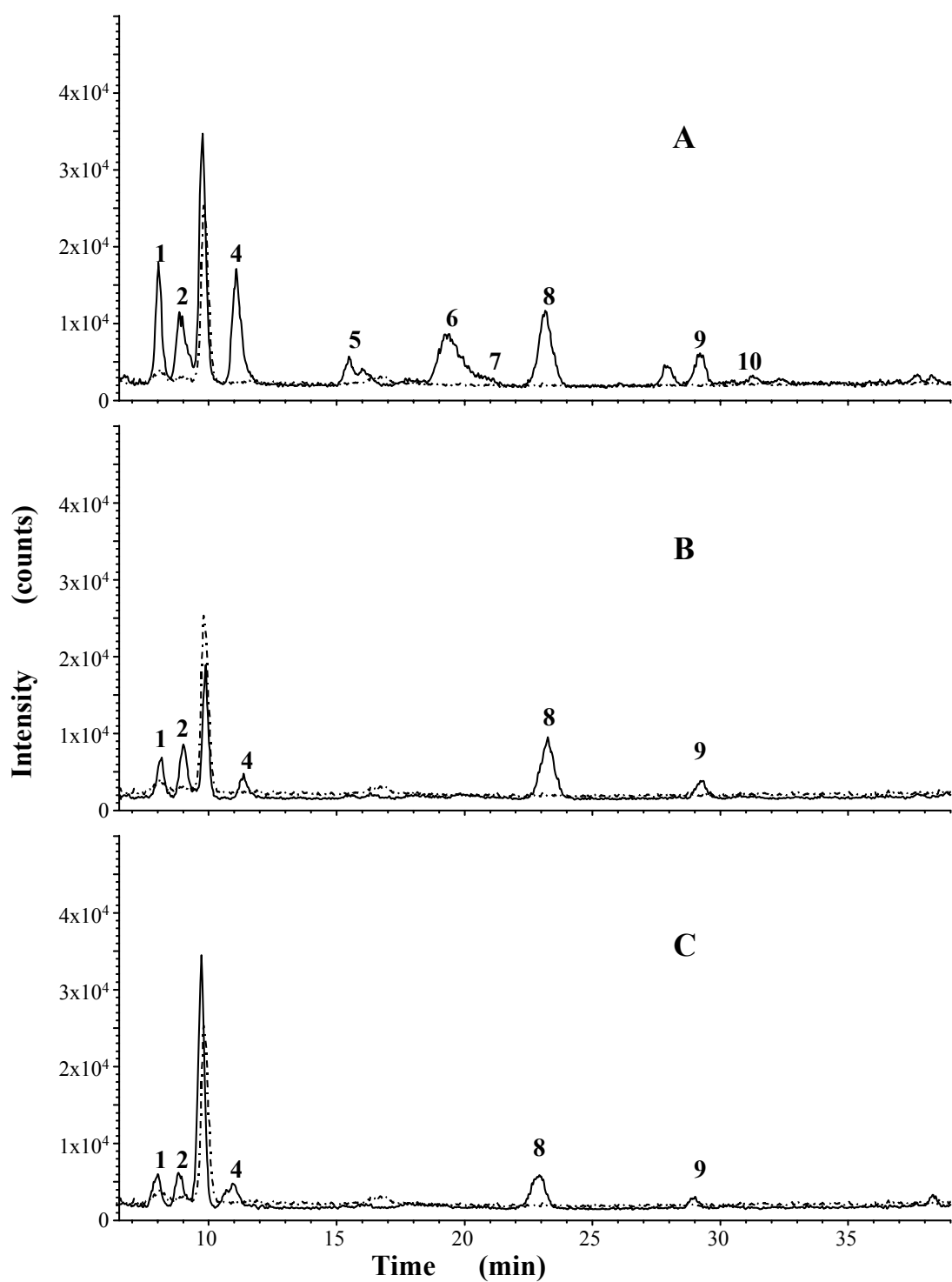


Figure 4.3 Negative SIM mode (Signal 3) MS-detected chromatograms of mouse plasma samples collected before (dotted lines) and after (solid lines) i.v. treatment of Thal (2 mg/kg). (A) 1 h, (B) 2 h, (C) 4 h.

4.3.2. Thalidomide metabolites in rabbits

Following p.o. administration (2 mg/kg) of thalidomide to rabbits, LC-MS plasma metabolite profiles were determined and the data were compared with parent drug concentrations, which were reported in a recent study by Chung et al.(2004a) investigating the disposition of thalidomide in this species. It was found that two different metabolic profiles existed in relation to the concentration of thalidomide in plasma. At all time points when the concentration of thalidomide was below 1 μ M, the metabolite profile showed hydrolysis products only (Peaks 1, 5 & 7) (Figures 4.4A & 4.4C). However, when the thalidomide plasma level was above 1 μ M, whether that was during the absorption or the elimination phase, hydroxylated metabolites (Peaks 2, 4, 6 & 8) were detected in addition to the hydrolysis products (Peaks 1, 3 & 5) (Figure 4.4B). While the MS peak areas of hydrolysis peaks, such as Peak 1 and Peak 5 were similar to each other in rabbit and mouse samples, the MS peak areas of Peaks 2, 4, 6 and 8 in rabbit samples were 26.8%, 43.7%, 3.6% and 6.2% respectively of their corresponding peak in murine samples, indicating a lower level of hydroxylation in rabbits compared with mice. Urine samples contained hydrolysis products (Peaks 1, 3 & 5) only (Figure 4.5A). Following i.v. administration, plasma samples collected before 2 h, when thalidomide concentration was above 1 μ M, hydrolysis (Peaks 1, 3 & 5) and hydroxylated products (Peaks 2, 4, 6, 8, 9 & 10) were detected (Figures 4.6A & 4.6B). However, after 2 h, when thalidomide concentrations had dropped below 1 μ M, the metabolite profiles showed only hydrolysis products (Peaks 1, 5 & 7) (Figure 4.6C). Urine samples following i.v. administration showed two hydrolysis products (Peaks 1 & 5) and one hydroxylation product (Peak 10) (Figure 4.5B).

4.3.3. Thalidomide Metabolites in Patients

Consistent with the results of Chapter 3, all plasma and urine samples from MMPs contained only Peaks 1, 5 and 7, corresponding to the hydrolysis products. Hydroxylated metabolites were not detected at any time point in plasma or in urine (Figures 4.7 & 4.8).

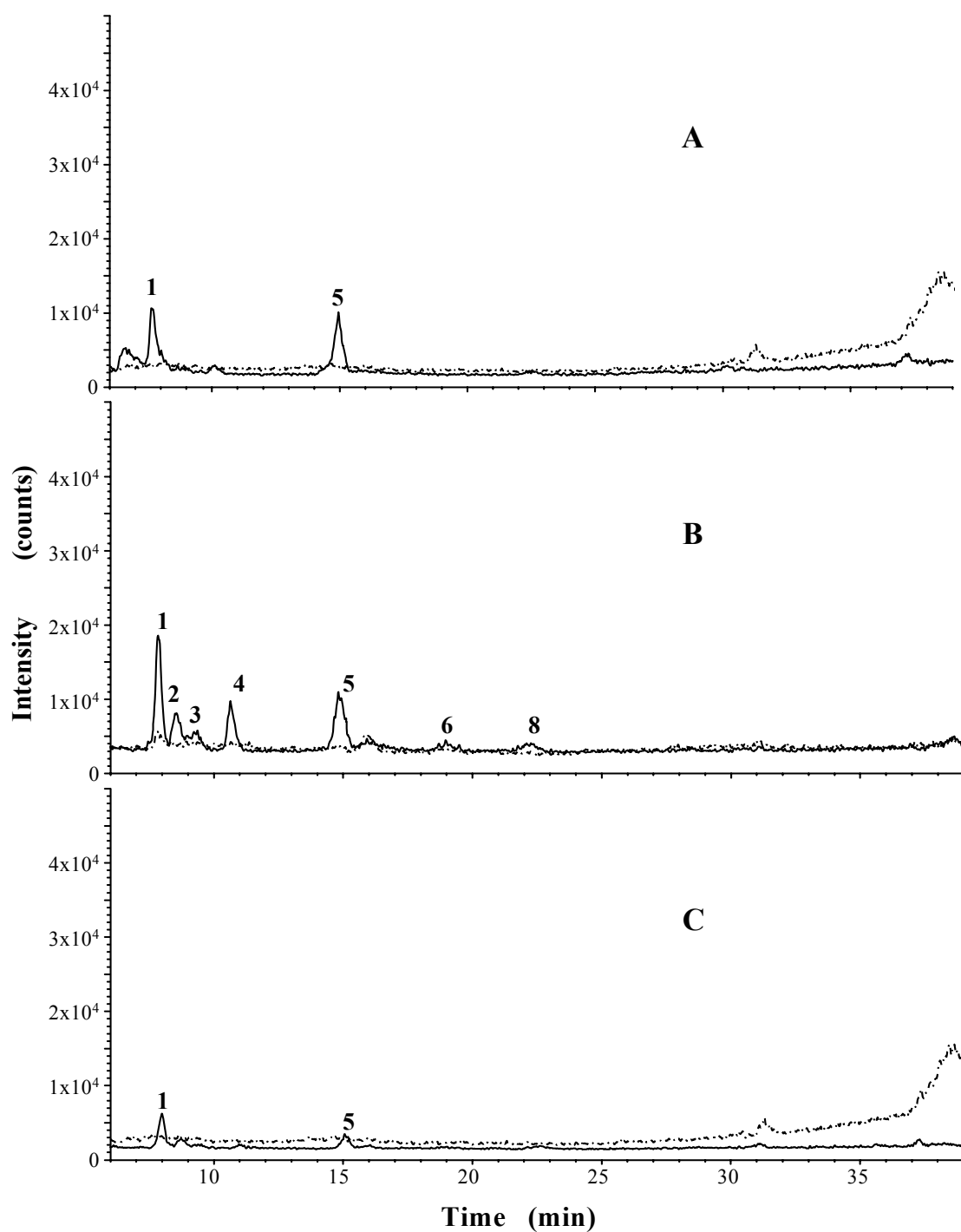


Figure 4.4 Negative SIM mode (Signal 3) MS-detected chromatograms of rabbit plasma samples collected before (dotted lines) and after p.o. treatment (solid lines). (A) 30 min, (B) 2h, (C) 6 h.

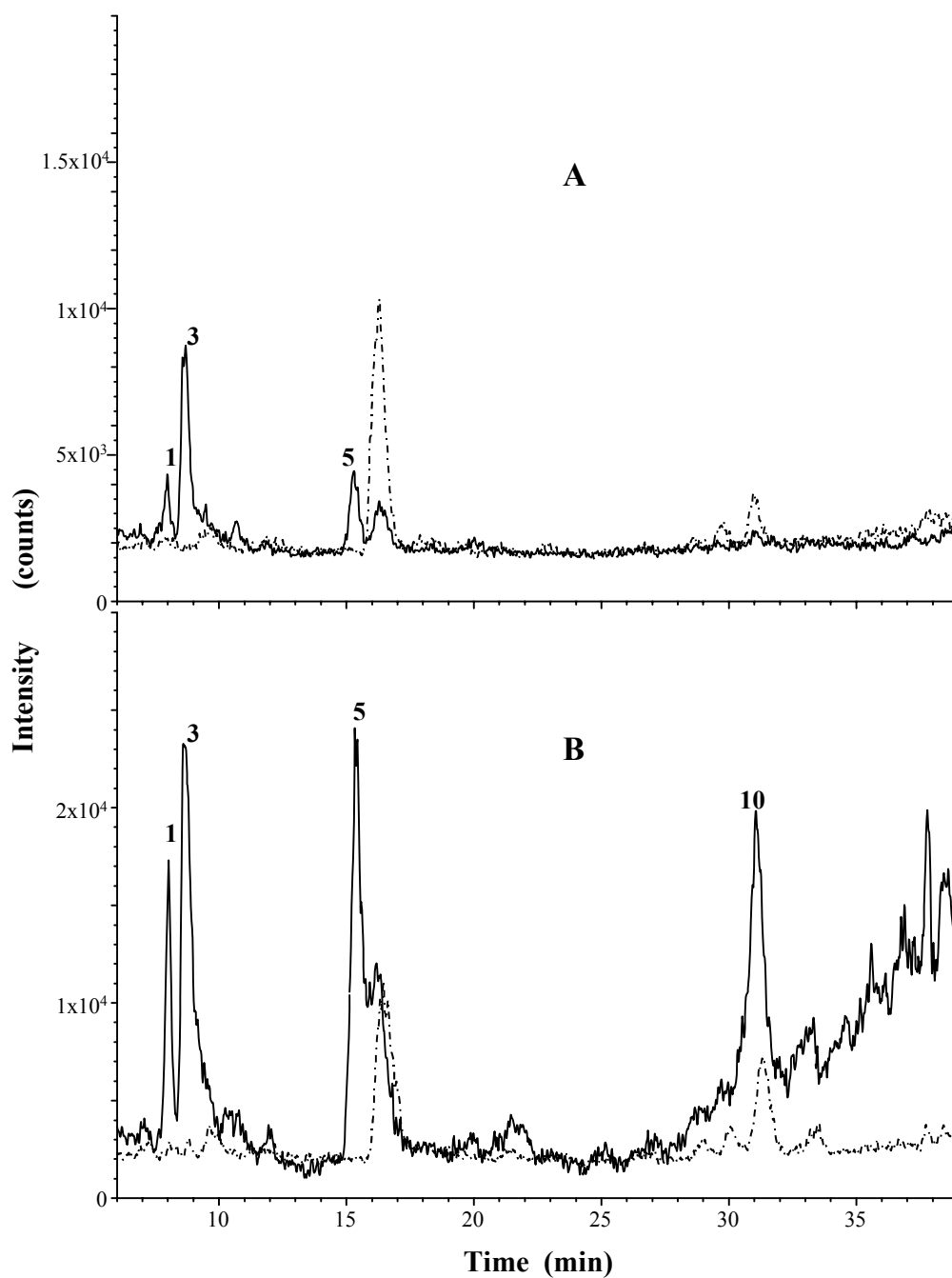


Figure 4.5 Negative SIM mode (Signal 3) MS-detected chromatograms of rabbit urine samples collected before (dotted lines) and after treatment (solid lines). (A) 3 h after p.o. administration, (B) 3 h after i.v. injection.

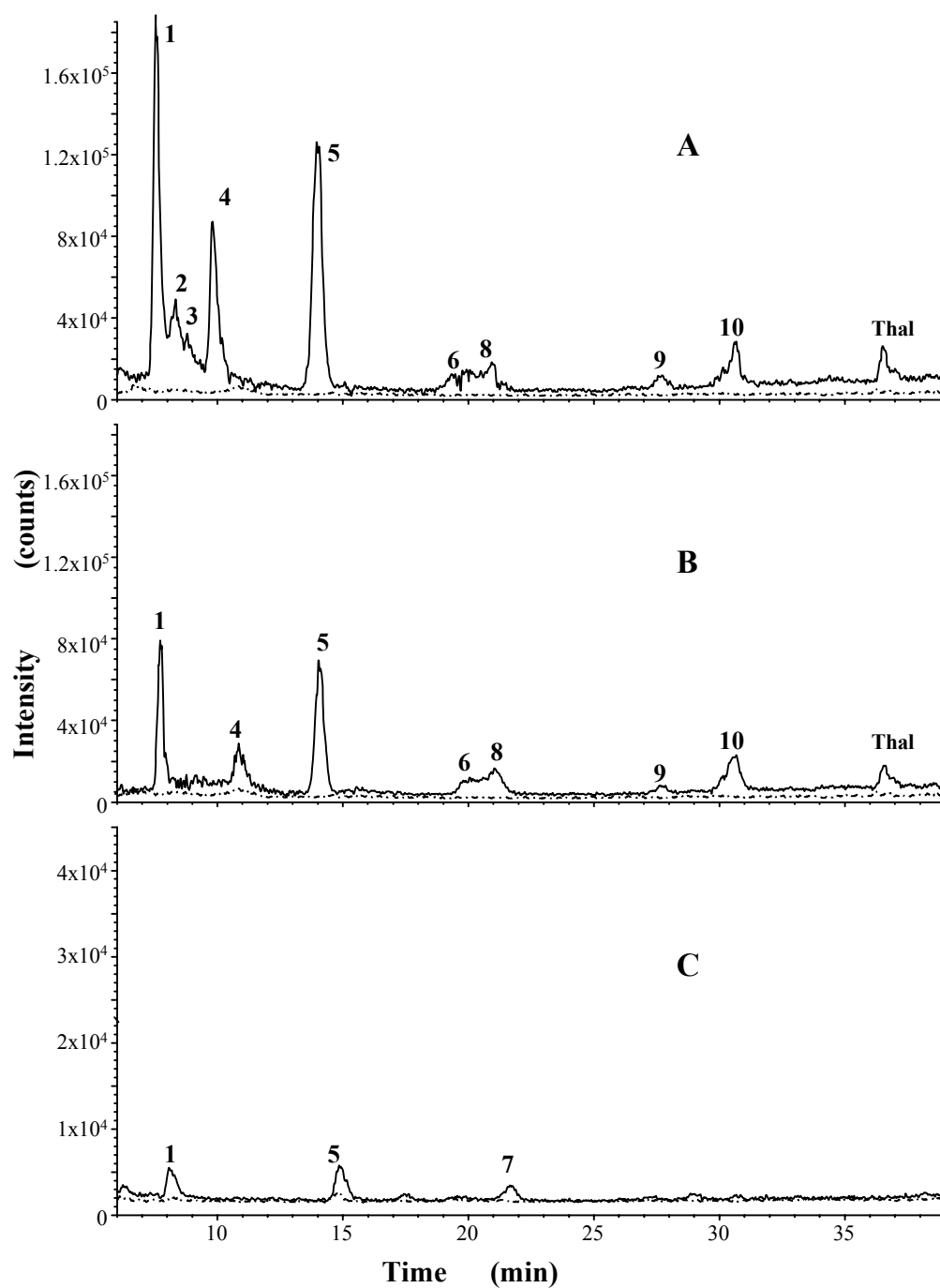


Figure 4.6 Negative SIM mode (Signal 3) MS-detected chromatograms of rabbit plasma samples collected before (dotted lines) and after i.v. treatment (solid lines). (A) 30 min, (B) 2h, (C) 4 h.

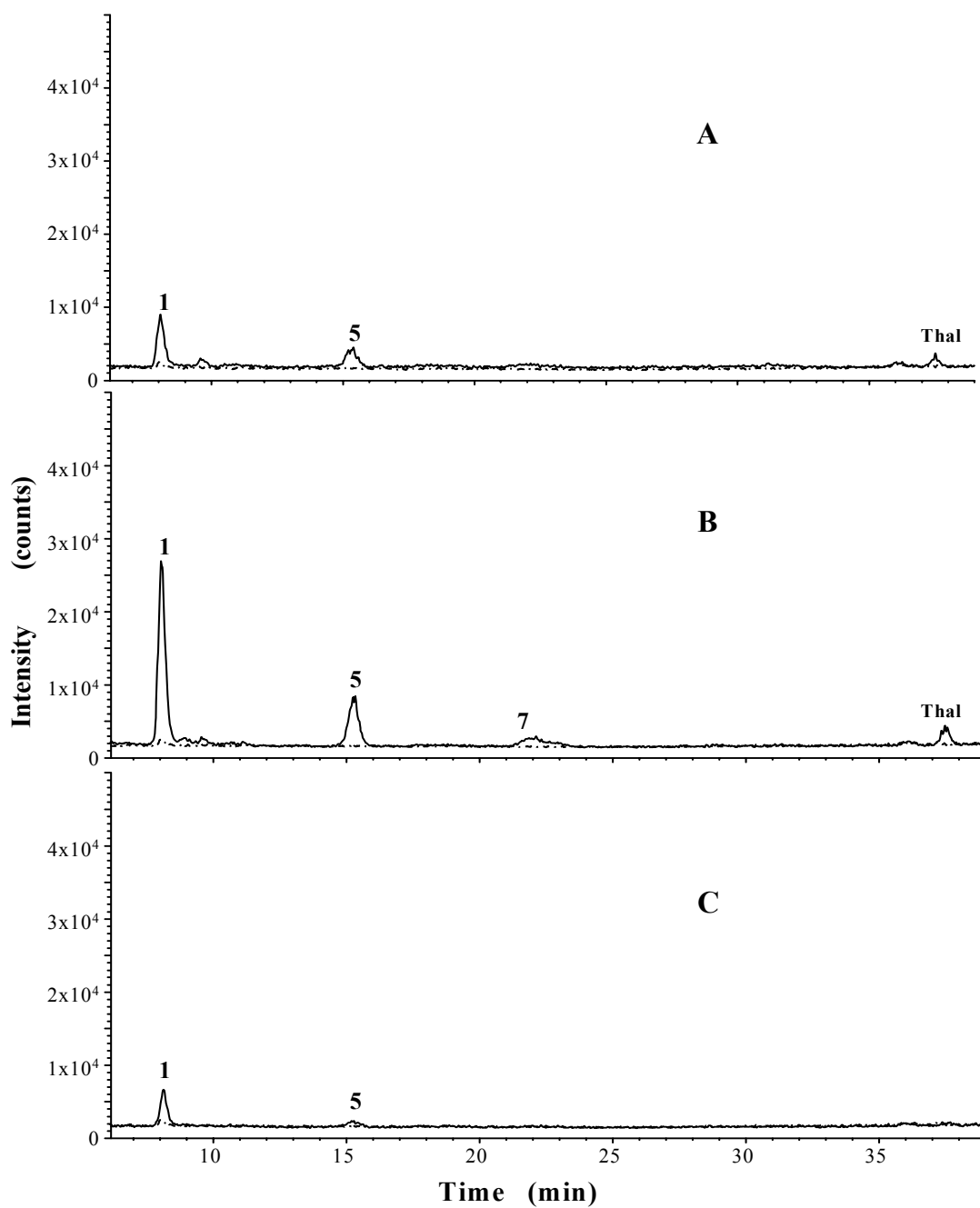


Figure 4.7 Negative SIM mode (Signal 3) MS-detected chromatograms of MMP plasma samples collected before (dotted lines) and after treatment (solid lines). (A) 1 h, from MMP 8, (B) 4 h, from MMP 10, (C) 24 h, from MMP 11.

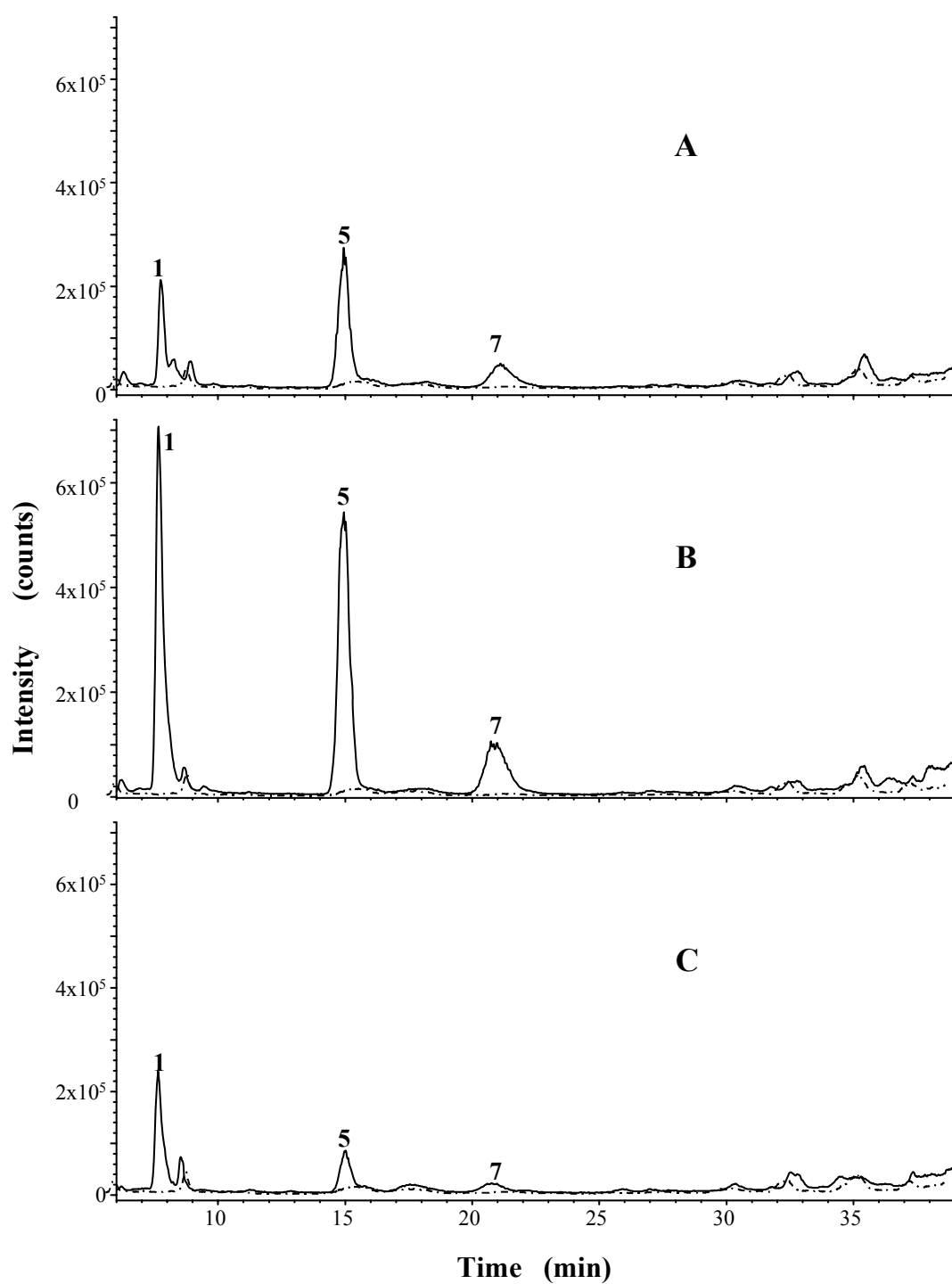


Figure 4.8 Negative SIM mode (Signal 3) MS-detected chromatograms of MMP 12 urine samples collected before (dotted lines) and after treatment (solid lines). (A) 4 h, (B) 8 h, (C) 24 h.

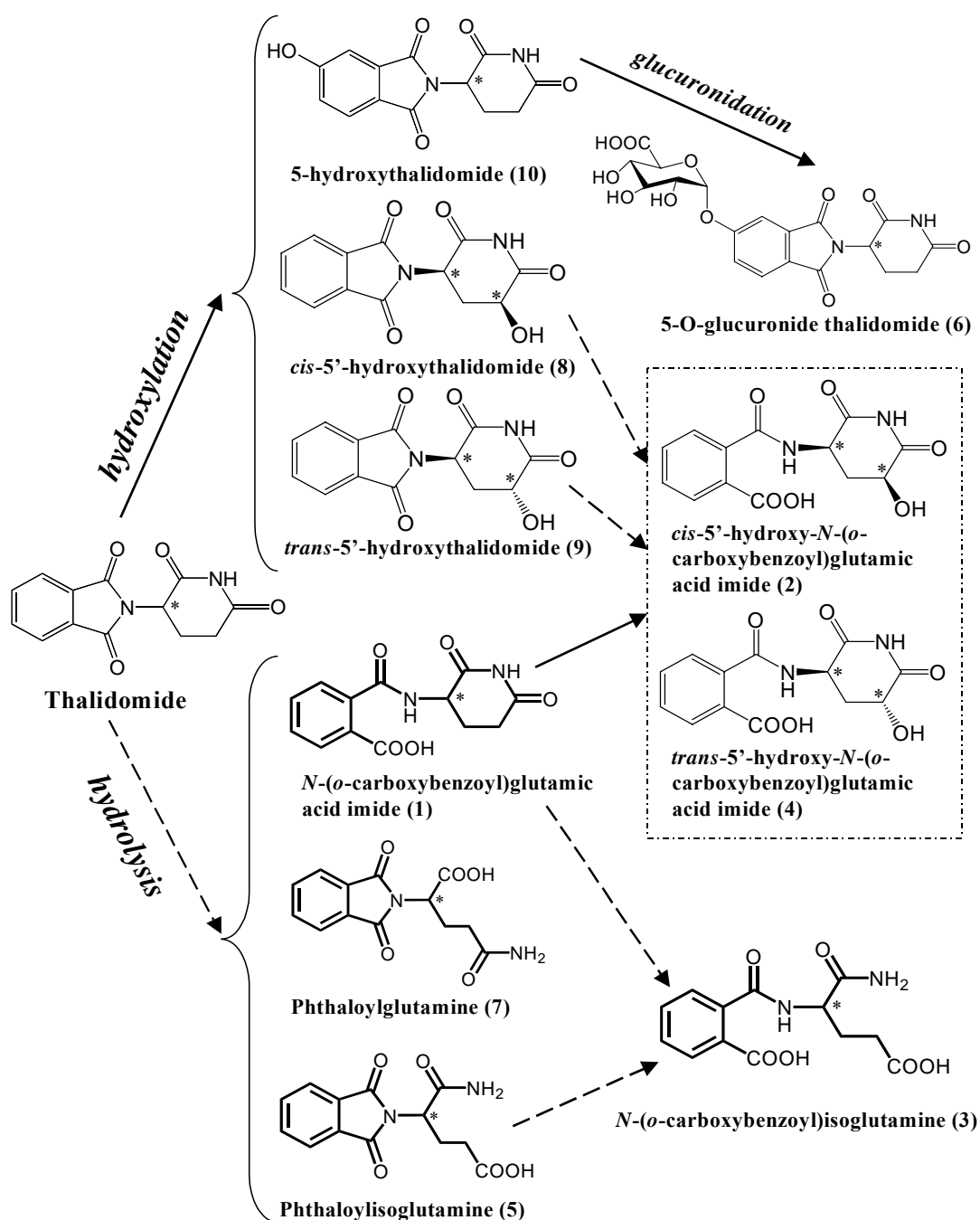


Figure 4.9 Thalidomide metabolism by hydrolysis (arrows with dashed lines) and CYP hydroxylation and UDPG transferase-mediated glucuronidation (arrows with solid lines) in mice, rabbits and MMPs. Unconfirmed metabolites are shown in dotted lines. Structures in bold are products formed via hydrolysis only. Numbers in brackets represent metabolite peak number in chromatograms.

4.4. Discussion

In mice, 10 metabolite peaks containing hydrolysis, hydroxylation and glucuronidation products were detectable in urine and plasma within 30 min of i.v. or p.o. administration (Figures 4.1 – 4.3). Hydroxylation products were detectable in rabbits only if the thalidomide concentration was above 1 μM in the plasma, irrespective of the route of administration and the phase of the pharmacokinetic profile (Figures 4.5 & 4.7). Hydroxylated products were not detected at any time point in any of the five MMPs in this study (Figures 4.7 & 4.8) and the results are consistent with those from Chapter 3. The biotransformation pathways for thalidomide that yield the various metabolites detected are summarized in Figure 4.9. It has been demonstrated that less than 1 % of the administered thalidomide dose was excreted, unchanged, in urine of most animals including mice, rabbits and humans (Williams et al., 1965). Therefore, the majority of the absorbed thalidomide is excreted in the form of metabolites (Schumacher et al., 1965a; Williams et al., 1965). Hydroxylation of thalidomide occurs extensively in mice, moderately in rabbits, but is undetectable in patients. Since hydroxylated and glucuronidated metabolites are much more soluble than the parent drug, greater metabolism along this pathway would facilitate more rapid elimination of thalidomide from the system. Consistent with this, a reverse correlation between the rate of elimination, reflected by $t_{1/2}$ (Chung et al., 2004a), and the amount of hydroxylation in the three species was obtained, suggesting that the inter-species differences in thalidomide pharmacokinetics are related to the rate at which it is hydroxylated. The results of this study are also consistent with previous reports that hydroxylated metabolites are barely detectable in humans (Teo et al., 2000a; Ando et al., 2002b), and thalidomide is an extremely poor substrate for the human CYP450 isoenzymes compared with those responsible in rodents (Teo et al., 2000a; Ando et al., 2002a).

If the parent drug rather than a hydroxylated metabolite is responsible for the *in vivo* effects, then thalidomide would be expected to be more effective in a species where it is slowly metabolised and eliminated. Consistent with this proposal, humans are more susceptible than rodents to the many of effects of thalidomide. While clinical responses

have been reported for human malignancies (Fife et al., 1998; Singhal et al., 1999; Barlogie et al., 2001a; Figg et al., 2001) (reviewed in Section 1.2), anti-tumour activity following single or multiple applications of thalidomide in mice has been difficult to obtain (Ching et al., 1995; Gutman et al., 1996; Myoung et al., 2001) (reviewed in Section 1.2.1). Based on their extent of metabolism, rabbits would be expected to be intermediate between humans and mice in their responsiveness to thalidomide, and it has been reported that daily high doses of thalidomide are effective in inhibiting tumour growth rabbits (Verheul et al., 1999). The susceptibility of rabbits at high doses, humans at low doses, and the resistance of rodents to thalidomide's teratogenicity (Schumacher et al., 1968b; Neubert and Neubert, 1997) also correlate with the metabolism and elimination of the parent drug.

Inter-individual variability in thalidomide metabolite formation was not observed in MMPs in this study despite differences in age (42-81 years), weight (52-105 kg), sex, and disease status. Nor were there any differences among metabolite profiles of MMPs in the previous study (Chapter 3). Thus, factors apart from drug metabolism are more important in determining a patient's outcome to thalidomide treatment. A recent study showed that MMPs who are genetically high TNF producers, respond better to thalidomide therapy (Neben et al., 2002b).

In conclusion, a method that allows the major thalidomide metabolites to be detected in a single HPLC run using LC-MS has been developed. Large inter-species difference in the degree to which it undergoes hydroxylation is seen that appears related to their responsiveness to thalidomide. The results suggest that species that metabolise and eliminate thalidomide quickly will be less responsive to the effects of the drug. Inter-species sensitivity to the activity of thalidomide is consistent with the extent of metabolism.

CHAPTER 5. IN VITRO METABOLISM OF THALIDOMIDE IN MURINE, RABBIT AND HUMAN LIVER MICROSOMES

5.1. Introduction

Previous studies in Chapters 2-4 have shown that hydroxylated metabolites are not detected in MMPs although they are found in mice and rabbits. However, studies *in vitro* have reported the formation of hydroxylated metabolites after incubation of thalidomide with human S9 liver fractions (Eriksson et al., 1998) or human liver microsomes (Ando et al., 2002a). Since cancer patients have been shown to have suppressed CYP2C19 activity (Williams et al., 2000), the primary enzyme responsible for the hydroxylation of thalidomide in humans (Ando et al., 2002a), the lack of hydroxylated metabolite detected in MMPs (Figures 3.1, 3.2, 4.7 & 4.8) could be as a result of suppressed CYP2C19 activity. In this study liver microsomes from healthy human donors that have been genotyped for CYP2C19 activity were used to determine the extent of hydroxylation of thalidomide *in vitro*.

Since the studies in Chapter 4 showed that thalidomide metabolite formation between mice, rabbits and MMPs were very different; this study also compares metabolite formation using microsomes prepared from livers of mice, rabbits and healthy human donors, to determine if the differences observed *in vivo* are also detected *in vitro*. The rates of formation of 5-OH Th formation using liver microsomes from the various species were used as an indicator of the rate of thalidomide metabolism. The objectives of this study are:

- a) To examine thalidomide metabolites formed *in vitro* using liver microsomes from mice, rabbits or humans.
- b) To determine the rate of formation of 5-OH Th *in vitro* using murine, rabbit and human liver microsomes.

5.2. Methods

5.2.1. Liver Microsome Preparation

Human livers HL5 and HL18 from the human liver bank, Department of Pharmacology and Clinical Pharmacology, Faculty of Medical and Health Sciences, University of Auckland that had been genotyped for CYP2C19 were used in this study. HL5 is *CYP2C19* *1/*1, a homozygous wild type which has an extensive metaboliser phenotype, while HL18 is *CYP2C19* *1/*2, is a heterozygote. Livers from C57Bl/6 mice, New Zealand White rabbits and human donors were rinsed in ice-cold phosphate buffer (pH 7.4) and blotted dry. Livers were then homogenized in 67 mM phosphate buffer containing 1.15% KCl in a volume that was 3 times their weights. The homogenate was then centrifuged at 10,000 x g for 20 min, and the supernatant was removed and centrifuged at 100,000 x g for 1 h. The supernatant was again removed and the remaining microsomal pellets were rinsed with phosphate buffer. The rinsed pellets were re-suspended in a small volume of phosphate buffer and stored at –80 °C until further required.

5.2.2. Bicinchoninic Acid (BCA) Protein Assay

Total protein concentrations in microsome preparations were determined by the BCA method using bovine serum albumin (BSA) to construct the calibration curve (Smith et al., 1985). Samples were diluted with fresh NaOH (1 M) to solubilise the proteins to concentrations that were within the calibration curve. BSA (31.25 – 2000 µg/ml) and samples (50 µl each) were added in duplicate to a flat-bottomed 96-well plate (Nalgene, Nunc International, Rochester, NY). BCA reagent (100 µl, 1:50 dilution of 1% copper sulphate in BCA solution, prepared immediately prior to use) was added to each well, and the plate incubated for 10 min at room temperature. The absorbance was read at 562 nm using a microtitre plate reader (Microplate Reader 3550, Bio-Rad Laboratories, Hercules, CA). Protein concentrations of samples were calculated from the BSA calibration curve.

5.2.3. *In Vitro* Metabolism

For the *in vitro* metabolism studies, thalidomide was dissolved in DMSO, and then diluted to various concentrations in 67 mM phosphate buffer (pH 7.4) with the final concentration of DMSO below 0.2% and incubated with 4 mM NADPH in a final volume of 300 μ l in a shaking water bath at 37 °C for 5 min. Microsomes were added to initiate the reaction. Boiled microsomes were used for the controls. The reaction mixture was then incubated in the shaking water bath at 37 °C and the reaction was terminated at indicated times by addition of 300 μ l 10% TCA containing phenacetin (final concentration 60 μ M) as an internal standard. The reaction mixture was then vortexed and centrifuged (3,000 x g) for 10 min to remove precipitated protein (Torano et al., 1999), and the supernatants were kept in –80 °C freezer until required.

5.2.4. Detection of Metabolites Formed *in vitro*

The supernatants prepared in Section 5.2.3 were processed by solid phase extraction as described previously (Section 2.2.3.1), and the dry residues were reconstituted in 300 μ l of mobile phase (10% ACN and 1% acetic acid in Milli Q water). Reconstituted samples (100 μ l each) were analysed immediately for metabolites using LC-MS as described in Section 4.2.4. Chromatograms of each sample were compared with control samples to determine whether there is any difference in the extent of hydrolysis and whether there is any metabolite formed other than spontaneous hydrolysis. The UV spectra and MS spectra of metabolite peaks in chromatograms were compared with that of authentic standards, and metabolites were identified as described in Section 2.3.2.

Chromatograms obtained through MS single-ion detection were used to determine the relative abundance of metabolites formed after incubation. The metabolite peak of interest was integrated using ChemStation Software (Agilent Technologies, Avondale, PA), and the area of the peak was used as a measure of relative abundance.

5.2.5. Assay of 5-OH Th

5-OH Th concentrations in samples prepared in Section 5.2.3 were determined using a method that was developed in this laboratory to assay for thalidomide concentrations (Chung et al., 2004). Duplicate aliquots (100 μ l) of samples were loaded onto a Waters Breeze chromatograph (Waters Associates, Milford, MA), which consisted of a M717plus auto-sampler, M1525 binary pump and M2487 dual wavelength absorbance detector. Separation was achieved using a 100 x 4.6 mm stainless steel Luna 5 μ m Phenylhexyl column and a mobile phase which consisted of: Solution A (100% ACN) and Solution B (10% ACN and 1% acetic acid in Milli Q water). The elution program was 100% solution B at 0.5 ml/min over 0-10 min, addition of 0-10 % solution A in a linear gradient at 1 ml/min over 10-15 min, 90% solution B and 10% solution A at 1 ml/min over 15-23 min, reduction of 10-0% solution A in a linear gradient at 0.5 ml/min over 23-27 min and 100% solution B at 0.5 ml/min over 27-30 min. Phenacetin and 5-OH Th were detected at UV wavelengths of 220 and 248 nm. Data acquisition and integration was achieved using Breeze™ Software (Milford, CA, USA). 5-OH Th concentrations were determined using calibration curve that was prepared with each run using a range of 5-OH Th concentrations (0.1-25 μ M). The ratios of area of the peaks to the area of the peak for the internal standard was calculated and plotted against concentration and linear regression analysis was used to obtain the line of best-fit, which in all the runs had an r^2 value of 0.999. The rate of formation of 5-OH Th (concentration/time) was plotted against thalidomide concentration, and the data was fitted using the Michaelis-Menten model. Maximum velocity of reaction (V_{\max}) and Michaelis-Menten constant (K_M) were determined by Prism 3.0 program (Graphpad Software Co., CA), as well as Lineweaver-Burk and Eadie-Hofstee models.

The intra-assay accuracy was 90-110% with a coefficient of variation (CV) of 5-9% (3 samples per concentration). Inter-assay accuracy was 96-104% with a CV of 2-4% (5 samples per concentration). For quality control, three concentrations of 5-OH Th (0.2, 5, and 25 μ M) were stored at -80°C , and these were included in each analysis and were found to be stable over a period of 14 days and within 3% of the validated value.

5.3. Results

5.3.1. Detection of Metabolites

A concentration of thalidomide of 400 μ M and an incubation time of 60 min were chosen based on the studies of Ando and co-workers (Ando et al., 2002). The degradation of thalidomide was shown in preliminary experiments to be less than 10% in phosphate buffer at 37 °C. Control incubations of thalidomide with boiled microsomes provided four peaks (1, 2, 5 & 6) that were products of hydrolysis (Figures 5.1 & 5.2). Incubation of thalidomide with rabbit and mouse liver microsomes (0.4 – 2 mg/ml) provided eleven peaks (1-11) in addition to the thalidomide peak (Table 5.1; Figures 5.1B & C). Of the seven peaks that were not present in the controls, 4 corresponded to 5-OH Th, 5'-OH CG, and *cis*- and *trans*- 5'-OH Th (4, 7, 10 and 11; Figures 5.1B & C) that had been previously characterised in Chapter 2. Metabolites in peaks 3, 8 and 9 all had a molecular mass that was 16 amu higher than 5-OH Th or 5'-OH Th and were suggested to be dihydroxylated metabolites. None of the retention times and UV spectra of these three “di-hydroxylated” metabolites however were comparable to that of authentic 5,6-dihydroxythalidomide. Peaks 8 and 9 could be *cis*-5,5'-dihydroxythalidomide and *trans*-5,5'-dihydroxythalidomide, but authentic standards are not available for confirmation. Peak 3 with a retention time of 10.4 min could be 5,*N*-dihydroxythalidomide, since hydroxylation on the glutamine ring renders the molecule more polar and will elute earlier, but again, it has not been confirmed as the authentic standard is not available.

Using human (HL18) liver microsomes only seven peaks (1, 2, 5-7 & 10-11) were detected (Figure 5.1A), in contrast to the 11 peaks obtained with murine or rabbit microsomes. Peaks corresponding to the hydroxylated metabolites, 5-OH Th (peak 11), *cis*-5'-OH Th (peak 7) and *trans*- 5'-OH Th (peak 10) (Figure 5.1A) were detected in addition to the four hydrolysis products (peaks 1, 2, 5, and 6). Hydroxylation metabolites were not produced at detectable levels using microsomes from donor HL5 however (Figure 5.3).

Table 5.1 Metabolite formed after incubating thalidomide with mouse and rabbit liver microsomes.

Peak	M.W. ^a	Metabolite	Structure
1*	276	CG	
2*	294	<i>N</i> -(<i>o</i> -carboxybenzoyl)isoglutamine	
3 ^{#b}	290	5, <i>N</i> -dihydroxythalidomide	
4 ^{#b}	292	5'-OH CG	
5*	276	PiG	
6*	276	PG	
7 [#]	274	<i>cis</i> -5'-OH Th	
8 ^{#b}	290	<i>cis</i> -5,5'-dihydroxythalidomide	
9 ^{#b}	290	<i>trans</i> -5,5'-dihydroxythalidomide	
10 [#]	274	<i>trans</i> -5'-OH Th	
11 [#]	274	5-OH Th	

* hydrolysis metabolite, [#] metabolite formed via hydroxylation, ^a Molecular Weight, ^b Proposed metabolite.

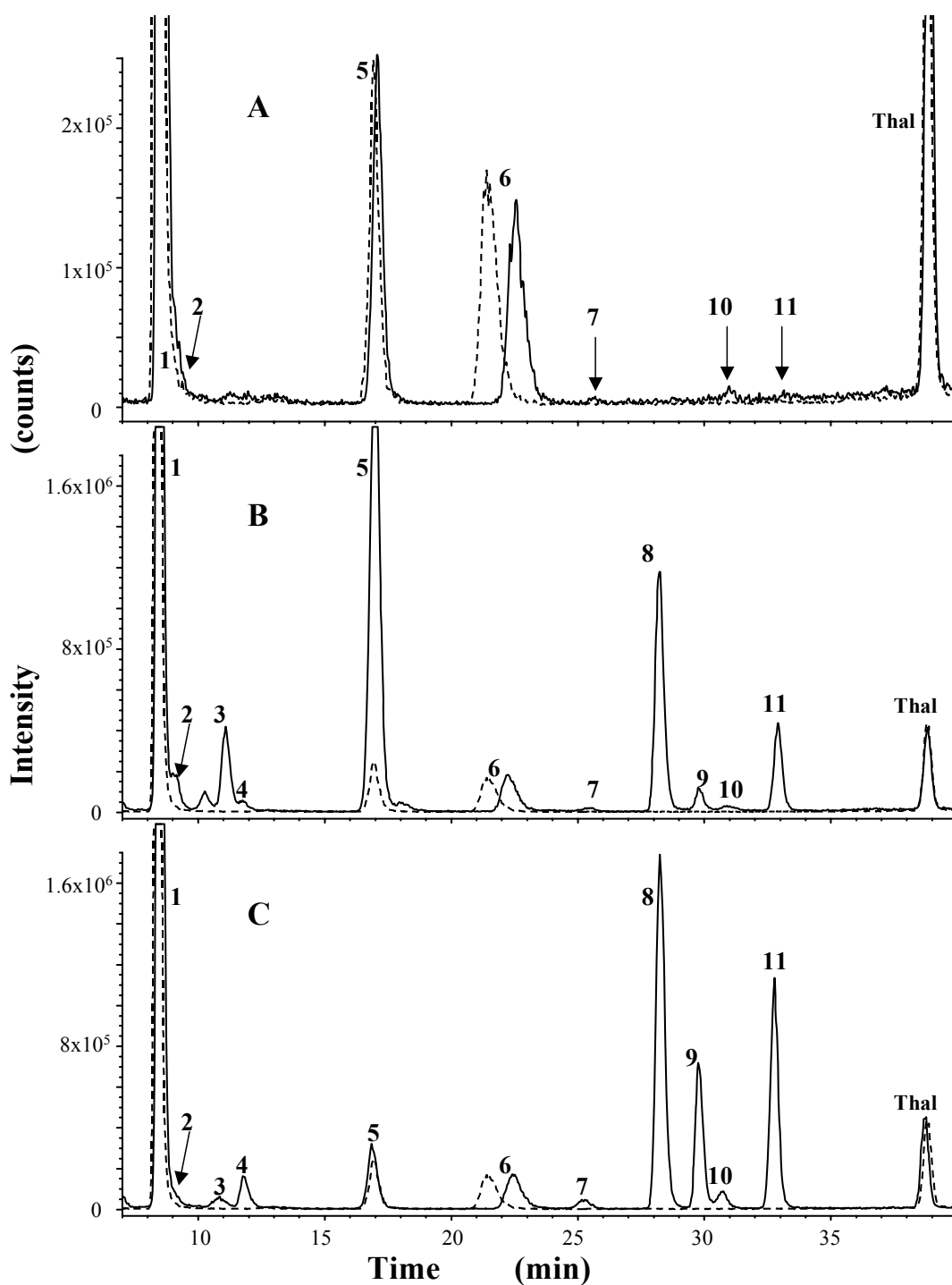


Figure 5.1 LC-MS chromatograms of Thal metabolites following incubation (60 min; 37°C) of Thal (400 μ M) with liver microsomes (solid lines) of (A) human HL18, (B) rabbits and (C) mice, or with boiled liver microsomes (dotted lines). Metabolites were detected by SIM mode (Signal 3) of MS as described in methods.

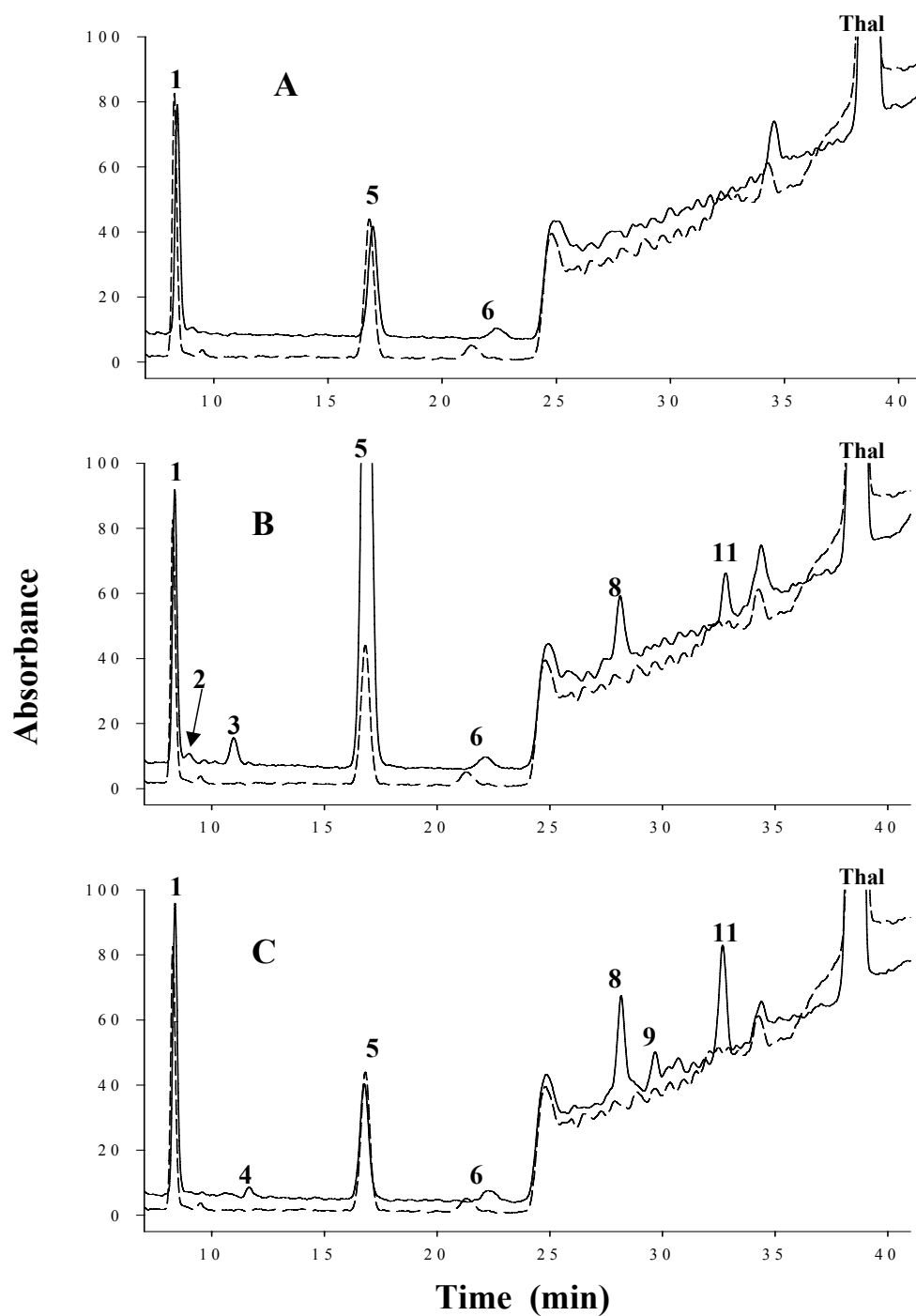


Figure 5.2 HPLC chromatograms with UV detection of Thal metabolites following incubation (60 min; 37°C) of Thal (400 μ M) with (A) human HL18, (B) rabbits and (C) mice liver microsomes (solid lines), or with boiled liver microsomes (dotted lines).

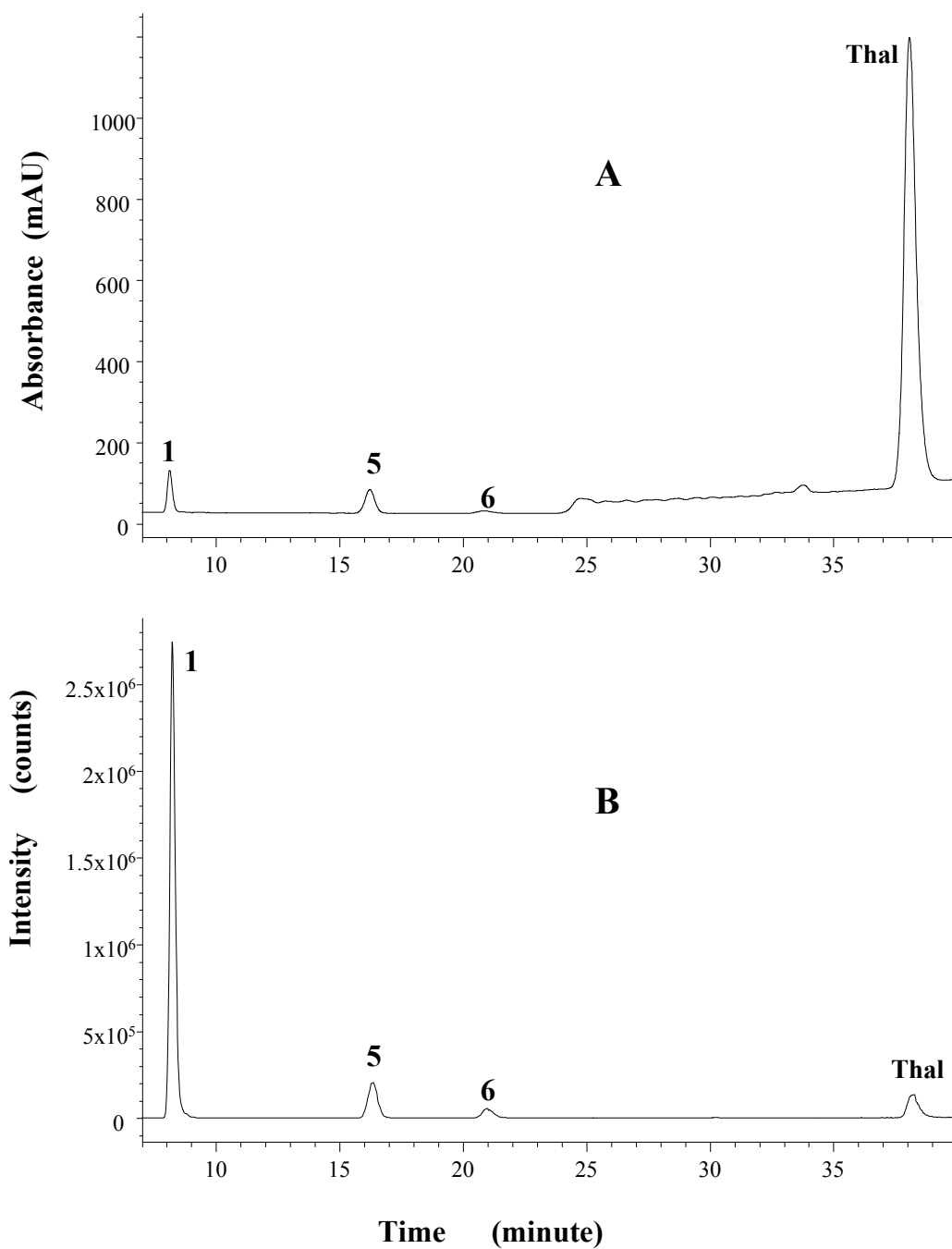


Figure 5.3 LC-MS chromatograms with UV (A) or MS negative SIM (B) detection of Thal metabolites following incubation (60 min; 37°C) of Thal (400 μ M) with 2 mg/ml human HL5 liver microsomes.

5.3.2. Relative Abundance of Metabolites

The area of their peaks obtained using MS single-ion detection was used as a measure of the relative abundance of the hydroxylated metabolites and is given in Table 5.2. The relative abundance of the hydroxylated metabolites using HL18 microsomes was much lower than that obtained with mouse or rabbit liver microsomes.

The relative abundance of hydrolysis products formed in three species was found to be similar to that in control samples with the exception of PiG (Peak 5) and *N*-(*o*-carboxybenzoyl)isoglutamine (Peak 2) which was much higher with rabbit microsomes (Figures 5.1 & 5.2; Table 5.3). The formation of PiG was found to increase linearly with increasing concentrations of rabbit microsomes ($r^2 = 0.983$; Figure 5.4) using a thalidomide concentration of 400 μ M. At thalidomide concentrations 12.5 μ M or higher, more PiG was formed using rabbit microsomes than mouse microsomes. However, similar amounts of PiG were produced by rabbit and murine microsomes at a thalidomide concentration of 6.25 μ M.

It was found that the peak UV absorbances of thalidomide and its metabolites were close to each other (220-245 nm, Figure 2.5); thus, as an estimation of metabolite formation, the areas of the relevant metabolite peaks in UV chromatograms was obtained from Figure 5.2 and were expressed as a percentage of the total area of all metabolite peaks plus the thalidomide peak. These are summarised in Table 5.4. Rabbit microsomes provided the highest overall transformation of thalidomide (25.7%) and human microsomes gave the lowest (7.9%). The formation of hydrolysis products using human (7.9%) and mouse liver microsomes (7.7%) was lower than that in rabbit liver microsomes (22.7%). Hydroxylation of thalidomide was highest with mouse microsomes (6.1%), and moderate with rabbit microsomes (3.0%), and was not measurable with human liver microsomes.

5.3.3. Rate of Metabolism of Thalidomide to 5-OH Th

In a preliminary study, thalidomide at 400 μ M was incubated with 0.4, 0.6, 0.8, 1.2, 1.6 or 2 mg/ml of liver microsomes for 60 min. The concentration of 5-OH Th formed was

plotted against liver microsomal protein concentrations and was shown to be linear between 0.4 – 2 mg/ml ($r^2 = 0.984$ and 0.985 respectively) using mouse and rabbit microsomes, and between 0.6 – 2 mg/ml ($r^2 = 0.986$) with human microsomes (Figure 5.5). The optimal reaction time was then determined by incubating thalidomide at 400 μ M with 2 mg/ml of liver microsomes for 10, 20, 30, 40, 50 or 60 min. 5-OH Th formation was linear between 10 – 30 min ($r^2 = 0.998$ and 0.999 respectively) with mouse and rabbit hepatic microsomes and between 40 – 60 min in the presence of human HL18 liver microsomes (Figure 5.6). Based on the results from these preliminary experiments, liver microsome concentration of 2 mg/ml for all three species, and a reaction time of 30 min for mouse and rabbit microsomes and a reaction time of 60 min for human microsomes were chosen as being appropriate for the determination of the rate of 5-OH Th formation.

Thalidomide at various concentrations (6.25 – 600 μ M) was incubated with 2 mg/ml of mouse and rabbit microsomes for 30 min or with 2 mg/ml of human microsomes for 60 min. 5-OH Th concentrations were measured as described in Section 5.2.5, using HPLC which was able to give complete separation of *cis*-5'-OH Th, *trans*-5'-OH Th, 5-OH Th, phenacetin and thalidomide (Figure 5.7). Formation of 5-OH Th above the limit of quantitation of 0.1 μ M was obtained using HL18 (*CYP2C19* *1/*2) human liver microsomes at concentrations above 0.6 mg/ml. 5-OH Th production was below the limit of detection using HL5 (*CYP2C19* *1/*1) liver microsomes however. The rate of formation of 5-OH Th with mouse and rabbit liver microsomes above 6.25 μ M followed Michaelis-Menten kinetics (Figure 5.8). The V_{\max} and K_M , were 45.2 ± 2.1 pmol/min/mg and 208.3 ± 23.1 μ M respectively for mouse microsomes, and 11.91 ± 0.5 pmol/min/mg and 88.02 ± 11.6 μ M respectively for rabbit microsomes. V_{\max} and K_M calculated using Lineweaver-Burk (Figure 5.9) and Eadie-Hofstee plots (Figure 5.10) produced similar results. The apparent intrinsic clearance (CL_{int}), calculated as V_{\max}/K_M , of thalidomide to 5-OH Th in mouse and rabbit microsomes was 0.217 and 0.135 ml/min/g, respectively. In human HL18 liver microsomes, 5-OH Th was only detectable at 3 thalidomide concentrations (200, 400 and 600 μ M), and the V_{\max} , K_M and CL_{int} calculated from those three concentrations using Michaelis-Menten model were 0.334 ± 0.02 pmol/min/mg, 85.8 ± 27.5 μ M and 0.004 ml/min/g, respectively.

Table 5.2 Comparison of relative levels of hydroxylated metabolites formed following a 60 min incubation of Thal with liver microsomal protein (2 mg/ml). Metabolites were determined by mass spectral detection using single ion monitoring. The response of each metabolite peak produced by mouse liver microsomes was normalized to 1.

	5, <i>N</i> -dOH Thal ¹ (3)*	5'-OH CG (4)	<i>cis</i> -5'- OH Thal (7)	<i>cis</i> -5,5'- dOH Thal ² (8)	<i>trans</i> - 5,5'- dOH Thal ³ (9)	<i>trans</i> - 5'-OH Thal (10)	5-OH Thal (11)
Mouse	1	1	1	1	1	1	1
Rabbit	4.59	0.26	0.34	0.68	0.13	0.27	0.37
Human	0	0	0.07	0	0	0.09	0.005

*Number in brackets represents peak number in chromatogram.

¹ 5,*N*-dihydroxythalidomide, ² *cis*-5,5'-dihydroxythalidomide, ³ *trans*-5,5'-dihydroxythalidomide.

Table 5.3 Comparison of relative levels of hydrolysis products formed following a 60 min incubation of Thal with liver microsomal protein (2 mg/ml). Hydrolysis products were determined by mass spectral detection using single-ion monitoring. The response of each peak produced by mouse liver microsomes was normalized to 1.

	CG (1)*	CiG ¹ (2)	PiG (5)	PG (6)
Control ²	1	1	1	1
Mouse	0.90-1.2	1	0.98-1.08	0.96-1.09
Rabbit	0.95-1.13	8.9-17.8	2.65-7.92	0.87-1.03
Human	0.90-1.01	1	0.88-1.1	0.84-1.05

* Number in brackets represents peak number in chromatogram.

¹ *N*-(*o*-Carboxybenzoyl)isoglutamine.

² Thalidomide solutions incubated with boiled liver microsomes of mouse, rabbit and human.

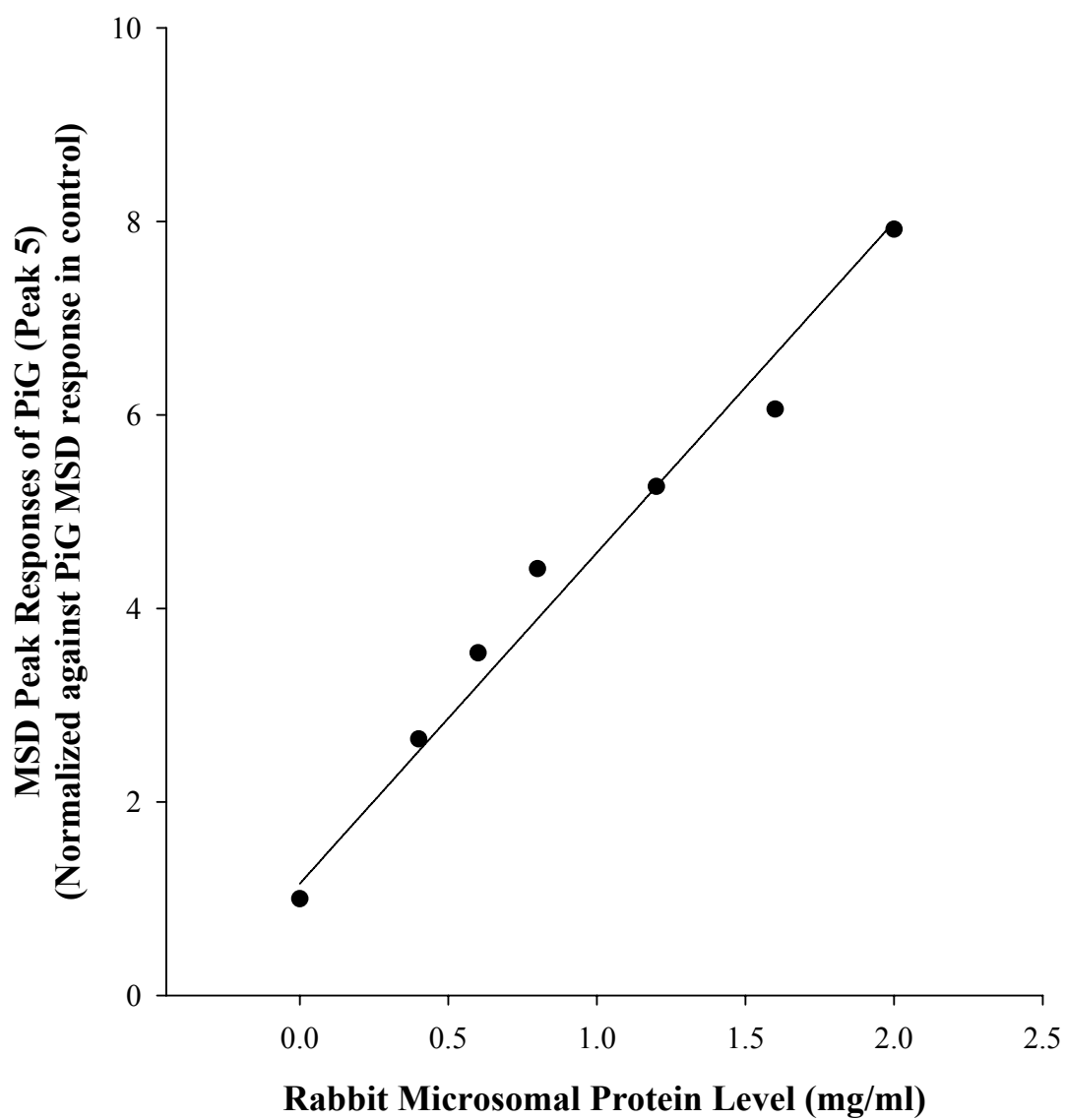


Figure 5.4 Enzymatic hydrolysis of PiG by rabbit liver microsomal protein in the presence of NADPH (4mM).

Table 5.4 Comparison of the total products of hydrolysis and hydroxylation formed following a 60 min incubation of Thal with liver microsomal protein (2 mg/ml).

Species	All metabolites of hydrolysis (%)*	All metabolites of hydroxylation (%)*	5-OH Th (%)*	Total metabolites (%)*
Mouse	7.7	6.1	2.5	13.8
Rabbit	22.7	3.0	1.1	25.7
Human	7.9	-	-	7.9

* The percentage was obtained by comparing the sum of the UV responses of all hydrolysis or/and hydroxylation peaks with the sum of the UV responses of all metabolite and parent peaks, including hydrolysis, hydroxylation and thalidomide peaks.

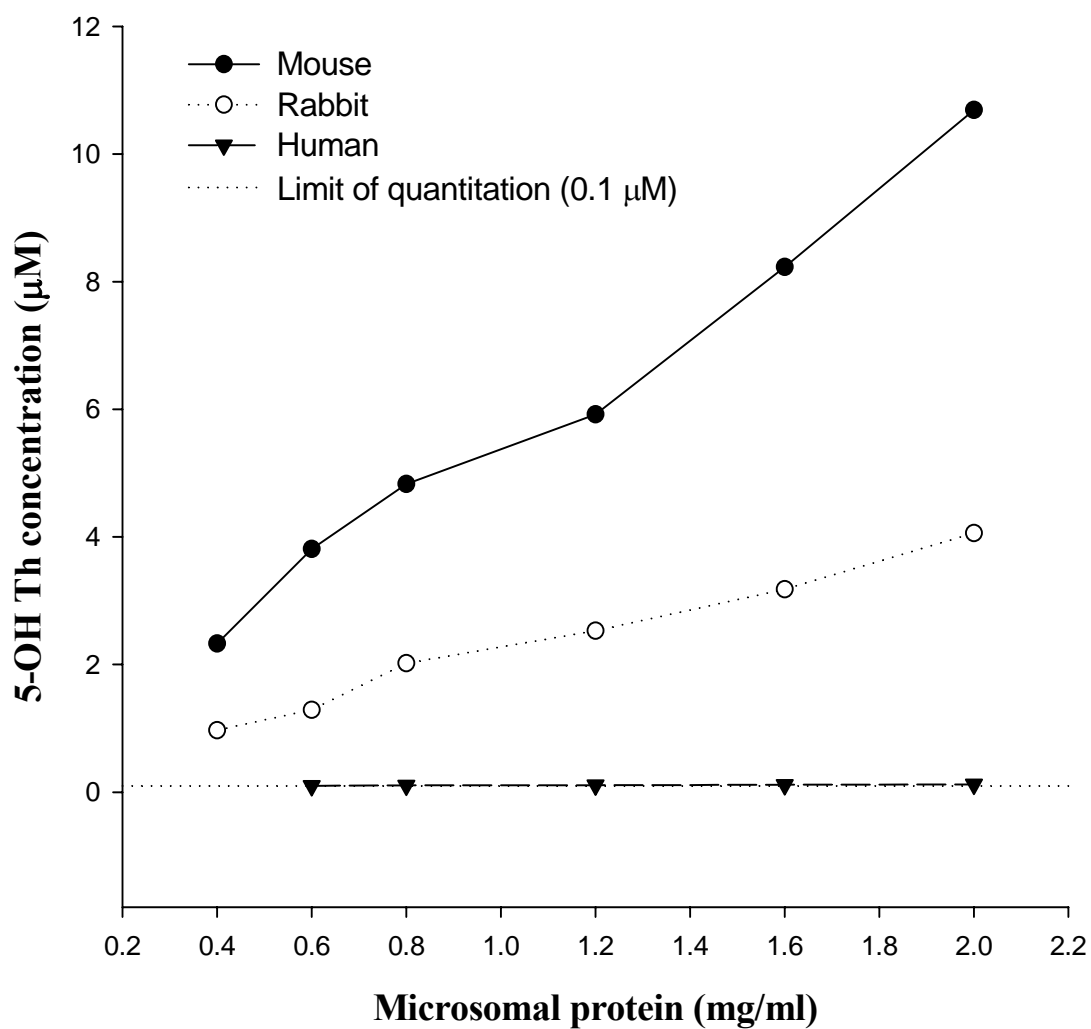


Figure 5.5 Concentration of 5-OH Th with different microsomal protein concentrations after incubating 400 μM of thalidomide with mouse, rabbit and human liver microsomes for 60 min.

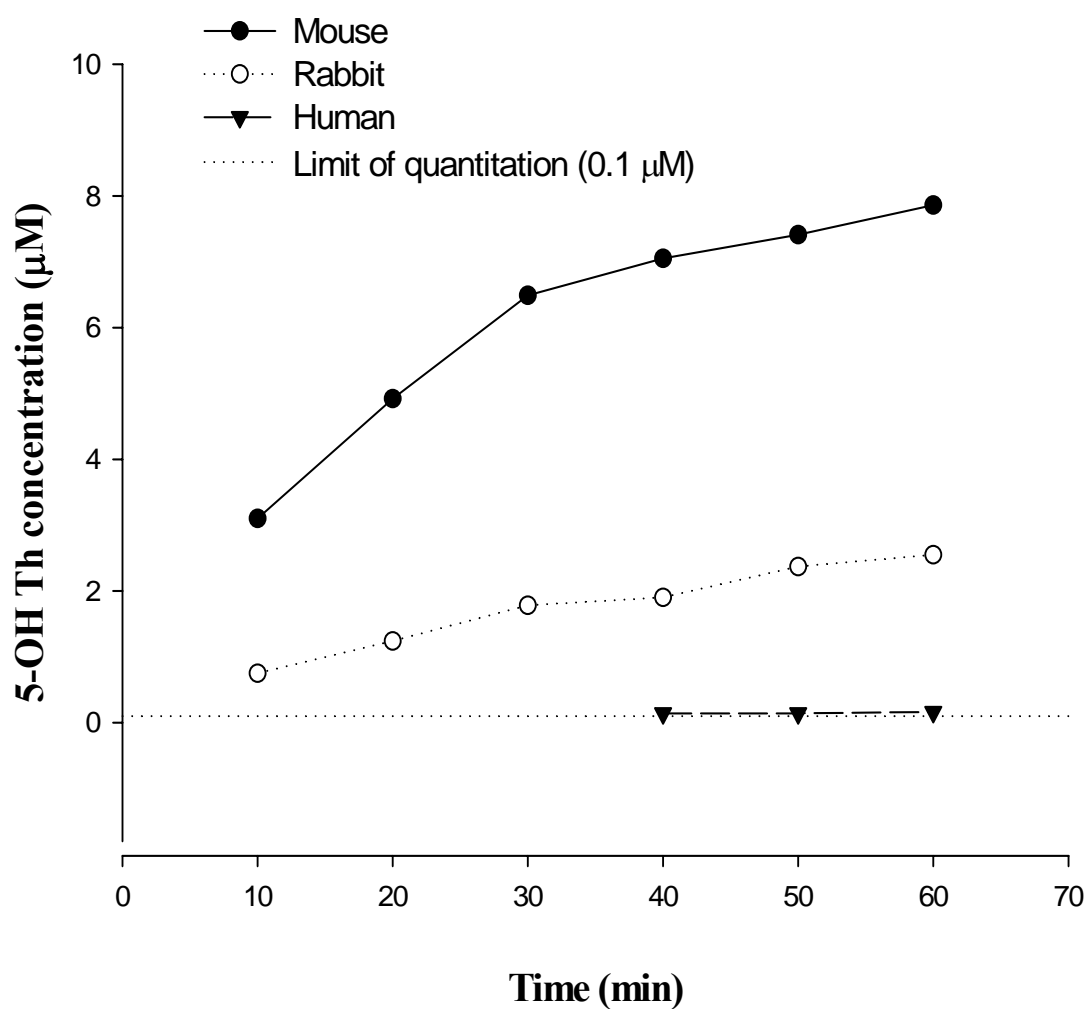


Figure 5.6 Concentration of 5-OH Th at different times after incubating 400 μM of thalidomide with 2 mg/ml of mouse, rabbit and human liver microsomes.

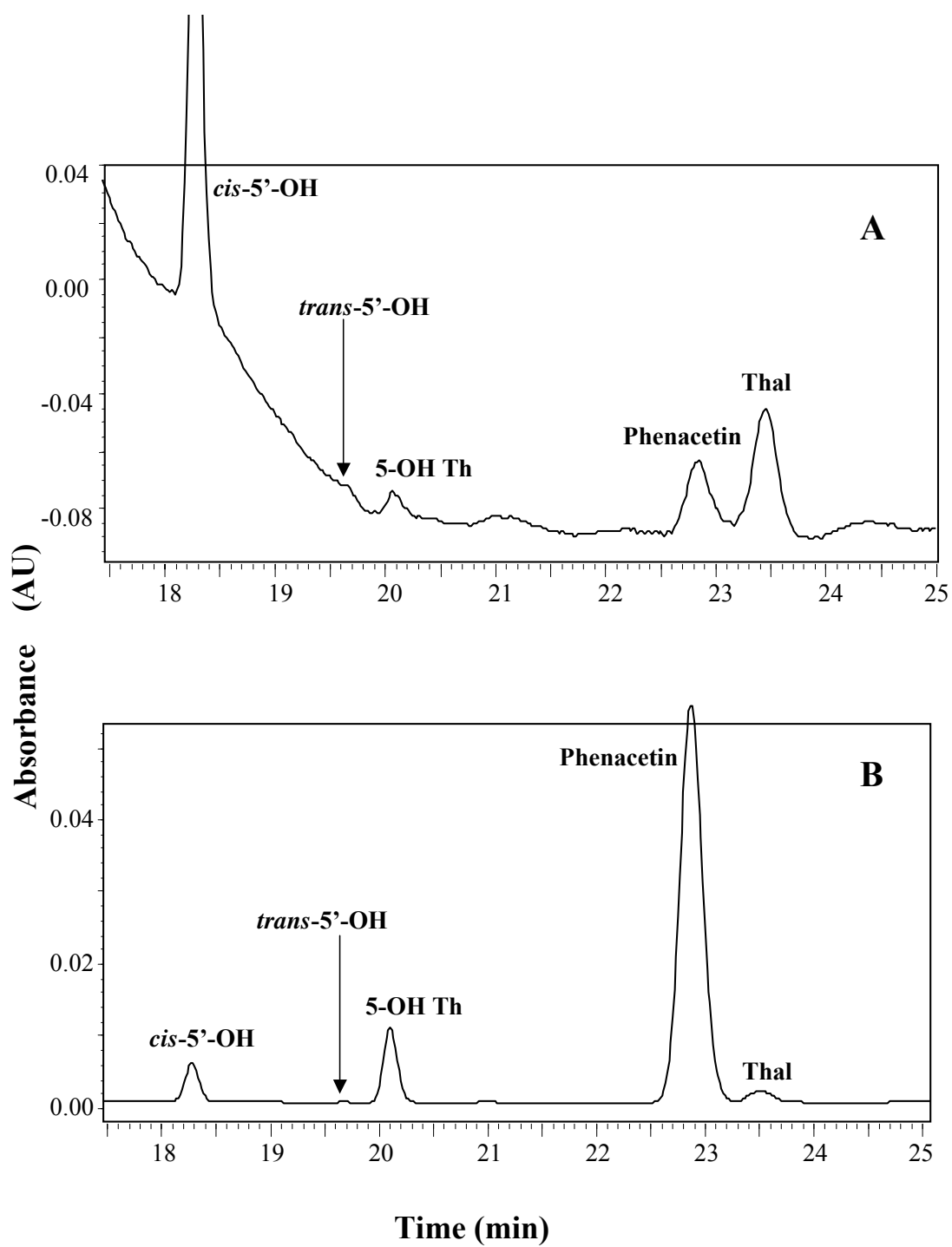


Figure 5.7 HPLC chromatograms showing complete separation of *cis*-5'-OH Th, *trans*-5'-OH Th, 5-OH Th, Phenacetin and Thal using UV detection at (A) 220 nm or (B) 248 nm.

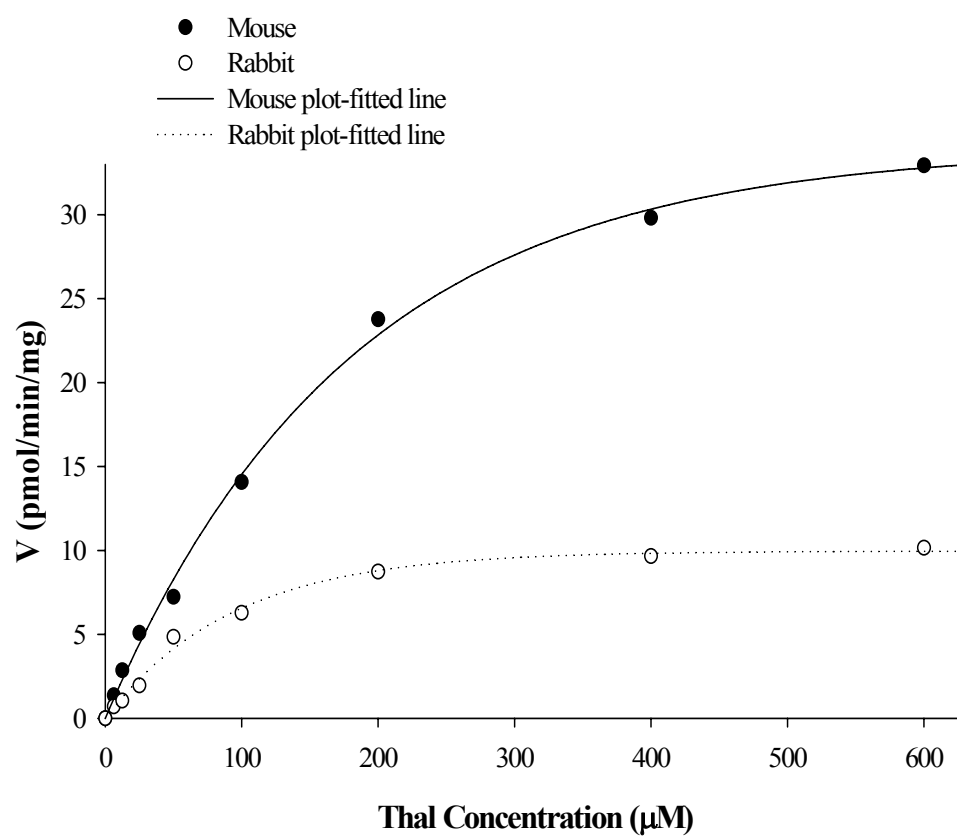


Figure 5.8 Formation of 5-OH Th in rabbit and mouse liver microsomes following incubation with Thal.

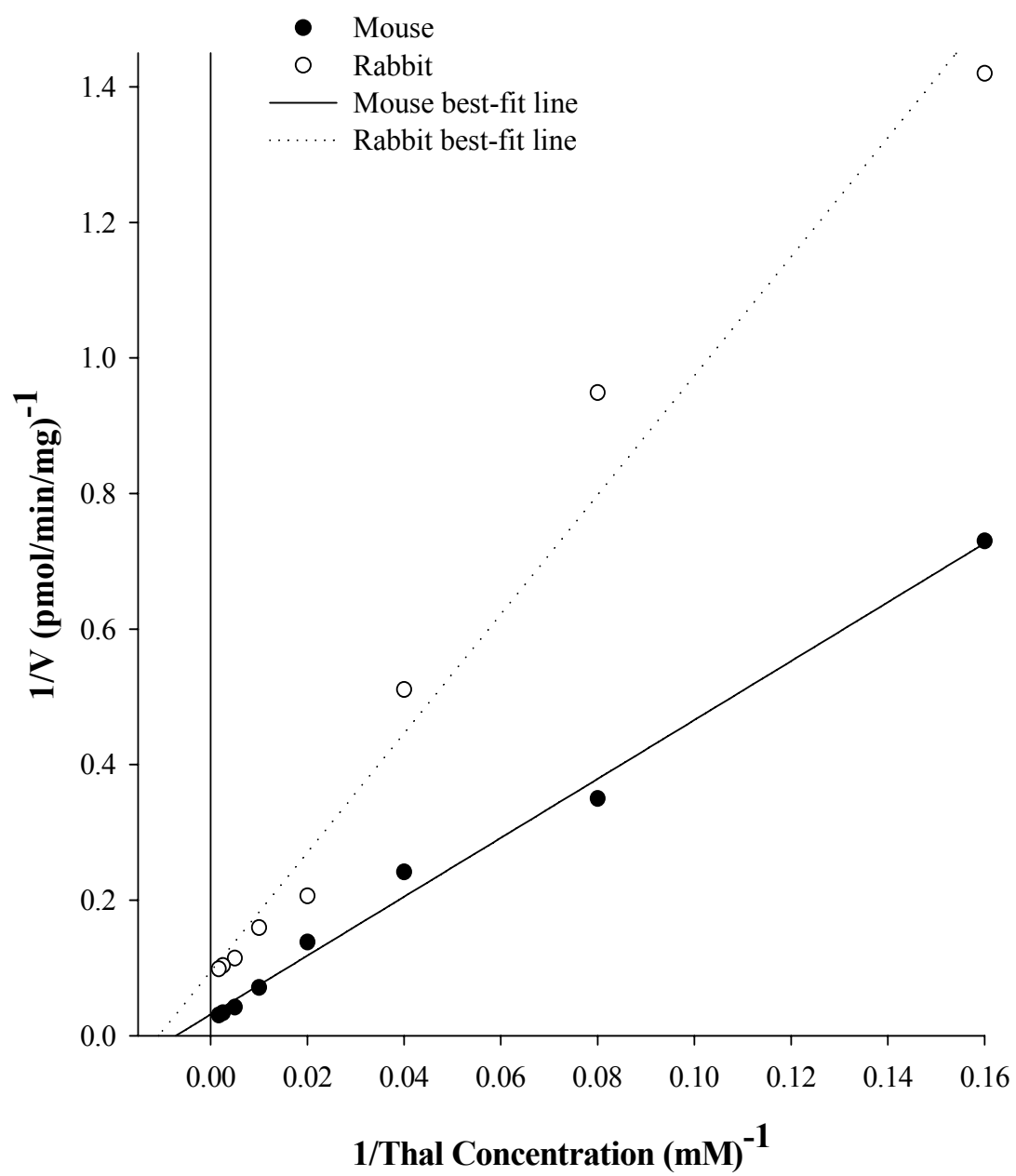


Figure 5.9 Lineweaver-Burk plots of thalidomide 5-hydroxylation by rabbit and mouse liver microsomes

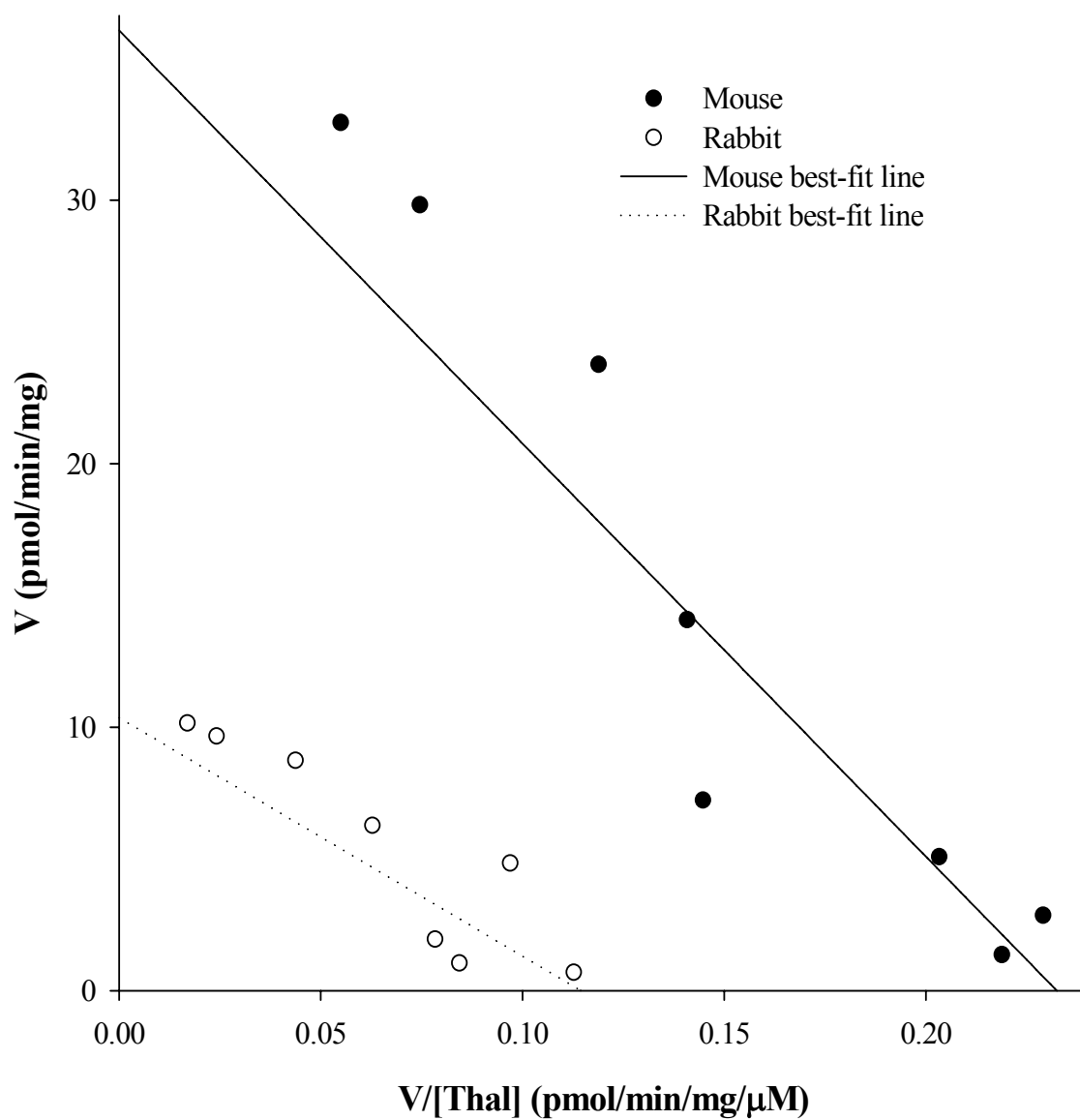


Figure 5.10 Eadie-Hofstee plots of thalidomide 5-hydroxylation by rabbit and mouse liver microsomes

5.4. Discussion

The studies in this chapter on thalidomide metabolism using microsomes from mice, rabbit and human livers have detected a greater number of different metabolites formed *in vitro* than *in vivo*. With murine and rabbit liver microsomes, three metabolites (3, 8 and 9), with masses consistent with dihydroxylated products that were not seen *in vivo* were detected. The mono-hydroxylated metabolites such as 5-OH Th are rapidly cleared *in vivo* by glucuronidation (Figure 2.9), and thus may not be available for dihydroxylation. Thal-5-*O*-glucuronide, which was detected *in vivo* (Figures 2.1, 4.1 & 4.4), was not detected *in vitro* since UDPG, a co-factor necessary for glucuronidation, is lacking in the microsomal preparations. Four metabolites, 5-OH Th, *cis*- and *trans*-5'-OH Th and 5'-OH CG (Figure 5.1), were observed both *in vitro* and *in vivo* (Figures 2.1, 4.1 & 4.4) in murine and rabbit microsomes. *In vitro* formation of 5-OH Th and *cis*-5'-OH Th, as well as of 5,6-dihydroxythalidomide and several unidentified metabolites, has been reported (Ando et al., 2002a). The identity of metabolites 3, 8, and 9 in this study has not been confirmed, but none of them corresponded to authentic 5,6-dihydroxythalidomide.

The hydrolysis of thalidomide in rats, humans and rabbits is considered not to be enzyme dependent (Faigle, 1962; Keberle et al., 1965; Schumacher et al., 1965; Williams et al., 1965). The studies here have provided evidence of enzymatic conversion of thalidomide to PiG in rabbit microsomes however. Hydrolysis of thalidomide to PiG (Peak 5) increased with increasing concentrations of rabbit hepatic microsomes (Figure 5.3), but was not seen with murine or human microsomes (Figures 5.1 & 5.2). These observations are consistent with a study by Schumacher and co-workers (Schumacher et al., 1968) who showed that the rate of hydrolysis of thalidomide was higher in rabbit livers than in rat livers, but it was not shown in their studies that the increased hydrolysis was related to PiG formation. The higher levels of *N*-(*o*-carboxybenzoyl)isoglutamine (Peak 2), formed by hydrolysis of PiG, seen with rabbit microsomes compared with mouse or human microsomes (Table 5.3) could be explained by the increased formation of PiG by enzymatic hydrolysis. Enzymatic hydrolysis occurred only at *in vitro* thalidomide concentrations at 12.5 μ M or above. PiG levels in plasma of mice and rabbits were similar following p.o. administration of

thalidomide at 2 mg/kg, suggesting significant enzymatic production of PiG as seen *in vitro* did not occur *in vivo* (Figures 4.1 & 4.4). The lack of enzymatic PiG formation could be because the plasma concentrations of thalidomide ($C_{\max} = 1.8 \pm 0.4 \mu\text{M}$, Chung et al., 2004a) following administration of 2 mg/kg to rabbits are below the concentrations required for enzymatic hydrolysis to occur.

The relative total metabolic clearance of thalidomide *in vitro* via both hydrolysis (enzymatic and non-enzymatic) and hydroxylation was greatest in the rabbit and lowest in human liver microsomes (Table 5.4). Since enzymatic hydrolysis of thalidomide in the rabbit may not occur at *in vivo* concentrations, and the rate of non-enzymatic hydrolysis is similar in all species (Figure 4.2, 4.4 & 4.7), enzymatic hydroxylation may be the rate-limiting step in the clearance of thalidomide. The study here showed significant differences in the degree of hydroxylation occurring in microsomes from the different species (Table 5.2), which correlated with the different rates of 5-OH formation (Section 5.3.3). The relative rates of 5-OH Th formation *in vitro* also correlate with the *in vivo* clearance of thalidomide in the three species. Mice were shown to clear thalidomide faster than rabbits, which were faster than humans (Chung et al., 2004a), and the rate of 5-OH Th formation in murine microsomes was 1.6 fold faster than that in rabbit microsomes and 50 fold faster than that in human microsomes.

Metabolism of thalidomide to 5-OH Th and *cis* 5'-OH Th has been shown to be catalysed by CYP2C subfamily *in vitro* (Ando et al., 2002a). However, kinetic parameters such as V_{\max} , K_M and CL_{int} of thalidomide to 5-OH Th in microsomes were not calculated as the formation of 5-OH Th in relation to time of incubation was non-linear in that study (Ando et al., 2002a). The study here used higher microsomal protein concentration and shorter incubation time to obtain the linear formation of 5-OH Th, allowing the V_{\max} , K_M and CL_{int} to be calculated, and the inter-species comparisons to be made. However, since products of further hydroxylation of *cis*-, *trans*-5'-OH Th and 5-OH Th were detected, the kinetics of formation of the primary hydroxylated metabolites of thalidomide (5-OH Th and *cis*-5'-OH Th) would be compromised by the rate(s) of the second hydroxylation step, and the kinetic parameters, in particular K_M , should be described as *apparent* only.

The overall rate of hydroxylation in human liver microsomes is very low irrespective of CYP2C19 genotype (Table 5.2, Figures 5.1 & 5.2). Hydroxylated metabolites were measurable using liver microsomes from HL18, a CYP2C19 heterozygote (*1/*2), but hydroxylation of thalidomide was not observed using liver microsomes from HL5, a homozygous wild type (*1/*1). In the study by Ando and co-workers (2002a) using microsomes from two human livers that were both genotyped as homozygous wild type (*1/*1), the rate of 5'-OH Th formation was low for one donor and was below the limit of quantification for another. In the same study, pooled human liver microsomes also did not produce quantifiable amounts of hydroxylated metabolites, although studies using purified CYP2C19 indicated that this enzyme was responsible for the hydroxylation of thalidomide in humans (Ando et al., 2002a). More recent studies showed that prostate cancer patients with an extensive metaboliser genotype did not hydroxylate thalidomide to any significant extent (Ando et al., 2002b). Thus, although CYP2C19 appears to be responsible for hydroxylation of thalidomide in humans, the CYP2C19 genotype of the patients does not appear to predict the degree of hydroxylation as shown here (Figures 5.1 & 5.3) and in the work of Ando and co-workers (2002a, 2002b). Irrespective of the involvement of CYP isoenzyme(s), the overall rate of metabolism of thalidomide is extremely low in human liver microsomes compared with mouse and rabbit microsomes.

In summary, the studies show huge differences in thalidomide metabolism using microsomes from mouse, rabbit and human livers. Highest degree of hydroxylation occurred using murine microsomes, and the lowest with human microsomes. The degree of hydroxylation obtained with the microsomes from the different species corresponded with the degree of hydroxylation that was observed *in vivo* in mice (Figure 4.2), rabbits (Figure 4.4) and MMPs (Figure 4.7). Hydroxylation in HL18 human microsomes occurred only at thalidomide concentrations above 200 µM, which is considerably higher than the plasma concentrations of 50 µM that are achieved using the highest dose of thalidomide (1,600 mg/day) during therapy (Figg et al., 1999). The *in vitro* studies are consistent with studies in Chapters 3 and 4, which showed no hydroxylated metabolites in patients with multiple myeloma, or in patients with Hansen's disease on thalidomide treatment (Teo et al., 2000).

CHAPTER 6. BIOLOGICAL ACTIVITY OF THALIDOMIDE'S HYDROLYSIS METABOLITES

6.1. Introduction

Thalidomide's anti-tumour activities have been mainly attributed to its anti-angiogenic properties (D'Amato et al., 1994; Kenyon et al., 1997; Kruse et al., 1998; Joussen et al., 1999), although there is increasing evidence of the involvement of cytokine modulation (Kenyon et al., 1997; Hideshima et al., 2001a; Hideshima et al., 2001b; Dmoszynska et al., 2002; Tosi et al., 2002; Li et al., 2003). Metabolites have been suggested to be responsible for the anti-angiogenic effects of thalidomide (Gordon et al., 1981; Ng et al., 2003), and hydroxylated metabolites have been found to be effective in inhibiting angiogenesis in a number of different assays (Marks et al., 2002; Price et al., 2002; Ng et al., 2003). Hydrolysis metabolites have not been reported to be anti-angiogenic, although they have been tested extensively for teratogenicity and shown to be non-teratogenic (Fabro et al., 1965; Smith et al., 1965; Fabro et al., 1967b; Meise et al., 1973). However, a recent report showed that thalidomide as well as its hydrolysis metabolites was able to inhibit gene transcription in multiple myeloma cell lines (Drucker et al., 2003), indicating that the hydrolysis metabolites could be effective in the treatment of multiple myeloma.

Results in Chapters 3 & 4 showed only three hydrolysis metabolites, PG, PiG and CG, and no hydroxylated metabolites in MMPs who were responding to thalidomide treatment (Figures 3.1, 3.2, 4.7 & 4.8). This strongly indicated that either thalidomide or the hydrolysis products were the active compounds. The ability of the hydrolysis metabolites to inhibit angiogenesis and to modulate cytokine production has been compared with thalidomide in this chapter. In this chapter, the hydrolysis metabolites have been compared with thalidomide in a number of different assays of activity that has previously been reported for thalidomide (Sampaio et al., 1991; Ching et al., 1995; Cao et al., 1999; Ng et al., 2003). The objectives of this study are:

- a) To determine whether the hydrolysis metabolites can enhance the anti-tumour action of DMXAA against Colon 38 tumours in mice.
- b) To investigate whether the hydrolysis metabolites inhibited tube formation by ECV304 cells in Matrigel layers as a determination of anti-angiogenic activity.
- c) To test whether the hydrolysis metabolites modulated DMXAA-induced TNF production in mice and LPS-induced TNF production in cultured human peripheral blood leucocytes (HPBL).
- d) To determine the stability of CG in solution.
- e) To determine CG concentrations in MMPs.

6.2. Methods

6.2.1. Tumour Growth Delay Determinations

Mice were implanted with Colon 38 tumours as described in Section 2.2.1, and were used for growth delay experiment when tumours have reached approximately 3-5 mm in diameter. Mice were divided into 10 groups, an untreated control group, a group treated i.p. with DMXAA at 25 mg/kg only, and 8 groups treated with DMXAA together with PG, PiG, CG or thalidomide at 100 mg/kg, or together with CG or thalidomide at 20 mg/kg or 4 mg/kg. DMXAA was dissolved in saline at 2.5 mg/ml and injected i.p. into mice in a volume of 10 μ l/g body weight. Thalidomide, PG, PiG and CG were dissolved in DMSO at 40, 8 or 1.6 mg/ml (for dosages of 100, 20, 4 mg/kg respectively) and injected i.p. in a volume of 2.5 μ l/g body weight. Tumours were measured 2-3 times weekly after treatment and tumour volumes were calculated as $0.52 \times a^2 \times b$, where a and b are the minor and major axes of the tumour. The arithmetic means and standard errors were calculated for each point, counting cured animals as having zero tumour volume, and expressed as fractions of the pre-treatment volume. Growth delay was determined as the difference in the number of days required for the tumour to reach four times the pre-treatment volume. Mice in which the tumour had completely disappeared were kept for 3 months to ensure that the tumours did not re-grow.

6.2.2. Modulation of TNF Production in Mice

Mice with Colon 38 tumours, approximately 5-7 mm in diameter, were divided into groups of 5. One group was untreated. Other groups were treated with DMXAA (25 mg/kg) alone; DMXAA (25 mg/kg) + thalidomide (100 mg/kg), DMXAA (25 mg/kg) + PG (100 mg/kg), DMXAA (25 mg/kg) + PiG (100 mg/kg), DMXAA (25 mg/kg) + CG (100 mg/kg), DMXAA (25 mg/kg) + thalidomide (20 mg/kg), DMXAA (25 mg/kg) + CG (20 mg/kg), and thalidomide, PG, PiG or CG only at 100 and 200 mg/kg. Three hours after treatment, mice were anaesthetized with halothane (NZ Pharmacology Ltd., Christchurch, New Zealand), and blood was collected from the ocular sinus and tumours were excised. Blood was coagulated overnight at 4 °C, and then centrifuged for 30 min at 2,000 x g and 4 °C, and the serum was removed and stored at -80 °C until use. Tumour tissues were weighed and homogenized in 1.5 ml α -minimal essential medium (α -MEM). The homogenates were centrifuged (2,000 x g, 30 min, 4 °C) and supernatant was removed and re-centrifuged (14,000 x g, 30 min, 4 °C). The final supernatants were removed and kept at -80 °C until use. TNF levels in serum and supernatants derived from tumour homogenates were assayed for TNF as described in Section 6.2.4.

6.2.3. Modulation of TNF Production *In vitro*

Blood (20 ml) each from seven healthy volunteers were collected into heparinized tubes, and was overlayed on top of 10 ml of Ficoll-Paque Plus (Amersham Biosciences AB, Uppsala, Sweden) in 50 ml Faclon polypropylene conical tubes (Becton Dickson Labware, Franklin Lakes, NJ). The tubes were centrifuged for 30 min at 300 x g and 4 °C, and the layer of cells was removed and re-suspended at 1×10^6 cells/ml in α -MEM medium supplemented with foetal bovine serum (FBS) (10% v/v), streptomycin sulphate (100 μ g/ml) and penicillin-G (100 units/ml). Cells were added to a 24-well plate (Nunc, Kamstrup, Roskilde, Denmark) with LPS (*Escherichia coli* serotype 055:B5; Sigma, St. Louis, MO) plus thalidomide or CG at 0.04, 0.2, 1, 5, 25 & 100 μ g/ml; or PG or PiG at 1, 5 & 25 μ g/ml in a final volume of 1 ml. Wells containing cells only and cells plus LPS only were included as controls. After 12 hours of

incubation, supernatants were removed and assayed immediately for TNF as described in Section 6.2.4.

6.2.4. TNF Assay

TNF was assayed using a commercially available ELISA kit (OpEIA human or murine TNF kit, PharMingen, San Diego, CA), according to the manufacturer's instructions. Samples (100 µl/well) in duplicate together with a serial dilution of TNF (31.25 – 2000 pg/ml) for the standard curve, were added to flat-bottom 96-well plates pre-coated with immobilised monoclonal anti-TNF antibody and incubated at room temperature for 2 h. The wells were then washed, biotinylated polyclonal antibody to TNF was added, followed by peroxidase-labelled streptavidin, and incubated at room temperature for 1 h. The wells were washed again, and the substrate (tetramethylbenzidine and hydrogen peroxide, from PharMingen's TMB substrate reagent set) was added and after 10 min the reaction was stopped with 2 N sulphuric acid. The absorbance at 450 nm was determined using a microtitre plate reader.

6.2.5. Inhibition of Tube Formation *In vitro*

Each well in a 24-well plate was coated with 300 µl of Matrigel which was allowed to solidified at 37 °C for 1 h. ECV304 cells (4×10^4) in a final volume of 1 ml of M-199 medium supplemented with 10% FBS, containing thalidomide, CG, PG and PiG at varying concentrations (2 – 25 µg/ml), were plated onto the Matrigel. After 15 – 18 h of incubation at 37 °C at 5% CO₂, the culture supernatant was aspirated. The cells were fixed and stained using Diff-Quick staining kit (Dade AG, Duding, Switzerland) according to the manufacturer's instructions. After removal of the staining solution the stained cells in each well were photographed along with a measuring ruler placed at the bottom edge of the photographing field (Olympus Camedia C-5050 professional digital camera, Olympus Optical, Tokyo, Japan). The total length of the tubes formed in the photographs was measured and divided by the area of the field (mm/mm²).

6.2.6. Cytotoxicity Assay

The 3-(4,5-dimethylthiazol-2-yl)-2,5-diphenyl tetrazolium bromide (MTT) assay, which measures mitochondrial metabolic activity, was used to determine cell viability. Cells (4×10^3 /well) were cultured with various concentrations of thalidomide, CG, PG and PiG in a final volume of 100 μ l M199 medium supplemented with 10% FBS, 100 μ g/ml streptomycin sulphate and 100 units/ml penicillin-G in flat-bottomed 96-well plates at 37 °C at 5% CO₂ for 18 h. At the end of the incubation period, 10 μ l of MTT (Sigma, St. Louis, MO, 5 mg/ml in PBS) was added to each well, and the cells were further incubated for 2 h. The supernatants were then removed and the formazan crystals in the cells were dissolved by the addition of 100 μ l of DMSO per well, and the absorbance at 590 nm was read using a plate reader. Each concentration of drug was tested in triplicate wells, and the mean \pm standard error of the mean (SEM) was calculated.

6.2.7. Stability and Plasma Concentrations of CG

6.2.7.1. Calibration Curves and Quality Controls

Standard curves were constructed by adding thalidomide (0.6-100 μ M) or CG (0.2-50 μ M) with phenacetin (60 μ M) as the internal standard in PBS for *in vitro* experiments or human plasma for the patient studies, and was processed as described in Section 5.2.5. Thalidomide in plasma at 0.6, 5, and 25 μ M and CG in plasma at 0.2, 5, and 25 μ M were stored at -80 °C and were included where appropriate as quality controls, and were found to be stable over a period of 14 days within 10% and 5% of the validated value respectively. The r^2 of calibration curves of thalidomide was 0.9995, and for CG calibration curves was 0.9999. The intra-assay recovery was 90-110% (8 samples per concentration) and the CV was 5-9% (4 samples per concentration), while the inter-assay recovery was 96-104% (15 per concentration) and the CV was 2-4% (6 samples per concentration).

6.2.7.2. Determination of CG Stability in vitro

CG (50 μM) with 60 μM of phenacetin (as an internal standard) at pH 3.5, 6.8, 7.1, 7.4, 7.7 and 8 were added to 8 mm clear polyethylene starburst conical snap vials (Alltech, Deerfield, IL), and incubated in the autosampler (Waters Associates, Milford, MA) at 37 °C. Aliquots (50 μl) of the solutions were then automatically loaded onto a Waters Breeze chromatograph at 0, 6, 12, 18 and 24 hours after incubation. The ratio of the area of the thalidomide peak or the CG peak to that of the phenacetin peak was determined as described in Section 5.2.5, and the concentration of thalidomide and CG was determined using the calibration curve. The percentage degradation of CG was calculated as: $[1 - (\text{CG concentration after incubation} / \text{starting concentration})] \times 100$.

6.2.7.3. Calculation of Plasma C_{max} , T_{max} , AUC and $t_{1/2}$ of CG in MMPs

Plasma samples processed for the studies in Chapter 4 (60 μl of each in duplicate) from 3 of the 5 MMPs, who took 200 mg thalidomide in the previous metabolite-detection studies in Chapter 4, were separated by HPLC (Sections 6.2.6.1). The concentration of CG was determined as described in Section 6.2.6.2. The non-compartment pharmacokinetic parameters, C_{max} , T_{max} , AUC, and $t_{1/2}$ were determined using WinNonlin Professional Software, version 4.0.1 (Mountain View, CA). Elimination $t_{1/2}$ was calculated as the ratio of 0.693 and the slope of the terminal phase of the log-linear concentration-time curve. The AUC was calculated as a function of time using the log-linear trapezoidal rule. Concentration was expressed as $\mu\text{mol/l}$ or $\mu\text{mol/kg}$ of the mean \pm SEM.

6.3. Results

6.3.1. Potentiation of Anti-tumour Activity of DMXAA in Mice by Thalidomide, PG, PiG and CG

Co-administration of thalidomide (100 mg/kg) was shown to potentiate the anti-tumour activity of DMXAA (Ching et al., 1995). To investigate whether the hydrolysis metabolites had the same activity, mice with Colon 38 tumours were treated with CG, PG, PiG and thalidomide at 100 mg/kg together with DMXAA (25 mg/kg), and the growth of the tumours were followed. Co-administration of PiG or PG with DMXAA did not inhibit tumour growth above that of DMXAA alone (Figure 6.1A). At 21 days after treatment, no significant difference in tumour volumes was observed between the DMXAA-treated group and those treated with DMXAA plus PG or DMXAA plus PiG (Figure 6.2). Co-administration of CG however produced greater inhibition of tumour growth than that of DMXAA alone and to a similar extent as thalidomide (Figure 6.1A). At 21 days after treatment, mice treated by CG or thalidomide combined with DMXAA had significantly smaller tumour volumes than those treated by DMXAA alone ($p < 0.05$, Figure 6.2).

CG was then compared with thalidomide at the lower doses of 20 mg/kg and 4 mg/kg for potentiation of DMXAA activity against Colon 38 tumours. At 20 mg/kg, CG plus DMXAA was more effective than thalidomide plus DMXAA or DMXAA alone (Figure 6.1B). At 21 days after treatment, mice treated by CG combined with DMXAA had significantly smaller tumour volume than those treated by DMXAA alone ($p < 0.05$). Tumour volumes from mice treated by thalidomide plus DMXAA were similar to those treated by DMXAA alone (Figure 6.2). At 4 mg/kg, neither CG nor thalidomide showed potentiation of DMXAA-induced anti-tumour effects (Figure 6.1C), and there was no significant difference between tumour volumes of mice treated with CG or thalidomide plus DMXAA or DMXAA alone at 21 days after treatment (Figure 6.2).

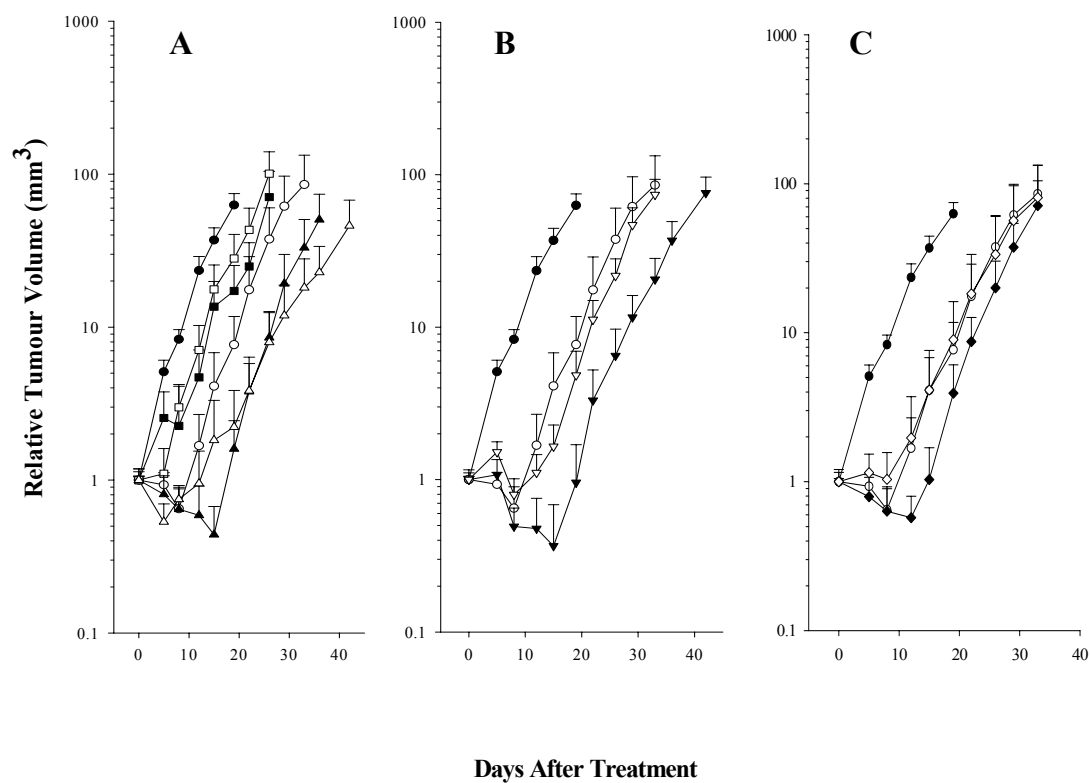


Figure 6.1 Tumour growth delay in mice untreated, or treated with DMXAA or DMXAA combined with Thal or hydrolysis products/metabolites of Thal.

- Control
- DMXAA 25mg/kg
- DMXAA 25mg/kg + PG 100mg/kg
- DMXAA 25mg/kg + PiG 100mg/kg
- ▲— DMXAA 25mg/kg + CG 100mg/kg
- △— DMXAA 25mg/kg + Thal 100mg/kg
- ▼— DMXAA 25mg/kg + CG 20mg/kg
- ▽— DMXAA 25mg/kg + Thal 20mg/kg
- ◆— DMXAA 25mg/kg + CG 4mg/kg
- ◇— DMXAA 25mg/kg + Thal 4mg/kg

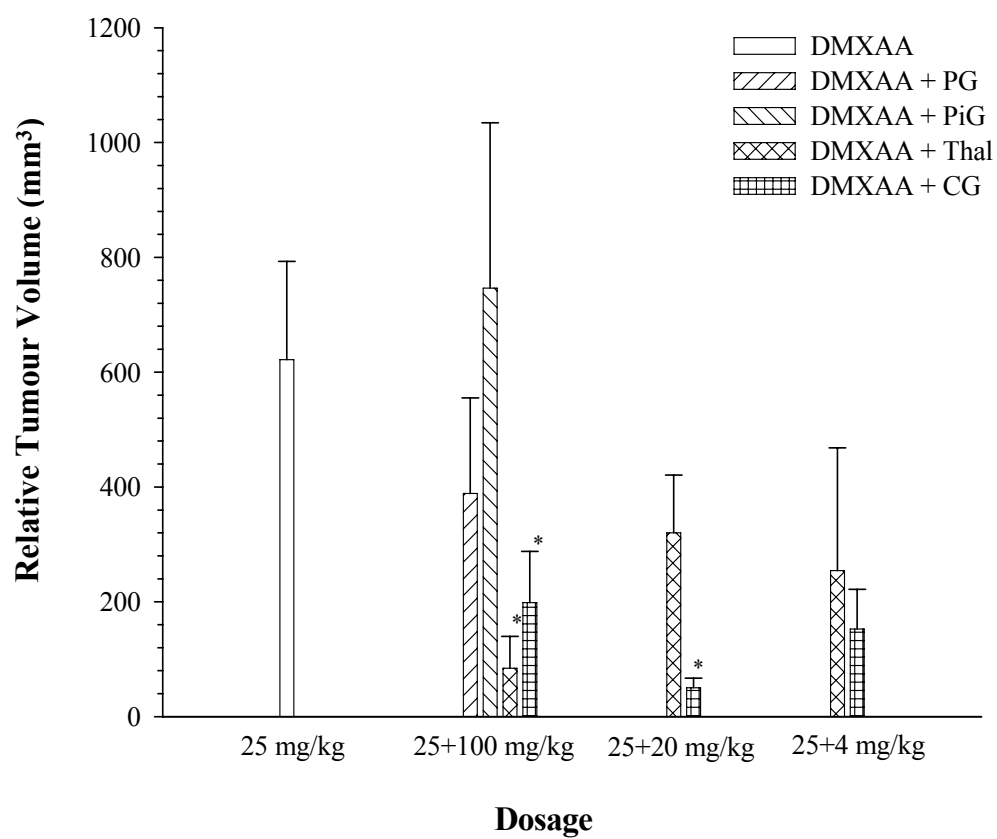


Figure 6.2 Colon 38 tumour volumes 21 days after treatment in mice. “*” represents significant difference ($p < 0.05$, student’s t -test) compared with DMXAA alone treatment.

6.3.2. Effects of Thalidomide, PG, PiG and CG on DMXAA-Induced TNF Production in Mice

Tumour-bearing mice were administered thalidomide, PG, PiG, CG or DMXAA alone, or administered DMXAA (25 mg/kg) plus PG (100 mg/kg), PiG (100 mg/kg), thalidomide (100 mg/kg or 20 mg/kg) or CG (100 mg/kg or 20 mg/kg). Serum and tumour samples of mice were assayed for TNF production 3 h after drug administration when the TNF levels were apparently influenced by DMXAA and thalidomide (Ching et al., 1995). TNF levels in serum and tumours from mice treated with PG, PiG, CG or thalidomide alone were similar to that of untreated mice (student's *t-test*). Mice treated with DMXAA alone (25 mg/kg) had a 20-fold (Figure 6.3A), and 50-fold increase respectively in serum and tumour TNF activity above those of control untreated mice (Figure 6.3B). Co-administration of PG and PiG had no effect on DMXAA-induced serum and tumour TNF level (Figure 6.3). Co-administered thalidomide reduced DMXAA-induced TNF levels in serum at 100 mg/kg and 20 mg/kg ($p < 0.05$, Figure 6.3A), but had no significant effect on DMXAA-induced intra-tumoural TNF levels (Figure 6.3B). CG significantly increased DMXAA-induced TNF production in tumours at doses of 100 mg/kg and 20 mg/kg ($p < 0.05$, Figure 6.3B), and decreased DMXAA-induced TNF levels in serum at 100 mg/kg (Figure 6.3A).

6.3.3. Effects of Thalidomide, PG, PiG and CG on LPS-induced TNF Production by HPBL in Culture

Significant TNF production was obtained when HPBL were cultured with 100 pg/ml of LPS (Figure 6.4), and that concentration was chosen for subsequent studies. HPBL were cultured with LPS plus thalidomide, PG, PiG or CG at various concentrations for 12 h, and the supernatants were assayed for TNF. PG or PiG had no significant effect on LPS-induced TNF production over all the concentrations tested (1, 5, 25 µg/ml, Figure 6.5), whereas thalidomide and CG significantly decreased LPS-induced TNF levels in a dose-dependent manner (Figure 6.5A) and to a similar extent (Figure 6.5B).

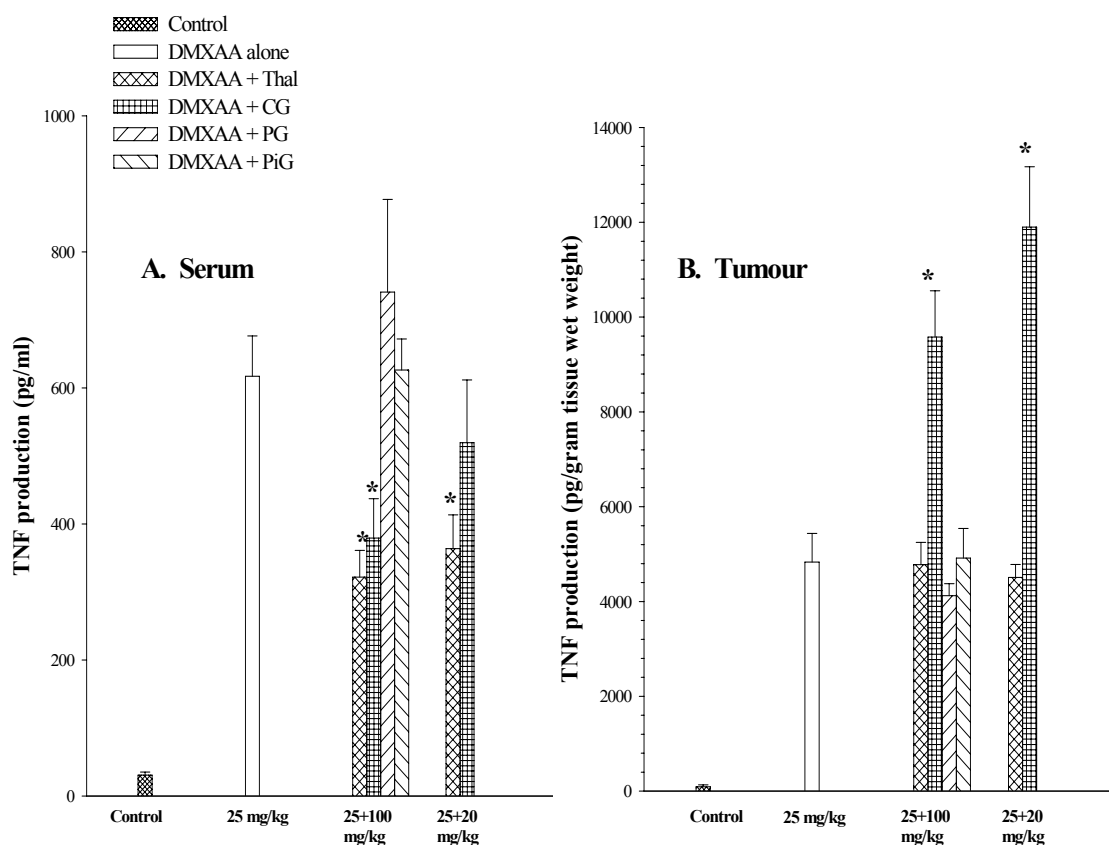


Figure 6.3 TNF levels in (A) serum and (B) tumour tissue of mice untreated, or treated with DMXAA alone or DMXAA combined with Thal or hydrolysis products/metabolites of Thal. “*” represents significant difference ($p < 0.05$, student’s t -test) compared with DMXAA alone treatment.

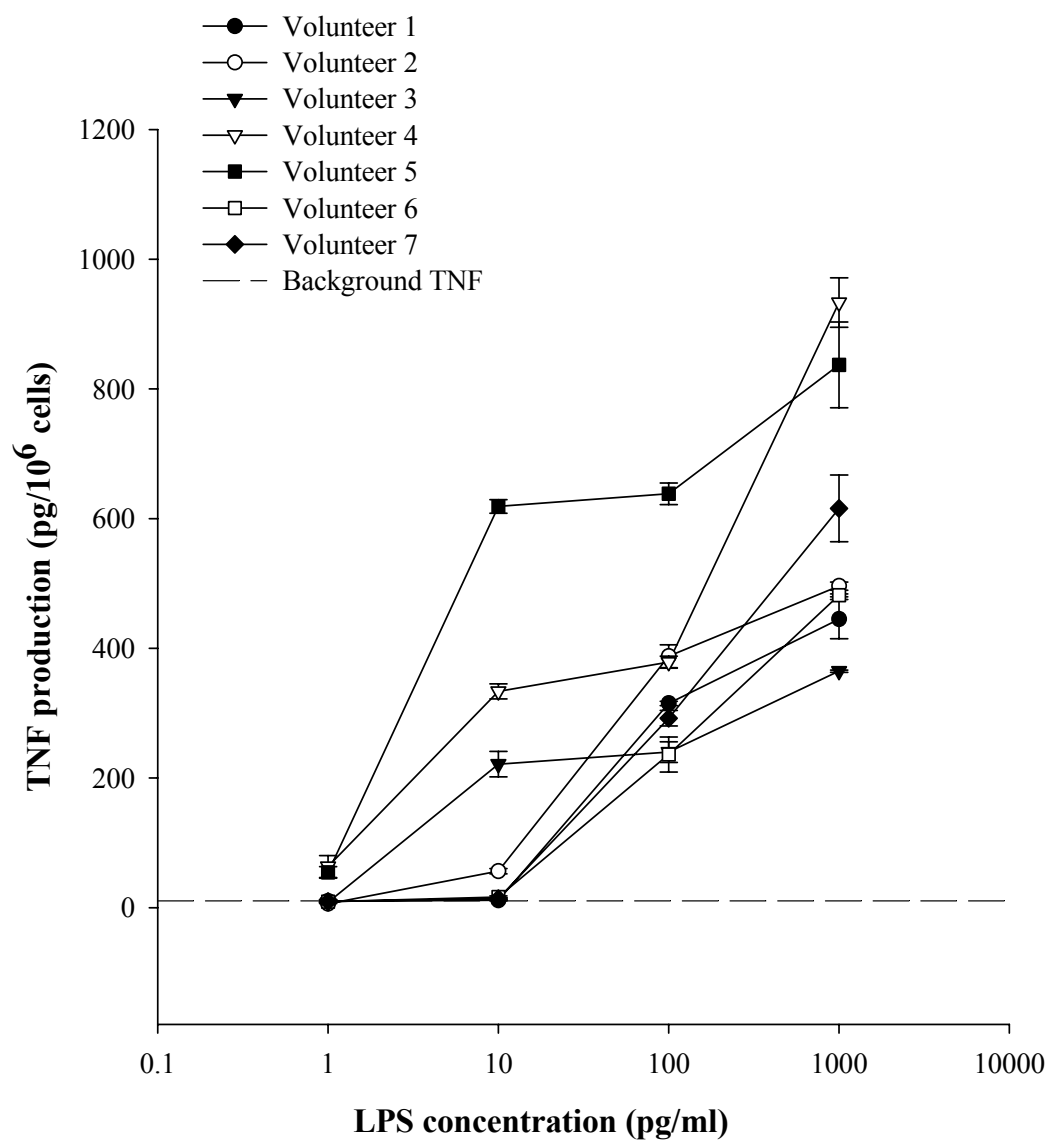


Figure 6.4 TNF production by HPBL from seven healthy volunteers at different concentrations of LPS.

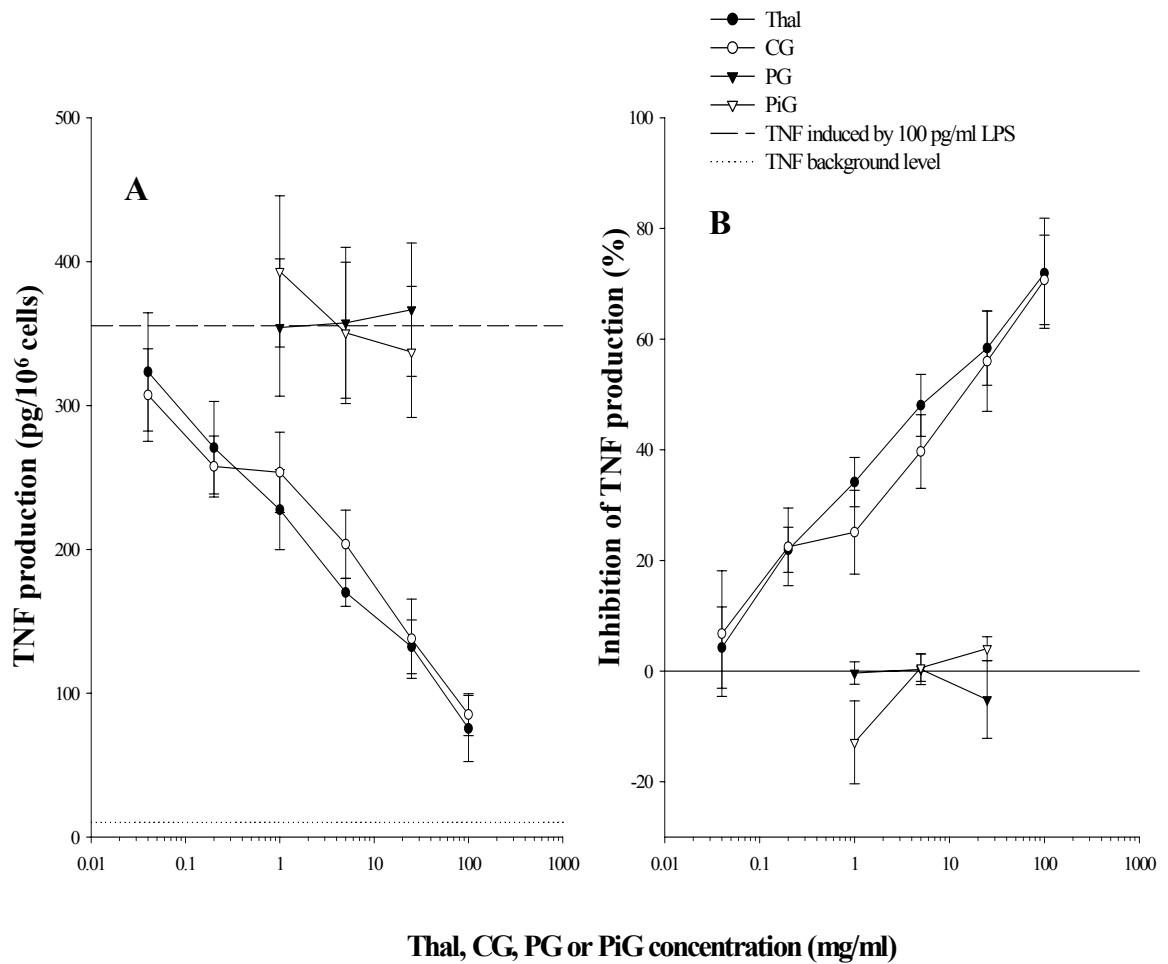


Figure 6.5 The effect of Thal, CG, PG or PiG on LPS-induced TNF production by HPBL from healthy human volunteers. (A) average TNF activity, (B) average percentage of inhibition.

6.3.4. Inhibition of Tube Formation in Matrigel

Tube formation by ECV304 cells on matrigel layers was used as an *in vitro* model for angiogenesis, and the ability of thalidomide or its hydrolysis metabolites to inhibit tube formation was tested. Near complete inhibition of tube formation was observed with thalidomide and CG at 250 µg/ml (Figures 6.6 & 6.7), and 38-41% inhibition (Figure 6.7) at the lowest concentration tested (2 µg/ml). PG and PiG however, did not show any inhibition on tube formation at all concentrations tested (Figure 6.6).

As a control that inhibition of tube formation was not as result of cytotoxicity of the drugs, ECV304 cells were cultured with thalidomide, PG, PiG and CG at the same the concentrations used for tube inhibition (2 – 250 µg/ml), and cell viability after 18 h was measured using the MTT assay (Section 6.2.6). No toxicity was observed with any of the compounds compared with untreated or DMSO-treated cultures.

6.3.5. Stability of CG at Different pHs

To examine its stability, CG was incubated at different pHs and at 0, 6, 12, 18 and 24 h after incubation, the concentrations of CG and thalidomide in solution was measured using HPLC assay which resolved CG, phenacetin and thalidomide completely with the retention times of 8.5, 22.8 and 23.6 min respectively (Figure 6.8). At pH 3.5, 7.7 and 8, 21.5%, 8.6% and 0% of CG was remaining in the solution after 24 h (Figure 6.9). CG was more stable at pH 6.8, 7.1 and 7.4. At pH 6.8, 81.75% of CG remained in solution after 24 h of incubation, and at pH 7.1 and 7.4, 50.1% and 46.6% respectively of CG remained in solution. Thalidomide was not detected in CG solutions with pH of 6.8, 7.1, 7.4, 7.7 or 8 after incubation. However, it was detected at pH of 3.5 after 6, 12, 18 and 24 h of incubation (Figure 6.9). Since the molar ratio of transformation from CG to thalidomide is 1:1, it was determined that 42% of CG was transformed into thalidomide after 24 h incubation at pH 3.5 (Figure 6.9).

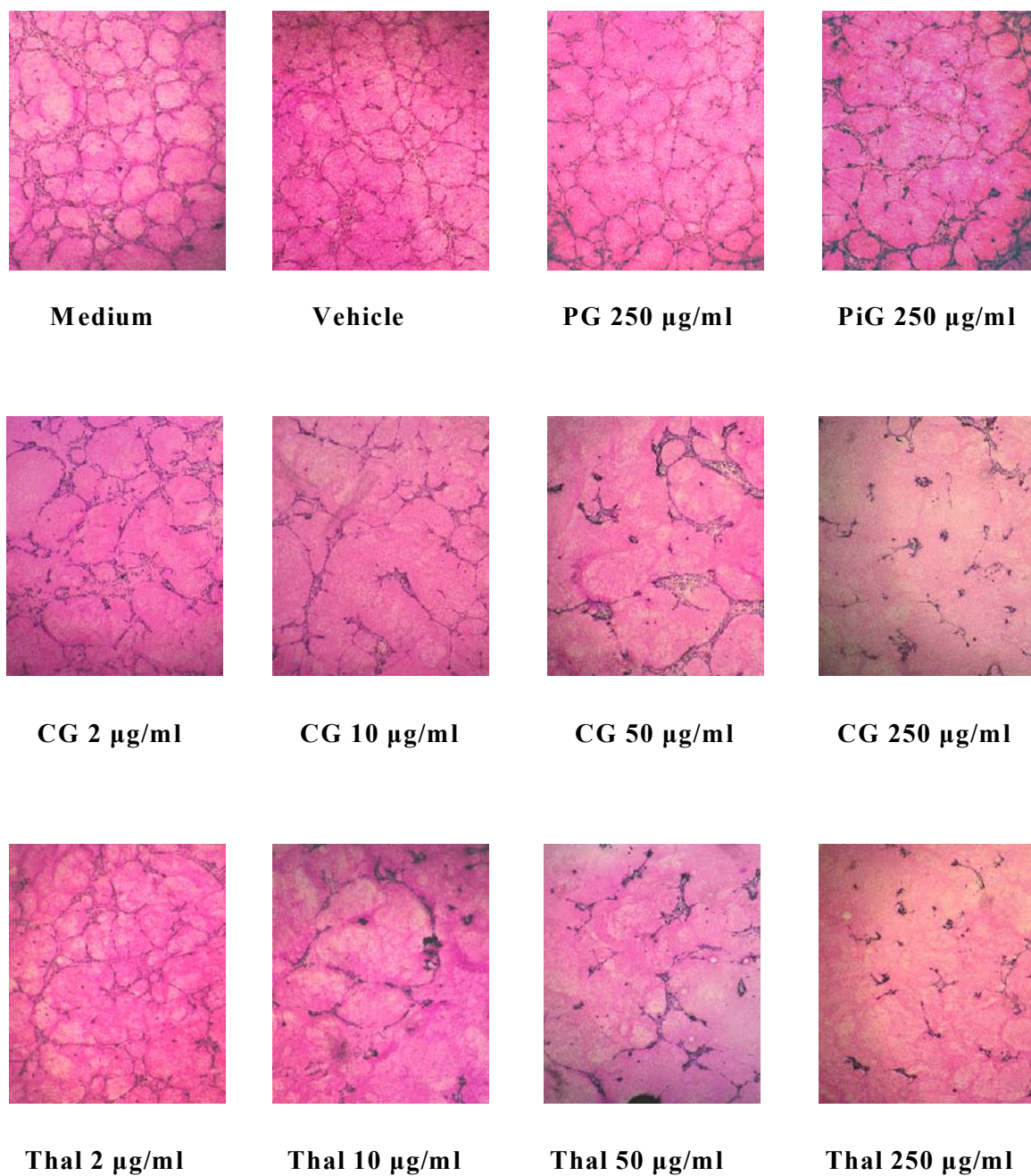


Figure 6.6 Effects of Thal, CG, PG and PiG on tube formation of ECV 304 cells in Matrigel. Cells were treated with medium only, medium with vehicle only and indicated concentrations of drugs.

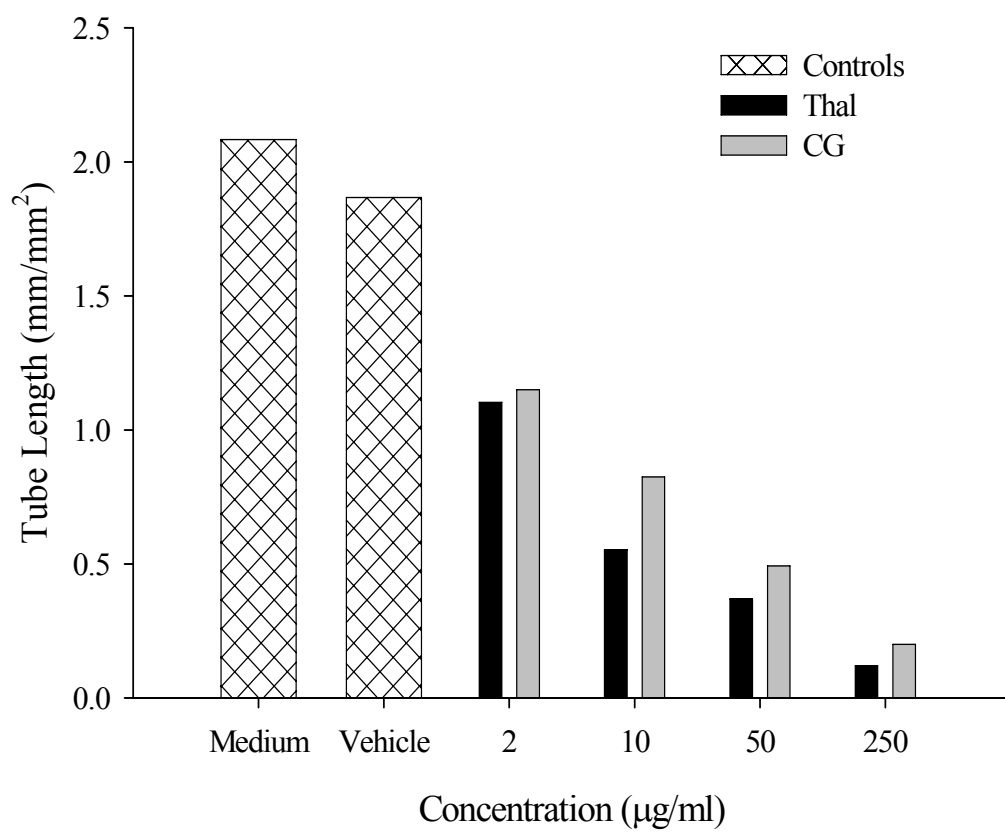


Figure 6.7 Inhibition of the tube formation of ECV 304 cells in Matrigel by Thal and CG at different concentrations.

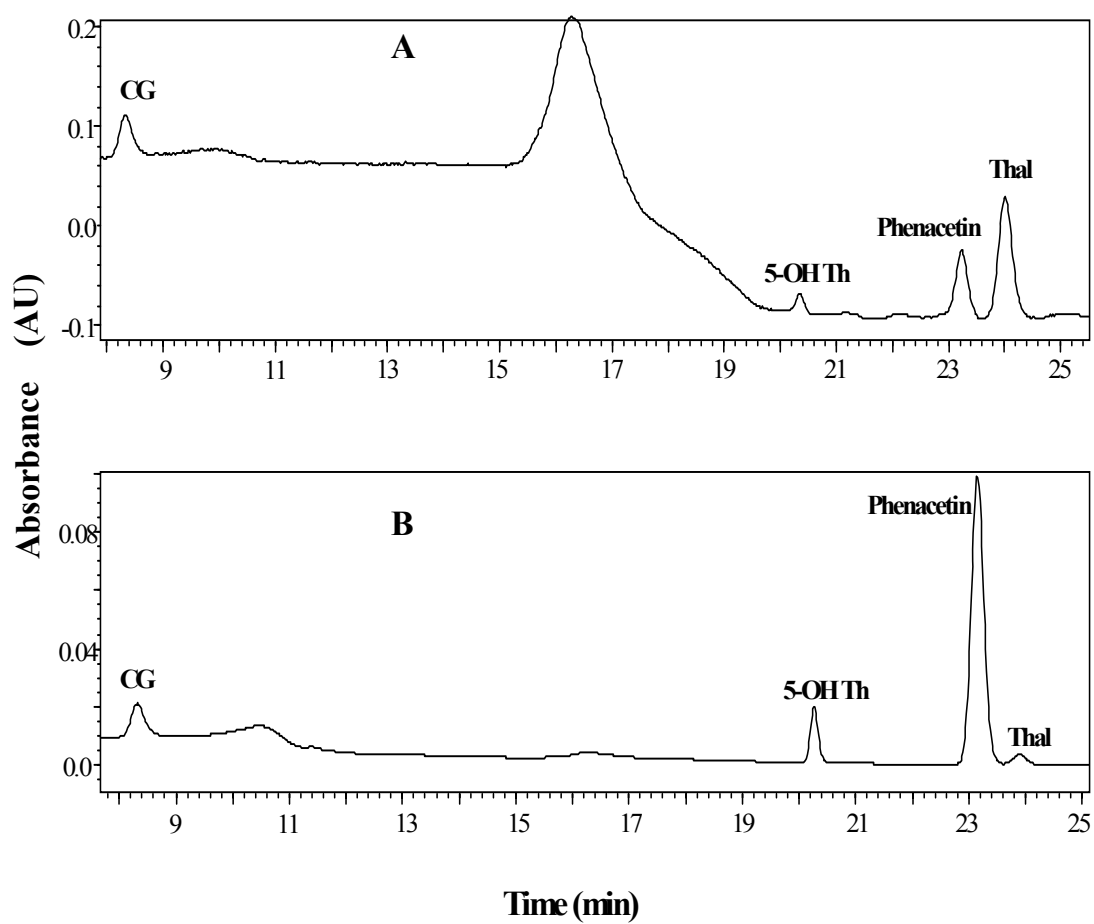


Figure 6.8 HPLC chromatograms showing complete separation of CG, phenacetin and Thal at wavelength of (A) 220 nm or (B) 248 nm.

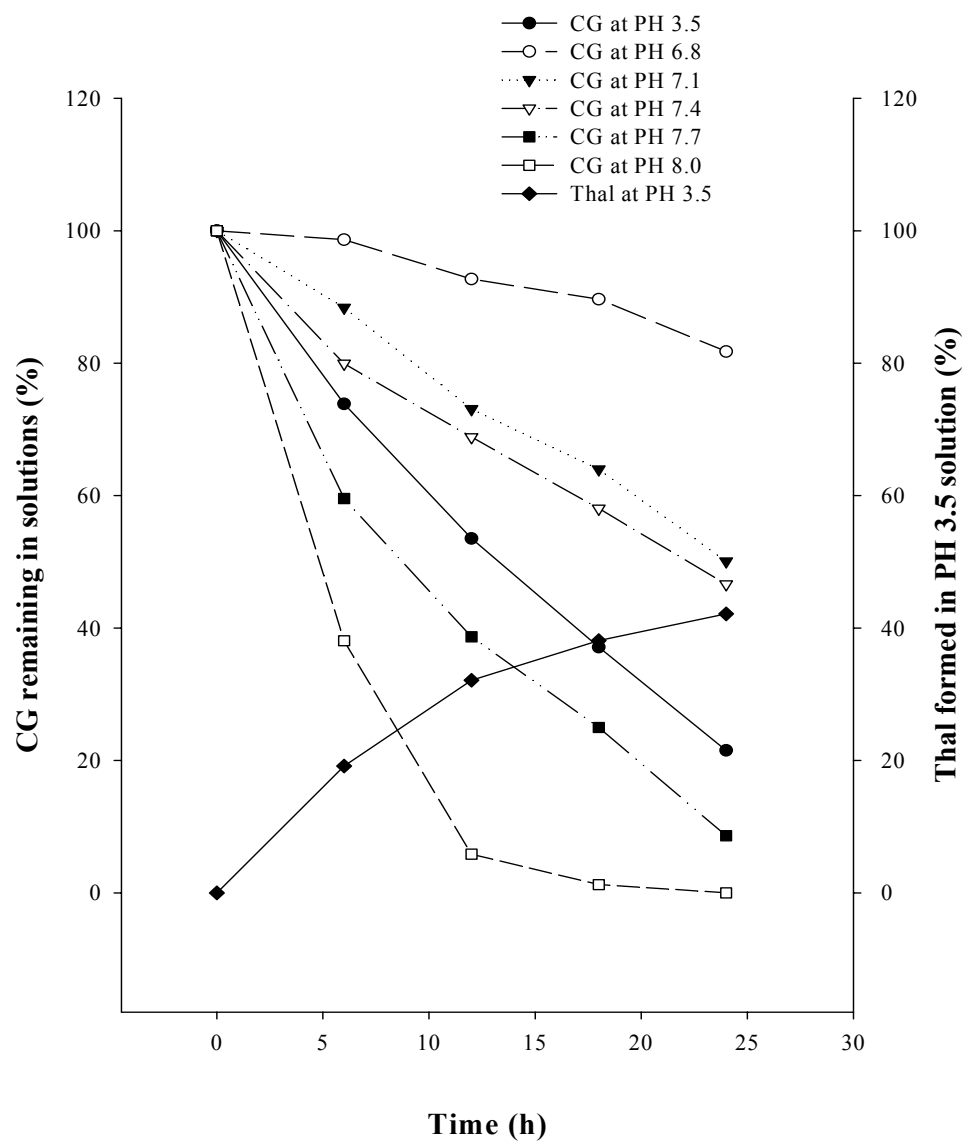


Figure 6.9 CG and Thal concentrations in PBS solutions at different pH during 24 h of incubation at 37 °C.

6.3.6. Plasma concentrations of CG in MMPs

The concentrations of CG in the plasma of 3 MMPs, who took 200 mg thalidomide and whose blood was collected for metabolite study in Chapter 4, were measured using method described in Section 6.2.7 and plotted against time after administration. The C_{\max} of CG ($5.88 \pm 0.05 \mu\text{M}$) was achieved after $5.69 \pm 0.13 \text{ h}$ (T_{\max}) (Figure 6.10). The elimination $t_{1/2}$ was $44.9 \pm 3.35 \text{ h}$ and the AUC of CG was $416 \pm 27 \mu\text{M}\cdot\text{h}$. The values of C_{\max} and T_{\max} of CG were found to be similar to those reported by Chung et al. (2004a) for thalidomide. The AUC and $t_{1/2}$ of CG were approximately 5 and 6 times higher than that of thalidomide (Figure 6.10; Table 6.1).

Table 6.1 Comparison of PK parameters of CG and Thal in MMPs.

	C_{\max} (μM)	T_{\max} (h)	$\text{AUC}_{0-\infty}$ ($\mu\text{M}\cdot\text{h}$)	$t_{1/2}$ (h)
CG	5.9 ± 0.1	5.7 ± 0.1	416 ± 27	44.9 ± 3.4
Thal*	5.4 ± 1.9	4.8 ± 1	81 ± 26	7.3 ± 0.6

* Thal PK parameters are from Chung et al., 2004a.

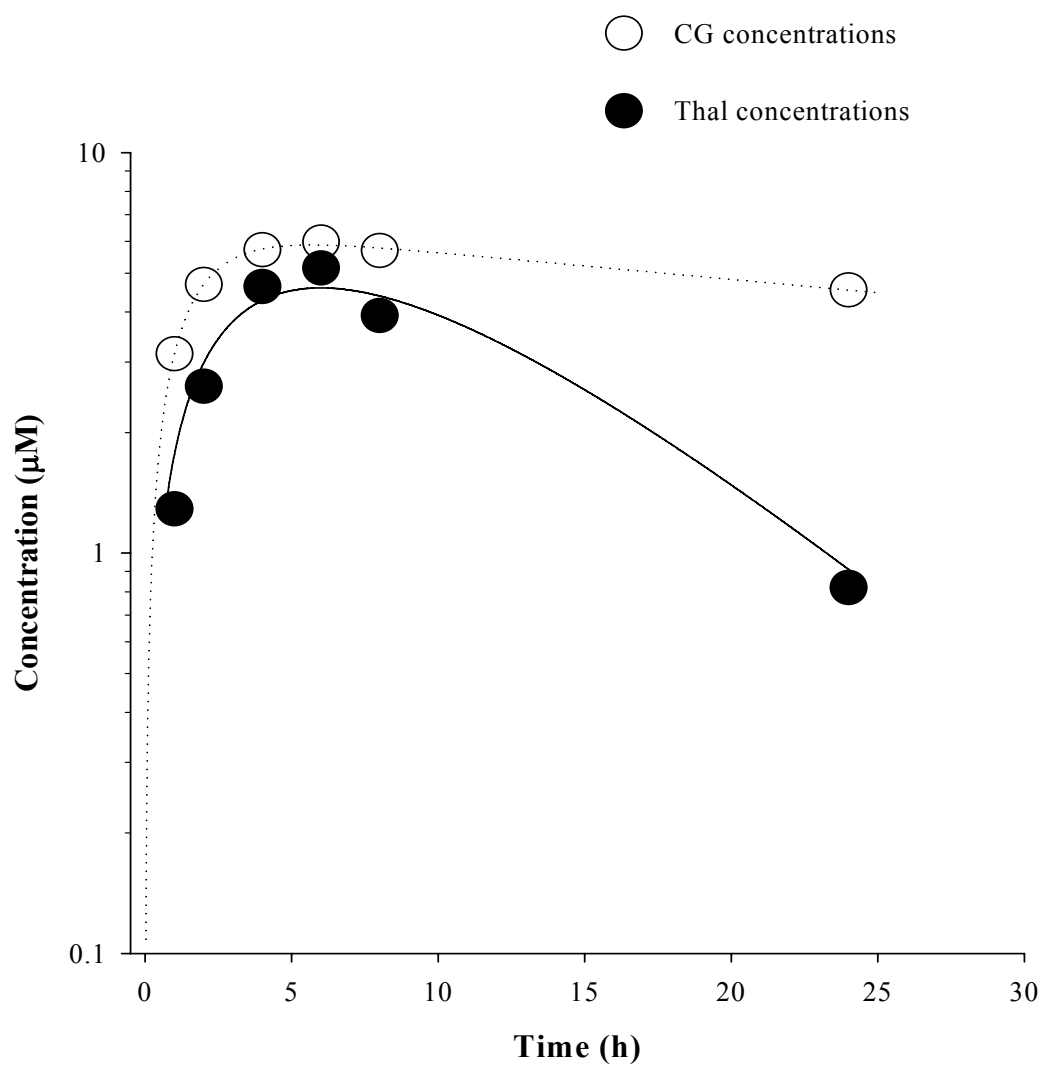


Figure 6.10 Plasma concentration-time profiles of CG (from samples of three MMPs) compared with that of thalidomide (redrawn from Chung et al., 2004a) after the treatment of 200 mg oral dose of thalidomide.

6.4. Discussion

The results in this Chapter have shown that of the three hydrolysis metabolites that were detected in all three species including MMPs, only CG showed activity in the biological assays that were carried out. Indeed, CG was as active as thalidomide in the *in vitro* assays of angiogenesis inhibition (Figures 6.6 & 6.7) and TNF inhibition (Figure 6.5) in human cell systems. The inhibition of tube formation was not due to cytotoxicity, as no loss of cell viability was observed at the same drug concentrations, and incubation time (Section 6.3.4). CG performed slightly better than thalidomide *in vivo* in modulating DMXAA-induced TNF production and anti-tumour responses in mice (Figures 6.1-3). CG provided greater tumour growth inhibition than thalidomide at doses at or above 20 mg/kg when combined with DMXAA (Figures 6.1 & 6.2). Thus CG possesses anti-angiogenic and cytokine modulatory activities, the two effects that perhaps form the basis of the anti-tumour properties of thalidomide.

Several studies have suggested that CG is unstable and will convert to thalidomide (Keberle et al., 1965; Schumacher et al., 1965b; Xiao et al., 2002), raising the possibility that perhaps the activities detected in the assays were due primarily to thalidomide that had been converted from CG. However, the stability studies here showed that CG was stable in solution at pHs between 6.8 – 7.4 (Figure 6.9), indicating that the active agent in the biological assays would have been CG and not thalidomide transformed from CG. The stability studies here showed that CG was more stable than thalidomide at physiological conditions, as only 1.3 – 20% of CG had degraded after 6 h, whereas Schumacher and co-workers showed that 25 – 50% of thalidomide had degraded after 5 h at pHs of 6.8 – 7.4 (Schumacher et al., 1965b). CG was unstable at low pH however, and 42% had converted to thalidomide at pH 3.5.

Concentrations of CG in plasma of MMPs were similar to those of thalidomide (Table 6.1, Figure 6.10) and were present for much longer periods. Thus, CG exposure is far greater than that of thalidomide. It is worthy to note that the observed *in vivo* plasma concentrations of CG were similar to or higher than the concentrations required for significant inhibition of TNF production and tube formation *in vitro* (Figures 6.5-7).

The results would strongly indicate that CG could be contributing to the therapeutic effects against multiple myeloma during thalidomide therapy. However, to conclusively prove this, more detailed pharmacokinetic studies would have to be undertaken with CG. The results from the current study are limited as it was not possible to perform detailed pharmacokinetic analysis from the data and so these conclusions are somewhat qualitative. It would be of interest to establish the degree to which CG converts thalidomide following administration of CG.

The results in this chapter suggest that CG would be better than thalidomide for clinical use, since it is more soluble (Scifinder Scholar Database, © 2003 American Chemical Society; calculated by Advanced Chemistry Development (ACD) Software Solaris V4.67 © 1994-2003 ACD), more stable at physiological conditions, and appears to be at least as active as thalidomide in the panel of biological assays performed here. A major advantage of using CG over thalidomide would be that CG appears to be non-teratogenic. CG was not teratogenic when tested in New Zealand White rabbits using various doses and routes of administration (Fabro and Smith, 1966). Nor was teratogenicity observed when CG was administered i.p. to pregnant mice (Meise et al., 1973). Its inability to cause teratogenicity was attributed to its polarity and not being able to cross the placental barrier (Keberle et al., 1965; Neubert and Neubert, 1997). Indeed, CG is the first metabolite peak eluted from the column (Figures 2.1, 4.1 & 6.8) consistent with it being the most polar of all the metabolites formed. On the other hand, when ^{14}C -labelled CG was administered to pregnant rabbits, the ratio of embryo ^{14}C /maternal plasma ^{14}C was 0.6 at 12 – 58 h after dosing (Fabro et al., 1967a), indicating that CG is able to cross the placenta, but is unable to cause teratogenicity.

In conclusion, CG has the same, if not better, activity as thalidomide, and since it is non-teratogenic, more stable and soluble than thalidomide under physiological conditions, it may be a more attractive clinical agent than thalidomide.

CHAPTER 7. GENERAL DISCUSSION

Thalidomide has been known for over half a century, but its mechanism of action is still not completely understood. It is known that different species have widely different sensitivity to thalidomide (Braun and Dailey, 1981; Gordon et al., 1981; Braun et al., 1986; Bauer et al., 1998). Studies in this thesis show major inter-species differences in the metabolism of thalidomide and suggest that the inter-species differences in the biological effects of thalidomide could be explained, at least in part, by differences in its metabolism. Another key finding to emerge from these studies is that the formation of hydroxylated metabolites is unlikely to be required for clinical anti-cancer activity, and that thalidomide or/and its hydrolysis product, CG, is/are the active agent(s). The implications of these findings are discussed.

7.1. Inter-Species Differences in Thalidomide Metabolism

The metabolism of thalidomide includes non-enzymatic hydrolysis, enzymatic hydrolysis and CYP-enzymatic hydroxylation (Chapter 3-5). The rate of hydroxylation appeared to be the rate-determining step in the metabolism of thalidomide (Figures 4.2, 4.4, 4.7 & 5.1). Hydroxylation, both *in vivo* and *in vitro*, occurred extensively with mouse (Figures 2.1, 4.2, 5.1 & 5.8), moderately with rabbit (Figures 4.4, 5.1 & 5.8) and was undetectable with human systems (Figures 3.2, 4.7 & 5.1). The degree of hydroxylation is correlated with the rate of thalidomide clearance in mice, rabbits and MMPs (Chung et al., 2004a). Thus, mice with the highest degree of hydroxylation also had the highest rate of clearance of thalidomide of the three species. Mice are also the least sensitive of the three species to thalidomide's teratogenicity (Section 4.1), and it is also the most difficult to detect anti-tumour activity using murine models (Section 1.2.1). Humans are much more responsive to thalidomide. The greater responsiveness of humans could be explained on the basis of its slower clearance of thalidomide, so that the active agent is present in the body for longer period compared with species such as mice where it is rapidly metabolised and cleared. Thus, inter-species

differences in the activity of thalidomide could be explained on the basis of differences in rates of metabolism and clearance of thalidomide.

7.2. The Active Agent in Thalidomide Therapy

A surprising result from the metabolite studies from MMPs, who were responding to thalidomide therapy, was the lack of detectable hydroxylated metabolites (Figures 3.2, 4.7 & 4.8). Hydroxylated metabolites have been shown to be anti-angiogenic and put forward as the prime candidates as the active anti-cancer agent (Marks et al., 2002; Price et al., 2002). The results in chapters 2 and 3 strongly suggest that the formation of hydroxylated products is not critical for clinical activity.

CYP2C19 has been identified as the enzyme responsible for hydroxylation of thalidomide in humans (Ando et al., 2002a). However, along with the studies by Ando and co-workers (2002a), the studies in chapter 5 did not find a correlation between the degree of hydroxylation and CYP2C19 genotype of the liver donor. Moreover, the CYP2C19 genotype and the presence of hydroxylated metabolites did not appear to be correlated with the clinical response of patients with prostate cancer to thalidomide therapy (Ando et al., 2002b). Thus, thalidomide is a poor substrate for CYP2C19, and CYP-catalysed hydroxylation may not play a strong part in the clinical response to thalidomide. The low involvement of CYP-mediated metabolism implicated in this study and other thalidomide-drug interaction studies (Trapnell et al., 1998; Scheffler et al., 1999), makes thalidomide an excellent partner for combination therapies. If the anti-cancer action of thalidomide is not dependent on CYP-enzymic activity, no competition for the metabolising enzymes with other CYP-activated anti-cancer drugs will be encountered, making thalidomide a favourable candidate for combination therapies.

The plasma and urine from MMPs who were responding to thalidomide therapy contained only thalidomide and three hydrolysis products (Figures 3.2, 4.7 & 4.8). The results strongly indicated that either thalidomide and/or its hydrolysis metabolite(s) is/are the active agent(s). The studies in chapter 6 showed that of the three hydrolysis products detected, CG had anti-angiogenic and TNF modulatory activities similar to

that of thalidomide. Moreover, CG was detectable in MMPs (Figure 6.10) at pharmacologically active concentrations. The stability study of CG *in vitro* (Figure 6.9) and the pharmacokinetic study of CG in MMPs (Figure 6.10) indicated that CG was more stable than thalidomide, and since CG appears as effective as thalidomide, the clinical effects may be due to a combination of both thalidomide and CG.

The clinical outcome of the 12 MMPs studied in this thesis showed that 3 patients had greater than 75% reduction in paraprotein level, which has been defined as a complete response (Singhal et al., 1999); 5 patients had greater than 25% reduction in paraprotein level, defined as a partial response; and one patient had good response with no object parameters to follow because of non-secretory myeloma (Professor Peter Browett, personal communication). The concentrations of thalidomide and CG in 3 MMPs, who took 200 mg thalidomide per day, were measured; and a prolonged exposure of both CG and thalidomide at concentrations, which inhibited TNF production *in vitro*, was observed (Figure 6.10). These results indicate that thalidomide at 200 mg/day is effective and maybe due to, or at least partially due to the high concentrations and long-time exposure of both CG and thalidomide. Since most of thalidomide's adverse effects appear at doses higher than 200 mg/day (Matthews and McCoy, 2003), it is suggested that thalidomide at 200 mg/day is a favourable dose for cancer therapy from the pharmacological point of view. This is in line with two recent studies which showed that thalidomide was effective at a dose of 200 mg/day and had less side-effects (Lee, 2002; Wechalekar et al., 2003).

7.3. Development of CG as A Clinical Agent

Since CG does not appear to be teratogenic (Fabro et al., 1965; Smith et al., 1965; Fabro et al., 1967b; Meise et al., 1973), it may be a more attractive clinical agent than thalidomide. It also has other properties that make it more advantageous than thalidomide. It is much more stable than thalidomide, both *in vitro* (Figure 6.9) and *in vivo* (Figure 6.10), and would be available for a longer period of time in the body. CG is most stable at pH 6.8 (Figure 6.9), and since tumour tissues have a lower pH (average range of 6.8-7.3) compared with normal tissues (pH 7.4 – 7.6) (Wike-Hooley et al., 1984), CG would have greater stability in tumour tissues providing a greater

degree of tumour-selectivity over normal tissues. On the other hand, CG converts to thalidomide at pH 3.5 (Figure 6.9), and low pHs will be encountered in the stomach following oral administration. However, since CG is also much more soluble (Section 6.4), it can easily be formulated for intravenous administrations to by-pass the stomach and to avoid the conversion to thalidomide and the risk of teratogenicity. Alternatively, CG could be given as pills that are dissolved only in the intestine.

It has been proposed that the high polarity of the molecule renders CG incapable of penetrating the placental barrier, and hence its inability to cause teratogenicity (Neubert and Neubert, 1997). Thus, using the ring-opened structure may disassociate the beneficial biological effects of thalidomide from the adverse effects. However, it must be considered that the high polarity of CG may be associated with low oral bioavailability through reduced absorption in the gut. This drawback would have to be addressed in future drug development studies. To avoid the possibility of its conversion back to thalidomide, and hence the possibility of teratogenicity, it may be possible to design analogues of CG where the middle ring of the molecule is not able to cyclize as depicted in Figure 7.1. However, with all drug development programmes, considerable preclinical research of the analogues will be necessary. The analogues will need to be screened for activity *in vitro*, followed by testing of the most potent candidates *in vivo* using animal models and their efficacy to thalidomide compared. Rodent models are the most widely used for preclinical evaluations. The studies in this thesis however, have identified potential difficulties with the use of mice as models for the evaluation of thalidomide due to widely different rates of metabolism leading to inter-species differences in bioavailability and hence activity of the drug. The analogues of CG will also need to be examined for inter-species variability in metabolism *in vitro*. If the analogues of CG also exhibit inter-species variability, it may be necessary to consider administering the analogues in a schedule that provides a similar bioavailability that would be expected to be encountered in humans.

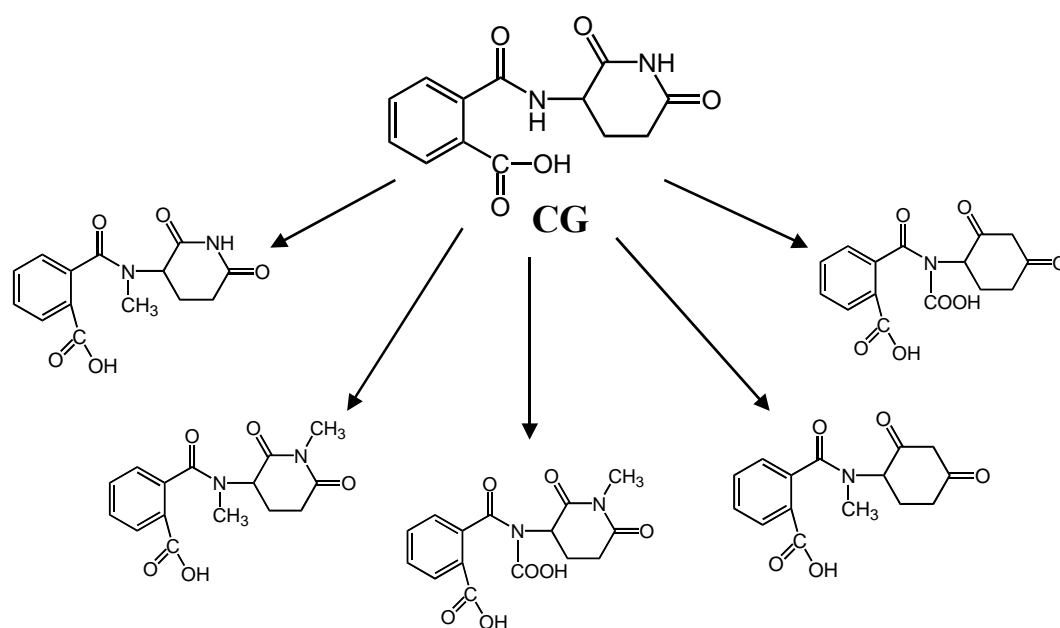


Figure 7.1 Proposed analogues of CG.

APPENDICES

Appendix 1. Chemicals and Reagents

Phthaloylglutamic acid, trichloroacetic acid (TCA), 2-hydroxypropyl- β -cyclodextrin (HPCD), β -glucuronidase, D-saccharic acid 1,4-lactone, phenacetin and β -nicotinamide adenine dinucleotide phosphate reduced form (NAPDH) were bought from Sigma-Aldrich (St Louis, MO, USA). Acetonitrile (ACN) and cetyltrimethylammonium bromide were bought from BDH Laboratory supplies (Poole, UK). Dimethylsulfoxide (DMSO) and 1-octanesulfonic acid were purchased from Riedel-de Haen AG (Seelze, Germany). Hydroxypropylcellulose was purchased from Glogon & Company Inc. (IL, USA). Glacial acetic acid was purchased from Panreac Quimica SA (Barcelona, Spain).

R-, *S*- racemic thalidomide (Thal) was a courtesy of Dr. George Muller of Celgene Corporation (Warren, NJ). DMXAA was synthesized in this laboratory (Rewcastle et al., 1991). 5'-hydroxythalidomide (5'-OH Th) was a generous gift from Professor Sven Bjorkman (Malmo University Hospital, Malmo, Sweden) and was a mixture of 5'-*cis* and 5'-*trans* diastereomers. Authentic standards of putative metabolites of thalidomide, including *N*-(*o*-carboxybenzoyl)glutamic acid imide (CG), 5-hydroxy-*N*-(*o*-carboxybenzoyl)glutamic acid imide, 4-hydroxyphthaloylisoglutamine, 4-hydroxyphthaloylglutamine, 4-hydroxythalidomide, 5-hydroxyphthaloylglutamine, 5-hydroxyphthaloylisoglutamine, phthaloylisoglutamine (PiG), phthaloylglutamine (PG), 5-hydroxythalidomide (5-OH Th), *N*-(*o*-carboxybenzoyl)isoglutamine, *N*-(*o*-carboxybenzoyl)glutamine and 5,6-dihydroxythalidomide were supplied by Associate Professor Brian Palmer of this laboratory and their structures were confirmed using 400 MHz ^1H NMR spectroscopy and MS.

Appendix 2. Publications Derived from this Thesis

Papers:

Jun Lu, N. Helsby, B.D. Palmer, P. Kestell, B.C. Baguley, M. Tingle and L-M. Ching. Thalidomide metabolism in liver microsomes of mice, rabbits and humans. *Journal of Pharmacology and Experimental Therapeutics*, **310**: 571-7. 2004.

Francisco Chung Jr., **Jun Lu**, B.D. Palmer, P. Kestell, P. Browett, B.C. Baguley, G. Muller and L-M. Ching. Thalidomide pharmacokinetics and metabolism in mice, rabbits and patients with multiple myeloma. *Clinical Cancer Research*, **10**: 5949-5956.

Jun Lu, B.D. Palmer, P. Kestell, P. Browett, B.C. Baguley, G. Muller and L-M. Ching. Thalidomide metabolites in mice and patients with multiple myeloma. *Clinical Cancer Research*, **9**: 1680-8. 2003.

Abstracts:

Francisco Chung Jr., **Jun Lu**, B.D. Palmer, P. Kestell, P. Browett, B.C. Baguley and L-M. Ching. Pharmacokinetic studies of thalidomide in mice, rabbits and multiple myeloma patients. In: *Proceedings of ASCEPT annual meeting 2003*, Vol. 10, Abstract 64.

Jun Lu, B.D. Palmer, P. Kestell, P. Browett, B.C. Baguley and L-M. Ching. Thalidomide metabolites in mice and multiple myeloma patients. In: *Proceedings of 94th Annual Meeting of American Association for Cancer Research*, **44**: 5479. 2003.

Jun Lu, L-M. Ching, P. Browett, P. Kestell, B.C. Baguley and B.D. Palmer. Thalidomide metabolites in mice, rabbits and multiple myeloma patients. In: *Proceedings of New Zealand Society for Oncology Annual Meeting 2003*, Abstract Number 11. 2003.

REFERENCES

- Agoston I, Dibbs ZI, Wang F, Muller G, Zeldis JB, Mann DL and Bozkurt B (2002) Preclinical and clinical assessment of the safety and potential efficacy of thalidomide in heart failure. *Journal of Cardiac Failure* **8**:306-314.
- Anderson KC (2001) Targeted therapy for multiple myeloma. *Seminars in Hematology* **38**:286-294.
- Anderson KC, Jones RM, Morimoto C, Leavitt P and Barut BA (1989) Response patterns of purified myeloma cells to hematopoietic growth factors. *Blood* **73**:1915-1924.
- Ando Y, Fuse E and Figg WD (2002a) Thalidomide metabolism by the CYP2C subfamily. *Clinical Cancer Research* **8**:1964-1973.
- Ando Y, Price DK, Dahut WL, Cox MC, Reed E and Figg WD (2002b) Pharmacogenetic associations of CYP2C19 genotype with in vivo metabolisms and pharmacological effects of thalidomide. *Cancer Biology & Therapy* **1**:669-673.
- Arrieta O, Guevara P, Tamariz J, Rembao D, Rivera E and Sotelo J (2002) Antiproliferative effect of thalidomide alone and combined with carmustine against C6 rat glioma. *International Journal of Experimental Pathology* **83**:99-104.
- Aweeka F, Trapnell C, Chernoff M, Jayewardene A, Spritzler J, Bellibas SE, Lizak P and Jacobson J (2001) Pharmacokinetics and pharmacodynamics of thalidomide in HIV patients treated for oral aphthous ulcers: ACTG protocol 251. AIDS Clinical Trials Group. *Journal of Clinical Pharmacology* **41**:1091-1097.
- Baidas SM, Winer EP, Fleming GF, Harris L, Pluda JM, Crawford JG, Yamauchi H, Isaacs C, Hanfelt J, Tefft M, Flockhart D, Johnson MD, Hawkins MJ, Lippman ME and Hayes DF (2000) Phase II evaluation of thalidomide in patients with metastatic breast cancer. *Journal of Clinical Oncology* **18**:2710-2717.
- Banks RE, Gearing AJ, Hemingway IK, Norfolk DR, Perren TJ and Selby PJ (1993) Circulating intercellular adhesion molecule-1 (ICAM-1), E-selectin and vascular cell adhesion molecule-1 (VCAM-1) in human malignancies. *British Journal of Cancer* **68**:122-124.
- Barlogie B, Desikan R, Eddlemon P, Spencer T, Zeldis J, Munshi N, Badros A, Zangari M, Anaissie E, Epstein J, Shaughnessy J, Ayers D, Spoon D and Tricot G (2001a) Extended survival in advanced and refractory multiple myeloma after single-agent thalidomide: identification of prognostic factors in a phase 2 study of 169 patients. *Blood* **98**:492-494.
- Barlogie B, Tricot G and Anaissie E (2001b) Thalidomide in the management of multiple myeloma. *Seminars in Oncology* **28**:577-582.

- Barosi G, Grossi A, Comotti B, Musto P, Gamba G and Marchetti M (2001) Safety and efficacy of thalidomide in patients with myelofibrosis with myeloid metaplasia. *British Journal of Haematology* **114**:78-83.
- Bataille R, Jourdan M, Zhang XG and Klein B (1989) Serum levels of interleukin 6, a potent myeloma cell growth factor, as a reflect of disease severity in plasma cell dyscrasias. *Journal of Clinical Investigation* **84**:2008-2011.
- Bauer KS, Dixon SC and Figg WD (1998) Inhibition of angiogenesis by thalidomide requires metabolic activation, which is species-dependent. *Biochemical Pharmacology* **55**:1827-1834.
- Bekker LG, Haslett P, Maartens G, Steyn L and Kaplan G (2000) Thalidomide-induced antigen-specific immune stimulation in patients with human immunodeficiency virus type 1 and tuberculosis. *Journal of Infectious Diseases* **181**:954-965.
- Bellamy WT, Richter L, Frutiger Y and Grogan TM (1999) Expression of vascular endothelial growth factor and its receptors in hematopoietic malignancies. *Cancer Research* **59**:728-733.
- Belo AV, Ferreira MA, Bosco AA, Machado RD and Andrade SP (2001) Differential effects of thalidomide on angiogenesis and tumor growth in mice. *Inflammation* **25**:91-96.
- Boughton BJ, Sheehan TM, Wood J, O'Brien D, Butler M, Simpson A and Hale KA (1995) High-performance liquid chromatographic assay of plasma thalidomide: stabilization of specimens and determination of a tentative therapeutic range for chronic graft-versus-host disease. *Annals of Clinical Biochemistry* **32**:79-83.
- Braun AG and Dailey JP (1981) Thalidomide metabolite inhibits tumor cell attachment to concanavalin A coated surfaces. *Biochemical & Biophysical Research Communications* **98**:1029-1034.
- Braun AG, Harding FA and Weinreb SL (1986) Teratogen metabolism: thalidomide activation is mediated by cytochrome P-450. *Toxicology & Applied Pharmacology* **82**:175-179.
- Breban M, Gombert B, Amor B and Dougados M (1999) Efficacy of thalidomide in the treatment of refractory ankylosing spondylitis. *Arthritis & Rheumatism* **42**:580-581.
- Caligaris-Cappio F, Gregoret MG, Merico F, Gottardi D, Ghia P, Parvis G and Bergui L (1992) Bone marrow microenvironment and the progression of multiple myeloma. *Leukemia & Lymphoma*. **8**:15-22.
- Cao Z, Joseph WR, Browne WL, Mountjoy KG, Palmer BD, Baguley BC and Ching LM (1999) Thalidomide increases both intra-tumoural tumour necrosis factor- α production and anti-tumour activity in response to 5,6-dimethylxanthenone-4-acetic acid. *British Journal of Cancer* **80**:716-723.

- Carlesimo M, Giustini S, Rossi A, Bonaccorsi P and Calvieri S (1995) Treatment of cutaneous and pulmonary sarcoidosis with thalidomide. *Journal of the American Academy of Dermatology* **32**:866-869.
- Chauhan D and Anderson KC (2003) Mechanisms of cell death and survival in multiple myeloma (MM): Therapeutic implications. *Apoptosis* **8**:337-343.
- Chen TL, Vogelsang GB, Petty BG, Brundrett RB, Noe DA, Santos GW and Colvin OM (1989) Plasma pharmacokinetics and urinary excretion of thalidomide after oral dosing in healthy male volunteers. *Drug Metabolism & Disposition* **17**:402-405.
- Cheng D, Kini AR, Rodriguez J, Burt RK, Peterson LC and Traynor AE (1999) Microvascular density and cytotoxic T cell activation correlate with response to thalidomide therapy in myeloma patients. *Blood* **94** (suppl. 1):315a.
- Ching LM, Goldsmith D, Joseph WR, Korner H, Sedgwick JD and Baguley BC (1999) Induction of intratumoral tumor necrosis factor (TNF) synthesis and hemorrhagic necrosis by 5,6-dimethylxanthenone-4-acetic acid (DMXAA) in TNF knockout mice. *Cancer Research* **59**:3304-3307.
- Ching LM, Xu ZF, Gummer BH, Palmer BD, Joseph WR and Baguley BC (1995) Effect of thalidomide on tumour necrosis factor production and anti-tumour activity induced by 5,6-dimethylxanthenone-4-acetic acid. *British Journal of Cancer* **72**:339-343.
- Chung F, Lu J, Palmer BD, Kestell P, Browett P, Baguley BC, Tingle MD and Ching LM (2004a) Thalidomide pharmacokinetics and metabolite formation in mice, rabbits and multiple myeloma patients. *Clinical Cancer Research* **10**: 5949-5956.
- Chung F, Wang LCS, Kestell P, Baguley BC and Ching LM (2004b) Modulation of thalidomide pharmacokinetics by cyclophosphamide or 5,6-dimethylxanthenone-4-acetic acid (DMXAA) in mice: the role of tumour necrosis factor. *Cancer Chemotherapy & Pharmacology* **53**:377-383.
- Coleman M, Leonard J, Lyons L, Pekle K, Nahum K, Pearse R, Niesvizky R and Michaeli J (2002) BLT-D (clarithromycin [Biaxin], low-dose thalidomide, and dexamethasone) for the treatment of myeloma and Waldenström's macroglobulinemia. *Leukemia & Lymphoma* **43**:1777-1782.
- Corral LG, Haslett PA, Muller GW, Chen R, Wong LM, Ocampo CJ, Patterson RT, Stirling DI and Kaplan G (1999) Differential cytokine modulation and T cell activation by two distinct classes of thalidomide analogues that are potent inhibitors of TNF- α . *Journal of Immunology* **163**:380-386.
- Dal Lago L, Richter MF, Cancela AI, Fernandes SA, Jung KT, Rodrigues AC, Costa TD, Di Leone LP and Schwartzmann G (2003) Phase II trial and pharmacokinetic study of thalidomide in patients with metastatic colorectal cancer. *Investigational New Drugs* **21**:359-366.

- D'Amato RJ, Loughnan MS, Flynn E and Folkman J (1994) Thalidomide is an inhibitor of angiogenesis. *Proceedings of the National Academy of Sciences of the United States of America* **91**:4082-4085.
- Davies FE, Raje N, Hideshima T, Lentzsch S, Young G, Tai YT, Lin B, Podar K, Gupta D, Chauhan D, Treon SP, Richardson PG, Schlossman RL, Morgan GJ, Muller GW, Stirling DI and Anderson KC (2001) Thalidomide and immunomodulatory derivatives augment natural killer cell cytotoxicity in multiple myeloma. *Blood* **98**:210-216.
- De AU and Pal D (1975) Possible antineoplastic agents I. *Journal of Pharmaceutical Sciences* **64**:262-266.
- Dimopoulos MA, Zervas K, Kouvatses G, Galani E, Grigoraki V, Kiamouris C, Vervessou E, Samantas E, Papadimitriou C, Economou O, Gika D, Panayiotidis P, Christakis I and Anagnostopoulos N (2001a) Thalidomide and dexamethasone combination for refractory multiple myeloma. *Annals of Oncology* **12**:991-995.
- Dimopoulos MA, Zomas A, Viniou NA, Grigoraki V, Galani E, Matsouka C, Economou O, Anagnostopoulos N and Panayiotidis P (2001b) Treatment of Waldenstrom's macroglobulinemia with thalidomide. *Journal of Clinical Oncology* **19**:3596-3601.
- Ding Q, Kestell P, Baguley BC, Palmer BD, Paxton JW, Muller G and Ching LM (2002) Potentiation of the antitumour effect of cyclophosphamide in mice by thalidomide. *Cancer Chemotherapy & Pharmacology* **50**:186-192.
- Dmoszynska A, Bojarska-Junak A, Domanski D, Rolinski J, Hus M and Soroka-Wojtaszko M (2002) Production of proangiogenic cytokines during thalidomide treatment of multiple myeloma. *Leukemia & Lymphoma*. **43**:401-406.
- Drucker L, Uziel O, Tohami T, Shapiro H, Radnay J, Yarkoni S, Lahav M and Lishner M (2003) Thalidomide down-regulates transcript levels of GC-rich promoter genes in multiple myeloma. *Molecular Pharmacology* **64**:415-420.
- Dunzendorfer S, Herold M and Wiedermann CJ (1999) Inducer-specific bidirectional regulation of endothelial interleukin-8 production by thalidomide. *Immunopharmacology* **43**:59-64.
- Eisen TG (2000) Thalidomide in solid tumors: the London experience. *Oncology (Huntington)* **14**:17-20.
- Elliott MA, Mesa RA, Li CY, Hook CC, Ansell SM, Levitt RM, Geyer SM and Tefferi A (2002) Thalidomide treatment in myelofibrosis with myeloid metaplasia. *British Journal of Haematology* **117**:288-296.
- Eriksson T and Bjorkman S (1997) Handling of blood samples for determination of thalidomide. *Clinical Chemistry* **43**:1094-1096.
- Eriksson T, Bjorkman S, Roth B, Bjork H and Hoglund P (1998a) Hydroxylated metabolites of thalidomide: formation in-vitro and in-vivo in man. *Journal of Pharmacy & Pharmacology* **50**:1409-1416.

- Eriksson T, Bjorkman S, Roth B, Fyge A and Hoglund P (1995) Stereospecific determination, chiral inversion in vitro and pharmacokinetics in humans of the enantiomers of thalidomide. *Chirality* **7**:44-52.
- Eriksson T, Bjorkman S, Roth B, Fyge A and Hoglund P (1998b) Enantiomers of thalidomide: blood distribution and the influence of serum albumin on chiral inversion and hydrolysis. *Chirality* **10**:223-228.
- Eriksson T, Bjorkman S, Roth B and Hoglund P (2000) Intravenous formulations of the enantiomers of thalidomide: pharmacokinetic and initial pharmacodynamic characterization in man. *Journal of Pharmacy & Pharmacology* **52**:807-817.
- Ezell TN, Maloney N, Githua JW and Taylor LD (2003) Exposure to the anti-TNF- α drug thalidomide induces apoptotic cell death in human T leukemic cells. *Cellular & Molecular Biology* **49**:1117-1124.
- Fabro S, Schumacher H, Smith RL, Stagg RB and Williams RT (1965) The metabolism of thalidomide: some biological effects of thalidomide and its metabolites. *British Journal of Pharmacology* **25**:352-362.
- Fabro S and Smith RL (1966) The teratogenic activity of thalidomide in the rabbit. *Journal of Pathology & Bacteriology* **91**:511-519.
- Fabro S, Smith RL and Williams RT (1967a) The fate of ^{14}C thalidomide in the pregnant rabbit. *Biochemical Journal* **104**:565-569.
- Fabro S, Smith RL and Williams RT (1967b) The fate of the hydrolysis products of thalidomide in the pregnant rabbit. *Biochemical Journal* **104**:570-574.
- Faid L, Van Riet I, De Waele M, Facon T, Schots R, Lacor P and Van Camp B (1996) Adhesive interactions between tumour cells and bone marrow stromal elements in human multiple myeloma. *European Journal of Haematology* **57**:349-358.
- Faigle JW (1962) The metabolic fate of thalidomide. *Experientia* **18**:389-397.
- Fife K, Howard MR, Gracie F, Phillips RH and Bower M (1998) Activity of thalidomide in AIDS-related Kaposi's sarcoma and correlation with HHV8 titre. *International Journal of STD & AIDS* **9**:751-755.
- Figg WD, Dahut W, Duray P, Hamilton M, Tompkins A, Steinberg SM, Jones E, Premkumar A, Linehan WM, Floeter MK, Chen CC, Dixon S, Kohler DR, Kruger EA, Gubish E, Pluda JM and Reed E (2001) A randomized phase II trial of thalidomide, an angiogenesis inhibitor, in patients with androgen-independent prostate cancer. *Clinical Cancer Research* **7**:1888-1893.
- Figg WD, Raje S, Bauer KS, Tompkins A, Venzon D, Bergan R, Chen A, Hamilton M, Pluda J and Reed E (1999) Pharmacokinetics of thalidomide in an elderly prostate cancer population. *Journal of Pharmaceutical Sciences* **88**:121-125.
- Fine HA, Figg WD, Jaeckle K, Wen PY, Kyritsis AP, Loeffler JS, Levin VA, Black PM, Kaplan R, Pluda JM and Yung WK (2000) Phase II trial of the antiangiogenic

- agent thalidomide in patients with recurrent high-grade gliomas. *Journal of Clinical Oncology* **18**:708-715.
- Fujita J, Mestre JR, Zeldis JB, Subbaramaiah K and Dannenberg AJ (2001) Thalidomide and its analogues inhibit lipopolysaccharide-mediated induction of cyclooxygenase-2. *Clinical Cancer Research* **7**:3349-3355.
- Fullerton PM and Kremer M (1961) Neuropathy after intake of thalidomide. *British Medical Journal*:855-858.
- Garcia-Sanz R, Gonzalez-Fraile MI, Sierra M, Lopez C, Gonzalez M and San Miguel JF (2002) The combination of thalidomide, cyclophosphamide and dexamethasone (ThaCyDex) is feasible and can be an option for relapsed/refractory multiple myeloma. *Hematology Journal* **3**:43-48.
- Geitz H, Handt S and Zwingenberger K (1996) Thalidomide selectively modulates the density of cell surface molecules involved in the adhesion cascade. *Immunopharmacology* **31**:213-221.
- Gordon GB, Spielberg SP, Blake DA and Balasubramanian V (1981) Thalidomide teratogenesis: evidence for a toxic arene oxide metabolite. *Proceedings of the National Academy of Sciences of the United States of America* **78**:2545-2548.
- Govindarajan R (2000) Irinotecan and thalidomide in metastatic colorectal cancer. *Oncology (Huntington)* **14**:29-32.
- Govindarajan R (2002) Irinotecan/thalidomide in metastatic colorectal cancer. *Oncology (Huntington)* **16**:23-26.
- Grabstald H and Golbey R (1965) Clinical experience with thalidomide in patients with cancer. *Clinical Pharmacology & Therapeutics* **6**:298-302.
- Grosshans E and Illy G (1984) Thalidomide therapy for inflammatory dermatoses. *International Journal of Dermatology* **23**:598-602.
- Gullestad L, Semb AG, Holt E, Skardal R, Ueland T, Yndestad A, Froland SS and Aukrust P (2002) Effect of thalidomide in patients with chronic heart failure. *American Heart Journal* **144**:847-850.
- Gunzler V, Hanauske-Abel HM, Tschank G and Schulte-Wissermann H (1986) Immunological effects of thalidomide. Inactivity of the drug and several of its hydrolysis products in mononucleocyte proliferation tests. *Arzneimittel-Forschung* **36**:1138-1141.
- Gupta A, Cohen BH, Ruggieri P, Packer RJ and Phillips PC (2003) Phase I study of thalidomide for the treatment of plexiform neurofibroma in neurofibromatosis 1. *Neurology* **60**:130-132.
- Gupta D, Treon SP, Shima Y, Hideshima T, Podar K, Tai YT, Lin B, Lentzsch S, Davies FE, Chauhan D, Schlossman RL, Richardson P, Ralph P, Wu L, Payvandi F, Muller G, Stirling DI and Anderson KC (2001) Adherence of multiple myeloma

- cells to bone marrow stromal cells upregulates vascular endothelial growth factor secretion: therapeutic applications. *Leukemia* **15**:1950-1961.
- Gutierrez-Rodriguez O (1984) Thalidomide. A promising new treatment for rheumatoid arthritis. *Arthritis & Rheumatism* **27**:1118-1121.
- Gutman M, Szold A, Ravid A, Lazauskas T, Merimsky O and Klausner JM (1996) Failure of thalidomide to inhibit tumor growth and angiogenesis in vivo. *Anticancer Research* **16**:3673-3677.
- Hallek M, Bergsagel PL and Anderson KC (1998) Multiple myeloma: increasing evidence for a multistep transformation process. *Blood* **91**:3-21.
- Haslett P, Hempstead M, Seidman C, Diakun J, Vasquez D, Freedman VH and Kaplan G (1997) The metabolic and immunologic effects of short-term thalidomide treatment of patients infected with the human immunodeficiency virus. *AIDS Research & Human Retroviruses* **13**:1047-1054.
- Haslett PA, Corral LG, Albert M and Kaplan G (1998) Thalidomide costimulates primary human T lymphocytes, preferentially inducing proliferation, cytokine production, and cytotoxic responses in the CD8⁺ subset. *Journal of Experimental Medicine* **187**:1885-1892.
- Haslett PA, Hanekom WA, Muller G and Kaplan G (2003) Thalidomide and a thalidomide analogue drug costimulate virus-specific CD8⁺ T cells in vitro. *Journal of Infectious Diseases* **187**:946-955.
- Haslett PA, Klausner JD, Makonkawkeyoon S, Moreira A, Metatratip P, Boyle B, Kunachiwa W, Maneekarn N, Vongchan P, Corral LG, Elbeik T, Shen Z and Kaplan G (1999) Thalidomide stimulates T cell responses and interleukin 12 production in HIV-infected patients. *AIDS Research & Human Retroviruses*. **15**:1169-1179.
- Hideshima T, Chauhan D, Podar K, Schlossman RL, Richardson P and Anderson KC (2001a) Novel therapies targeting the myeloma cell and its bone marrow microenvironment. *Seminars in Oncology* **28**:607-612.
- Hideshima T, Chauhan D, Richardson P, Mitsiades C, Mitsiades N, Hayashi T, Munshi N, Dang L, Castro A, Palombella V, Adams J and Anderson KC (2002) NF-kappa B as a therapeutic target in multiple myeloma. *Journal of Biological Chemistry* **277**:16639-16647.
- Hideshima T, Chauhan D, Schlossman RL, Richardson P and Anderson KC (2001b) The role of tumor necrosis factor alpha in the pathophysiology of human multiple myeloma: therapeutic applications. *Oncogene*. **20**:4519-4527.
- Hideshima T, Chauhan D, Shima Y, Raje N, Davies FE, Tai YT, Treon SP, Lin B, Schlossman RL, Richardson P, Muller G, Stirling DI and Anderson KC (2000) Thalidomide and its analogs overcome drug resistance of human multiple myeloma cells to conventional therapy. *Blood* **96**:2943-2950.

- Horowitz SB and Stirling AL (1999) Thalidomide-induced toxic epidermal necrolysis. *Pharmacotherapy* **19**:1177-1180.
- Hsu C, Chen CN, Chen LT, Wu CY, Yang PM, Lai MY, Lee PH and Cheng AL (2003) Low-dose thalidomide treatment for advanced hepatocellular carcinoma. *Oncology* **65**:242-249.
- Huang PH and McBride WG (1990) Thalidomide induced alteration in secondary structure of rat embryonic DNA in vivo. *Teratogenesis, Carcinogenesis, & Mutagenesis* **10**:281-294.
- Huang PH, McBride WG and Tuman WG (1999) Interaction of thalidomide with DNA of rabbit embryos: a possible explanation for its immunosuppressant and teratogenic effects. *Pharmacology & Toxicology* **85**:103-104.
- Hussein MA (2003) Modifications to therapy for multiple myeloma: pegylated liposomal Doxorubicin in combination with vincristine, reduced-dose dexamethasone, and thalidomide. *Oncologist* **3**:39-45.
- Huupponen R and Pyykko K (1995) Stability of thalidomide in human plasma. *Clinical Chemistry* **41**:1199.
- Jacobson JM, Greenspan JS, Spritzler J, Ketter N, Fahey JL, Jackson JB, Fox L, Chernoff M, Wu AW, MacPhail LA, Vasquez GJ and Wohl DA (1997) Thalidomide for the treatment of oral aphthous ulcers in patients with human immunodeficiency virus infection. National Institute of Allergy and Infectious Diseases AIDS Clinical Trials Group. *New England Journal of Medicine* **336**:1487-1493.
- Johnke H and Zachariae H (1993) Thalidomide treatment of prurigo nodularis. *Ugeskrift for Laeger* **155**:3028-3030.
- Jonsson NA (1972) Chemical structure and teratogenic properties. IV. An outline of a chemical hypothesis for the teratogenic action of thalidomide. *Acta Pharmaceutica Suecica* **9**:543-562.
- Jourdan M, Tarte K, Legouffe E, Brochier J, Rossi JF and Klein B (1999) Tumor necrosis factor is a survival and proliferation factor for human myeloma cells. *European Cytokine Network*. **10**:65-70.
- Joussen AM, Germann T and Kirchhof B (1999) Effect of thalidomide and structurally related compounds on corneal angiogenesis is comparable to their teratological potency. *Graefes Archive for Clinical & Experimental Ophthalmology* **237**:952-961.
- Juliussen G, Celsing F, Turesson I, Lenhoff S, Adriansson M and Malm C (2000) Frequent good partial remissions from thalidomide including best response ever in patients with advanced refractory and relapsed myeloma. *British Journal of Haematology* **109**:89-96.
- Keberle H, Faigle JW, Fritz H, Knusel F, Loustalot P and Schmid K (1965) Theories on the mechanism of action of thalidomide, in *Embryopathic Activity of Drugs*

- (Robson JM, Sullivan FM and Smith RL eds) pp 210-233, J. & A. Churchill Ltd., London.
- Keifer JA, Guttridge DC, Ashburner BP and Baldwin AS, Jr. (2001) Inhibition of NF-kappa B activity by thalidomide through suppression of IkappaB kinase activity. *Journal of Biological Chemistry* **276**:22382-22387.
- Kelsey FO (1988) Thalidomide update: regulatory aspects. *Teratology* **38**:221-226.
- Kenyon BM, Browne F and D'Amato RJ (1997) Effects of thalidomide and related metabolites in a mouse corneal model of neovascularization. *Experimental Eye Research* **64**:971-978.
- Kestell P, Zhao L, Baguley BC, Palmer BD, Muller G, Paxton JW and Ching LM (2000) Modulation of the pharmacokinetics of the antitumour agent 5,6-dimethylxanthenone-4-acetic acid (DMXAA) in mice by thalidomide. *Cancer Chemotherapy & Pharmacology* **46**:135-141.
- Kim I, Uchiyama H, Chauhan D and Anderson KC (1994) Cell surface expression and functional significance of adhesion molecules on human myeloma-derived cell lines. *British Journal of Haematology* **87**:483-493.
- Klausner JD, Freedman VH and Kaplan G (1996) Thalidomide as an anti-TNF-alpha inhibitor: implications for clinical use. *Clinical Immunology & Immunopathology* **81**:219-223.
- Koch HP and Czejka MJ (1986) Evidence for the intercalation of thalidomide into DNA: clue to the molecular mechanism of thalidomide teratogenicity? *Zeitschrift fur Naturforschung - Section C - Biosciences*. **41**:1057-1061.
- Kotoh T, Dhar DK, Masunaga R, Tabara H, Tachibana M, Kubota H, Kohno H and Nagasue N (1999) Antiangiogenic therapy of human esophageal cancers with thalidomide in nude mice. *Surgery* **125**:536-544.
- Krenn M, Gamcsik MP, Vogelsang GB, Colvin OM and Leong KW (1992) Improvements in solubility and stability of thalidomide upon complexation with hydroxypropyl-beta-cyclodextrin. *Journal of Pharmaceutical Sciences* **81**:685-689.
- Kruse FE, Joussen AM, Rohrschneider K, Becker MD and Volcker HE (1998) Thalidomide inhibits corneal angiogenesis induced by vascular endothelial growth factor. *Graefes Archive for Clinical & Experimental Ophthalmology* **236**:461-466.
- Kumar S, Gertz MA, Dispenzieri A, Lacy MQ, Geyer SM, Iturria NL, Fonseca R, Hayman SR, Lust JA, Kyle RA, Greipp PR, Witzig TE and Rajkumar SV (2003) Response rate, durability of response, and survival after thalidomide therapy for relapsed multiple myeloma.[comment]. *Mayo Clinic Proceedings* **78**:34-39.
- Larkin M (1999) Low-dose thalidomide seems to be effective in multiple myeloma. *Lancet* **354**:925.
- Lee CK, Barlogie B, Munshi N, Zangari M, Fassas A, Jacobson J, van Rhee F, Cottler-Fox M, Muwalla F and Tricot G (2003) DTPACE: an effective, novel combination

- chemotherapy with thalidomide for previously treated patients with myeloma. *Journal of Clinical Oncology* **21**:2732-2739.
- Lee FC (2002) Second response to lower-dose thalidomide in a patient with multiple myeloma. *Blood* **99**:4248; discussion 4249.
- Leleu X, Magro L, Fawaz A, Bauters F, Facon T and Yakoub-Agha I (2002) Efficacy of a low dose of thalidomide in advanced multiple myeloma. *Blood* **100**:1519-1520.
- Lentzsch S, Rogers MS, LeBlanc R, Birsner AE, Shah JH, Treston AM, Anderson KC and D'Amato RJ (2002) S-3-Amino-phthalimido-glutarimide inhibits angiogenesis and growth of B-cell neoplasias in mice. *Cancer Research* **62**:2300-2305.
- Lenz W (1962) Thalidomide and congenital abnormalities. *Lancet* **1**:45.
- Li J, Luo S, Hong W, Zhou Z and Zou W (2002) Influence of thalidomide on interleukin-6 and its transmission in multiple myeloma patients. *Aizheng (Chinese Journal of Oncology)* **24**:254-256.
- Li J, Luo SK, Hong WD, Zhou ZH and Zou WY (2003) Influence of thalidomide on bone marrow microenvironment in refractory and relapsed multiple myeloma. *Aizheng (Chinese Journal of Oncology)* **22**:346-349.
- Little RF, Wyvill KM, Pluda JM, Welles L, Marshall V, Figg WD, Newcomb FM, Tosato G, Feigal E, Steinberg SM, Whitby D, Goedert JJ and Yarchoan R (2000) Activity of thalidomide in AIDS-related Kaposi's sarcoma. *Journal of Clinical Oncology* **18**:2593-2602.
- Liu L and Wells PG (1995) DNA oxidation as a potential molecular mechanism mediating drug-induced birth defects: phenytoin and structurally related teratogens initiate the formation of 8-hydroxy-2'-deoxyguanosine in vitro and in vivo in murine maternal hepatic and embryonic tissues. *Free Radical Biology & Medicine*. **19**:639-648.
- Londono F (1973) Thalidomide in the treatment of actinic prurigo. *International Journal of Dermatology* **12**:326-328.
- Luzzio FA, Mayorov AV, Ng SS, Kruger EA and Figg WD (2003) Thalidomide metabolites and analogues. 3. Synthesis and antiangiogenic activity of the teratogenic and TNFalpha-modulatory thalidomide analogue 2-(2,6-dioxopiperidine-3-yl)phthalimidine. *Journal of Medicinal Chemistry* **46**:3793-3799.
- Luzzio FA, Thomas EM and Figg WD (2000) Thalidomide metabolites and analogs. Part 2: Cyclic derivatives of 2-N-phthalimido-2S,3S (3-hydroxy) ornithine. *Tetrahedron Letters* **41**:7151-7155.
- Lyon AW, Duran G and Raisys VA (1995) Determination of thalidomide by high performance liquid chromatography: methodological strategy for clinical trials. *Clinical Biochemistry* **28**:467-470.

- Mall JW, Philipp AW, Mall W and Pollmann C (2002) Long-term survival of a patient with small-cell lung cancer (SCLC) following treatment with thalidomide and combination chemotherapy. *Angiogenesis*. **5**:11-13.
- Marks MG, Shi J, Fry MO, Xiao Z, Trzyna M, Pokala V, Ihnat MA and Li PK (2002) Effects of putative hydroxylated thalidomide metabolites on blood vessel density in the chorioallantoic membrane (CAM) assay and on tumor and endothelial cell proliferation. *Biological & Pharmaceutical Bulletin* **25**:597-604.
- Matthews SJ and McCoy C (2003) Thalidomide: a review of approved and investigational uses. *Clinical Therapeutics*. **25**:342-395.
- McBride W (1961) Thalidomide and congenital abnormalities. *Lancet* **2**:1358.
- McHugh SM, Rifkin IR, Deighton J, Wilson AB, Lachmann PJ, Lockwood CM and Ewan PW (1995) The immunosuppressive drug thalidomide induces T helper cell type 2 (Th2) and concomitantly inhibits Th1 cytokine production in mitogen- and antigen-stimulated human peripheral blood mononuclear cell cultures. *Clinical & Experimental Immunology* **99**:160-167.
- Meise W, Ockenfels H and Kohler F (1973) Teratological tests of the hydrolysis products of thalidomide. *Experientia* **29**:423-424.
- Mellin GW and Katzenstein M (1962) The saga of thalidomide. *The New England Journal of Medicine* **267**:1238-1244.
- Meyring M, Chankvetadze B and Blaschke G (2000) Simultaneous separation and enantioseparation of thalidomide and its hydroxylated metabolites using high-performance liquid chromatography in common-size columns, capillary liquid chromatography and nonaqueous capillary electrochromatography. *Journal of Chromatography* **876**:157-167.
- Minchinton AI, Fryer KH, Wendt KR, Clow KA and Hayes MM (1996) The effect of thalidomide on experimental tumors and metastases. *Anti-Cancer Drugs* **7**:339-343.
- Minor JR and Piscitelli SC (1996) Thalidomide in diseases associated with human immunodeficiency virus infection. *American Journal of Health-System Pharmacy* **53**:429-431.
- Mitsiades N, Mitsiades CS, Poulaki V, Chauhan D, Richardson PG, Hideshima T, Munshi N, Treon SP and Anderson KC (2002a) Biologic sequelae of nuclear factor-kappaB blockade in multiple myeloma: therapeutic applications. *Blood* **99**:4079-4086.
- Mitsiades N, Mitsiades CS, Poulaki V, Chauhan D, Richardson PG, Hideshima T, Munshi NC, Treon SP and Anderson KC (2002b) Apoptotic signaling induced by immunomodulatory thalidomide analogs in human multiple myeloma cells: therapeutic implications. *Blood* **99**:4525-4530.

- Moehler TM, Neben K, Benner A, Egerer G, Krasniqi F, Ho AD and Goldschmidt H (2001) Salvage therapy for multiple myeloma with thalidomide and CED chemotherapy. *Blood* **98**:3846-3848.
- Mohla S, Weilbacher KN, Cher ML, Oyajobi BO, Poznak CV and Clohisy DR (2003) Third North American Symposium on Skeletal Complications of Malignancy: summary of the scientific sessions. *Cancer*. **97**:719-725.
- Moller DR, Wysocka M, Greenlee BM, Ma X, Wahl L, Flockhart DA, Trinchieri G and Karp CL (1997) Inhibition of IL-12 production by thalidomide. *Journal of Immunology* **159**:5157-5161.
- Moraes MO, Sarno EN, Teles RM, Almeida AS, Saraiva BC, Nery JA and Sampaio EP (2000) Anti-inflammatory drugs block cytokine mRNA accumulation in the skin and improve the clinical condition of reactional leprosy patients. *Journal of Investigative Dermatology*. **115**:935-941.
- Moreira AL, Sampaio EP, Zmuidzinas A, Frindt P, Smith KA and Kaplan G (1993) Thalidomide exerts its inhibitory action on tumor necrosis factor alpha by enhancing mRNA degradation. *Journal of Experimental Medicine* **177**:1675-1680.
- Motzer RJ, Berg W, Ginsberg M, Russo P, Vuky J, Yu R, Bacik J and Mazumdar M (2002) Phase II trial of thalidomide for patients with advanced renal cell carcinoma. *Journal of Clinical Oncology*. **20**:302-306.
- Muckter H (1965) Thalidomide and tumor. *Antimicrobial Agents & Chemotherapy* **5**:531-538.
- Muckter H and More E (1966) Thalidomide and cancer. *Arzneimittel-Forschung* **16**:129-134.
- Myoung H, Hong SD, Kim YY, Hong SP and Kim MJ (2001) Evaluation of the anti-tumor and anti-angiogenic effect of paclitaxel and thalidomide on the xenotransplanted oral squamous cell carcinoma. *Cancer Letters* **163**:191-200.
- Neben K, Moehler T, Benner A, Kraemer A, Egerer G, Ho AD and Goldschmidt H (2002a) Dose-dependent effect of thalidomide on overall survival in relapsed multiple myeloma. *Clinical Cancer Research* **8**:3377-3382.
- Neben K, Moehler T, Kraemer A, Benner A, Egerer G, Ho AD and Goldschmidt H (2001) Response to thalidomide in progressive multiple myeloma is not mediated by inhibition of angiogenic cytokine secretion. *British Journal of Haematology* **115**:605-608.
- Neben K, Mytilineos J, Moehler TM, Preiss A, Kraemer A, Ho AD, Opelz G and Goldschmidt H (2002b) Polymorphisms of the tumor necrosis factor-alpha gene promoter predict for outcome after thalidomide therapy in relapsed and refractory multiple myeloma. *Blood* **100**:2263-2265.
- Neubert R and Neubert D (1997) Peculiarities and possible mode of actions of thalidomide, in *Drug Toxicity in Embryonic Development II* (Kavlock RJ and Daston GP eds) pp 41-119, Springer-Verlag, Berlin.

- Ng SS, Gutschow M, Weiss M, Hauschildt S, Teubert U, Hecker TK, Luzzio FA, Kruger EA, Eger K and Figg WD (2003) Antiangiogenic activity of N-substituted and tetrafluorinated thalidomide analogues. *Cancer Research* **63**:3189-3194.
- Nguyen M, Chanh T, Barsky S, Sun JR, McBride W, Pegram M, Pietras R, Love S and Glaspy J (1997) Thalidomide and chemotherapy combination: preliminary results of preclinical and clinical studies. *International Journal of Oncology* **10**:965-969.
- Nilsson K, Jernberg H and Pettersson M (1990) IL-6 as a growth factor for human multiple myeloma cells--a short overview. *Current Topics in Microbiology & Immunology*. **166**:3-12.
- Noormohamed FH, Youle MS, Higgs CJ, Kook KA, Hawkins DA, Lant AF and Thomas SD (1999) Pharmacokinetics and hemodynamic effects of single oral doses of thalidomide in asymptomatic human immunodeficiency virus-infected subjects. *AIDS Research & Human Retroviruses* **15**:1047-1052.
- Offidani M, Marconi M, Corvatta L, Olivieri A, Catarini M and Leoni P (2003) Thalidomide plus oral melphalan for advanced multiple myeloma: a phase II study. *Haematologica* **88**:1432-1433.
- Olson KB, Hall TC, Horton J, Khung CL and Hosley HF (1965) Thalidomide (N-phthaloylglutamimide) in the treatment of advanced cancer. *Clinical Pharmacology & Therapeutics* **6**:292-297.
- Osman K, Comenzo R and Rajkumar SV (2001) Deep venous thrombosis and thalidomide therapy for multiple myeloma. *New England Journal of Medicine* **344**:1951-1952.
- Paget S (1889) Distribution of secondary growths in cancer of the breast. *Lancet* **1**:571-572.
- Palumbo A, Giaccone L, Bertola A, Pregno P, Bringhen S, Rus C, Triolo S, Gallo E, Pileri A and Boccadoro M (2001) Low-dose thalidomide plus dexamethasone is an effective salvage therapy for advanced myeloma. *Haematologica* **86**:399-403.
- Parentin F, Da Pozzo S, Lepore L and Perissutti P (2001) Thalidomide effectiveness for bilateral chronic idiopathic anterior uveitis in a three-year-old child. *Ophthalmologica* **215**:70-73.
- Parman T, Wiley MJ and Wells PG (1999) Free radical-mediated oxidative DNA damage in the mechanism of thalidomide teratogenicity. *Nature Medicine* **5**:582-585.
- Piscitelli SC, Figg WD, Hahn B, Kelly G, Thomas S and Walker RE (1997) Single-dose pharmacokinetics of thalidomide in human immunodeficiency virus-infected patients. *Antimicrobial Agents & Chemotherapy* **41**:2797-2799.
- Podar K, Tai YT, Davies FE, Lentzsch S, Sattler M, Hideshima T, Lin BK, Gupta D, Shima Y, Chauhan D, Mitsiades C, Raje N, Richardson P and Anderson KC (2001) Vascular endothelial growth factor triggers signaling cascades mediating multiple myeloma cell growth and migration. *Blood*. **98**:428-435.

- Pollard M (1996) Thalidomide promotes metastasis of prostate adenocarcinoma cells (PA-III) in L-W rats. *Cancer Letters* **101**:21-24.
- Price DK, Ando Y, Kruger EA, Weiss M and Figg WD (2002) 5'-OH-Thalidomide, a metabolite of thalidomide, inhibits angiogenesis. *Therapeutic Drug Monitoring* **24**:104-110.
- Rajkumar SV, Dispenzieri A, Fonseca R, Lacy MQ, Geyer S, Lust JA, Kyle RA, Greipp PR, Gertz MA and Witzig TE (2001) Thalidomide for previously untreated indolent or smoldering multiple myeloma. *Leukemia* **15**:1274-1276.
- Rajkumar SV, Fonseca R, Dispenzieri A, Lacy MQ, Lust JA, Witzig TE, Kyle RA, Gertz MA and Greipp PR (2000a) Thalidomide in the treatment of relapsed multiple myeloma. *Mayo Clinic Proceedings* **75**:897-901.
- Rajkumar SV, Hayman S, Fonseca R, Dispenzieri A, Lacy MQ, Geyer S, Wellik L, Lust JA, Kyle RA, Greipp PR, Gertz MA and Witzig TE (2000b) Thalidomide plus dexamethasone (Thal/Dex) and thalidomide alone (Thal) as first line therapy for newly diagnosed myeloma (MM). *Blood* **96 (suppl. 1)**:168a.
- Rajkumar SV, Hayman S, Gertz MA, Dispenzieri A, Lacy MQ, Greipp PR, Geyer S, Iturria N, Fonseca R, Lust JA, Kyle RA and Witzig TE (2002) Combination therapy with thalidomide plus dexamethasone for newly diagnosed myeloma. *Journal of Clinical Oncology* **20**:4319-4323.
- Randall T (1990) Thalidomide has 37-year history. *JAMA* **263**:1474.
- Raza A, Meyer P, Dutt D, Zorat F, Lisak L, Nascimben F, du Randt M, Kaspar C, Goldberg C, Loew J, Dar S, Gezer S, Venugopal P and Zeldis J (2001) Thalidomide produces transfusion independence in long-standing refractory anemias of patients with myelodysplastic syndromes. *Blood* **98**:958-965.
- Reyes-Teran G, Sierra-Madero JG, Martinez del Cerro V, Arroyo-Figueroa H, Pasquetti A, Calva JJ and Ruiz-Palacios GM (1996) Effects of thalidomide on HIV-associated wasting syndrome: a randomized, double-blind, placebo-controlled clinical trial. *Aids* **10**:1501-1507.
- Richardson P, Hideshima T and Anderson KC (2002) Thalidomide in multiple myeloma. *Biomedicine and Pharmacotherapy* **56**:115-128.
- Roodman GD (2002) Role of the bone marrow microenvironment in multiple myeloma. *Journal of Bone & Mineral Research*. **17**:1921-1925.
- Rowland TL, McHugh SM, Deighton J, Dearman RJ, Ewan PW and Kimber I (1998) Differential regulation by thalidomide and dexamethasone of cytokine expression in human peripheral blood mononuclear cells. *Immunopharmacology* **40**:11-20.
- Sampaio EP, Sarno EN, Galilly R, Cohn ZA and Kaplan G (1991) Thalidomide selectively inhibits tumor necrosis factor alpha production by stimulated human monocytes. *Journal of Experimental Medicine* **173**:699-703.

- Scheffler MR, Colburn W, Kook KA and Thomas SD (1999) Thalidomide does not alter estrogen-progesterone hormone single dose pharmacokinetics. *Clinical Pharmacology & Therapeutics* **65**:483-490.
- Schumacher H, Blake DA and Gillette JR (1968a) Disposition of thalidomide in rabbits and rats. *Journal of Pharmacology & Experimental Therapeutics* **160**:201-211.
- Schumacher H, Blake DA, Gurian JM and Gillette JR (1968b) A comparison of the teratogenic activity of thalidomide in rabbits and rats. *Journal of Pharmacology & Experimental Therapeutics* **160**:189-200.
- Schumacher H, Smith RL and Williams RT (1965a) The metabolism of thalidomide: the fate of thalidomide and some of its hydrolysis products in various species. *British Journal of Pharmacology* **25**:338-351.
- Schumacher H, Smith RL and Williams RT (1965b) The metabolism of thalidomide: the spontaneous hydrolysis of thalidomide in solution. *British Journal of Pharmacology* **25**:324-337.
- Scott WJ, Fradkin R and Wilson JG (1977) Nonconfirmation of thalidomide induced teratogenesis in rats and mice. *Teratology* **16**:333-335.
- Settles B, Stevenson A, Wilson K, Mack C, Ezell T, Davis MF and Taylor LD (2001) Down-regulation of cell adhesion molecules LFA-1 and ICAM-1 after in vitro treatment with the anti-TNF-alpha agent thalidomide. *Cellular & Molecular Biology* **47**:1105-1114.
- Shannon E, Aseffa A, Pankey G, Sandoval F and Lutz B (2000) Thalidomide's ability to augment the synthesis of IL-2 in vitro in HIV-infected patients is associated with the percentage of CD4+ cells in their blood. *Immunopharmacology* **46**:175-179.
- Shannon EJ, Sandoval F and Krahenbuhl JL (1997) Hydrolysis of thalidomide abrogates its ability to enhance mononuclear cell synthesis of IL-2 as well as its ability to suppress the synthesis of TNF-alpha. *Immunopharmacology* **36**:9-15.
- Sheskin J (1965) Further observation with thalidomide in lepra reactions. *Leprosy Review* **36**:183-187.
- Singhal S and Mehta J (2002) Thalidomide in cancer. *Biomedicine & Pharmacotherapy*. **56**:4-12.
- Singhal S, Mehta J, Desikan R, Ayers D, Roberson P, Eddlemon P, Munshi N, Anaissie E, Wilson C, Dhodapkar M, Zeddis J and Barlogie B (1999) Antitumor activity of thalidomide in refractory multiple myeloma. *New England Journal of Medicine* **341**:1565-1571.
- Smith RL, Fabro S, Schumacher H and Williams RT (1965) Studies on the relationship between the chemical structure and embryotoxic activity of thalidomide and related compound, in *Embryopathic Activity of Drugs* (Robson JM, Sullivan FM and Smith RL eds) pp 195-209, J. & A. Churchill Ltd., London.

- Somers GF (1960) Pharmacological properties of thalidomide, a new sedative hypnotic drug. *British Journal of Pharmacology* **15**:111-116.
- Srkalovic G, Elson P, Trebisky B, Karam MA and Hussein MA (2002) Use of melphalan, thalidomide, and dexamethasone in treatment of refractory and relapsed multiple myeloma. *Medical Oncology* **19**:219-226.
- Stebbing J, Benson C, Eisen T, Pyle L, Smalley K, Bridle H, Mak I, Sapunar F, Ahern R and Gore ME (2001) The treatment of advanced renal cell cancer with high-dose oral thalidomide. *British Journal of Cancer* **85**:953-958.
- Steins MB, Padro T, Bieker R, Ruiz S, Kropff M, Kienast J, Kessler T, Buechner T, Berdel WE and Mesters RM (2002) Efficacy and safety of thalidomide in patients with acute myeloid leukemia. *Blood* **99**:834-839.
- Stephens TD, Bunde CJ and Fillmore BJ (2000) Mechanism of action in thalidomide teratogenesis. *Biochemical Pharmacology* **59**:1489-1499.
- Stephens TD, Bunde CJW, Torres RD, Hackett DA, Stark MR, Smith DM and Fillmore BJ (1998) Thalidomide inhibits limb development through its antagonism of IGF-I + FGF-2 + heparin. *Teratology* **57**:112.
- Stevens RJ, Andujar C, Edwards CJ, Ames PR, Barwick AR, Khamashta MA and Hughes GR (1997) Thalidomide in the treatment of the cutaneous manifestations of lupus erythematosus: experience in sixteen consecutive patients. *British Journal of Rheumatology* **36**:353-359.
- Stirling DI (1998) Thalidomide and its impact in dermatology. *Seminars in Cutaneous Medicine & Surgery* **17**:231-242.
- Streicher HZ, Vereshchagina LA and Schoenfeldt M (2003) Clinical trials referral resource. Current clinical trials of thalidomide. *Oncology (Huntington)* **17**:369-371, 374-365, 379-380.
- Strupp C, Germing U, Aivado M, Misgeld E, Haas R and Gattermann N (2002) Thalidomide for the treatment of patients with myelodysplastic syndromes. *Leukemia* **16**:1-6.
- Suzuki H, Yasukawa K, Saito T, Goitsuka R, Hasegawa A, Ohsugi Y, Taga T and Kishimoto T (1992) Anti-human interleukin-6 receptor antibody inhibits human myeloma growth *in vivo*. *European Journal of Immunology* **22**:1989-1993.
- Tanaka A, Hasegawa A and Urakubo G (1965) Metabolic fate of thalidomide in rats. *Chemical & Pharmaceutical Bulletin* **13**:1263-1265.
- Teo SK, Colburn WA and Thomas SD (1999) Single-dose oral pharmacokinetics of three formulations of thalidomide in healthy male volunteers. *Journal of Clinical Pharmacology* **39**:1162-1168.
- Teo SK, Sabourin PJ, O'Brien K, Kook KA and Thomas SD (2000a) Metabolism of thalidomide in human microsomes, cloned human cytochrome P-450 isozymes,

- and Hansen's disease patients. *Journal of Biochemical & Molecular Toxicology* **14**:140-147.
- Teo SK, Scheffler MR, Kook KA, Tracewell WG, Colburn WA, Stirling DI and Thomas SD (2000b) Effect of a high-fat meal on thalidomide pharmacokinetics and the relative bioavailability of oral formulations in healthy men and women. *Biopharmaceutics & Drug Disposition* **21**:33-40.
- Teo SK, Scheffler MR, Kook KA, Tracewell WG, Colburn WA, Stirling DI and Thomas SD (2001) Thalidomide dose proportionality assessment following single doses to healthy subjects. *Journal of Clinical Pharmacology* **41**:662-667.
- Thompson MA, Witzig TE, Kumar S, Timm MM, Haug J, Fonseca R, Greipp PR, Lust JA and Rajkumar SV (2003) Plasma levels of tumour necrosis factor alpha and interleukin-6 predict progression-free survival following thalidomide therapy in patients with previously untreated multiple myeloma. *British Journal of Haematology* **123**:305-308.
- Tosi P, Zamagni E, Cellini C, Cangini D, Tura S, Baccarani M and Cavo M (2001) Rapid response and early relapse after thalidomide plus dexamethasone salvage therapy in patients with advanced relapsed and refractory multiple myeloma. *Blood* **98**:163a.
- Tosi P, Zamagni E, Cellini C, Ronconi S, Patriarca F, Ballerini F, Musto P, Di Raimondo F, Ledda A, Lauria F, Masini L, Gobbi M, Vacca A, Ria R, Cangini D, Tura S, Baccarani M and Cavo M (2002) Salvage therapy with thalidomide in patients with advanced relapsed/refractory multiple myeloma. *Haematologica* **87**:408-414.
- Trapnell CB (1998) Clinical pharmacology of thalidomide. *AIDS Clinical Care* **10**:3, 8.
- Trapnell CB, Donahue SR, Collins JM, Flockhart DA, Thacker D and Abernethy DR (1998) Thalidomide does not alter the pharmacokinetics of ethinyl estradiol and norethindrone. *Clinical Pharmacology & Therapeutics* **64**:597-602.
- Tricot G (2000) New insights into role of microenvironment in multiple myeloma. *Lancet* **355**:248-250.
- Tseng JE, Glisson BS, Khuri FR, Shin DM, Myers JN, El-Naggar AK, Roach JS, Ginsberg LE, Thall PF, Wang X, Teddy S, Lawhorn KN, Zentgraf RE, Steinhaus GD, Pluda JM, Abbruzzese JL, Hong WK and Herbst RS (2001) Phase II study of the antiangiogenesis agent thalidomide in recurrent or metastatic squamous cell carcinoma of the head and neck. *Cancer* **92**:2364-2373.
- Turk BE, Jiang H and Liu JO (1996) Binding of thalidomide to alpha1-acid glycoprotein may be involved in its inhibition of tumor necrosis factor alpha production. *Proceedings of the National Academy of Sciences of the United States of America* **93**:7552-7556.
- Uchiyama H, Barut BA, Chauhan D, Cannistra SA and Anderson KC (1992) Characterization of adhesion molecules on human myeloma cell lines. *Blood* **80**:2306-2314.

- Urashima M, Chen BP, Chen S, Pinkus GS, Bronson RT, Dederda DA, Hoshi Y, Teoh G, Ogata A, Treon SP, Chauhan D and Anderson KC (1997) The development of a model for the homing of multiple myeloma cells to human bone marrow. *Blood* **90**:754-765.
- Vacca A, Di Loreto M, Ribatti D, Di Stefano R, Gadaleta-Caldarola G, Iodice G, Caloro D and Dammacco F (1995) Bone marrow of patients with active multiple myeloma: angiogenesis and plasma cell adhesion molecules LFA-1, VLA-4, LAM-1, and CD44. *American Journal of Hematology* **50**:9-14.
- Vacca A, Ribatti D, Presta M, Minischetti M, Iurlaro M, Ria R, Albini A, Bussolino F and Dammacco F (1999) Bone marrow neovascularization, plasma cell angiogenic potential, and matrix metalloproteinase-2 secretion parallel progression of human multiple myeloma. *Blood* **93**:3064-3073.
- Vacca A, Ribatti D, Roncali L, Ranieri G, Serio G, Silvestris F and Dammacco F (1994) Bone marrow angiogenesis and progression in multiple myeloma. *British Journal of Haematology* **87**:503-508.
- Verbon A, Juffermans NP, Speelman P, van Deventer SJ, ten Berge IJ, Guchelaar HJ and van der Poll T (2000) A single oral dose of thalidomide enhances the capacity of lymphocytes to secrete gamma interferon in healthy humans. *Antimicrobial Agents & Chemotherapy*. **44**:2286-2290.
- Verheul HM, Panigrahy D, Yuan J and D'Amato RJ (1999) Combination oral antiangiogenic therapy with thalidomide and sulindac inhibits tumour growth in rabbits. *British Journal of Cancer* **79**:114-118.
- Vidriales MB and Anderson KC (1996) Adhesion of multiple myeloma cells to the bone marrow microenvironment: implications for future therapeutic strategies. *Molecular Medicine Today*. **2**:425-431.
- Vogelsang GB, Santos GW, Colvin OM and Chen T (1988) Thalidomide for graft-versus-host disease. *Lancet* **1**:827.
- Walchner M, Meurer M, Plewig G and Messer G (2000) Clinical and immunologic parameters during thalidomide treatment of lupus erythematosus. *International Journal of Dermatology*. **39**:383-388.
- Wang ML, Mu HR, Liu YF, Li YG, Wu HG and Sui HT (2003) The short-term outcomes of patients with acute leukemia treated by thalidomide. *Chung Hua Nei Ko Tsa Chih Chinese Journal of Internal Medicine* **42**:296-299.
- Weber D, Rankin K, Gavino M, Delasalle K and Alexanian R (2003) Thalidomide alone or with dexamethasone for previously untreated multiple myeloma. *Journal of Clinical Oncology* **21**:16-19.
- Webster LK, Ellis AG, Kestell P and Rewcastle GW (1995) Metabolism and elimination of 5,6-dimethylxanthenone-4-acetic acid in the isolated perfused rat liver. *Drug Metabolism & Disposition* **23**:363-368.

- Wechalekar AD, Chen CI, Sutton D, Reece D, Voralia M and Stewart AK (2003) Intermediate dose thalidomide (200mg daily) has comparable efficacy and less toxicity than higher doses in relapsed multiple myeloma. *Leukemia and Lymphoma* **44**:1147-1149.
- Wettstein AR and Meagher AP (1997) Thalidomide in Crohn's disease. *Lancet* **350**:1445-1446.
- Wike-Hooley JL, Haveman J and Reinhold HS (1984) The relevance of tumour pH to the treatment of malignant disease. *Radiotherapy & Oncology* **2**:343-366.
- Williams ML, Bhargava P, Cherrouk I, Marshall JL, Flockhart DA and Wainer IW (2000) A discordance of the cytochrome P450 2C19 genotype and phenotype in patients with advanced cancer. *British Journal of Clinical Pharmacology* **49**:485-488.
- Williams RT, Schumacher H, Fabro S and Smith RL (1965) The chemistry and metabolism of thalidomide, in *Embryopathic Activity of Drugs* (Robson JM, Sullivan FM and Smith RL eds) pp 167-193, J. & A. Churchill Ltd., London.
- Wohl DA, Aweeka FT, Schmitz J, Pomerantz R, Cherng DW, Spritzler J, Fox L, Simpson D, Bell D, Holohan MK, Thomas S, Robinson W, Kaplan G, Teppler H, National Institute of A and Infectious Diseases ACTG (2002) Safety, tolerability, and pharmacokinetic effects of thalidomide in patients infected with human immunodeficiency virus: AIDS Clinical Trials Group 267. *Journal of Infectious Diseases* **185**:1359-1363.
- Xiao Z, Schaefer K, Firestine S and Li PK (2002) Solid-phase synthesis of thalidomide and its analogues. *Journal of Combinatorial Chemistry* **4**:149-153.
- Yakoub-Agha I, Attal M, Dumontet C, Delannoy V, Moreau P, Berthou C, Lamy T, Grosbois B, Dauriac C, Dorvaux V, Bay JO, Monconduit M, Harousseau JL, Duguet C, Duhamel A and Facon T (2002) Thalidomide in patients with advanced multiple myeloma: a study of 83 patients--report of the Intergroupe Francophone du Myelome (IFM). *Hematology Journal* **3**:185-192.
- Yakoub-Agha I, Moreau P, Leyvraz S, Berthou C, Payen C, Dumontet C, Grosbois B, Beris P, Duguet C, Attal M, Harousseau JL and Facon T (2000) Thalidomide in patients with advanced multiple myeloma. *Hematology Journal* **1**:186-189.
- Zhai Y and Lu ZJ (2003) Effect of thalidomide on tumor growth in mouse hepatoma h22 model. *Aizheng (Chinese Journal of Oncology)* **22**:1301-1306.
- Zhang HB, Chen SL, Liu JZ, Xiao B, Chen ZB and Wang HJ (2003) The changes of gene expression in multiple myeloma treated with thalidomide. *Chung Hua Nei Ke Tsa Chih (Chinese Journal of Internal Medicine)* **42**:300-302.
- Zhu X, Zhang YP, Klopman G and Rosenkranz HS (1999) Thalidomide and metabolites: indications of the absence of 'genotoxic' carcinogenic potentials. *Mutation Research* **425**:153-167.

Zwingerberger K and Wnendt S (1996) Immunomodulation by thalidomide: systematic review of the literature and of unpublished observations. *Journal of Inflammation* **46**:177-211.

Thalidomide Metabolites in Mice and Patients with Multiple Myeloma¹

Jun Lu, Brian D. Palmer, Phillip Kestell, Peter Browett, Bruce C. Baguley, George Muller, and Lai-Ming Ching²

Auckland Cancer Society Research Centre [J. L., B. D. P., P. K., B. C. B., L.-M. C.] and Department of Molecular Medicine and Pathology [P. B.], Faculty of Medical and Health Sciences, The University of Auckland, Auckland 92019, New Zealand, and Celgene Corporation, Warren, New Jersey [G. M.]

ABSTRACT

Purpose: This research examines the profile of metabolites of thalidomide that are formed in refractory multiple myeloma patients undergoing thalidomide therapy in comparison with those that are detected in healthy mice.

Experimental Design: Urine or plasma samples from patients during thalidomide therapy (100–400 mg daily), or from mice treated i.p. (100 mg/kg) or p.o. with thalidomide (50 mg/kg) were analyzed using liquid chromatography-mass spectrometry. Metabolites in each of the peaks observed in the UV- and mass spectrometry-detected high-performance liquid chromatography traces were identified by comparison of retention times and spectra with those of authentic standards.

Results: Plasma and urine samples from mice 4 h after treatment with thalidomide contained eight major metabolites formed by hydroxylation and/or hydrolysis of thalidomide. In contrast, urine samples from seven multiple myeloma patients at steady state levels of thalidomide therapy showed the presence of only three hydrolysis breakdown products and no hydroxylated metabolites.

Conclusions: Our results show that thalidomide metabolite profiles in multiple myeloma patients differ considerably from those in mice. The lack of measurable hydroxylated metabolites in urine and in 1 case plasma of these patients suggests that such metabolites are not responsible for the therapeutic effects of thalidomide in multiple myeloma. We suggest that thalidomide may act directly, down-regulating growth factors essential for multiple myeloma growth.

INTRODUCTION

Thalidomide (α -phthalimidoglutarimide), marketed initially for its sedatory effects (1) and later discovered to be effective in controlling acute symptoms associated with a number of inflammatory and autoimmune diseases (2, 3), has shown promise recently in the treatment of cancer (4). The clinical evaluation of thalidomide as an anticancer agent followed the demonstration that thalidomide could inhibit angiogenesis (5). Activity against renal carcinomas (6) and gliomas (7) has been observed, and thalidomide is also being trialled for the treatment of prostate cancers (8). The observation that patients with refractory multiple myeloma show an increase in bone marrow vascularity suggested that thalidomide might be used as an antiangiogenic agent (9). Although the resultant clinical trials with thalidomide have had outstanding results, no significant decrease in marrow microvessel density has been observed in patients responding to thalidomide therapy (10), suggesting that mechanisms other than antiangiogenesis may be involved in its clinical action.

Biotransformation of thalidomide occurs by hydrolysis (11–13) or by hepatic CYP-450-mediated hydroxylation (14), and both types of products are generally referred to as metabolites. Hydroxylated metabolites are present only in trace amounts after oral administration to humans but can be detected *in vitro* after incubation of thalidomide with human liver enzyme preparations (15, 16). Hepatic CYP2C19 activity is important for the 5- and 5'-hydroxylation of thalidomide in humans (15).

The teratogenic properties of thalidomide appear to require prior biotransformation (14, 17), and chirally stable hydrolysis products and arene intermediates have been implicated (18–20). On the other hand, the antiangiogenic effects and anticancer activities of thalidomide have been attributed to the formation of hydroxylated derivatives (21–23). The synthesis of hydroxylated thalidomide analogues has provided a number of compounds with potent antiangiogenic/antimetastatic activities (23), strengthening the hypothesis that hydroxylated thalidomide metabolites are responsible for antiangiogenic effects. The formation of thalidomide metabolites appears to be highly species-dependent and, whereas microsomal preparations from human, primates, or rabbits support the production of active metabolites, microsomes from rodents generally produce negative results (17, 19). These *in vitro* studies are consistent with the greater *in vivo* sensitivity to the effects of thalidomide observed in humans and rabbits as compared with that in rodents. However, inhibition of angiogenesis by thalidomide can be demonstrated in corneal assays with both rabbits and mice (5, 24, 25).

Because hydroxylated products of thalidomide have been proposed to be responsible for its antitumor effects, we have searched for the presence of these metabolites in multiple myeloma patients undergoing thalidomide therapy. We have developed methodologies where both hydrolysis and hydroxylated

Received 9/23/02; revised 2/3/03; accepted 2/4/03.

The costs of publication of this article were defrayed in part by the payment of page charges. This article must therefore be hereby marked *advertisement* in accordance with 18 U.S.C. Section 1734 solely to indicate this fact.

¹Supported by the Marsden Research Fund and the Auckland Cancer Society.

²To whom requests for reprints should be addressed, at Auckland Cancer Society Research Centre, Faculty of Medical and Health Sciences, The University of Auckland, Private Bag 92019, Auckland, New Zealand. Phone: 64-9-3737-999; Fax: 64-9-3737-502; E-mail: l.ching@auckland.ac.nz.

metabolites of thalidomide can be detected in the one HPLC³ run using LC-MS, and have compared metabolite profiles in urine of mice and of patients with multiple myeloma. We have identified eight urinary metabolites in mice, including hydroxylated metabolites, but have not been able to detect these hydroxylated products in urine of patients treated with thalidomide. We have discussed the implications of these results to the mode of action of thalidomide in multiple myeloma.

MATERIALS AND METHODS

Materials. Racemic thalidomide for murine studies was synthesized at Celgene Corporation (Warren, NJ). OSA sodium salt was purchased from Riedel-de Haen (Seeize, Germany). Trichloroacetic acid, phthaloylglutamic acid, and β -glucuronidase were purchased from Sigma-Aldrich. CTAB and ACN were purchased from BDH Laboratory Supplies (Poole, United Kingdom), DMSO was purchased from Riedel-de Haen AG, and hydroxypropylcellulose was purchased from Glogau & Company Inc. (Melrose Park, IL).

Authentic Standards. Phthaloylglutamine and phthaloylisoglutamine were prepared by reaction of glutamine and isoglutamine, respectively, with *N*-carboethoxyphthalimide at room temperature in aqueous sodium carbonate solution. 4-Hydroxyphthaloylglutamine and 5-hydroxyphthaloylglutamine were synthesized by condensation of 3-hydroxyphthalic anhydride and 4-hydroxyphthalic anhydride, respectively, with glutamine in refluxing dry pyridine. Each was dehydrated using 1,1'-carbonyldiimidazole and 4-(dimethylamino)pyridine in refluxing *p*-dioxane to give 4-hydroxythalidomide and 5-hydroxythalidomide. Similar reactions of 3- and 4-hydroxyphthalic anhydride with isoglutamine gave 4-hydroxyphthaloylisoglutamine and 5-hydroxyphthaloylisoglutamine, respectively. α -Aminoglutaramide was obtained as the hydrochloride salt starting from *N*-(carbobenzoyloxy)glutamine as described elsewhere (26). It was reacted with phthalic anhydride or 4-hydroxyphthalic anhydride in the presence of triethylamine, in dry tetrahydrofuran at room temperature to give *N*-(*o*-carboxybenzoyl)glutamic acid imide and 5-hydroxy-*N*-(*o*-carboxybenzoyl)glutamic acid imide, respectively. Similar reaction of phthalic anhydride with glutamine or isoglutamine at room temperature gave *N*-(*o*-carboxybenzoyl)glutamine and *N*-(*o*-carboxybenzoyl)isoglutamine, respectively. All of the synthetic standards were purified by chromatography on silica, and their structures were confirmed using 400 MHz ¹H NMR spectroscopy and MS. 5'-Hydroxythalidomide was a generous gift from Prof. Sven Bjorkman (Malmo University Hospital, Malmo, Sweden) and was a mixture of 5'-*cis* and 5'-*trans* diastereomers.

Mouse Studies. Male 8–12-week-old C57/Bl/6 mice bred at the Animal Resources Unit, Faculty of Medical and Health Sciences, University of Auckland were used for all of the experiments. Mice were housed under conditions of constant

temperature and humidity according to institutional ethical guidelines. Thalidomide, dissolved in DMSO (40 mg/ml) was administered by i.p. injection (100 mg/kg, 2.5 μ l/g body weight). For p.o. administration, thalidomide was suspended in 0.3% hydroxypropylcellulose (10 mg/ml) and administered using a gavage tube (50 mg/kg, 5 μ l/g body weight). After drug administration, mice were placed in metabolic cages with water and food supplied, and urine over the 4-h period was collected. After 4 h, murine blood samples were collected in heparinized tubes during terminal halothane (NZ Pharmacology Ltd., Christchurch, New Zealand) anesthesia, centrifuged, and the plasma removed. Mouse plasma samples (300 μ l each) and urine samples (100 μ l each) were then acidified by adding 1 N HCl up to 1 ml. Acidified samples were loaded onto 1 ml/100 mg preconditioned C18 Bond Elut columns (Varian, Harbor City, CA) using an automated sample preparation with an extraction column system (ASPEC; Gilson Medical, Meddleton, WI). The columns were washed with 1 ml of Milli-Q water, and the compounds of interest were then eluted using 1 ml of 100% ACN. The eluates were evaporated to dryness using a centrifugal evaporator (Jouan, St. Nazaire, France) and residues reconstituted in 100- μ l mobile phase for HPLC analysis.

Human Studies. Seven patients undergoing treatment with thalidomide for refractory multiple myeloma at Auckland Hospital were recruited for these studies. The thalidomide dosages of the patients ranged between 100 and 400 mg/day. Urine samples on 3 consecutive months of treatment as well as a plasma sample on one occasion was obtained from 1 patient with a >75% reduction in his IgG paraprotein on 100 mg thalidomide/day. Control samples of urine were obtained from healthy volunteers as well as a pretreatment sample from 1 of the patients. Urine (3.33 ml) or heparinized blood (0.8 ml) were acidified by adding 1 N HCl to 10 ml, and processed as described for murine samples. Dried residues of the samples were reconstituted in 500- μ l mobile phase for urine samples and in 400- μ l mobile phase for plasma samples.

LC-MS Analysis. Reconstituted samples were analyzed by LC-MS using an Agilent 1100 Series LC/MSD system (Agilent Technologies, Avondale, PA) using an atmospheric pressure chemical ionization interface. All of the samples were analyzed first using MSD set on negative-ion scan mode with a molecular weight range from 70 to 1000 a.m.u. to identify each of the peaks. Then, samples were reanalyzed on negative single-ion monitoring mode at the molecular weights 257, 273, 275, 276, 289, 291, 293, 294, and 449 a.m.u. (corresponding to each of the peaks) coupled with a second MSD signal set on negative-ion scan mode. This provided better sensitivity and reduced background noise. The other MS conditions were: fragmentor and capillary voltage of the interface, 100 and 3500 V, respectively; drying gas flow rate, 5 liter/min; corona current, 10 μ A; gas temperature, 350°C; vaporizing temperature, 500°C; and nebulizing pressure, 35 p.s.i. Samples were also analyzed concurrently using diode array UV detection at 230 nm. The UV spectra of individual metabolite peaks were compared with those generated by the authentic standards (which had the same retention times), and the percentage match between the spectra determined using ChemStation Rev. A.08.04 (Agilent Technologies). Chromatographic separation was achieved with a LUNA 5 μ Phenylhexyl 100 \times 4.6 mm stainless steel column (Phe-

³ The abbreviations used are: HPLC, high performance liquid chromatography; LC-MS, liquid chromatography-mass spectrometry; OSA, 1-octanesulfonic acid; CTAB, cetyltrimethylammonium bromide; ACN, acetonitrile; NMR, nuclear magnetic resonance; MSD, mass spectral detection; MS, mass spectrometry.

nomenex, Torrance, CA) using a combination of the following solutions: solution A, which contained 80% ACN and 1% acetic acid in water, and solution B, which contained 10% ACN and 1% acetic acid in water. The elution program was 100% solution B at 0.5 ml/min over 0–20 min, addition of 0–20% solution A in a linear gradient at 0.7 ml/min over 20–45 min, and 100% solution B at 0.5 ml/min over 45–55 min.

Resolution of Phthaloylglutamine and Phthaloylisoglutamine by HPLC. The chromatographic conditions used in the LC-MS analyses did not allow the separation of phthaloylglutamine and phthaloylisoglutamine. The mobile phase was modified by the addition of the ion pair reagents CTAB and OSA. Analysis of these two compounds was performed using a Waters semipreparative HPLC system (Waters Associates, Milford, MA) consisting of a 717PLUS auto sampler, 1525 binary HPLC pump, 100 × 10.0 mm stainless steel LUNA 5 μ Phenylhexyl column (Phenomenex) and a model 2487 dual λ absorbance detector set at 230 nm, and the peak containing a mixture of phthaloylisoglutamine and phthaloylglutamine was collected with a Gilson model-202 fraction collector (Gilson Medical Electronics, Middleton, MI). The mobile phase consisted of 10% ACN and 1% acetic acid in Milli-Q water, and the flow rate was 0.5 ml/min isocratic. The collected eluant was dried using a Virtis Freeze-Mobile 6 model freeze drier (Virtis Co. Inc., Gardiner, NY). The reconstituted dried samples were analyzed by the same Waters HPLC system but using a LUNA 5 μ Phenylhexyl 100 × 4.6 mm stainless steel column instead of 100 × 10.0 mm stainless steel LUNA 5 μ Phenylhexyl column, and a mobile phase of 10% ACN and 1% acetic acid in Milli-Q water, 48 mg/liter OSA, and 32 mg/liter CTAB. Peaks were monitored by UV at 230 nm using an isocratic flow rate of 0.5 ml/min.

Thalidomide Glucuronide Identification. The fraction containing the glucuronide metabolite of thalidomide was collected and dried using the same procedure as that described above for the phthaloylisoglutamine/phthaloylglutamine fraction. The method of identification was adapted from that of Webster *et al.* (27) used to identify glucuronidation of 5,6-dimethylxanthene-4-acetic acid. In brief, the dried residue was reconstituted in 0.1 M PBS (pH 5.5), and two aliquots of 500- μ l reconstituted metabolite solution were incubated at 37°C for 45 min and 90 min with 2000 units/ml β -glucuronidase plus 20 mM D-saccharic acid 1,4-lactone, respectively. Another two aliquots of 500- μ l reconstituted metabolite solution were incubated together without β -glucuronidase as control. The reaction was initiated by addition of β -glucuronidase and D-saccharic acid 1,4-lactone, and stopped by addition of 50 μ l of 10% trichloroacetic acid. The mixture was centrifuged at 3000 × *g* for 15 min to remove precipitated protein. The supernatant was removed then injected into LC-MS, and analyzed using the same procedure used to analyze mouse and human plasma and urine samples.

RESULTS

Detection of Thalidomide Metabolites in Mice. Mice were treated with thalidomide either i.p. (100 mg/kg) or p.o. (50 mg/kg), and urine and plasma samples were collected at 4 h and analyzed using LC-MS. The UV profiles of urine and plasma

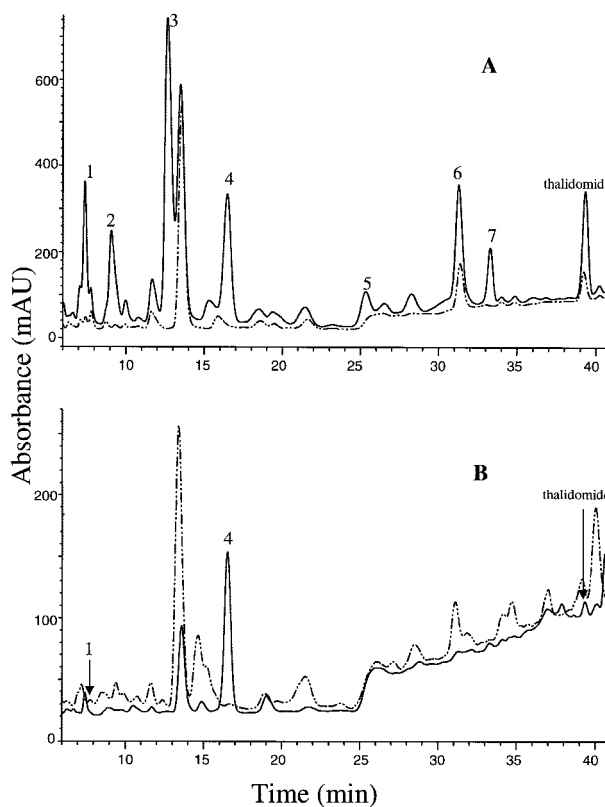


Fig. 1 A, UV-detected chromatograms of urine from mice without treatment (—) and up to 4 h after p.o. administration of thalidomide (50 mg/kg). B, patient 7 with multiple myeloma: pretreatment (—) and after thalidomide (100 mg/day p.o., - - -).

from both untreated and treated mice showed a number of peaks (Fig. 1A), and differences in the UV profiles were used to detect metabolites. Peaks were considered to be metabolite peaks if they gave signals on MS-negative ion scan mode and negative single-ion monitoring mode (Fig. 2A and Fig. 3A), and if the mass spectrum of the peak contained additional ions to those in untreated control samples. An example for peak 6, is shown for scan mode in Figs. 2, B and C, and for single ion monitoring in Fig. 3, A and B. By these criteria, seven metabolite peaks, in addition to the thalidomide peak, were identified in the urine from mice treated with thalidomide (Fig. 1A).

Identification of Biotransformation Products. Possible metabolites with molecular weights corresponding to the MS signals of each of the peaks were deduced, and authentic samples of the majority of these were obtained. The retention times, UV spectra, mass spectra, and single ion monitoring chromatographic profiles of metabolite peaks and authentic standards were compared. Results are summarized in Table 1. Peak 1, with a molecular mass of 276, was identified as *N*-(*o*-carboxybenzoyl)glutamic acid imide on the basis that they had the same retention time, and their UV spectra shared 93.5% identity to each other (Fig. 4A). Peak 2, with a mass of 292, could correspond to a variety of possible hydroxylated hydrolysis products. Therefore, we synthesized 5- and 4-hydroxyphthaloylisoglutamine, 5- and 4-hydroxyphthaloylglutamine, and 5- and 4-

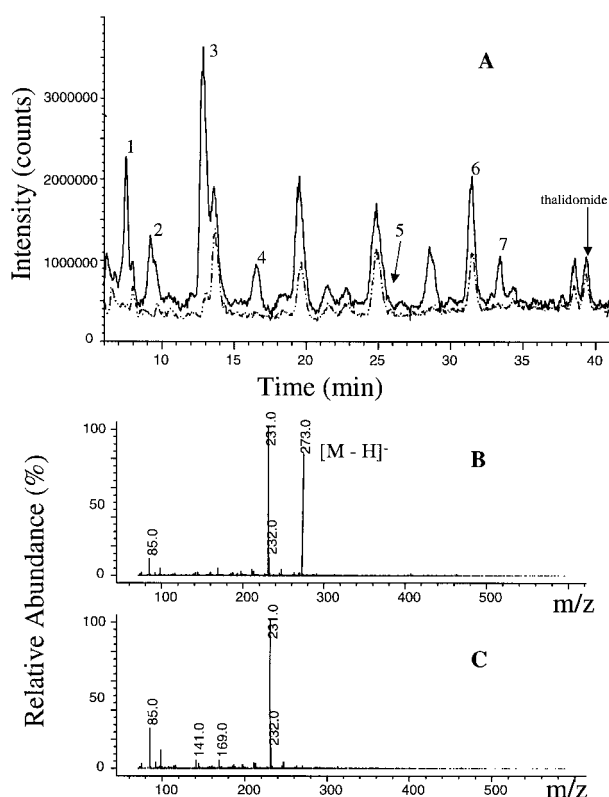


Fig. 2 A, total ion MS-detected chromatogram of urine from mice without treatment (—) and up to 4 h after p.o. administration of thalidomide (50 mg/kg, ---). B, mass spectrum of peak 6 using negative ion-scan mode showing an $[M-H]^-$ mass of 273 amu. C, mass spectrum at the retention time corresponding to peak 6 in untreated mouse urine.

hydroxy-*N*-(*o*-carboxybenzoyl)glutamic acid imide, and found they all had different retention times to peak 2. *N'*-hydroxy-*N*-(*o*-carboxybenzoyl)glutamic acid imide also has a mass of 292, but metabolites resulting from *N*-hydroxylation of the imide ring of thalidomide have never been detected (15, 16, 28, 29), and it is unlikely that this is the compound in peak 2. We suggest that the most likely candidate for peak 2 is 5'-hydroxy-*N*-(*o*-carboxybenzoyl)glutamic acid imide, although the authentic compound is not yet available for confirmation.

Peak 3, a major component of the urine extracts, showed two molecular ions, corresponding to components with molecular weights of 450 and 274. It eluted just before an unidentified host component (present in urine of untreated mice) that had a molecular weight of 179. The molecular weight of the larger component suggested that it was an *O*-glucuronide derivative of thalidomide, whereas that of the smaller component suggested that it was a fragment ion resulting from loss of glucuronic acid. Therefore, peak 3 was collected, a portion was treated with β -glucuronidase, and both portions were rechromatographed (Fig. 5A). Exposure to β -glucuronidase caused the appearance of a new component, peak II, with a mass spectrum corresponding to a molecular weight of 274 (Fig. 5B). This was identified as 5-hydroxythalidomide on the basis that it has the same retention time, and its UV spectrum shares >99% identity with

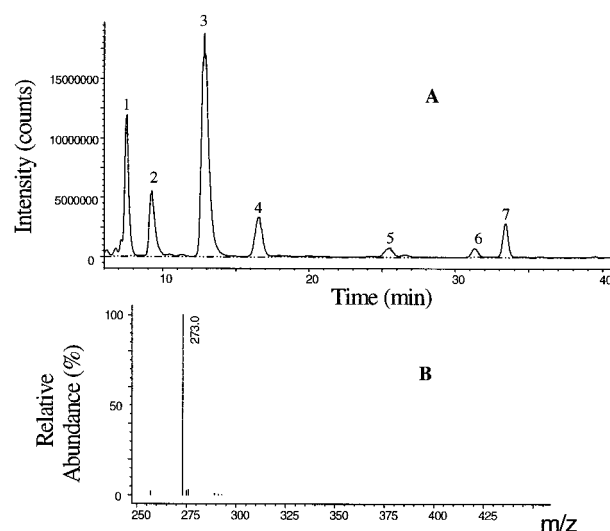


Fig. 3 A, single-ion monitoring mode MS-detected chromatogram of urine from mice without treatment (—) and up to 4 h after p.o. administration of thalidomide (50 mg/kg, ---). B, mass spectrum using negative single-ion monitoring mode of peak 6 showing a $[M-H]^-$ response of 273 amu.

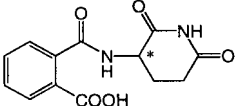
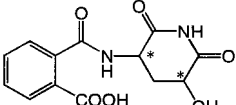
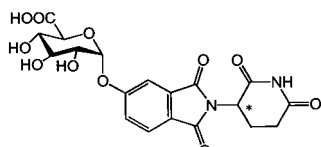
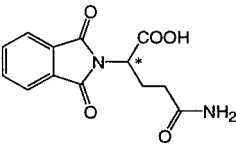
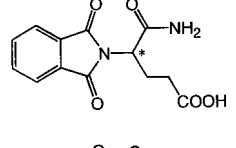
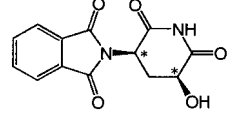
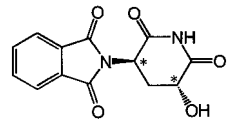
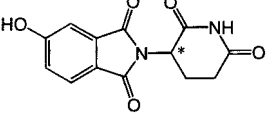
that of authentic material. Peak I had a molecular weight of 450 (its reduced retention time was because of the lower loading of the column), and the decrease in its proportion after exposure to β -glucuronidase strongly suggested that it was thalidomide-5-*O*-glucuronide. The peak eluting at 12.8 min (molecular weight 179) corresponded to the unidentified host component. No evidence of glucuronidation at the 5'-position was found.

Peak 4 had a molecular mass of 276, and identical UV and mass spectra to authentic phthaloylisoglutamine. However, authentic phthaloylglutamine also has the same mass and has a very similar retention time, and it was necessary to determine whether both might be present in peak 4. Therefore, this fraction was collected and reanalyzed by HPLC using the mobile phase containing CTAB and OSA that allows separation of phthaloylisoglutamine and phthaloylglutamine with respective retention times of 15.1 min and 12.7 min (Fig. 6A). The sample collected from peak 4 resolved into two fractions (Fig. 6B), indicating that both phthaloylglutamine and phthaloylisoglutamine were present.

Peaks 5, 6, and 7 were identified as *cis*-5'-hydroxythalidomide, *trans*-5'-hydroxythalidomide, and 5-hydroxythalidomide, respectively, on the basis of similarity of UV spectra (Fig. 4, B-D) and identity of retention time (Table 1). The same number of metabolite peaks in UV profiles was obtained in urine after p.o. or i.p. administration (Fig. 7). The profile obtained in plasma contained smaller-sized but the same number of peaks compared with the urine profile from mice administered thalidomide i.p. at the same dose (Fig. 8A).

Thalidomide Metabolites in Multiple Myeloma Patients. Seven patients with refractory multiple myeloma, receiving between 100 and 400 mg thalidomide daily, were recruited for this study. Urine samples from patients on thalidomide therapy were analyzed for metabolites using the same procedure as that for murine samples. A pretreatment

Table 1 Metabolite peaks in UV profiles from murine urine after thalidomide treatment

Peak no.	Retention time (min)	Molecular weight	Match of UV spectra ^a	Metabolite	Structure
1	7.4	276	93.5%	<i>N</i> -(<i>o</i> -carboxybenzoyl)-glutamic acid imide	
2	9.1	292		5'-hydroxy- <i>N</i> -(<i>o</i> -carboxybenzoyl)glutamic acid imide ^b	
3	12.8	450		thalidomide-5- <i>O</i> -glucuronide	
4a ^c	16.5	276		phthaloylglutamine	
4b ^c	16.5	276		phthaloylisoglutamine	
5	25.4	274	98%	<i>cis</i> -5'-hydroxy-thalidomide	
6	31.3	274	98%	<i>trans</i> -5'-hydroxy-thalidomide	
7	33.3	274	>99%	5-hydroxythalidomide	

* Chiral centre.

^a See Fig. 4.^b Proposed metabolite.^c Peak 4 separates into 4a and 4b with retention times of 12.7 and 15.1 min, respectively, on HPLC with mobile phase containing CTAB and OSA.

sample from one patient (Fig. 1B) showed no significant difference to those from healthy individuals, and peaks observed in untreated controls were not included in the analysis. Applying the same criteria as those used for defining murine metabolite peaks, only two metabolite peaks were detected in the UV profile of all seven of the patients' urine (Fig. 1B; Fig. 8B). The first of these peaks was the same as peak 1 in the murine profile,

corresponding to *N*-(*o*-carboxybenzoyl)glutamic acid imide, whereas the second was identical to peak 4. This second peak was reanalyzed by HPLC using the ion-paired mobile phase, and like the corresponding peak in mice, it could be resolved into two components corresponding to phthaloylglutamine and phthaloylisoglutamine (Fig. 6C).

Patient 1, who showed a >75% reduction in paraprotein

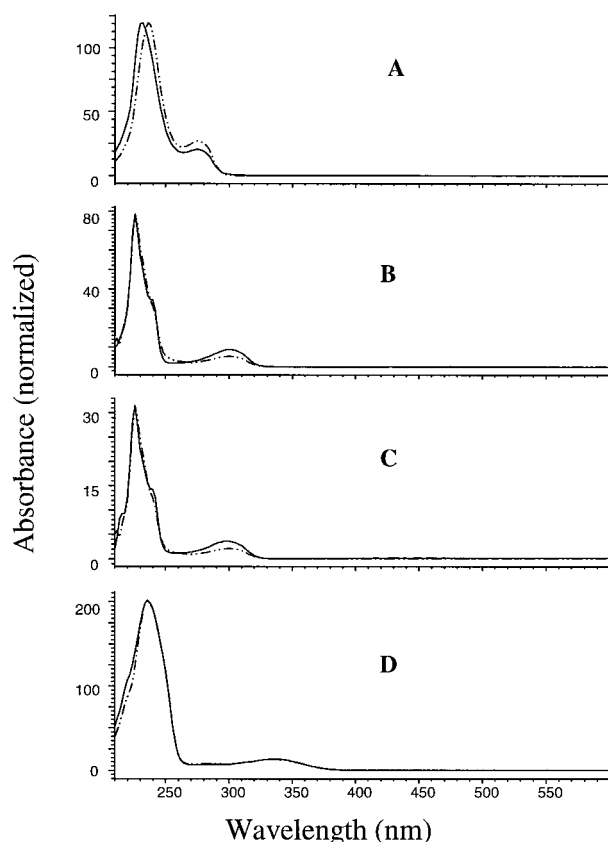


Fig. 4 UV spectra of metabolite peaks (—) compared with UV spectra of corresponding authentic standards (---). A, peak 1 and *N*-(*o*-carboxybenzoyl)glutamic acid imide. B, peak 5 and *cis*-5'-hydroxythalidomide. C, peak 6 and *trans*-5'-hydroxythalidomide. D, peak 7 and 5-hydroxythalidomide.

level on thalidomide, was studied while on a dose of 100 mg/day. Urine samples collected on 3 consecutive months of treatment were analyzed, but no variations in the metabolite profiles were seen over this period. This patient also provided a blood sample 15 h after 1 of his daily thalidomide doses. Thalidomide metabolites were not detected in this plasma although they were detectable in a urine sample collected at the same time (Fig. 8B).

DISCUSSION

The results confirm the formation in mice of three first-step hydrolysis products, *N*-(*o*-carboxybenzoyl)glutamic acid imide, phthaloylisoglutamine, and phthaloylglutamine, as well as three first-step hydroxylation products, 5-hydroxythalidomide, and *cis*- and *trans*-5'-hydroxythalidomide. In addition, we provide evidence of a second-step transformation of 5-hydroxythalidomide to produce thalidomide-5-*O*-glucuronide. A scheme for these transformation steps is shown in Fig. 9. Although several studies report the presence of unidentified metabolite peaks (15, 16, 30), glucuronidated thalidomide metabolites have not been documented previously. Glucuronidation confers greater solubility to a compound, and the formation of glucuronidated metabolites may facilitate faster metabolism and excretion via

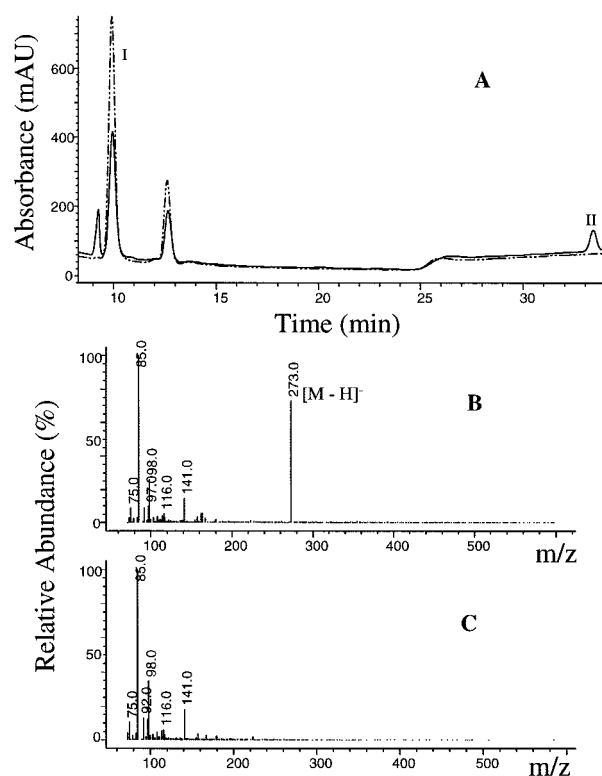


Fig. 5 A, UV-detected chromatogram of peak 3 after treatment with β -glucuronidase (—) and without treatment (---). B, mass spectrum of the Peak 2 formed after β -glucuronidase treatment showing an $[M-H]^-$ mass of 273 amu corresponding to 5-hydroxythalidomide. C, mass spectrum at the retention time corresponding to peak 2 in the untreated control.

this route. Indeed, the thalidomide-5-*O*-glucuronide was the largest metabolite peak in mouse urine. Glucuronidation occurred only at the 5-position, and no evidence for the formation of thalidomide-5'-*O*-glucuronide was found.

Although we have not been able to validate the structure by comparison with authentic material, we suggest that the metabolite in peak 2 is 5'-hydroxy-*N*-(*o*-carboxybenzoyl)glutamic acid imide, which can be formed either by second-step hydrolysis of 5'-hydroxythalidomide or second step hydroxylation of *N*-(*o*-carboxybenzoyl)glutamic acid imide. Other authentic standards with the same mass have been ruled out, because they have different HPLC retention times.

We found striking differences in the urinary thalidomide metabolite profiles between mice and patients with multiple myeloma. In the murine profiles, seven peaks containing eight metabolites formed by hydrolysis or hydroxylation (Fig. 1A; Fig. 8A; Table 1) were observed, whereas in the profiles of patients with multiple myeloma, only three products were detectable, all produced by hydrolysis (Table 2; Fig. 1B; Fig. 8B). Because p.o. and i.p. administration of thalidomide to mice produced essentially identical metabolite profiles (Fig. 7), the differences are unlikely to be because of an altered route of administration and may, therefore, reflect differences in metabolism. It has been found that the quantities of 5- and 5'-hydroxy

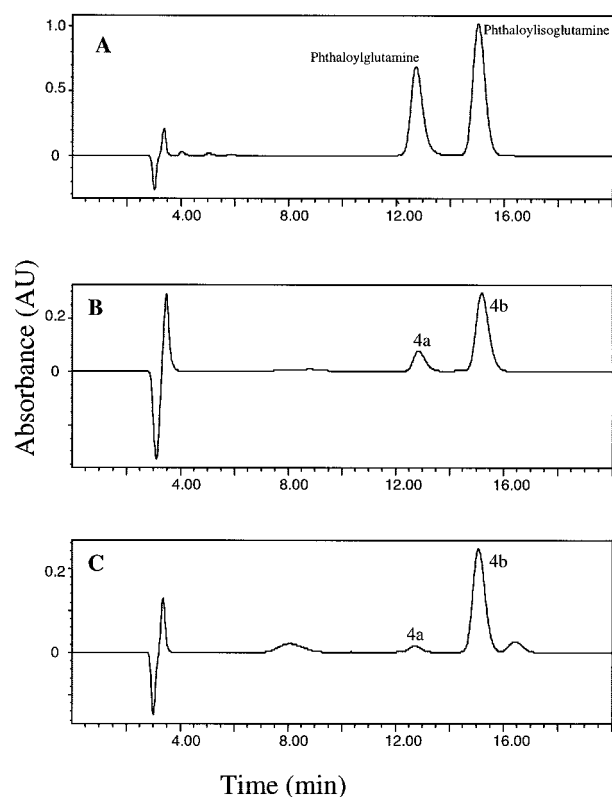


Fig. 6 HPLC chromatograms using mobile phase containing CTAB and OSA showing complete separation of: A, phthaloylglutamine and phthaloylisoglutamine authentic standards; B, separation of the peak 4 fraction from mice urine; and C, separation of the equivalent of peak 4 from patient urine into two peaks showing the presence of both phthaloylglutamine and phthaloylisoglutamine.

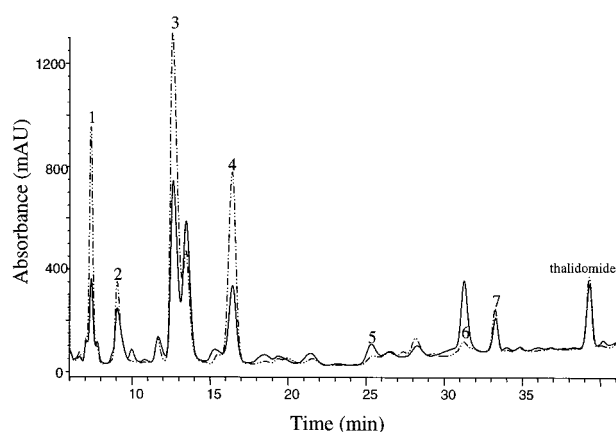


Fig. 7 Comparison of UV-detected chromatograms of urine from mice administered thalidomide p.o. (—) or i.p. (---).

thalidomide metabolites, thought to be produced by CYP2C19 activity in human liver microsomes, are ~10-fold lower than those obtained with liver microsomes from rodents, where CYP2C6 is the primary enzyme responsible (15). Thus, thalid-

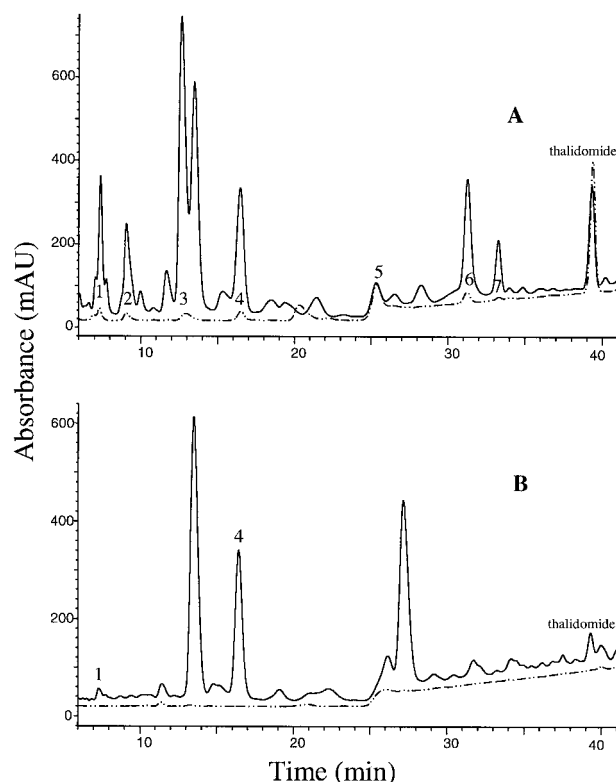


Fig. 8 Comparison of UV-detected chromatograms of urine (—) or plasma (---) from (A) mice given thalidomide (50 mg/kg) p.o.; and (B) patient 1 ~15 h after a prior dose of thalidomide (100 mg daily).

omide appears a much poorer substrate for the human CYP enzymes involved compared with the equivalent rodent enzymes, explaining the lower level of hydroxylation of thalidomide in humans.

Because plasma samples were only analyzed in one patient (Fig. 8B), we cannot exclude the possibility that hydroxylated thalidomide metabolites are produced in plasma of humans but do not appear in urine. However, in patients with Hansen's disease given a single p.o. dose of 400 mg thalidomide, no metabolites were detected in plasma, and the 5-hydroxy metabolite, although detected in urine, was below the limits of quantitation (29). Furthermore, in a study using healthy male volunteers, the plasma concentration of 5'-hydroxythalidomide was of the order of 0.1% of that of thalidomide, although both 5'- and 5-hydroxy metabolites were formed *in vitro* in the presence of human S9 liver fractions (16). In addition to the intrinsically lower amounts of hydroxylation in humans, it is possible that this pathway is suppressed in multiple myeloma patients as a result of their disease. A study involving 16 patients with advanced cancer showed a reduction in metabolic activity, correlating with decreased CYP2C19 activity, as compared with healthy volunteers (31).

The lack of detectable hydroxylated metabolites in multiple myeloma patients who are responding to thalidomide therapy suggests that such metabolites are not responsible for the therapeutic effect. Because hydroxylated metabolites have been implicated in the inhibition of angiogenesis, the results also

Table 2 Metabolites in mouse and patient urine samples

Metabolites	Mice oral 50 mg/kg	Patient 1 male 55 y 100 mg	Patient 2 female 47 y 400 mg	Patient 3 male 50 y 200 mg	Patient 4 male 63 y 400 mg	Patient 5 male 68 y 200 mg	Patient 6 female 75 y 300 mg	Patient 7 female 81 y 100 mg
Hydrolysis								
<i>N</i> -(<i>o</i> -carboxybenzoyl)glutamic acid imide (1)	+	+	+	+	+	+	+	+
Phthaloylglutamine (4a)	+	+	+	+	+	+	+	+
Phthaloylisoglutamine (4b)	+	+	+	+	+	+	+	+
Hydroxylation								
5'-hydroxy <i>N</i> -(<i>o</i> -carboxybenzoyl)-glutamic acid imide (2)	+	+	+	+	+	+	+	+
Thalidomide-5- <i>O</i> -glucuronide (3)	+	+	+	+	+	+	+	+
<i>cis</i> -5'-hydroxythalidomide (5)	+	+	+	+	+	+	+	+
<i>trans</i> -5'-hydroxythalidomide (6)	+	+	+	+	+	+	+	+
5-hydroxythalidomide (7)	+	+	+	+	+	+	+	+

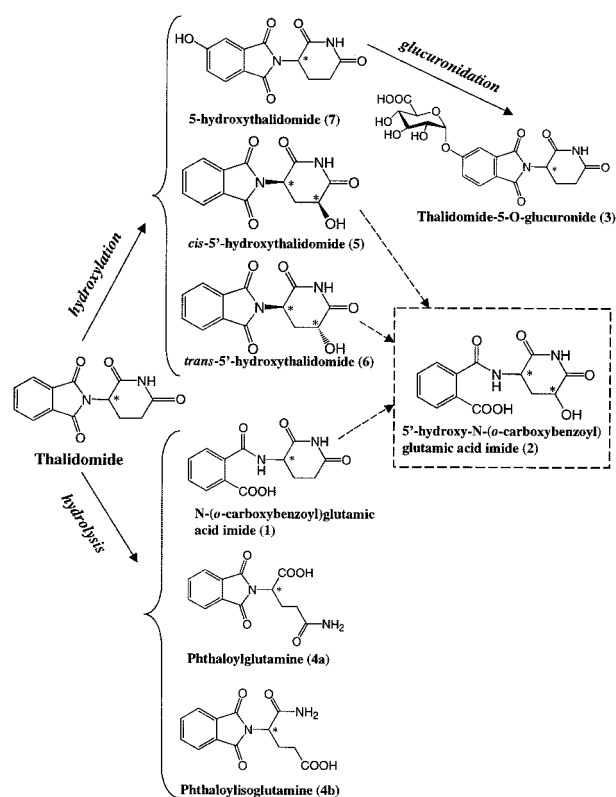


Fig. 9 Proposed pathways of biotransformation of thalidomide in mice. Unconfirmed steps or metabolites are shown in ----.

imply that the primary mechanism of action of thalidomide in responding multiple myeloma patients does not involve antiangiogenesis. An alternative explanation is that thalidomide itself is the active agent and exerts its activity by immunomodulation. The progression of multiple myeloma is strongly dependent on interleukin-6 and vascular endothelial growth factor production triggered by adhesion of the tumor cells to bone marrow stromal cells (32, 33). The ability of thalidomide to inhibit the biosynthesis of a range of cytokines, including interleukin-6, is well documented (34–36), and inhibition of growth factors necessary for tumor cell survival provides an alternative mechanism of action of thalidomide in the therapy of multiple myeloma. Inhibition of cytokine biosynthesis by thalidomide is not dependent on prior hepatic activation and occurs efficiently *in vitro* in the absence of metabolic enzymes (37). Rather, this activity is dependent on the intact parent compound and is lost on hydrolysis (38). We suggest that down-regulation of essential growth factors is the basis of the therapeutic effects of thalidomide in multiple myeloma.

REFERENCES

- Mellin, G. W., and Katzenstein, M. The saga of thalidomide. *N. Eng. J. Med.*, 267: 1238–1244, 1962.
- Zwingenberger, K., and Wnendt, S. Immunomodulation by thalidomide: systematic review of the literature and of unpublished observations. *J. Inflamm.*, 46: 177–211, 1995.

3. Calabrese, L., and Resztak, K. Thalidomide revisited: pharmacology and clinical applications. *Expert Opin. Investig. Drugs*, 7: 2043–2060, 1998.
4. Eisen, T. G. Thalidomide in solid tumors: the London experience. *Oncology (Huntington)*, 14: 17–20, 2000.
5. D'Amato, R. J., Loughnan, M. S., Flynn, E., and Folkman, J. Thalidomide is an inhibitor of angiogenesis. *Proc. Natl. Acad. Sci. USA*, 91: 4082–4085, 1994.
6. Eisen, T., Boshoff, C., Mak, I., Sapunar, F., Vaughan, M. M., Pyle, L., Johnston, S. R., Ahern, R., Smith, I. E., and Gore, M. E. Continuous low dose Thalidomide: a phase II study in advanced melanoma, renal cell, ovarian and breast cancer. *Br. J. Cancer*, 82: 812–817, 2000.
7. Fine, H. A., Figg, W. D., Jaeckle, K., Wen, P. Y., Kyritsis, A. P., Loeffler, J. S., Levin, V. A., Black, P. M., Kaplan, R., Pluda, J. M., and Yung, W. K. Phase II trial of the antiangiogenic agent thalidomide in patients with recurrent high-grade gliomas. *J. Clin. Oncol.*, 18: 708–715, 2000.
8. Figg, W. D., Raje, S., Bauer, K. S., Tompkins, A., Venzon, D., Bergan, R., Chen, A., Hamilton, M., Pluda, J., and Reed, E. Pharmacokinetics of thalidomide in an elderly prostate cancer population. *J. Pharm. Sci.*, 88: 121–125, 1999.
9. Vacca, A., Ribatti, D., Roncali, L., Ranieri, G., Serio, G., Silvestris, F., and Dammacco, F. Bone marrow angiogenesis and progression in multiple myeloma. *Br. J. Haematol.*, 87: 503–508, 1994.
10. Singhal, S., Mehta, J., Desikan, R., Ayers, D., Roberson, P., Edelman, P., Munshi, N., Anaissie, E., Wilson, C., Dhodapkar, M., Zeddis, J., and Barlogie, B. Antitumor activity of thalidomide in refractory multiple myeloma. *N. Eng. J. Med.*, 341: 1565–1571, 1999.
11. Faigle, J. W. The metabolic fate of thalidomide. *Experientia*, 18: 389–397, 1962.
12. Schumacher, H., Smith, R. L., and Williams, R. T. The metabolism of thalidomide: the fate of thalidomide and some of its hydrolysis products in various species. *Br. J. Pharmacol.*, 25: 338–351, 1965.
13. Schumacher, H., Smith, R. L., and Williams, R. T. The metabolism of thalidomide: the spontaneous hydrolysis of thalidomide in solution. *Br. J. Pharmacol.*, 25: 324–337, 1965.
14. Braun, A. G., Harding, F. A., and Weinreb, S. L. Teratogen metabolism: thalidomide activation is mediated by cytochrome P-450. *Toxicol. Appl. Pharmacol.*, 82: 175–179, 1986.
15. Ando, Y., Fuse, E., and Figg, W. D. Thalidomide metabolism by the CYP2C subfamily. *Clin. Cancer Res.*, 8: 1964–1973, 2002.
16. Eriksson, T., Bjorkman, S., Roth, B., Bjork, H., and Hoglund, P. Hydroxylated metabolites of thalidomide: formation *in-vitro* and *in-vivo* in man. *J. Pharm. Pharmacol.*, 50: 1409–1416, 1998.
17. Bauer, K. S., Dixon, S. C., and Figg, W. D. Inhibition of angiogenesis by thalidomide requires metabolic activation, which is species-dependent. *Biochem. Pharmacol.*, 55: 1827–1834, 1998.
18. Eriksson, T., Bjorkman, S., Roth, B., Fyge, A., and Hoglund, P. Enantiomers of thalidomide: blood distribution and the influence of serum albumin on chiral inversion and hydrolysis. *Chirality*, 10: 223–228, 1998.
19. Gordon, G. B., Spielberg, S. P., Blake, D. A., and Balasubramanian, V. Thalidomide teratogenesis: evidence for a toxic arene oxide metabolite. *Proc. Natl. Acad. Sci. USA*, 78: 2545–2548, 1981.
20. Reist, M., Carrupt, P. A., Francotte, E., and Testa, B. Chiral inversion and hydrolysis of thalidomide: mechanisms and catalysis by bases and serum albumin, and chiral stability of teratogenic metabolites. *Chem. Res. Toxicol.*, 11: 1521–1528, 1998.
21. Price, D. K., Ando, Y., Kruger, E. A., Weiss, M., and Figg, W. D. 5'-OH-Thalidomide, a metabolite of thalidomide, inhibits angiogenesis. *Ther. Drug Monit.*, 24: 104–110, 2002.
22. Luzzio, F. A., Thomas, E. M., and Figg, W. D. Thalidomide metabolites and analogs. Part 2: Cyclic derivatives of 2-N-phthalimido-2S, 3S (3-hydroxy) ornithine. *Tetrahedron Lett.*, 41: 7151–7155, 2000.
23. Marks, M. G., Shi, J., Fry, M. O., Xiao, Z., Trzyna, M., Pokala, V., Ihnat, M. A., and Li, P. K. Effects of putative hydroxylated thalidomide metabolites on blood vessel density in the chorioallantoic membrane (CAM) assay and on tumor and endothelial cell proliferation. *Biol. Pharm. Bull.*, 25: 597–604, 2002.
24. Kruse, F. E., Jousen, A. M., Rohrschneider, K., Becker, M. D., and Volcker, H. E. Thalidomide inhibits corneal angiogenesis induced by vascular endothelial growth factor. *Graefes Arch. Clin. Exp. Ophthalmol.*, 236: 461–466, 1998.
25. Kenyon, B. M., Browne, F., and D'Amato, R. J. Effects of thalidomide and related metabolites in a mouse corneal model of neovascularization. *Exp. Eye Res.*, 64: 971–978, 1997.
26. Kaldor, S. W., Hammond, M., Dressman, B. A., Labus, J. M., Chadwell, F. W., Kline, A. D., and Heinz, B. A. Glutamine-derived aldehydes for the inhibition of human rhinovirus 3C protease. *Bioorg. Med. Chem. Lett.*, 5: 2021–2026, 1995.
27. Webster, L. K., Ellis, A. G., Kestell, P., and Rewcastle, G. W. Metabolism and elimination of 5, 6-dimethylxanthene-4-acetic acid in the isolated perfused rat liver. *Drug Metab. Dispos.*, 23: 363–368, 1995.
28. Wein, C., and Blaschke, G. Investigation of the *in vitro* biotransformation and simultaneous enantioselective separation of thalidomide and its neutral metabolites by capillary electrophoresis. *J. Chromatogr. B Biomed. Appl.*, 674: 287–292, 1995.
29. Teo, S. K., Sabourin, P. J., O'Brien, K., Kook, K. A., and Thomas, S. D. Metabolism of thalidomide in human microsomes, cloned human cytochrome P-450 isozymes, and Hansen's disease patients. *J. Biochem. Mol. Toxicol.*, 14: 140–147, 2000.
30. Meyring, M., Muhlenbrock, C., and Blaschke, G. Investigation of the stereoselective *in vitro* biotransformation of thalidomide using a dual cyclodextrin system in capillary electrophoresis. *Electrophoresis*, 21: 3270–3279, 2000.
31. Williams, M. L., Bhargava, P., Cherrouk, I., Marshall, J. L., Flockhart, D. A., and Wainer, I. W. A discordance of the cytochrome P450 2C19 genotype and phenotype in patients with advanced cancer. *Br. J. Clin. Pharmacol.*, 49: 485–488, 2000.
32. Suzuki, H., Yasukawa, K., Saito, T., Goitsuka, R., Hasegawa, A., Ohsugi, Y., Taga, T., and Kishimoto, T. Anti-human interleukin-6 receptor antibody inhibits human myeloma growth *in vivo*. *Eur. J. Immunol.*, 22: 1989–1993, 1992.
33. Gupta, D., Treon, S. P., Shima, Y., Hideshima, T., Podar, K., Tai, Y. T., Lin, B., Lentzsch, S., Davies, F. E., Chauhan, D., Schlossman, R. L., Richardson, P., Ralph, P., Wu, L., Payvandi, F., Muller, G., Stirling, D. I., and Anderson, K. C. Adherence of multiple myeloma cells to bone marrow stromal cells upregulates vascular endothelial growth factor secretion: therapeutic applications. *Leukemia (Baltimore)*, 15: 1950–1961, 2001.
34. Dunsendorfer, S., Herold, M., and Wiedermann, C. J. Inducer-specific bidirectional regulation of endothelial interleukin-8 production by thalidomide. *Immunopharmacology*, 43: 59–64, 1999.
35. Moller, D. R., Wysocka, M., Greenlee, B. M., Ma, X., Wahl, L., Flockhart, D. A., Trinchieri, G., and Karp, C. L. Inhibition of IL-12 production by thalidomide. *J. Immunol.*, 159: 5157–5161, 1997.
36. Rowland, T. L., McHugh, S. M., Deighton, J., Dearman, R. J., Ewan, P. W., and Kimber, I. Differential regulation by thalidomide and dexamethasone of cytokine expression in human peripheral blood mononuclear cells. *Immunopharmacology*, 40: 11–20, 1998.
37. Sampaio, E. P., Sarno, E. N., Galilly, R., Cohn, Z. A., and Kaplan, G. Thalidomide selectively inhibits tumor necrosis factor α production by stimulated human monocytes. *J. Exp. Med.*, 173: 699–703, 1991.
38. Shannon, E. J., Sandoval, F., and Krahenbuhl, J. L. Hydrolysis of thalidomide abrogates its ability to enhance mononuclear cell synthesis of IL-2 as well as its ability to suppress the synthesis of TNF- α . *Immunopharmacology*, 36: 9–15, 1997.

Metabolism of Thalidomide in Liver Microsomes of Mice, Rabbits, and Humans

Jun Lu, Nuala Helsby, Brian D. Palmer, Malcolm Tingle, Bruce C. Baguley, Philip Kestell, and Lai-Ming Ching

Auckland Cancer Society Research Centre, Faculty of Medical and Health Sciences, The University of Auckland, Auckland, New Zealand (J.L., N.H., B.D.P., B.C.B., P.K., L.-M.C.); and Department of Pharmacology and Clinical Pharmacology, Faculty of Medical and Health Sciences, The University of Auckland, Auckland, New Zealand (M.T.)

Received March 2, 2004; accepted April 5, 2004

ABSTRACT

Thalidomide is increasingly important in clinical treatment, not only of various inflammatory conditions but also in multiple myeloma and other malignancies. Moreover, the metabolism of thalidomide varies considerably among different species, indicating a need to understand its mechanistic basis. Our previous *in vivo* studies showed the plasma half-life of thalidomide to be much shorter in mice than in humans, with rabbits showing intermediate values. We were unable to detect hydroxylated thalidomide metabolites in humans and suggested that interspecies differences in thalidomide hydroxylation might account for the differences in plasma half-life. We sought here to establish whether these species differences in the formation of hydroxylated thalidomide metabolites could be discerned from *in vitro* studies. Liver microsomes of mice, rabbit, and human donors were incubated with thalidomide and analyzed using liquid chromatography-mass spectrometry. Hydrolysis prod-

ucts were detected for all three species, and the rates of formation were similar to those for spontaneous hydrolysis, except in rabbits where phthaloylisoglutamine formation increased linearly with microsomal enzyme concentration. Multiple hydroxylation products were detected, including three dihydroxylated metabolites not observed *in vivo*. Thalidomide-5-O-glucuronide, detected *in vivo*, was absent *in vitro*. The amount of 5-hydroxythalidomide formed was high in mice, lower in rabbits, and barely detectable in humans. We conclude that major interspecies differences in hepatic metabolism of thalidomide relate closely to the rate of *in vivo* metabolite formation. The very low rate of *in vitro* and *in vivo* hydroxylation in humans strongly suggests that thalidomide hydroxylation is not a requirement for clinical anticancer activity.

Thalidomide (α -phthalimidoglutarimide, Thal), despite its teratogenicity (McBride, 1961; Lenz, 1962), is attracting increasing clinical interest, initially as an anti-inflammatory agent (Sheskin, 1965; Zwingenberger and Wnendt, 1996; Calabrese and Fleischer, 2000) and more recently for the treatment of malignancies, particularly of multiple myeloma (Singhal et al., 1999; Eisen, 2000). Differences in metabolism among different species represent an important feature of its pharmacology. It has been suggested that Thal exerts its teratogenicity through an active metabolite, which is produced by human and rabbit liver microsome preparations but not by mouse liver microsomes (Gordon et al., 1981). After *in vivo* administration, Thal is both hydrolyzed chemically to a series of acid derivatives and hydroxylated by liver enzymes. In a previous study (Chung et al., 2004), we showed that the

plasma half-life of Thal in mice was much shorter than that in patients with multiple myeloma, with New Zealand White rabbits showing an intermediate half-life. We also showed that hydroxylated metabolites were not detected in multiple myeloma patients but were found in C57/Bl/6 mice and rabbits, suggesting that relative rates of Thal hydroxylation in different species could account for the differences in plasma pharmacokinetics, hence the differences in biological sensitivity. In this communication, we have addressed the question of whether these species differences are reflected in the *in vitro* activity of liver microsomal enzymes.

There have been a number of other studies on the *in vitro* metabolism of Thal in different species. Ando and coworkers compared the ability of liver microsomes from five different species to form 5-hydroxythalidomide (5-OH Thal) and *cis*-5'-OH Thal and found that human microsomes had the lowest activity (Ando et al., 2002a). The formation of 5,6-dihydroxythalidomide was also reported, with CYP2C19 identified

Article, publication date, and citation information can be found at <http://jpet.aspetjournals.org>.
DOI: 10.1124/jpet.104.067793.

ABBREVIATIONS: Thal, thalidomide; 5-OH Thal, 5-hydroxythalidomide; 5'-OH Thal, 5'-hydroxythalidomide; HPLC, high-performance liquid chromatography; LC-MS, liquid chromatography-mass spectrometry; P450, cytochrome P450; ACN, acetonitrile.

as responsible for the hydroxylation of Thal in humans. Another study (Eriksson et al., 1998) has compared the formation of hydroxylated metabolites in vitro using human S9 liver fractions and in vivo in healthy human volunteers: both 5-OH Thal and *cis*-5'-OH Thal were formed in vitro but only *cis*-5'-OH Thal was detected in vivo. However, Teo et al., (2000) did not detect any metabolites after incubating Thal with human liver microsomes or in the plasma of patients with Hansen's disease, although trace amounts of 5-OH Thal were detected in urine. We have taken advantage of progress in the chemical synthesis of Thal metabolites, together with the development of high-performance liquid chromatography (HPLC) and LC-MS technologies, to determine the rate of 5-OH Thal formation in liver microsomes of mice, rabbits, and humans, as well as to characterize all the major metabolites formed in vitro to compare them with those formed in vivo.

Materials and Methods

Materials. Thal was kindly provided by Dr. George Muller (Celgene Corporation, Warren, NJ). Phthaloylglutamic acid, trichloroacetic acid, and NADPH were from Sigma-Aldrich (St. Louis, MO); acetonitrile (ACN) was from BDH (Poole, Dorset, UK); and glacial acetic acid was from Panreac Quimica SA (Barcelona, Spain). Phthaloylisoglutamine, 4-hydroxyphthaloylisoglutamine, 5-hydroxyphthaloylisoglutamine, 5-OH Thal, phthaloylglutamine, 4-hydroxyphthaloylglutamine, 5-hydroxyphthaloylglutamine, 4-hydroxythalidomide, *N*-(*o*-carboxybenzoyl)glutamine, *N*-(*o*-carboxybenzoyl)isoglutamine, *N*-(*o*-carboxybenzoyl)glutamic acid imide, and 5-hydroxy-*N*-(*o*-carboxybenzoyl)glutamic acid imide were synthesized as described previously (Lu et al., 2003), and their structures were confirmed using 400-MHz ^1H nuclear magnetic resonance spectroscopy and mass spectrometry. 5,6-Dihydroxythalidomide was prepared by reaction of 5,6-dimethoxyphthalic anhydride (Barfield et al., 1975) with glutamine in refluxing pyridine (16 h), followed by cyclization of the product with *N,N*-carbonyldiimidazole and catalytic 4-(*N,N*-dimethylamino)pyridine in refluxing *p*-dioxane (16 h) and finally demethylation with pyridinium hydrochloride melt at 210°C (20 min). 5'-OH Thal was a generous gift from Professor Sven Bjorkman (Malmo University Hospital, Malmo, Sweden) and was a mixture of 5'-*cis* and 5'-*trans* diastereoisomers.

Liver Microsome Preparation. All studies with animals and humans conformed to institutional ethical guidelines. Human livers were obtained from two liver donors, HL5 and HL18, and stored in the human liver bank at the Department of Pharmacology and Clinical Pharmacology (Faculty of Medical and Health Sciences, University of Auckland). These livers have been genotyped for CYP2C19; HL18 is CYP2C19 $^{*1}/^{*2}$ and HL5 is CYP2C19 $^{*1}/^{*1}$. Pooled C57/Bl/6 mouse livers and livers from New Zealand White rabbit and human donors were rinsed in ice-cold phosphate buffer (pH 7.4) and blotted dry. Liver weights were recorded. Livers were then homogenized in 67 mM phosphate buffer containing 1.15% KCl (volume of buffer was 3 times the weight of the liver). The homogenate was then centrifuged at 10,000g for 20 min, and the supernatant was removed and centrifuged at 100,000g for 1 h. The supernatant was again removed and the remaining microsomal pellets were rinsed with phosphate buffer. The rinsed pellets were resuspended in a small volume of phosphate buffer and stored at -80°C until analysis. The protein content of microsomes of all three species was determined using bicinchoninic acid assay (Smith et al., 1985).

Microsomal Incubation and Sample Preparation for HPLC and LC-MS. In the preliminary control experiments, the degradation of 400 μM Thal was <10% in phosphate buffer at 37°C. The rate of Thal hydroxylation was linear with respect to microsomal protein concentration (0.4–2 mg/ml) and time (10–30 min) in mouse and rabbit hepatic microsomes and linear between 0.6–2 mg/ml and 40–60 min in the presence of human liver microsomes. Incubations were carried out in a shaking water bath at 37°C for 30 min for

mouse and rabbit microsomes and 60 min for human microsomes. The reaction mixture consisted of 67 mM phosphate buffer (pH 7.4), 4 mM NADPH, Thal (6.25–600 μM), and 2 mg/ml microsomes in a final volume of 300 μl . Thal was dissolved in dimethyl sulfoxide and then diluted in phosphate buffer (final concentration of dimethyl sulfoxide was <0.2%). After a 5-min preincubation, the reaction was initiated by addition of hepatic microsomes. Boiled microsomes were added to the control incubations. The reaction was terminated by addition of 300 μl of 10% trichloroacetic acid containing phenacetin as an internal standard and was then vortexed and centrifuged (3000g) for 10 min to remove precipitated protein (Torano et al., 1999). The supernatants were processed by solid phase extraction as described previously (Lu et al., 2003), and the dry residues were reconstituted in 300 μl of mobile phase. Reconstituted samples were analyzed for 5-OH Thal concentration (200 μl each) using HPLC and metabolite identification (100 μl each) determined by LC-MS immediately afterward.

Detection and Identification of Metabolites Formed in Vitro Using LC-MS. Samples (100 μl) from preliminary in vitro incubations (using 2 mg/ml liver microsomes, 400 μM Thal, and 60-min incubation time) and the final in vitro incubations (using 2 mg/ml liver microsomes, 6.25–600 μM Thal, and incubation time of 30 min for rabbit and mouse, 60 min for human) were analyzed together with authentic standards using an Agilent 1100 series LC-MS system (Agilent Technologies, Avondale, PA) as described previously (Lu et al., 2003) with two modifications. The proportions of solution A (80% ACN, 1% glacial acetic acid, and 19% Milli Q water) and solution B (9.5% ACN, 1% glacial acetic acid, and 89.5% Milli Q water) in the mobile phase were altered slightly to improve resolution; all samples were analyzed using diode array UV detection at 230 nm and mass spectral detection set on negative-ion scan mode with a molecular weight range of 70 to 1000 amu, negative single-ion monitoring mode, with the sensitivity of 1 pg, at the molecular weights 257, 273, 275, 276, 289, 291, 293, 294, and 449, and positive single-ion monitoring mode at the molecular weights 259, 275, 277, 278, 291, 293, 295, 296, and 451 (corresponding to each of the peaks) simultaneously. Chromatograms of each sample were compared with control samples and authentic standards, and molecular masses of metabolites were obtained by mass spectral detection. The relative abundances of peaks of interest in negative single-ion mass spectral-detected chromatograms or UV-detected chromatograms were obtained from integration using ChemStation Software (Agilent Technologies).

In Vitro 5-OH Thal Formation. Samples were analyzed for 5-OH Thal concentrations using HPLC. Solutions containing a range of concentrations of 5-OH Thal, together with phenacetin as internal standard, were processed alongside with samples. 5-OH Thal concentrations were determined using the method developed from this laboratory with slight modifications of HPLC run time and mobile phase (Chung et al., 2004). In brief, duplicate aliquots (100 μl) of reconstituted samples were loaded onto a Waters Breeze chromatograph (Waters, Milford, MA), which consisted of a model 717plus auto-sampler, model 1525 binary pump, and model 2487 dual wavelength absorbance detector. Compounds of interest were separated using a 100 \times 4.6-mm stainless steel Luna 5- μm Phenylhexyl column (Phenomenex, Torrance, CA) as well as a combination of the following solutions: solution A, which contained 100% acetonitrile, and solution B, which contained 10% acetonitrile and 1% acetic acid in Milli Q water. The elution program was 100% solution B at 0.5 ml/min over 0 to 10 min, addition of 0 to 10% solution A in a linear gradient at 1 ml/min over 10 to 15 min, 90% solution B and 10% solution A at 1 ml/min over 15 to 23 min, subtraction of 10 to 0% solution A in a linear gradient at 0.5 ml/min over 23 to 27 min and 100% solution B at 0.5 ml/min over 27 to 30 min. Phenacetin, Thal, and 5-OH Thal were detected at ultraviolet wavelengths of 220 and 248 nm. The retention times of 5-OH Thal and phenacetin were 20.1 and 22.8 min, respectively. Data acquisition and integration were achieved using Breeze Software (Waters, Milford, MA). A calibration

curve of 5-OH Thal in phosphate buffer was prepared fresh for each HPLC run. To construct the calibration curve, the peak/area ratios relative to the internal standard were plotted against 5-OH Thal concentrations and the best-fit straight line was obtained by linear regression analysis. The range of calibration curve of 5-OH Thal was 0.1–25 μM ($r^2 = 0.999$). The intra-assay accuracy and precision were acceptable with relative recoveries and coefficient of variation of 90 to 110% and 5 to 9% ($n = 3$), respectively. Similar results were achieved for interassay accuracy and precision with relative recoveries and coefficient of variations of 96 to 104 and 2 to 4% ($n = 5$). Quality control liver microsomes with three nominal 5-OH Thal concentrations (0.2, 5, and 25 μM) added were stored at -80°C . These were included in each analysis and were found to be stable over a period of 14 days and within 3% of the validated value, respectively. Reconstituted samples (100 μl each in duplicate) were injected onto HPLC and 5-OH Thal concentrations were determined

using calibration curve described above. The 5-OH Thal concentrations were used to calculate the rate of formation. Michaelis-Menten models were used to describe the in vitro enzyme kinetics, and the kinetic parameters were determined by Prism 3.0 program (Graph-Pad Software Inc., San Diego, CA).

Results

Metabolites Formed after Incubation of Thal with Hepatic Microsomes. After incubation of Thal (400 μM) with rabbit and mouse liver microsomes (0.4–2 mg/ml) for 60 min in the presence of NADPH (4 mM), 11 peaks (1–11), in addition to Thal (Table 1; Fig. 1, B and C) were resolved. In contrast, only seven peaks (1, 2, 5–7, and 10–11) were detected using human (HL18) liver microsomes (Fig. 1A). Four

TABLE 1

Metabolites formed after incubating Thal with mouse and rabbit liver microsomes

Peak	M.W. ^a	Metabolite	Structure
1*	276	<i>N</i> -(<i>o</i> -carboxybenzoyl)glutamic acid imide	
2*	294	<i>N</i> -(<i>o</i> -carboxybenzoyl)isoglutamine	
3 [#]	290	Unknown dihydroxythalidomide	—
4 ^{#b}	292	5'-hydroxy- <i>N</i> -(<i>o</i> -carboxybenzoyl)glutamic acid imide	
5*	276	phthaloylisoglutamine	
6*	276	phthaloylglutamine	
7 [#]	274	<i>cis</i> -5'-hydroxythalidomide	
8 ^{#b}	290	<i>cis</i> -5,5'-dihydroxythalidomide	
9 ^{#b}	290	<i>trans</i> -5,5'-dihydroxythalidomide	
10 [#]	274	<i>trans</i> -5'-hydroxythalidomide	
11 [#]	274	5-hydroxythalidomide	

* hydrolysis metabolite, [#] metabolite formed via hydroxylation, ^a Molecular Weight, ^b Proposed metabolite.

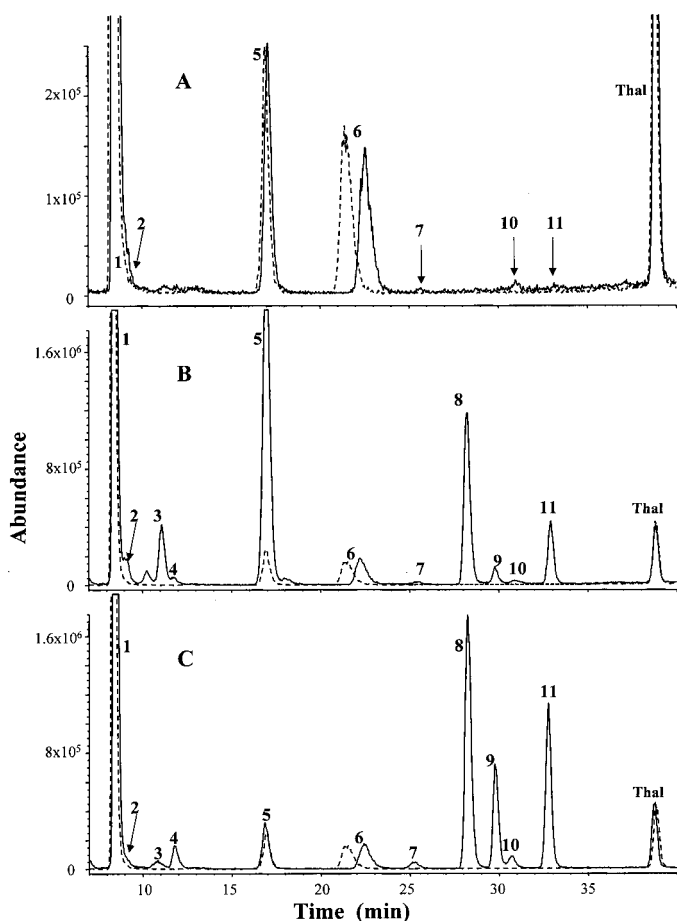


Fig. 1. LC-MS chromatograms of Thal metabolites after incubation (60 min; 37°C) of Thal (400 μ M) with liver microsomes (solid lines) of humans (A), rabbits (B), and mice (C), or with boiled liver microsomes (dotted lines). Metabolites were detected by single ion monitoring mass spectrometry as described under *Materials and Methods*.

peaks (1, 2, 5, and 6) in the control incubations (with boiled microsomes) were identified by UV and mass spectral analysis and comparison with authentic standards as products of hydrolysis (Figs. 1 and 2). Four of the remaining seven peaks formed by mouse and rabbit liver microsomes were identified as the previously reported hydroxyl derivatives (Lu et al., 2003; Chung et al., 2004), namely, 5-OH Thal and 5'-hydroxy-*N*-(*o*-carboxybenzoyl)glutamic acid imide plus *cis*- and *trans*-5'-OH Thal (4, 7, 10, and 11; Fig. 1, B and C). The remaining three peaks (3, 8, and 9) were products of further hydroxylation reactions because they had an identical molecular mass that was 16 amu higher than 5-OH Thal or 5'-OH Thal and were therefore assigned as dihydroxylated metabolites. None of these metabolites had retention times and UV spectra similar to authentic 5,6-dihydroxythalidomide. Peaks 8 and 9 could possibly correspond to *cis*-5,5'-dihydroxythalidomide and *trans*-5,5'-dihydroxythalidomide, although authentic compounds were not available for confirmation. Peak 3 was unidentified. Apart from the four hydrolysis products (1, 2, 5, and 6) observed in control incubations, human liver microsomes from donor HL18 catalyzed the formation of three hydroxylated metabolites, 5-OH Thal (11), *cis*-5'-OH Thal (7), and *trans*-5'-OH Thal (10) (Fig. 1A). However, microsomes from HL5 failed to produce any detectable hydroxylation metabolites.

A comparison of the relative formation of hydroxylated metabolites by hepatic microsomes in the different species indicates that metabolic rate via hydroxylation is mouse > rabbit > human (Table 2). In particular, the relative abundance of each of the hydroxylated metabolite peaks produced by HL18 microsomes was much lower than the corresponding peak formed by mouse or rabbit liver microsomes (Table 2). Similarly, the relative amount of hydroxylated metabolites was higher in the presence of mouse liver microsomes compared with rabbit liver microsomes, with the exception of peak 3.

The relative amount of hydrolysis products formed in microsomes from all three species did not differ significantly from the amount in control samples regardless of microsomal concentrations, with the exception of phthaloylisoglutamine (peak 5) and *N*-(*o*-carboxybenzoyl)isoglutamine (peak 2) in rabbit microsomal solutions (Figs. 1 and 2; Table 3). The formation of phthaloylisoglutamine exhibited a linear relationship with rabbit microsomal protein concentration ($r^2 = 0.983$; Fig. 3). Hence, it seems that the hydrolysis of Thal to phthaloylisoglutamine in rabbit microsomes, at high substrate concentrations (400 μ M), is an enzymatic process. Increased formation of *N*-(*o*-carboxybenzoyl)isoglutamine (peak 2) may be a consequence of the hydrolysis of the phtha-

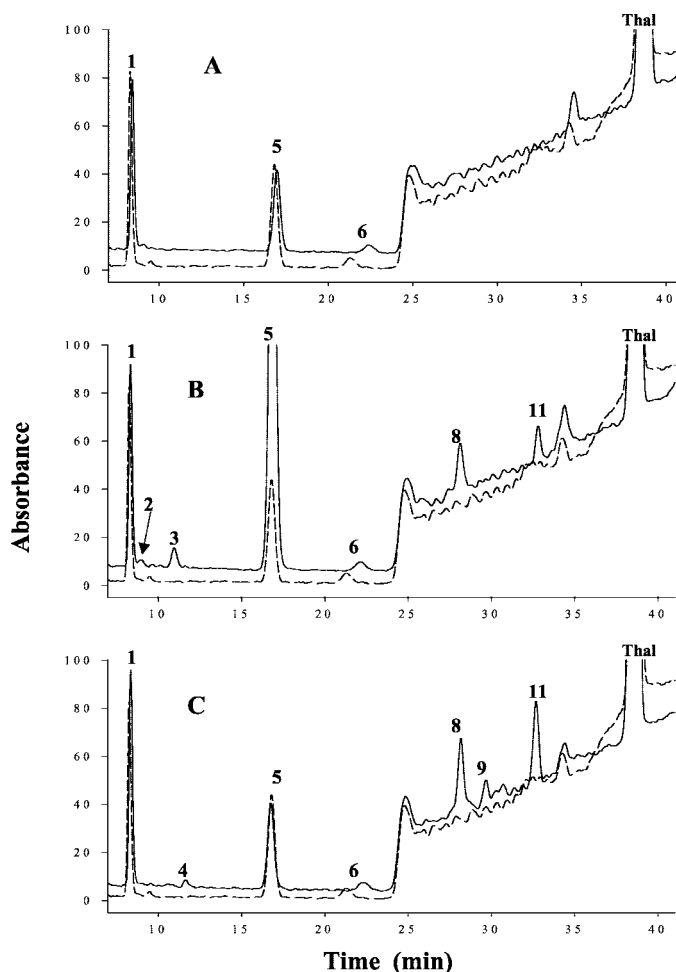


Fig. 2. HPLC chromatograms with UV detection of Thal metabolites after incubation (60 min; 37°C) of Thal (400 μ M) with liver microsomes (solid lines) of humans (A), rabbits (B), and mice (C), or with boiled liver microsomes (dotted lines).

TABLE 2

Comparison of relative levels of hydroxylated metabolites formed following a 60-min incubation of Thal with liver microsomal protein (2 mg/ml). Metabolites were determined by mass spectral detection using single ion monitoring. The response of each metabolite peak produced by mouse liver microsomes was normalized to 1.

	Unknown Dihydroxylated Metabolite (3) ^a	5'-OH CG ^b (4)	<i>cis</i> -5'-OH Thal (7)	<i>cis</i> -5,5'-OH Thal ^c (8)	<i>trans</i> -5,5'-OH Thal ^d (9)	<i>trans</i> -5'-OH Thal (10)	5-OH Thal (11)
Mouse	1	1	1	1	1	1	1
Rabbit	4.59	0.26	0.34	0.68	0.13	0.27	0.37
Human	0	0	0.07	0	0	0.09	0.005

^a Number in parentheses represents peak number in chromatogram.

^b 5'-hydroxy-*N*-(*o*-carboxybenzoyl)glutamic acid imide.

^c *cis*-5,5'-Dihydroxythalidomide.

^d *trans*-5,5'-Dihydroxythalidomide.

TABLE 3

Comparison of relative levels of hydrolysis products formed following a 60-min incubation of Thal with liver microsomal protein (2 mg/ml).

Hydrolysis products were determined by mass spectral detection by using single ion monitoring. The response of each peak produced by mouse liver microsomes was normalized to 1.

	CG (1) ^a	CiG ^b (2)	PiG (5)	PG (6)
Control ^c	1	1	1	1
Mouse	0.90–1.2	1	0.98–1.08	0.96–1.09
Rabbit	0.95–1.13	8.9–17.8	2.65–7.92	0.87–1.03
Human	0.90–1.01	1	0.88–1.1	0.84–1.05

^a Number in parentheses represents peak number in chromatogram.

^b *N*-(*o*-Carboxybenzoyl)isoglutamine.

^c Thalidomide solutions incubated with boiled liver microsomes of mouse, rabbit, and human.

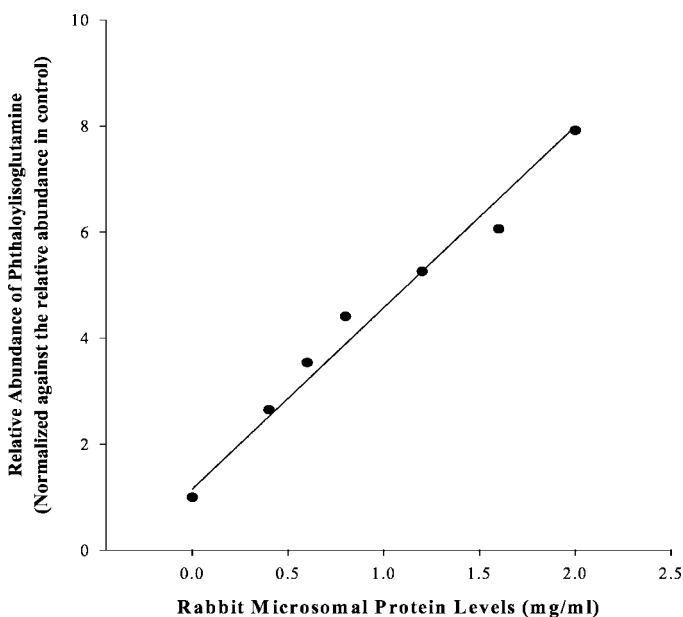


Fig. 3. Enzymatic hydrolysis of phthaloylisoglutamine by rabbit liver microsomal protein in the presence of NADPH (4 mM).

limide ring of phthaloylisoglutamine (peak 5). Another finding in accordance with the above-mentioned finding is that incubating rabbit and mouse microsome with Thal at 6.25 μ M did not show difference in phthaloylisoglutamine formation, but when Thal concentrations were raised to 12.5 μ M and above, rabbit liver microsome formed more phthaloylisoglutamine than mice.

The relative percentages of metabolite formation were obtained by comparing the peak areas of metabolites detected by UV with the sum of peak areas of all the metabolites and thalidomide (Fig. 2). A comparison of the relative total formation of hydrolysis products and hydroxylated metabolites

TABLE 4

Comparison of the total products of hydrolysis and hydroxylation formed following a 60-min incubation of Thal with liver microsomal protein (2 mg/ml).

Species	All Metabolites of Hydrolysis ^a	All Metabolites of Hydroxylation ^a	5-OH Th ^a	Total Metabolites ^a
	%			
Mouse	7.7	6.1	2.5	13.8
Rabbit	22.7	3.0	1.1	25.7
Human	7.9			7.9

^a The percentage was obtained by comparing the sum of the UV responses of all hydrolysis or/and hydroxylation peaks with the sum of the UV responses of all metabolite and parent peaks, including hydrolysis, hydroxylation, and thalidomide peaks.

in microsomes from the three species indicates that rabbit has the highest overall metabolic clearance of Thal (25.7%), mainly due to enzymatic hydrolysis (Table 4). In human and mouse liver microsomes, the formation of hydrolysis products was lower (7.7–7.9%) and due solely to nonenzymatic hydrolysis (Table 4). In contrast, metabolic clearance of Thal via hydroxylation was negligible in human liver microsomes and highest in mouse microsomes (6.1%).

Rate of 5-OH Thal Formation. Previous studies have indicated that the formation of 5-OH Thal may be catalyzed by CYP2C19 (Ando et al., 2002a). To determine the relative rates of metabolism of Thal to 5-OH Thal in the three species, the enzyme kinetics of 5-OH Thal formation was determined. HPLC with UV detection resolved the hydroxylated metabolites (*cis*- and *trans*-5'-OH Thal and 5-OH Thal) and internal

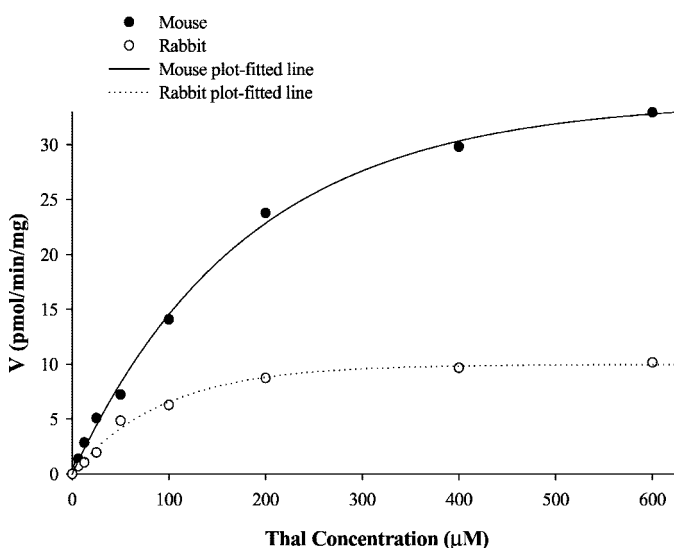


Fig. 4. Formation of 5-OH Thal in rabbit and mouse liver microsomes after incubation with Thal.

standard (phenacetin) from Thal with retention times of 18.3, 19.6, 20.1, 22.8, and 23.6 min, respectively. The formation of 5-OH Thal increased linearly with mouse and rabbit microsomal protein concentrations up to 2 mg/ml ($r^2 = 0.984$ and 0.985 , respectively), whereas the formation of 5-OH Thal by human liver microsomes was close to the limit of detection. Microsomes from donor HL18 (*CYP2C19* *1/*2) formed measurable amounts of 5-OH Thal (quantitative limit of $0.1 \mu\text{M}$) at microsomal concentrations higher than 0.6 mg/ml , whereas 5-OH Thal formed by microsomes from donor HL5 (*CYP2C19* *1/*1) was below the limit of detection. The formation of 5-OH Thal also increased with incubation time in the presence of 2 mg/ml mouse and rabbit liver microsomes and was linear up to 30 min ($r^2 = 0.998$ and 0.999 for mouse and rabbit, respectively), whereas 5-OH Thal formation by human liver microsomes (HL18) required an incubation time of greater than 40 min. Microsomes from mouse and rabbit formed measurable 5-OH Thal at concentrations of Thal above $6.25 \mu\text{M}$. The formation of 5-OH Thal followed Michaelis-Menten kinetics (Fig. 4) and the kinetic parameters V_{max} (maximum velocity of reaction) and K_M (Michaelis-Menten constant) were 45.2 pmol/min/mg and $208.3 \mu\text{M}$ for mouse microsomes, and $11.91 \text{ pmol/min/mg}$ and $88.02 \mu\text{M}$ for rabbit microsomes, respectively. Previous reports have indicated that the metabolism of Thal to 5-OH and *cis*-5'-OH Thal may be important routes of metabolic clearance catalyzed by *CYP2C19* in vitro (Ando et al., 2002a), but the kinetic parameters of Thal to 5-OH Thal in microsomes were not calculated due to the nonlinear formation of 5-OH Thal. We used conditions optimized for 5-OH Thal formation (higher microsomal protein concentration and shorter incubation time) to calculate the kinetic parameters because it seemed to be the major route of metabolism detected in vivo (Lu et al., 2003; Chung et al., 2004). However, as products of further hydroxylation of *cis*-, *trans*-5'-OH Thal, and 5-OH Thal were detected in the present in vitro study, kinetic parameters of formation of the primary hydroxylated metabolites of Thal (5-OH and *cis*-5'-OH) are compromised by the rate(s) of the second hydroxylation step; hence, the kinetic parameters, in particular K_M , can only be described as *apparent*. The apparent intrinsic clearance (CL_{int}) ($\text{CL}_{\text{int}} = V_{\text{max}}/K_M$) of Thal to 5-OH Thal in mouse and rabbit microsomes was 0.217 and 0.135 ml/min/g , respectively. Therefore, the apparent in vitro intrinsic clearance was 1.6-fold greater in mouse than rabbit microsomes. In contrast, the V_{max} , K_M , and CL_{int} from Thal to 5-OH Thal in HL18 microsomes were $0.334 \text{ pmol/min/mg}$, $85.8 \mu\text{M}$, and 0.004 ml/min/g , respectively. However, given that the data were calculated only from three concentration points (200 , 400 , and $600 \mu\text{M}$), where detectable 5-OH Thal was formed, the results are only an estimate of the kinetics of formation of 5-OH Thal in human microsomes. A comparison of the apparent CL_{int} of Thal to 5-OH Thal in the different species and in vivo plasma clearance of Thal (Cl/F) determined previously (unpublished data) are shown in Table 5. The relative rates of metabolism of Thal to 5-OH Thal in the three species in vitro correlates with the total in vivo clearance of Thal. Mouse has the highest rate of in vivo clearance (0.03 l/min/kg) and the highest rate of in vitro clearance to 5-OH Thal, whereas the negligible in vitro clearance of Thal to 5-OH Thal occurs in human liver microsomes corresponds to the very low in vivo clearance of Thal (0.0023 l/min/kg).

TABLE 5

Inter-species comparison of apparent in vitro kinetic parameters (V_{max} , hepatic intrinsic clearance) and in vivo plasma clearance

Species	Apparent V_{max}	Apparent CL_{int} to 5-OH Th	Cl/F at Oral Dose of 2 mg/kg ^a
	pmol/min/mg	ml/min/g	l/min/kg
Mouse	32.1–36.4	0.217	0.03
Rabbit	10.4–10.6	0.135	0.0167
Human	≈ 0.334	≈ 0.004	0.0023^b

^a Unpublished data.

^b Thal dose for multiple myeloma patients was 200 mg/kg , or 1.9 to 3.8 mg/kg according to patients' body weight.

Discussion

Numerous hydrolysis and metabolic products have been detected after the in vitro incubation of Thal with microsomes prepared from mouse, rabbit, and human liver. Some of the metabolites have been previously identified from in vivo studies (Lu et al., 2003; Chung et al., 2004) and include 5-OH Thal, *cis*- and *trans*-5'-OH Thal, and 5'-hydroxy-*N*-(*o*-carboxybenzoyl)glutamic acid imide. In addition, three metabolites (3, 8, and 9), with masses consistent with dihydroxylation have been detected. These were not observed in vivo, and it is possible that their sources, monohydroxylated metabolites, are rapidly cleared by glucuronidation, as in the case of 5-OH Thal (Lu et al., 2003). In vitro formation of 5-OH Thal and *cis*-5'-OH Thal, as well as of 5,6-dihydroxythalidomide and several unidentified metabolites, has been reported (Ando et al., 2002a). However, in our study none of metabolites (3, 8, and 9) corresponded to authentic 5,6-dihydroxythalidomide. Thal-5-*O*-glucuronide, which has been detected in our in vivo study, was also not detected, possibly due to the lack of uridine diphosphate glucuronide as a cofactor in the in vitro experiment setting.

Nonenzymatic hydrolysis of Thal was observed in this study, confirming previous results from other groups in a number of species, including rats, humans, and rabbits (Faigle, 1962; Keberle et al., 1965; Schumacher et al., 1965; Williams et al., 1965). In addition, we have found evidence of significant enzymatic hydrolysis of Thal to phthaloylisoglutamine in rabbit hepatic microsomes. This confirms an earlier report (Schumacher et al., 1968) indicating that the rate of hydrolysis of Thal was higher in rabbit liver than in rat liver, although the specific hydrolysis pathway from Thal to phthaloylisoglutamine was not identified. Because no differences in the relative amounts of phthaloylisoglutamine in the plasma of mice and rabbits after administration of Thal (2 mg/kg p.o.) were observed (Chung et al., 2004), enzymatic hydrolysis would be expected to occur only at the high Thal concentrations used in in vitro experiments ($\geq 12.5 \mu\text{M}$) and not at plasma concentrations ($C_{\text{max}} < 2.2 \mu\text{M}$) that are observed in vivo (Chung et al., 2004). Thalidomide is mainly excreted in the form of metabolites as shown by that less than 1% of the administered dose is excreted unchanged in urine in many species (Smith et al., 1965). Total metabolic clearance of Thal in vitro via both hydrolysis (enzymatic and nonenzymatic) and hydroxylation was greatest in the rabbit and negligible in human liver microsomes. However, because enzymatic hydrolysis of Thal in the rabbit may not occur at in vivo concentrations, clearance via hydroxylation may be more important.

Although hydroxylated metabolites were measurable in

human microsomal incubations with donor liver HL18, no metabolism of Thal was observed with another human liver donor HL5. This is in agreement with previous reports (Ando et al., 2002a) where of two human livers, one produced metabolites at or below the limit of quantification, and the other source had very low rate of metabolite formation. Ando et al. (2002a) indicated that this was related to the relative expression of CYP2C19; however, pooled human liver microsomes were also very poor metabolizers of Thal. Of the two livers used in this study, one HL5 was homozygous wild type (*1/*1) for CYP2C19, and the other liver HL18 was a heterozygote for the mutant allele (*1/*2). Although, in vitro studies with purified CYP2C19 indicated that this enzyme is involved in the hydroxylation of Thal, more recent in vivo studies (Ando et al., 2002b) have indicated that some patients with an extensive metabolizer genotype do not hydroxylate Thal to any significant extent. The role of CYP2C19 in the metabolism of Thal requires further study, but importantly, regardless of the P450 isozyme(s) involved, the overall rate of metabolism of Thal is negligible in human liver in comparison with mouse and rabbit.

In conclusion, the results support previous reports of low in vitro metabolic clearance of Thal in humans (Ando et al., 2002a) and suggest that there is minimal involvement of the hepatic P450 system in Thal metabolism. The data support in vivo data showing that hydroxylated metabolites are not detectable in patients with multiple myeloma (Lu et al., 2003; Chung et al., 2004) or with Hansen's disease (Teo et al., 2000). Hydroxylated metabolites can be detected in vitro but only at concentrations of Thal (200–600 μ M) that are well above the highest plasma concentrations of Thal (50 μ M) that have reported in human studies (Figg et al., 1999). These results suggest that Thal is unlikely to interact with other drugs extensively metabolized by human P450 system (Trapnell et al., 1998; Scheffler et al., 1999; Teo et al., 2000), which makes it a good candidate for combined chemotherapy. The data also strongly suggest that hydroxylated metabolites are unlikely to be involved in the mechanism of action of Thal in humans and that the parent compound and/or its hydrolysis product(s) are involved in its action.

References

- Ando Y, Fuse E, and Figg WD (2002a) Thalidomide metabolism by the CYP2C subfamily. *Clin Can Res* **8**:1964–1973.
- Ando Y, Price DK, Dahut WL, Cox MC, Reed E, and Figg WD (2002b) Pharmacogenetic associations of CYP2C19 genotype with in vivo metabolisms and pharmacological effects of thalidomide. *Cancer Biol Ther* **1**:669–673.
- Barfield M, Spear RJ, and Sternhell S (1975) Interproton spin-spin coupling across a dual path in 2,5-dihydrofurans and phthalans. *J Am Chem Soc* **97**:5160–5167.
- Calabrese L and Fleischer AB (2000) Thalidomide: current and potential clinical applications. *Am J Med* **108**:487–495.
- Chung F, Lu J, Palmer BD, Kestell P, Browett P, Baguley BC, Tingle MD and Ching

- LM (2004) Thalidomide pharmacokinetics and metabolite formation in mice, rabbits and multiple myeloma patients. *Clin Cancer Res*, in press.
- Chung F, Wang LCS, Kestell P, Baguley BC, and Ching LM (2004) Modulation of thalidomide pharmacokinetics by cyclophosphamide or 5,6-dimethylxanthine-4-acetic acid (DMXAA) in mice: the role of tumour necrosis factor. *Cancer Chemother Pharmacol* **53**:377–383.
- Eisen TG (2000) Thalidomide in solid tumors: the London experience. *Oncology (Huntington)* **14**:17–20.
- Eriksson T, Bjorkman S, Roth B, Bjork H, and Hoglund P (1998) Hydroxylated metabolites of thalidomide: formation in-vitro and in-vivo in man. *J Pharm Pharmacol* **50**:1409–1416.
- Faigle JW (1962) The metabolic fate of thalidomide. *Experientia* **18**:389–397.
- Figg WD, Raje S, Bauer KS, Tompkins A, Venzon D, Bergan R, Chen A, Hamilton M, Pluda J, and Reed E (1999) Pharmacokinetics of thalidomide in an elderly prostate cancer population. *J Pharm Sci* **88**:121–125.
- Gordon GB, Spielberg SP, Blake DA, and Balasubramanian V (1981) Thalidomide teratogenesis: evidence for a toxic arene oxide metabolite. *Proc Natl Acad Sci USA* **78**:2545–2548.
- Keberle H, Faigle JW, Fritz H, Knusel F, Loustalot P, and Schmid K (1965) Theories on the mechanism of action of thalidomide, in *Embryopathic Activity of Drugs* (Robson JM, Sullivan FM, and Smith RL eds) pp 210–233, J. & A. Churchill Ltd., London.
- Lenz W (1962) Thalidomide and congenital abnormalities. *Lancet* **1**:45.
- Lu J, Palmer BD, Kestell P, Browett P, Baguley BC, Muller G, and Ching LM (2003) Thalidomide metabolites in mice and patients with multiple myeloma. *Clin Cancer Res* **9**:1680–1688.
- McBride W (1961) Thalidomide and congenital abnormalities. *Lancet* **2**:1358.
- Scheffler MR, Colburn W, Kook KA, and Thomas SD (1999) Thalidomide does not alter estrogen-progesterone hormone single dose pharmacokinetics. *Clin Pharmacol Ther* **65**:483–490.
- Schumacher H, Blake DA, and Gillette JR (1968) Disposition of thalidomide in rabbits and rats. *J Pharmacol Exp Ther* **160**:201–211.
- Schumacher H, Smith RL, and Williams RT (1965) The metabolism of thalidomide: the fate of thalidomide and some of its hydrolysis products in various species. *Br J Pharmacol* **25**:338–351.
- Sheskin J (1965) Further observation with thalidomide in lepra reactions. *Leprosy Rev* **36**:183–187.
- Singhal S, Mehta J, Desikan R, Ayers D, Roberson P, Eddlemon P, Munshi N, Anaissie E, Wilson C, Dhodapkar M, et al. (1999) Antitumor activity of thalidomide in refractory multiple myeloma. *N Engl J Med* **341**:1565–1571.
- Smith PK, Krohn RI, Hermanson GT, Mallia AK, Garter FH, Provenzano MD, Fujimoto EK, Goeke NM, Olson BJ, and Klenk DC (1985) Measurement of protein using bichinchoninic acid. *Anal Biochem* **150**:76–85.
- Smith RL, Fabro S, Schumacher H, and Williams RT (1965) Studies on the relationship between the chemical structure and embryotoxic activity of thalidomide and related compound, in *Embryopathic Activity of Drugs* (Robson JM, Sullivan FM, and Smith RL eds) pp 195–209, J. & A. Churchill Ltd., London.
- Teo SK, Sabourin PJ, O'Brien K, Kook KA, and Thomas SD (2000) Metabolism of thalidomide in human microsomes, cloned human cytochrome P-450 isozymes and Hansen's disease patients. *J Biochem Toxicol* **14**:140–147.
- Torano JS, Verbon A, and Guchelaar HJ (1999) Quantitative determination of thalidomide in human serum with high-performance liquid chromatography using protein precipitation with trichloroacetic acid and ultraviolet detection. *J Chromatogr Biomed Appl* **734**:203–210.
- Trapnell CB, Donahue SR, Collins JM, Flockhart DA, Thacker D, and Abernethy DR (1998) Thalidomide does not alter the pharmacokinetics of ethinyl estradiol and norethindrone. *Clin Pharmacol Ther* **64**:597–602.
- Williams RT, Schumacher H, Fabro S, and Smith RL (1965) The chemistry and metabolism of thalidomide, in *Embryopathic Activity of Drugs* (Robson JM, Sullivan FM, and Smith RL eds) pp 167–193, J. & A. Churchill Ltd., London.
- Zwingerberger K and Wnendt S (1996) Immunomodulation by thalidomide: systematic review of the literature and of unpublished observations. *J Inflamm* **46**:177–211.

Address correspondence to: Dr. Lai-Ming Ching, The Auckland Cancer Society Research Center, Faculty of Medical and Health Sciences, The University of Auckland, Private Bag 92019, Auckland, New Zealand. E-mail: l.ching@auckland.ac.nz

Thalidomide Pharmacokinetics and Metabolite Formation in Mice, Rabbits, and Multiple Myeloma Patients

Francisco Chung,¹ Jun Lu,¹ Brian D. Palmer,¹
Philip Kestell,¹ Peter Browett,²
Bruce C. Baguley,¹ Malcolm Tingle,³ and
Lai-Ming Ching¹

¹Auckland Cancer Society Research Centre, ²Department of Molecular Medicine and Pathology, ³Department of Pharmacology and Clinical Pharmacology, Faculty of Medical and Health Sciences, The University of Auckland, Auckland, New Zealand.

ABSTRACT

Purpose: Thalidomide has a variety of biological effects that vary considerably according to the species tested. We sought to establish whether differences in pharmacokinetics could form a basis for the species-specific effects of thalidomide.

Experimental Design: Mice and rabbits were administered thalidomide (2 mg/kg) p.o. or i.v., and plasma concentrations of thalidomide were measured after drug administration using high performance liquid chromatography. Plasma samples from five multiple myeloma patients over 24 hours after their first dose of thalidomide (200 mg) were similarly analyzed and all data were fitted to a one-compartment model. Metabolites of thalidomide in plasma were identified simultaneously using liquid chromatography-mass spectrometry.

Results: Plasma concentration-time profiles for the individual patients were very similar to each other, but widely different pharmacokinetic properties were found between patients compared with those in mice or rabbits. Area under the concentration curve values for mice, rabbits, and multiple myeloma patients were 4, 8, and 81 $\mu\text{mol/L} \cdot \text{hour}$, respectively, and corresponding elimination half-lives were 0.5, 2.2, and 7.3 hours, respectively. Large differences were also observed between the metabolite profiles from the three species. Hydrolysis products were detected for all species, and the proportion of hydroxylated metabolites was higher in mice than in rabbits and undetectable in patients.

Conclusions: Our results show major interspecies differences in the pharmacokinetics of thalidomide that are related to the altered degree of metabolism. We suggest that the interspecies differences in biological effects of thalidomide may be attributable, at least in part, to the differences in its metabolism and hence pharmacokinetics.

INTRODUCTION

Thalidomide has a number of biological activities that have led to its clinical application to a variety of diseases. After demonstration of its efficacy in the control of erythema nodosum leprosum (1), thalidomide was evaluated for the management of numerous inflammatory and autoimmune diseases, including Crohn's disease (2) and rheumatoid arthritis (3). Its application as an anti-inflammatory agent is thought to be derived from its ability to inhibit the biosynthesis of proinflammatory cytokines such as tumor necrosis factor- α (4). After the demonstration that it could inhibit angiogenesis in the rabbit cornea (5), it was also evaluated for the treatment of cancer. Although activity was modest against renal carcinomas (6), gliomas (7), and prostate cancers (8), it was outstanding against refractory multiple myeloma (9), and thalidomide has been put forward as a 1st line treatment for this disease (10). However, thalidomide has an unfavorable effect, *i.e.*, its teratogenicity (11, 12), which led to its withdrawal when it was first marketed in the 1950s as a sedative and antiemetic (13). The difficulties in determining thalidomide's teratogenic properties during its initial development were perhaps because of the widely disparate interspecies sensitivities to the action of thalidomide. Rodents appear resistant to the teratogenicity of thalidomide, whereas rabbits and humans were highly susceptible (14). It has been suggested that the antiangiogenic and teratogenic effects are caused by stable metabolites, and species specific differences in thalidomide metabolism form the basis for the interspecies differences in the action of thalidomide (15).

Biotransformation of thalidomide can occur by nonenzymatic hydrolysis (16, 17) or by hepatic cytochrome P450-catalyzed hydroxylation (18), with all products often referred to as metabolites. Considerable interspecies differences in the production of hydroxylated metabolites have been observed. A 20-fold higher production of hydroxylated metabolites was found with rodent liver microsomes than with human liver microsomes (18). Two hydroxylated products were obtained when thalidomide was incubated with human liver enzymes, but only one of these could be found in low concentrations in plasma samples from healthy male volunteers (19). In patients with Hansen's disease, no hydroxylated metabolites were detected in plasma whereas one was detected in urine by tandem mass spectrometry but mostly at levels below the limit of quantitation, and *in vitro* studies indicated that thalidomide was a poor substrate for human cytochrome P450 isoenzymes (20). Among patients with prostate cancer, *cis*-5'-hydroxythalido-

Received 3/2/04; revised 4/22/04; accepted 5/5/04.

Grant support: Marsden Research Fund and the Health Research Council of New Zealand.

The costs of publication of this article were defrayed in part by the payment of page charges. This article must therefore be hereby marked *advertisement* in accordance with 18 U.S.C. Section 1734 solely to indicate this fact.

Note: F. Chung and J. Lu contributed equally to this work.

Requests for reprints: Lai-Ming Ching, Auckland Cancer Society Research Centre, Faculty of Medical and Health Sciences, The University of Auckland, Private Bag 92019, Auckland, New Zealand. Phone: 64-9-3737-999; Fax: 64-9-3737-502; E-mail: l.ching@auckland.ac.nz.

©2004 American Association for Cancer Research.

midate and 5-hydroxythalidomide were detectable in only 48% and 32% of individuals, respectively (21). In a previous study, we have used liquid chromatography-mass spectrometry to show that whereas hydroxylated metabolites of thalidomide were present in the plasma and urine of mice, none were detectable in the urine of multiple myeloma patients on thalidomide therapy (22).

In this report we have extended those studies to compare thalidomide pharmacokinetics and metabolite formation in mice, rabbits, and multiple myeloma patients. Our results suggest that differences in the rates by which the drug is metabolized may provide a basis for interspecies differences in the response to thalidomide.

MATERIALS AND METHODS

Materials. Thalidomide for animal studies was kindly provided by Dr. George Muller (Celgene Corp., Warren, NJ). 2-Hydroxypropyl- β -cyclodextrin and trichloroacetic acid were purchased from Sigma-Aldrich. Acetonitrile was purchased from BDH Laboratory Supplies (Poole, United Kingdom). Glacial acetic acid was purchased from Panreac Quimica SA (Barcelona, Spain).

Authentic Standards. Phthaloylglutamic acid was purchased from Sigma-Aldrich (St. Louis, MO). Phthaloylisoglutamine, 4-hydroxyphthaloylisoglutamine, 5-hydroxyphthaloylisoglutamine, phthaloylglutamine, 4-hydroxyphthaloylglutamine, 5-hydroxyphthaloylglutamine, 4-hydroxythalidomide, 5-hydroxythalidomide, *N*-(*o*-carboxybenzoyl)glutamine, *N*-(*o*-carboxybenzoyl)isoglutamine, *N*-(*o*-carboxybenzoyl)glutamic acid imide, and 5-hydroxy-*N*-(*o*-carboxybenzoyl)glutamic acid imide were synthesized as described previously (22), and their structures were confirmed using 400 MHz ^1H nuclear magnetic resonance spectroscopy and mass spectrometry. 5'-Hydroxythalidomide was a generous gift from Professor Sven Bjorkman (Malmo University Hospital, Malmo, Sweden) and was a mixture of 5'-*cis*- and 5'-*trans* diastereomers.

Murine Studies. Female 8 to 12 week-old C57Bl/6 mice bred at the Animal Resources Unit, Faculty of Medical and Health Sciences, University of Auckland, were housed under conditions of constant temperature and humidity according to institutional ethical guidelines. Thalidomide was dissolved in 2-hydroxypropyl- β -cyclodextrin (1 mg/ml) and administered p.o. (gavage needle) or i.v. (tail-vein; 2 mg/kg, 2 $\mu\text{L/g}$ body weight). In another set of experiments, thalidomide was administered p.o. or i.v. at a dose of 20 mg/kg dissolved in 30% dimethylsulfoxide in polypropylene glycol solution (8 mg/ml). Mice were bled at 5, 15, and 30 minutes, and 1, 2, 4, and 6 hours after treatment. Three mice were used for each time point plus an untreated control group. The mice used for the 6-hour time point were placed in metabolic cages with water and food, and urine was collected over the first 4 hours after treatment. Blood samples were collected into heparinized tubes during terminal halothane (NZ Pharmacology Ltd., Christchurch, New Zealand) anesthesia, centrifuged, and the plasma removed. Plasma (200 μL for pharmacokinetic studies and 300 μL for metabolite studies) and urine (100 μL) were acidified by adding 10% trichloroacetic acid up to 1 ml. Samples were centrifuged at $3000 \times g$ for 10 minutes to remove precipitated protein and then

processed using solid phase extraction as described previously (22). Dried plasma and urine residues were reconstituted in 100 μL and 1,000 μL mobile phase, respectively, for analysis.

Rabbit Studies. Three female New Zealand White rabbits supplied by Animal Resource Unit of the University of Auckland were used between 6 and 12 months-old for all of the experiments according to institutional ethical guidelines. Thalidomide was dissolved in 2-hydroxypropyl- β -cyclodextrin (1 mg/ml) and administered p.o. using a polyethylene plastic tube, or i.v. via ear-vein injection (2 mg/kg in a volume of 2 ml/kg). After drug administration, rabbits were placed in metabolic cages with water and food for urine collection over a 6-hour period. Blood samples were collected into heparinized tubes from the ear-vein at 15 and 30 minutes and 1, 2, 3, 4, 6, and 8 hours for the p.o. studies, and at 15 and 30 minutes and 1, 1.5, 2, 3, 4, and 8 hours for i.v. studies. Control urine and plasma samples for each rabbit were obtained before thalidomide administration. Plasma (200 and 300 μL for pharmacokinetics and metabolite studies, respectively) and urine (100 μL) were processed as described for the murine samples. Dried residues were reconstituted in 200 or 100 μL of mobile phase, respectively, for urine samples and plasma samples.

Clinical Studies. All clinical studies conformed to institutional ethical guidelines. Three male and two female Caucasian patients who were beginning their thalidomide therapy for refractory multiple myeloma at Auckland Hospital were recruited for these studies. Their ages ranged from 42 to 81 years, and their weights ranged from 52 to 105 kg. All patients had been instructed not to take nonprescription medications or drink alcohol. Blood was collected into heparinized tubes at 1, 2, 4, 6, 8, and 24 hours after the patients' first dose of thalidomide ($2 \times 100\text{-mg}$ tablets p.o.). Urine samples were collected whenever possible. A control sample of blood and urine was obtained from the patients before treatment. Blood samples were centrifuged and plasma collected and quickly stored at -80°C until analysis. Plasma (200 and 300 μL , respectively, for pharmacokinetics and metabolite studies) was acidified by adding 10% trichloroacetic acid up to 1 ml and centrifuged to remove precipitated protein. Urine samples (3.33-ml each) were acidified by adding 10% trichloroacetic acid up to 10 ml. All samples were processed as described for murine samples. Dried residues from plasma and urine samples were reconstituted in 100 and 1,000 μL mobile phase, respectively.

Pharmacokinetic Determination. Thalidomide concentrations were measured using a specific high performance liquid chromatography assay as described previously (23). Concentration-time data were analyzed using Pharsight WinNonlin 4.01 software (Mountain View, CA) and fitted either to a one-compartmental i.v. model or one-compartmental p.o. model with first-order absorption and elimination. C_{max} and T_{max} were determined visually from the plasma time-concentration profile. The elimination rate constant (λ) was determined from the terminal linear portion of the concentration *versus* time curve. The terminal $t_{1/2}$ was calculated as $\ln(2)/\lambda$. The area under the plasma thalidomide concentration *versus* time curve (AUC_{0-t}) from time zero to the last quantifiable concentration (C_t) was calculated by trapezoidal rule. Area under the concentration-time curve (AUC) extrapolated to infinity was calculated from ($\text{AUC}_{0-t} + C_t/\lambda$).

Metabolite Studies. Reconstituted samples were analyzed together with authentic standards using an Agilent 1100 series liquid chromatography-mass spectrometry system (Agilent Technologies, Avondale, PA) as described previously (22) with two modifications. The proportions of solution A (80% acetonitrile, 1% glacial acetic acid, and 19% Milli Q water) and solution B (9.5% acetonitrile, 1% glacial acetic acid, and 89.5% Milli Q water) in the mobile phase were altered slightly to improve resolution; all samples were analyzed using diode array UV detection at 230 nm and mass spectral detection set on negative-ion scan mode with a M_r range of 70 to 1,000 atomic mass units, negative single-ion monitoring mode, with the sensitivity of 1 pg, at the M_r 257, 273, 275, 276, 289, 291, 293, 294 and 449, and positive single-ion monitoring mode at the M_r 259, 275, 277, 278, 291, 293, 295, 296 and 451 (corresponding to each of the peaks) simultaneously.

Statistical Analysis. All pharmacokinetic data are presented as means \pm SD, and because of limitations on the volume of blood samples obtainable from mice, murine pharmacokinetic parameters were calculated by modeling group mean data using Pharsight v4.01. Student's t test was used to calculate the statistical significance between groups, with a probability value $P < 0.05$ considered significant.

RESULTS

Thalidomide Pharmacokinetics in Mice. After p.o. administration of thalidomide at 2 mg/kg, the peak concentration was 4.3 ± 0.9 $\mu\text{mol/L}$ after 0.5 hour (Fig. 1A). When given i.v., the highest concentration was 7.7 ± 0.3 $\mu\text{mol/L}$, observed after 5 minutes (Fig. 1B), and the $t_{1/2}$ was 0.5 to 0.8 hour. The AUC after p.o. administration (4.3 ± 0.8 $\mu\text{mol/L} \cdot \text{hour}$) was signif-

Table 1 Thalidomide pharmacokinetic parameters in plasma in mice, rabbits, and patients

Route	Dosage (mg/kg)	C_{\max} ($\mu\text{mol/L}$)	T_{\max} (h)	$\text{AUC}_{0-\infty}$ ($\mu\text{mol/L} \cdot \text{h}$)	$t_{1/2}$ (h)
Mice					
p.o.	2	4.3 ± 0.9	0.50	4.3 ± 0.8	0.5 ± 0.20
	20	12.0 ± 3.0	1.00	44.0 ± 6.0	1.2 ± 0.05
i.v.	2	$7.7 \pm 0.3^*$	$\leq 0.08^*$	8.7 ± 0.7	0.8 ± 0.10
	20	$59 \pm 7^*$	$\leq 0.08^*$	60.0 ± 7.0	0.7 ± 0.10
Rabbits					
p.o.	2	1.8 ± 0.4	1.5 ± 0.9	8 ± 0.2	2.2 ± 0.3
i.v.	2	$7.2 \pm 0.6^*$	0.25^*	8 ± 1.0	0.7 ± 0.1
Patients					
p.o.†					
P1	1.95	3.5	4	49	6.7
P2	2.11	3.8	4	69	7.7
P3	2.60	5.1	4	72	7.8
P4	3.51	7.2	6	107	7.7
P5	3.85	7.5	6	110	6.5
Mean \pm SD		5.4 ± 1.9	4.8 ± 1	81 ± 26	7.3 ± 0.6

* C_{\max} and T_{\max} values limited by the first time-point of analysis.

† Patients were treated with 200-mg tablets, and the dose was normalized.

icantly lower than that obtained with i.v. (8.7 ± 0.7 $\mu\text{mol/L} \cdot \text{hour}$) administration (Table 1). The calculated bioavailability, based on AUC, was 50%. Thalidomide concentrations were also measured after a dose of 20 mg/kg, which was used previously in our *in vivo* studies (ref. 24; Fig. 1A and B). This 10-fold increase in dose resulted in a 10-fold increase in AUC after p.o. administration of thalidomide (Table 1). The C_{\max} was increased only 3-fold (12 ± 3 $\mu\text{mol/L}$) and occurred after 1 hour

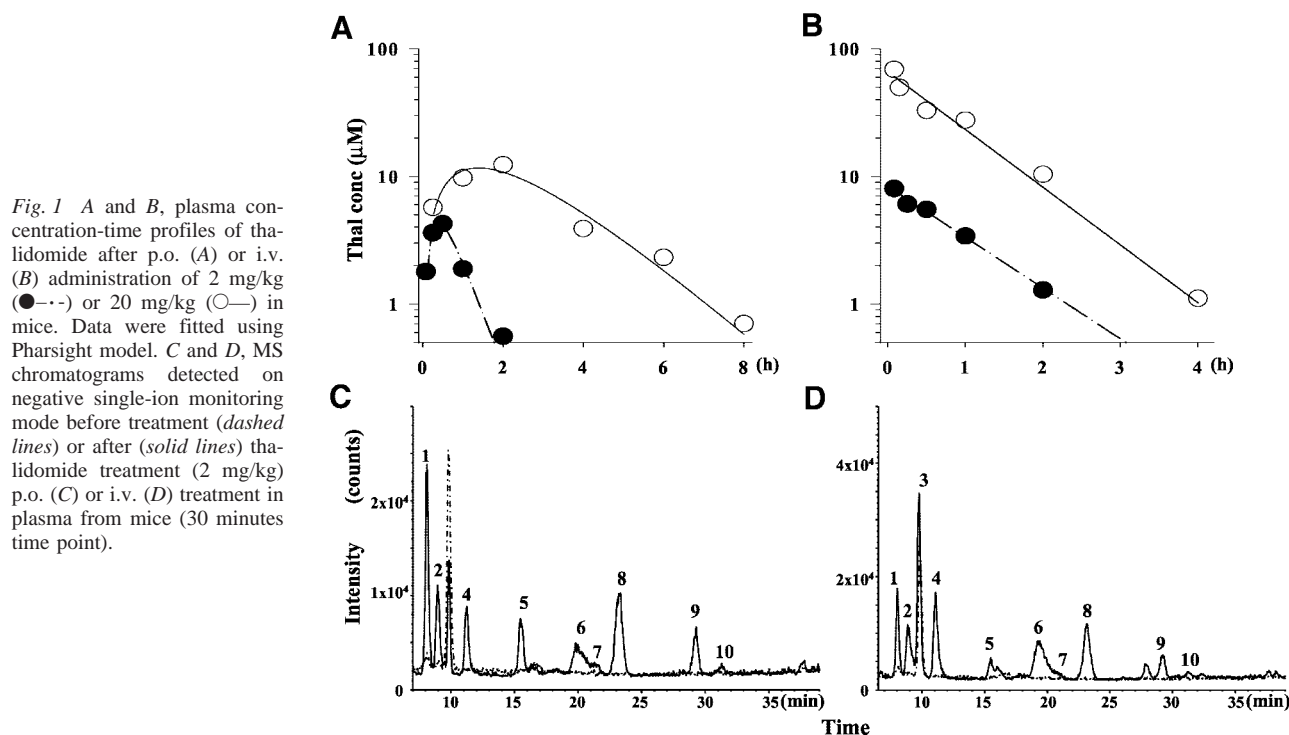


(Table 1), and the $t_{1/2}$ increased by 3- and 2-fold respectively at 20 mg/kg compared with 2 mg/kg p.o. thalidomide. Intravenous administration of thalidomide at 20 mg/kg also produced a proportionate increase in AUC ($60 \pm 7 \mu\text{mol/L} \cdot \text{hour}$) but with no significant change in $t_{1/2}$ (0.7 ± 0.1 hour).

Thalidomide Pharmacokinetics in Rabbits. Rabbits were administered thalidomide 2 mg/kg either p.o. (Fig. 2A) or i.v. (Fig. 2B). The C_{max} after p.o. administration ($1.8 \mu\text{mol/L}$) was 4-fold lower than that observed after i.v. administration ($7.2 \mu\text{mol/L}$). The T_{max} was 1.5 hours, and the bioavailability of thalidomide was 100%. The $t_{1/2}$ of p.o. administered thalidomide was 3-fold higher than that for i.v. administration (Table 1).

Thalidomide Pharmacokinetics in Multiple Myeloma Patients. Thalidomide was absorbed slowly in patients (Fig. 3A-E), with the mean peak concentration ($5.2 \pm 1.9 \mu\text{mol/L}$) achieved after 4.5 ± 1 hour. The elimination $t_{1/2}$ in patients was 7.6 ± 0.6 hours, 15- and 3-fold longer than that in mice and rabbits, respectively. The AUC, $83 \pm 14 \mu\text{mol/L} \cdot \text{hour}$, was 20- and 10-fold higher than in mice and rabbits, respectively (Table 1). In two patients, total 24-hour urines were collected for analysis, and unchanged thalidomide was found to account for 0.9% of the administered dose.

Thalidomide Metabolites in Mice. Metabolite profiles were monitored by liquid chromatography-mass spectrometry as described previously (22), with a modification in the solvent allowing separation of phthaloylisoglutamine (peak 5) from phthaloylglutamine (peak 7), as well as separation of the *cis*- and *trans*-5'-hydroxy-*N*-(*o*-carboxybenzoyl)glutamic acid imides (peaks 2 and 4). On the basis of their relative polarities, peak 2 and peak 4 would be expected to be the *cis*- and the *trans*-isomer, respectively, but this has yet to be validated with au-

thentic standards. The modification also provided a better resolution of *N*-(*o*-carboxybenzoyl)isoglutamine (peak 3). All plasma samples exhibited the same metabolite profile regardless of the route of administration (Fig. 1C and D), which contained peaks 1, 5, and 7 corresponding to hydrolysis products, plus peaks 2, 4, 6, 8, 9, and 10 corresponding to hydroxylated and glucuronidated metabolites (Table 2). Urine samples contained the same peaks with the addition of peak 3, *N*-(*o*-carboxybenzoyl)isoglutamine, which was masked in plasma samples by a background component present in untreated controls. Although i.v. (Fig. 1D) or p.o. (Fig. 1C) administration produced the same number of metabolite peaks, the plasma metabolite peaks at 2 hours or earlier were higher after i.v. administration compared with p.o. administration.

Thalidomide Metabolites in Rabbits. After p.o. administration to rabbits, two different metabolic profiles were observed in plasma, dependent on the concentration of the parent thalidomide present. At all time points when the concentration of thalidomide was below $1 \mu\text{mol/L}$, the metabolite profile showed hydrolysis products only (peaks 1, 5, and 7; Fig. 2D). However, when the thalidomide plasma level was above $1 \mu\text{mol/L}$, whether during the absorption or the elimination phase, hydroxylated metabolites (peaks 2, 4, 6, and 8) were detected in addition to the hydrolysis products (peaks 1, 3, and 5; Fig. 2C). The mass spectral peak areas of peaks 2, 4, 6, and 8 in rabbit samples were 26.8, 43.7, 3.6, and 6.2%, respectively, of their corresponding peak in murine samples, indicating a lower level of hydroxylation in rabbits compared with mice. Urine samples contained hydrolysis products (peaks 1, 3, and 5) only. After i.v. administration, plasma samples collected before 2 hours, when thalidomide concentration was above $1 \mu\text{mol/L}$, hydrolysis

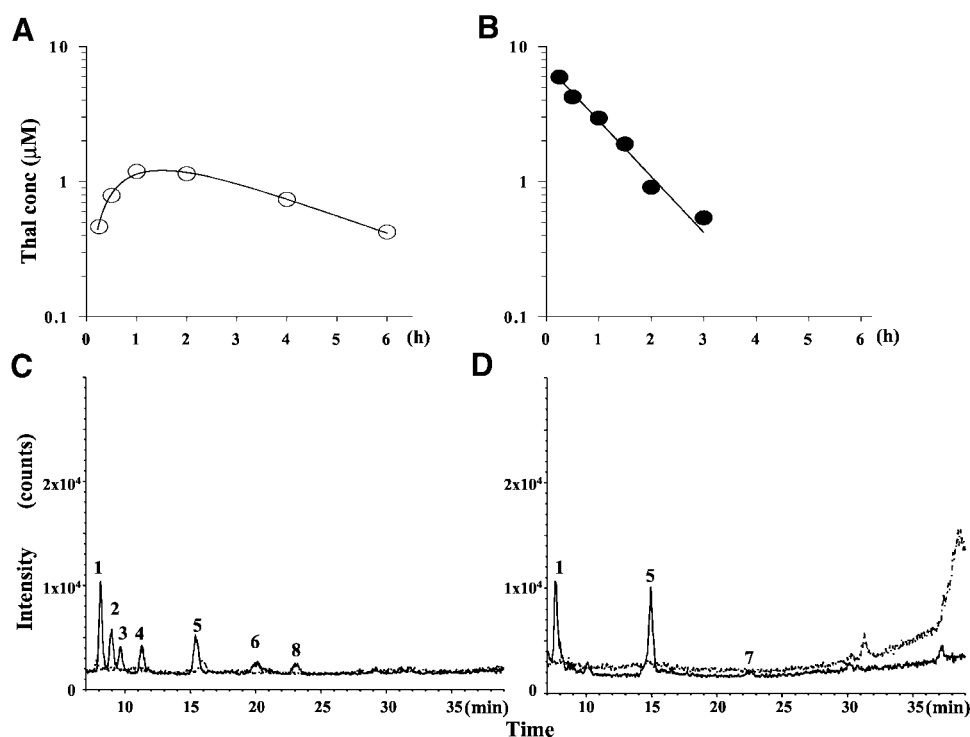


Fig. 2 A and B, plasma concentration-time profiles of thalidomide after p.o. (○; A) or i.v. administration (●; B) of 2 mg/kg to rabbits. Data were collected from three rabbits and fitted using Pharsight model. C and D, MS chromatograms detected on negative single-ion monitoring mode before (dashed lines) or after (solid lines) 2 hours (C) or 30 minutes (D) of thalidomide (2 mg/kg) p.o. treatment in plasma from rabbits.

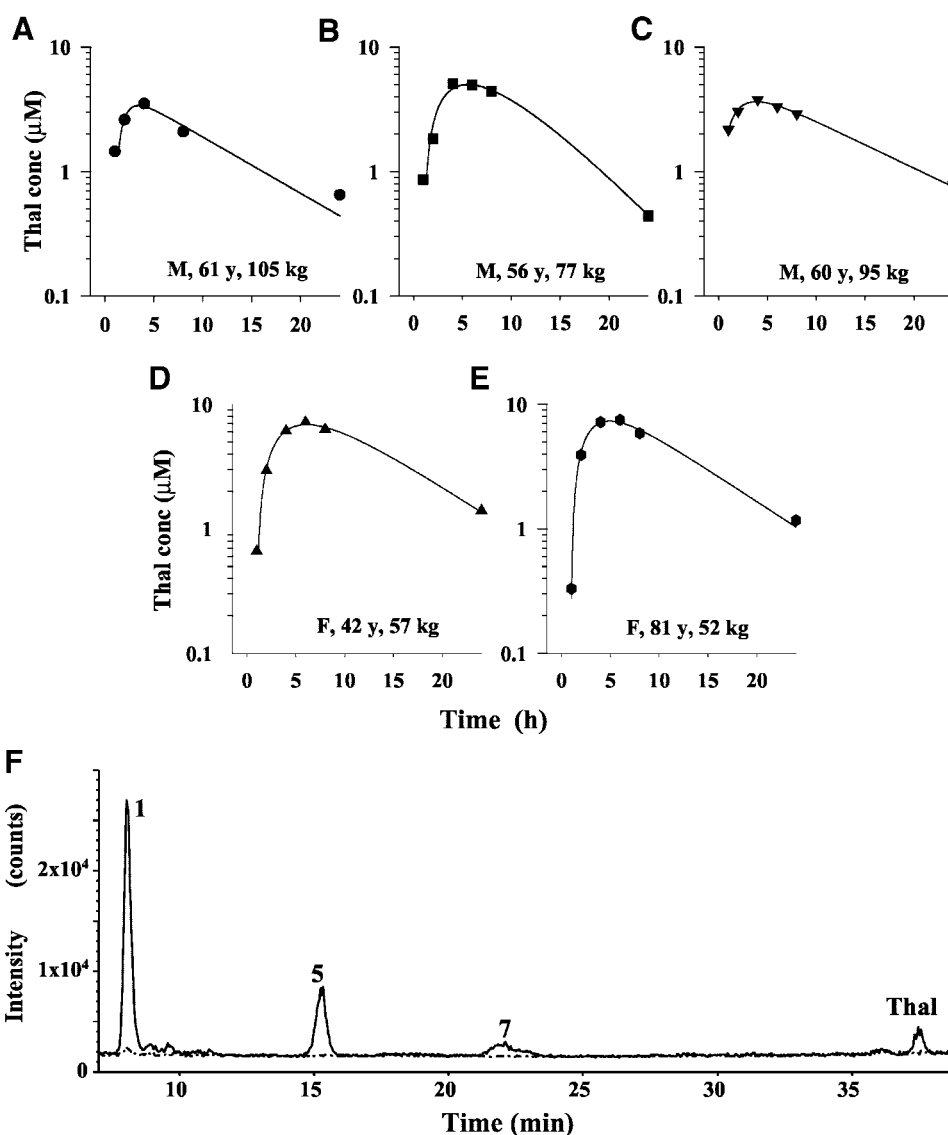


Fig. 3 A–E, plasma concentration-time profiles of thalidomide after an oral dose of 200 mg for each of five multiple myeloma patients ●, ■, ▲, ●, represent different patients. F, representative MS chromatogram detected on negative single-ion monitoring mode before (dashed line) or after (solid line) thalidomide (2 mg/kg p.o.) treatment in plasma from patient 2 (4-hour time point).

products (peaks 1, 3, and 5), and hydroxylated products (peaks 2, 4, 6, 8, 9, and 10) were detected. However, after 2 hours, when thalidomide concentrations had dropped below 1 µmol/L, the metabolite profiles showed only hydrolysis products (peaks 1, 5, and 7). Urine samples after i.v. administration showed two hydrolysis products (peaks 1 and 5) and one hydroxylation product (peak 10; data not shown).

Thalidomide Metabolites in Patients. All plasma and urine samples from multiple myeloma patients contained only peaks 1, 5, and 7, corresponding to the hydrolysis products; hydroxylated metabolites were not detected at any time point in urine or in plasma (Fig. 3F). Very little inter-individual variability in thalidomide pharmacokinetics and metabolite formation was seen in five patients despite differences in age (42–81 years), weight (52–105 kg), sex, and disease status (Fig. 3, Table 1).

DISCUSSION

This study, the first detailed comparison of thalidomide pharmacokinetics and metabolite formation in mice, rabbits, and patients with multiple myeloma, was carried out to determine whether thalidomide pharmacokinetics could explain the interspecies differences in biological response. Widely different pharmacokinetic parameters for thalidomide were found (Fig. 4; Table 1). In mice, bioavailability was 50%, and the elimination was rapid whereas in rabbits bioavailability was 100% and $t_{1/2}$ was longer, and in multiple myeloma patients the $t_{1/2}$ was even longer. We hypothesize that differences in metabolism are the principal cause of the observed interspecies differences in pharmacokinetics. Our observation in two multiple myeloma patients, that <1% of the administered thalidomide dose was excreted unchanged in urine, is in agreement with data for other species including mice and rabbits (25). In mice, 10 metabolite

Table 2 Metabolite peaks in UV and MS profiles of mouse urine after p.o. thalidomide

Peak No.	Molecular weight	Metabolite	Structure
1*	276	<i>N</i> -(<i>o</i> -carboxybenzoyl)glutamic acid imide	
2†,‡	292	<i>cis</i> -5'-Hydroxy- <i>N</i> -(<i>o</i> -carboxybenzoyl)glutamic acid imide	
3*	294	<i>N</i> -(<i>o</i> -carboxybenzoyl)isoglutamine	
4†,‡	292	<i>trans</i> -5'-Hydroxy- <i>N</i> -(<i>o</i> -carboxybenzoyl)glutamic acid imide	
5*	276	Phthaloylisoglutamine	
6†	450	Thalidomide-5- <i>O</i> -glucuronide	
7*	276	Phthaloylglutamine	
8†	274	<i>cis</i> -5'-Hydroxythalidomide	
9†	274	<i>trans</i> -5'-Hydroxythalidomide	
10†	274	5-Hydroxythalidomide	

* Hydrolysis product.

† Hydroxylation product.

‡ Not yet confirmed by comparison with authentic standard.

peaks corresponding to hydrolysis, hydroxylation, and glucuronidation products were detectable in urine and plasma within 30 minutes of i.v. (Fig. 1D) or p.o. (Fig. 1C) administration. Hydroxylation products were detectable in rabbits only if the thalidomide concentration was above 1 $\mu\text{mol/L}$ in the plasma, irrespective of the route of administration and the phase of the pharmacokinetic profile (Fig. 2). In contrast, hydroxylated metabolites were not detected in any sample from the five multiple myeloma patients in this study (Fig. 3F). Thus, hydroxylation of thalidomide occurs extensively in mice, moderately in rabbits, and undetectably in patients. Because hydroxylated and glucu-

ronidated metabolites are much more soluble than the parent drug, greater metabolism along this pathway would facilitate more rapid elimination of thalidomide from the system. Consistent with this, a reverse correlation between the rate of elimination and the amount of hydroxylation in the three species was obtained, suggesting that the interspecies differences in thalidomide pharmacokinetics are related to the rate at which it is hydroxylated.

The results confirm our previous finding that hydroxylated products are not detectable in multiple myeloma patients (22). If the parent drug, or one of its hydrolysis products, is responsible

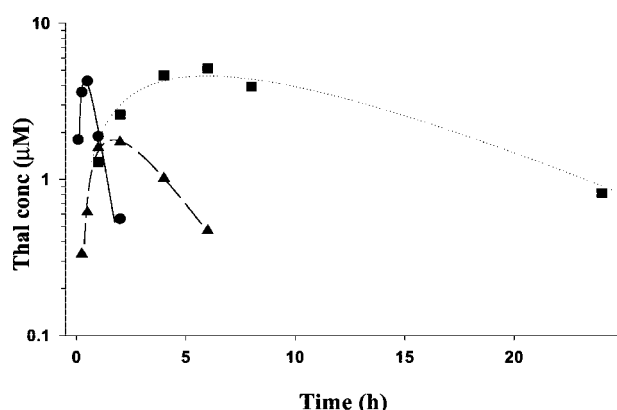


Fig. 4 Comparison of thalidomide pharmacokinetics in mice (2 mg/kg, ●), rabbits (2 mg/kg, ▲) and multiple myeloma patients (200 mg, combined data from five individuals, ■).

for the *in vivo* effects, thalidomide would be expected to be more effective in a species in which it is hydroxylated slowly. Consistent with this proposal, humans are more susceptible than rodents to many of the effects of thalidomide including antitumor effects. Although clinical responses have been reported for renal carcinomas (6), gliomas (7), prostate cancers (8), and in particular for multiple myeloma (9, 26), evidence for antitumor activity after single or multiple dose administration of thalidomide to mice has been difficult to obtain (27, 28). On the basis of the AUC values determined in the present study (Table 1), rabbits would be expected to be intermediate between humans and mice in their responsiveness to thalidomide, and there is a single report of daily high doses of thalidomide (200 mg/kg/day) achieving a 55% reduction in tumor volume of V2 carcinomas in rabbits (29). The teratogenicity of thalidomide in rabbits at high doses and in humans at low doses, as well as the resistance of rodents to teratogenicity (14), may also be related to the AUC and exposure to the parent drug (Table 1).

Thalidomide modulates the biosynthesis of a number of cytokines that are essential to the growth and survival of multiple myeloma cells, suggesting that its primary mechanism of action in multiple myeloma patients involves down-regulation of cytokine synthesis (30, 31). Consistent with this, a recent study has shown that multiple myeloma patients who are genetically high tumor necrosis factor- α producers respond better to thalidomide therapy (32). Inhibition of cytokine biosynthesis by thalidomide does not require hepatic activation (4) and we suggest that the long plasma half-life of thalidomide in multiple myeloma patients, which is a result of a low rate of metabolism, is important for such down-regulation. These considerations are relevant to the development of newer thalidomide analogs, some of which have been reported to have more consistent pharmacokinetic profiles than thalidomide and are currently undergoing clinical trial (33).

REFERENCES

1. Sheskin J. Further observation with thalidomide in lepra reactions. *Leprosy Rev* 1965;36:183-7.
2. Wettstein AR, Meagher AP. Thalidomide in Crohn's disease. *Lancet* 1997;350:1445-6.

3. Gutierrez-Rodriguez O. Thalidomide. A promising new treatment for rheumatoid arthritis. *Arthritis Rheum* 1984;27:1118-21.
4. Sampaio EP, Sarno EN, Galilly R, Cohn ZA, Kaplan G. Thalidomide selectively inhibits tumor necrosis factor alpha production by stimulated human monocytes. *J Exp Med* 1991;173:699-703.
5. D'Amato RJ, Loughnan MS, Flynn E, Folkman J. Thalidomide is an inhibitor of angiogenesis. *Proc Natl Acad Sci USA* 1994;91:4082-85.
6. Motzer RJ, Berg W, Ginsberg M, et al. Phase II trial of thalidomide for patients with advanced renal cell carcinoma. *J Clin Oncol* 2002;20:302-6.
7. Fine HA, Figg WD, Jaeckle K, et al. Phase II trial of the antiangiogenic agent thalidomide in patients with recurrent high-grade gliomas. *J Clin Oncol* 2000;18:708-15.
8. Figg WD, Dahut W, Duray P, et al. A randomized phase II trial of thalidomide, an angiogenesis inhibitor, in patients with androgen-independent prostate cancer. *Clin Cancer Res* 2001;7:1888-93.
9. Singhal S, Mehta J, Desikan R, et al. Antitumor activity of thalidomide in refractory multiple myeloma. *N Engl J Med* 1999;341:1565-71.
10. Weber D, Rankin K, Gavino M, Delasalle K, Alexanian R. Thalidomide alone or with dexamethasone for previously untreated multiple myeloma. *J Clin Oncol* 2003;21:16-9.
11. Lenz W. Thalidomide and congenital abnormalities. *Lancet* 1962;1:45.
12. McBride W. Thalidomide and congenital abnormalities. *Lancet* 1961;2:1358.
13. Randall T. Thalidomide has 37-year history. *J Am Med Assoc* 1990;263:1474.
14. Neubert R, Neubert D. Peculiarities and possible mode of actions of thalidomide. In: Kavlock RJ, Daston GP, editors. *Drug toxicity in embryonic development II*. Berlin: Springer-Verlag, 1997. p. 41-119.
15. Bauer KS, Dixon SC, Figg WD. Inhibition of angiogenesis by thalidomide requires metabolic activation, which is species-dependent. *Biochem Pharmacol* 1998;55:1827-34.
16. Schumacher H, Smith RL, Williams RT. The metabolism of thalidomide: the spontaneous hydrolysis of thalidomide in solution. *Br J Pharmacol* 1965;25:324-37.
17. Schumacher H, Smith RL, Williams RT. The metabolism of thalidomide: the fate of thalidomide and some of its hydrolysis products in various species. *Br J Pharmacol* 1965;25:338-51.
18. Ando Y, Fuse E, Figg WD. Thalidomide metabolism by the CYP2C subfamily. *Clin Cancer Res* 2002;8:1964-73.
19. Eriksson T, Bjorkman S, Roth B, Bjork H, Hoglund P. Hydroxylated metabolites of thalidomide: formation in-vitro and in-vivo in man. *J Pharm Pharmacol* 1998;50:1409-16.
20. Teo SK, Sabourin PJ, O'Brien K, Kook KA, Thomas SD. Metabolism of thalidomide in human microsomes, cloned human cytochrome P-450 isozymes, and Hansen's disease patients. *J Biochem Toxicol* 2000;14:140-7.
21. Ando Y, Price DK, Dahut WL, Cox MC, Reed E, Figg WD. Pharmacogenetic associations of CYP2C19 genotype with in vivo metabolisms and pharmacological effects of thalidomide. *Cancer Biol Ther* 2002;1:669-73.
22. Lu J, Palmer BD, Kestell P, et al. Thalidomide metabolites in mice and patients with multiple myeloma. *Clin Cancer Res* 2003;9:1680-8.
23. Chung F, Wang LCS, Kestell P, Baguley BC, Ching LM. Modulation of thalidomide pharmacokinetics by cyclophosphamide or 5,6-dimethylxanthine-4-acetic acid (DMXAA) in mice: the role of tumor necrosis factor. *Cancer Chemother Pharmacol* 2004;53:377-83.
24. Ding Q, Kestell P, Baguley BC, et al. Potentiation of the antitumor effect of cyclophosphamide in mice by thalidomide. *Cancer Chemother Pharmacol* 2002;50:186-92.
25. Smith RL, Fabro S, Schumacher H, Williams RT. Studies on the relationship between the chemical structure and embryotoxic activity of thalidomide and related compound. In: Robson JM, Sullivan FM, and Smith RL, editors. *Embryopathic activity of drugs*. London: J & A Churchill Ltd; 1965. p. 195-209.

26. Barlogie B, Desikan R, Eddlemon P, et al. Extended survival in advanced and refractory multiple myeloma after single-agent thalidomide: identification of prognostic factors in a phase 2 study of 169 patients. *Blood* 2001;98:492–4.
27. Cao Z, Joseph WR, Browne WL, et al. Thalidomide increases both intra-tumoural tumour necrosis factor- α production and anti-tumour activity in response to 5,6-dimethylxanthenone-4-acetic acid. *Br J Cancer* 1999;80:716–23.
28. Ching LM, Xu ZF, Gummer BH, Palmer BD, Joseph WR, Baguley BC. Effect of thalidomide on tumour necrosis factor production and anti-tumour activity induced by 5,6-dimethylxanthenone-4-acetic acid. *Br J Cancer* 1995;72:339–43.
29. Verheul HM, Panigrahy D, Yuan J, D'Amato RJ. Combination oral antiangiogenic therapy with thalidomide and sulindac inhibits tumour growth in rabbits. *Br J Cancer* 1999;79:114–8.
30. Gupta D, Treon SP, Shima Y, et al. Adherence of multiple myeloma cells to bone marrow stromal cells upregulates vascular endothelial growth factor secretion: therapeutic applications. *Leukemia* 2001;15:1950–61.
31. Hideshima T, Chauhan D, Schlossman RL, Richardson P, Anderson KC. The role of tumor necrosis factor α in the pathophysiology of human multiple myeloma: therapeutic applications. *Oncogene* 2001;20:4519–27.
32. Neben K, Mytilineos J, Moehler TM, et al. Polymorphisms of the tumor necrosis factor- α gene promoter predict for outcome after thalidomide therapy in relapsed and refractory multiple myeloma. *Blood* 2002;100:2263–5.
33. Richardson PG, Schlossman RL, Weller E, et al. Immunomodulatory drug CC-5013 overcomes drug resistance and is well tolerated in patients with relapsed multiple myeloma. *Blood* 2002;100:3063–7.